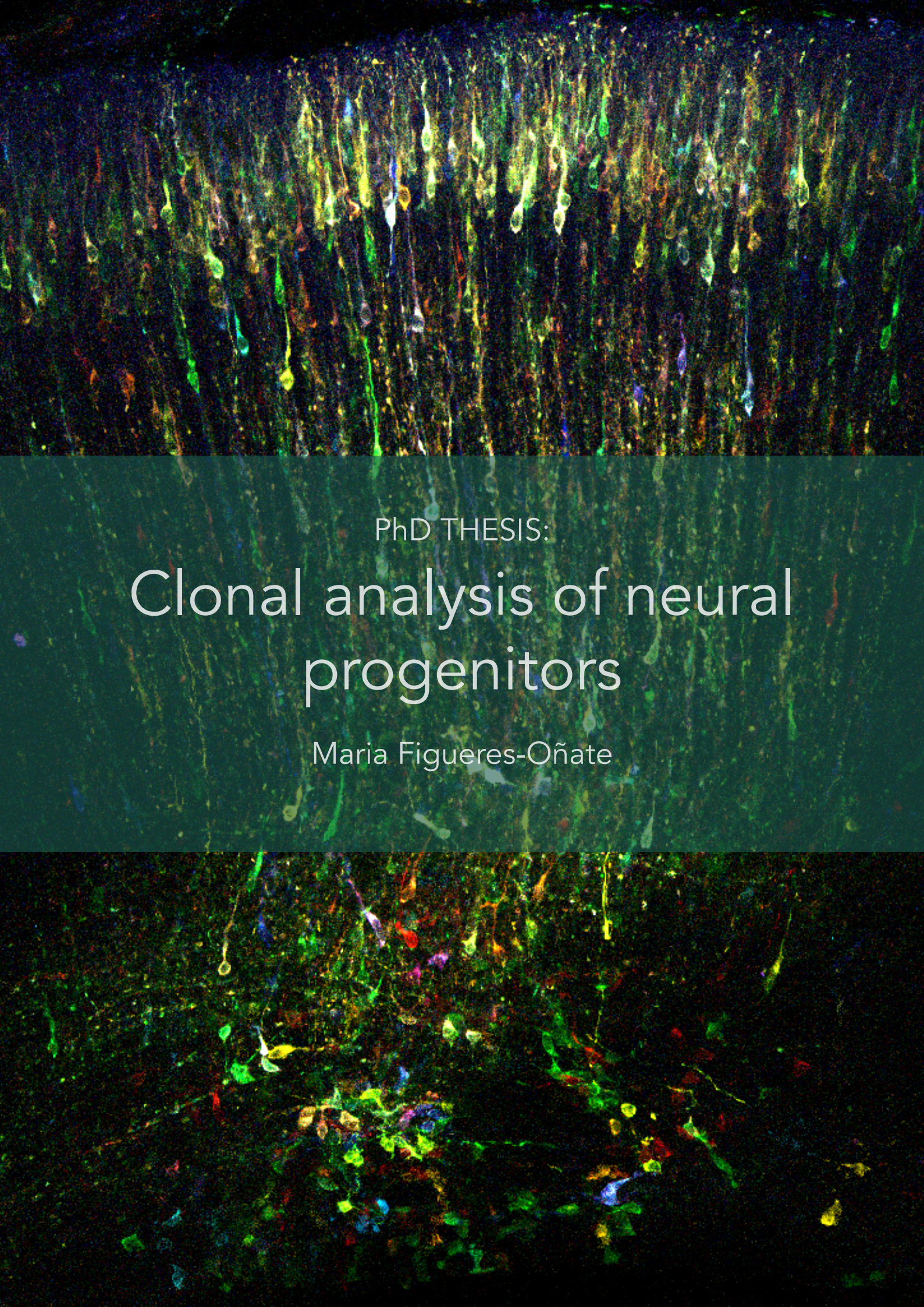

PhD THESIS:

Clonal analysis of neural progenitors

Maria Figueres-Oñate

UNIVERSIDAD AUTÓNOMA DE MADRID

FACULTAD DE MEDICINA

DEPARTAMENTO DE ANATOMÍA, HISTOLOGÍA
Y NEUROCIENCIA

PhD THESIS SUMMARY

CLONAL ANALYSIS OF NEURAL PROGENITORS

Maria Figueres Oñate

Department of Molecular, Cellular and Developmental Neurobiology
Laboratory Olfactive system and its development
Doctoral advisor Laura López Mascaraque
Instituto Cajal
Consejo Superior de Investigaciones Científicas(CSIC)

INSTITUTO CAJAL

CSIC
CONSEJO SUPERIOR DE INVESTIGACIONES CIENTÍFICAS

UAM
UNIVERSIDAD AUTONOMA DE MADRID

INSTITUTO CAJAL
CSIC
CONSEJO SUPERIOR DE INVESTIGACIONES CIENTÍFICAS

MINISTERIO DE ECONOMÍA Y COMPETITIVIDAD

LAURA LOPEZ MASCARAQUE, Científica Titular del Consejo Superior de Investigaciones Científicas

CERTIFICA que el presente trabajo titulado "*Clonal Analysis of Neural Progenitors*", ha sido realizado bajo mi dirección por Dña. María Figueres Oñate, en el Departamento de Neurobiología Molecular, Celular y del Desarrollo del Instituto Cajal (CSIC) de Madrid. Dicho trabajo reúne todos los requisitos científicos y formales para ser defendido como Tesis Doctoral y optar al grado de Doctora con mención Internacional por la Universidad Autónoma de Madrid.

Y para que conste a los efectos oportunos firmo el presente documento en Madrid a uno de Septiembre de 2016.

Dra. Laura López Mascaraque

AVDA. DOCTOR ARCE, 37
28002 - MADRID, ESPAÑA
TEL.: 91 585 47 50
FAX: 91 585 47 54
http://www.cajal.csic.es

But how I was astonished, as I looked at a white wall through the prism, that it stayed white! That only where it came upon some darkened area, it showed some colour, then at last, around the window sill all the colours shone... It didn't take long before I knew here was something significant about colour to be brought forth, and I spoke as through an instinct out loud, that the Newtonian teachings were false.

Goethe

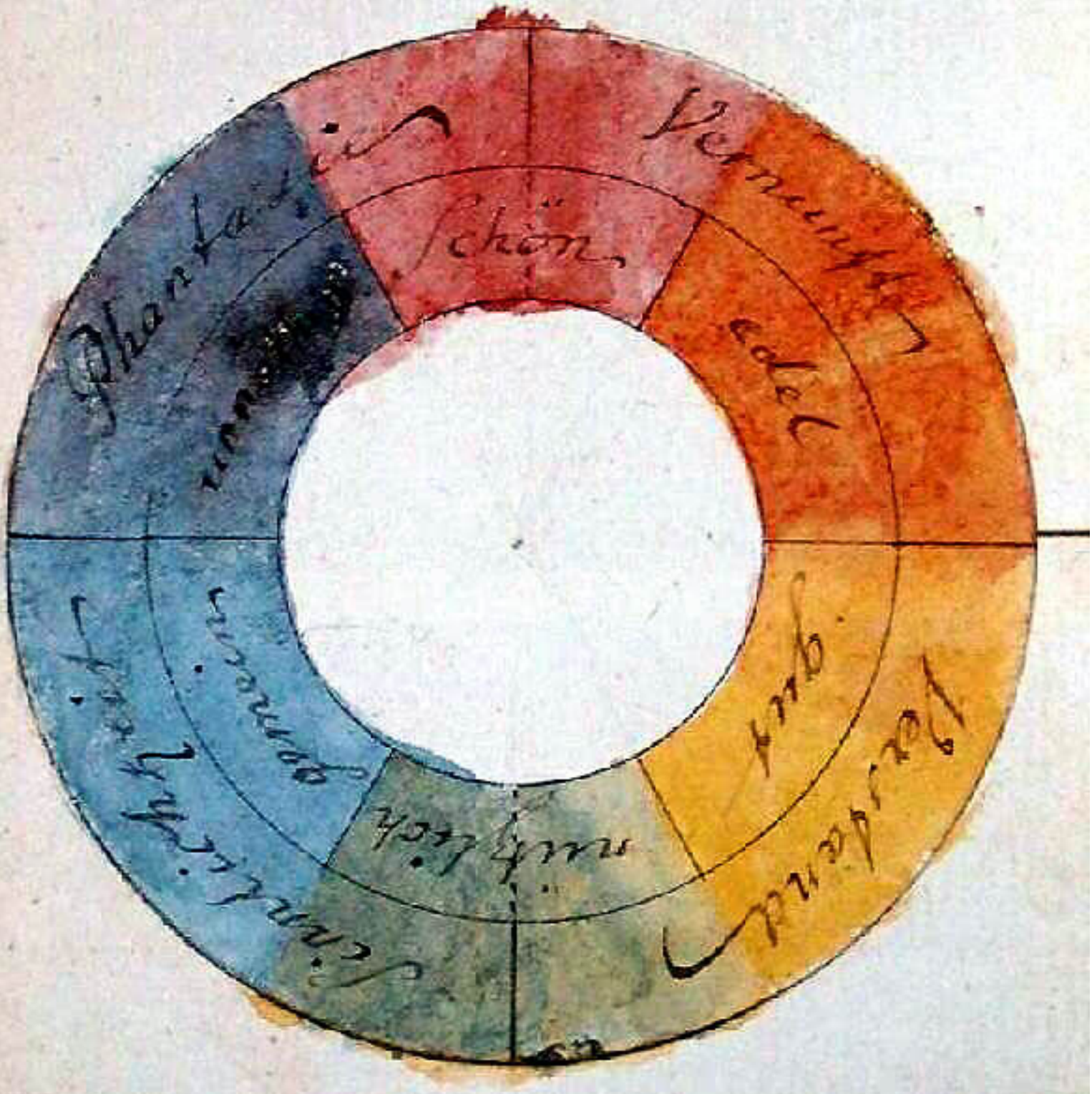

Goethe's symmetric colour wheel with associated symbolic qualities (1809)

Agradecimientos

Es en estos momentos, cuando echas la vista atrás y empiezas a hacer memoria de toda la gente que te ha ido acompañando en cada etapa de la que ha consistido esta tesis, cuando te das cuenta de como pasa el tiempo y todo lo que hemos ido caminando pasito a pasito, lo que se ha aprendido tanto personal como científicamente, lo que hemos crecido Porque todo el periodo que conlleva la realización de una tesis doctoral es una experiencia vital única, porque creces con ella, aprendes muchísimo tanto en el ámbito laboral como en el personal.

Y empezando por el principio, gracias a Laura por acogerme en su laboratorio, por su implicación y haberme permitido cosechar mi carrera científica. Gracias a todos y cada uno de los miembros que pasó por el A-21 y a los que siguen hoy en día presentes. Gracias por enseñarme ciencia, curiosidades y compartir nuestras vidas más allá de lo laboral, por haber sentido vuestro apoyo en muchas de las situaciones más complicadas. También mil gracias al Cajal y a sus gentes por esos viernes siempre con cañas, por compartir tantas risas, complicidades, agobios, sonrisas y buenos días.

Gracias a Spotify, por Brain food, Deep focus, concentración indie-rock… por ser la banda sonora de esta tesis.

Gracias a todos mis amigos "extracientíficos" por escuchar atentamente durante horas historias sobre células de colores y progenitores neurales, por poner interés en lo que hago y por apoyarme siempre.

Gracias a mi familia, a mis padres, los cuales me demuestran y enseñan día a día que el amor incondicional, desinteresado y absoluto existe y que ellos son los más especialistas en proporcionármelo en todo momento. Gracias por haberme inculcado todo lo que soy. No podría tener unos padres de los que estar más orgullosa.

Gracias a Juanma por regalarme cada día su paciencia, complicidad, apoyo y amor, que buena parte son los cimientos de esta tesis.

Gracias de corazón a todo el mundo que ha compartido su tiempo conmigo y ha hecho posible de algún modo u otro que hoy me encuentre escribiendo los agradecimientos de mi tesis doctoral.

Infinitas gracias.

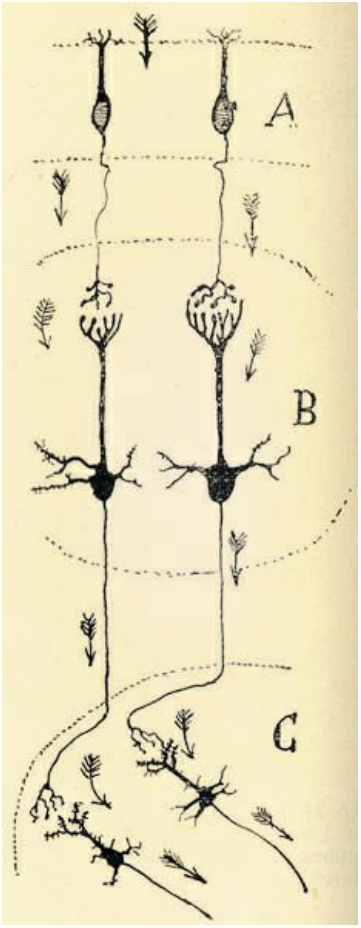

Esquema destinado a mostrar la dirección de la onda nerviosa en la mucosa y centros olfativos. — A, mucosa olfativa; B, bulbo olfatorio del cerebro; C, lóbulo esfenoidal del cerebro, donde acaban las vías nacidas del bulbo.

¿Cuál es la dirección del impulso nervioso dentro de la neurona? ¿Propágase como el sonido o como la luz en todas direcciones, o marcha constantemente en un solo sentido a la manera del agua de la aceña?

Santiago Ramón y Cajal.
Recuerdos de mi vida.
Historia de mi labor científica (1917)
Capitulo VIII.

Abbreviations

APC Adenomatous Polyposis Coli

BrdU 5-bromo-2′-deoxyuridine

CB Calbindin

cc Corpus callosum

CNPase 2′,3′-Cyclic-nucleotide 3′phosphodiesterase

CR Calretinin

Cre^{ERT2} Inducible Cre-recombinase enzyme

CSF Cerebrospinal fluid

Ctx Cerebral cortex

DCX Doublecortin

DDC DOPA decarboxylase

DNA Deoxyribonucleic acid

EGFP Enhanced green fluorescent protein

EPL External plexiform layer

GABA gamma-Aminobutyric acid

GAD67 Glutamate decarboxylase 67

GcL Granular cell Layer

GFAP Glial fibrillary acidic protein

GL Glomerular layer

hyPBase hyperactive transposase of the piggyBac system

IPC Intermediate Progenitor cell

IPL internal plexiform layer

LGE Lateral ganglionic eminence

LOT Lateral olfactory tract

MBP Myelin Basic Protein antibody

mCerulean monomeric Cerulean fluorescent protein

mCherry monomeric cherry fluorescent protein

MCL Mitral cell layer

MGE Medial ganglionic eminence

mKO monomeric Kusabira Orange fluorescent protein

mT-Sapphire monomeric Turbo shapphire fluorescent protein

NB Neuroblast

NEC Neuroepithelial cell

NeuN Neuronal Nuclei

NG2 Neural/glial antigen 2

NPC Neural progenitor cell

NSC Neural Stem cell

OB Olfactory Bulb

OE Olfactory epithelium

OEC Olfactory ensheathing cells

Olig2 Oligodentrocyte transcription factor 2

ONL Olfactory neurons layer

OSN Olfactory sensory neuron

PCD Programed cell death

PDGFRα Alpha-type platelet-derived growth factor receptor.

PV Parvalbumin

Reel Reelin

RGC Radial glial cell

RMS Rostral migratory stream

S100β S100 calcium binding protein □

SEZ Subependimal Zone

SOM Somatostatin

SVZ Subventricular Zone

TAP Transit-amplifying progenitor

Tbr1 T-box, brain, 1

Tbr2 T-box, brain, 2

TH Tyrosine hydroxylase

UbC UbiqutinC promoter

VZ ventricular zone

YFP Yellow fluorescent protein

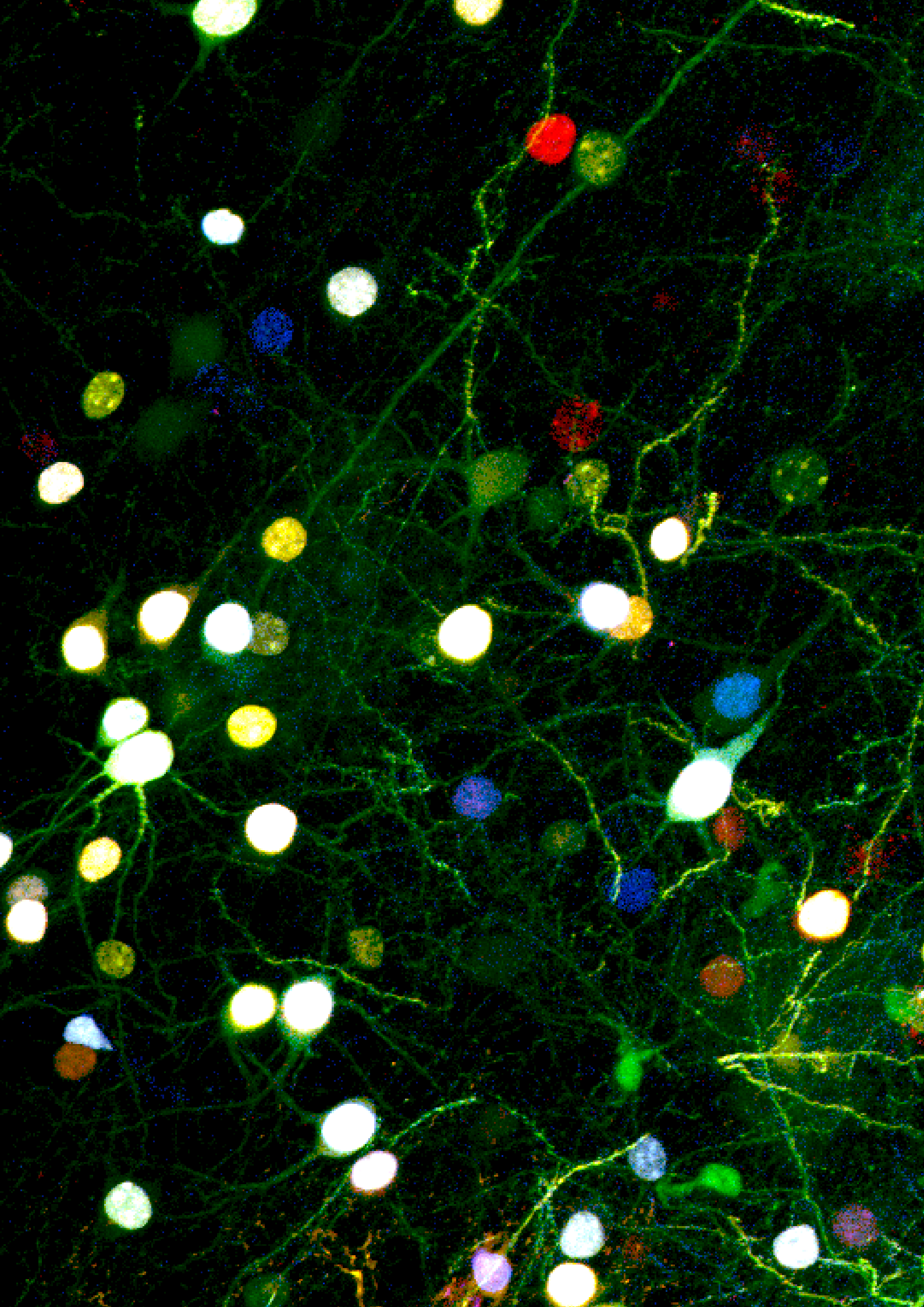

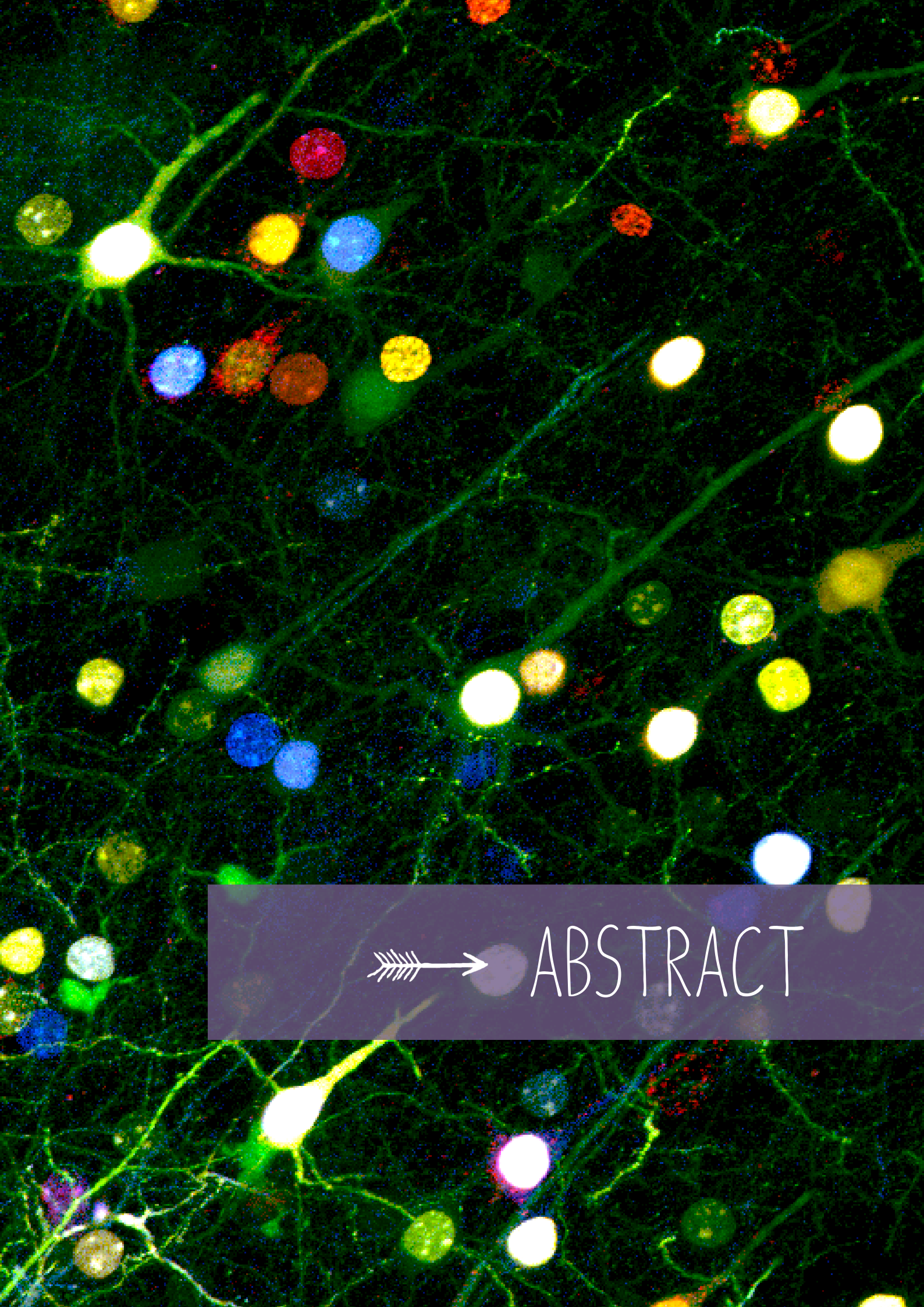

ABSTRACT

A key question in developmental neurobiology is how a pool of progenitors proliferates and differentiates to create an adult brain of appropriate size and cellular composition. So important is the control of the final size, as the appropriate distribution of cells with different embryonic origins. Each neural progenitor should produce a certain number of neuronal/glial cells encompassing a clone, and all these clones together will result in the adult functional nervous system.

The overall goal of this thesis was aimed to develop an in vivo lineage-tracing genetic method to trace all the neural progeny derived from a single cell, UbC-StarTrack. This will allow to follow cell dispersion of the progeny from embryonic and postnatal mice neural progenitors, independently of their lineage. To validate the method we selected as an experimental system the olfactory bulb, since it is one of the main regions of embryonic and adult neurogenesis. Then, the main experimental approach was based on gene transfection by electroporation with a combination of diverse fluorescent reporter proteins. This produced inheritable marks that enabled the long-term in vivo tracing of the different neural cells from its generation, during embryonic development, to its final fate in the adult brain. First, we analyzed the fate of embryonic progenitors lining either the ventricular surface or the ependymal layer of the olfactory bulbs. Second, we addressed the fate of postnatal progenitors form the dorso-lateral region of the ventricular surface, to finally perform a clonal analysis of newly generated olfactory bulb cells from those postnatal SVZ progenitors.

This thesis will advance the understanding of cell heterogeneity that can be decoded by studying their ontogenetic origin, and could yield to track cell lineages to understand their functional clonal relationships.

Una de las preguntas más importantes en Neurobiología del Desarrollo es como un grupo de progenitores prolifera y se diferencia para crear un cerebro con el tamaño y composición celular adecuado. Tan importante es el control del tamaño final, como la correcta distribución de células con distinto origen embrionario. Cada progenitor debe generar un determinado numero de células gliales/neuronales y estos clones resultarán en el sistema nervioso central adulto funcional.

El objetivo general del trabajo presentado en esta Tesis Doctoral fue generar un método de análisis clonal ubicuo con el propósito de trazar toda la progenie de células individuales, seguir clones pertenecientes a distintos linajes neurales provenientes de progenitores tanto embrionarios como postnatales. El método desarrollado se basa en la identificación de células hermanas mediante el análisis del especifico código de colores que expresan, generado por la combinación aleatoria de distintos reporteros fluorescentes en las células progenitoras y transmitido de manera equitativa a toda la descendencia. Los estudios de análisis clonal de los distintos linajes neurales se han centrado en el sistema olfativo del ratón, ya que es uno de los centros donde tiene lugar la neurogénesis tanto en estadios embrionarios como postnatales. El principal enfoque experimental llevado a cabo, se basa en la transfección mediante electroporación de distintos constructos genómicos que expresan proteínas fluorescentes diferentes bajo un promotor ubicuo. Esto produce marcas estables hereditables que permiten el marcaje in vivo a largo plazo de células neurales desde su generación en el desarrollo embrionario hasta su destino final en el cerebro adulto.

El presente trabajo de tesis contiene los detalles de la generación de un método ubicuo de análisis clonal al que hemos denominado UbC-StarTrack, en primer lugar haciendo una comparativa de la expresión de vectores integrados en el genoma vs. vectores que permanecen sin integrar. En segundo lugar, hemos analizado la descendencia de progenitores embrionarios, posicionados en la superficie del ventrículo lateral o de la zona ependimaria intrabulbar, que convergen en el bulbo olfativo adulto. Seguidamente, examinamos el destino de progenitores postnatales localizados en la región dorso-lateral adyacente a los ventrículos laterales. Para concluir, mostramos los resultados clonales preliminares obtenidos con el método de análisis clonal desarrollado en las células generadas a partir de progenitores postnatales, implicadas en la neurogénesis en adulto que tiene lugar en el sistema olfativo del ratón.

Con todo esto, este trabajo de Tesis Doctoral exhibe un avance en el conocimiento de la heterogeneidad celular, siendo ésta decodificada a través de su ontogenia. Además, abre un nuevo campo al estudio de los distintos tipos celulares no sólo por su linaje sino por su relación clonal, haciendo posible el análisis de la interrelación entre los clones obtenidos y sus implicaciones fisiológicas.

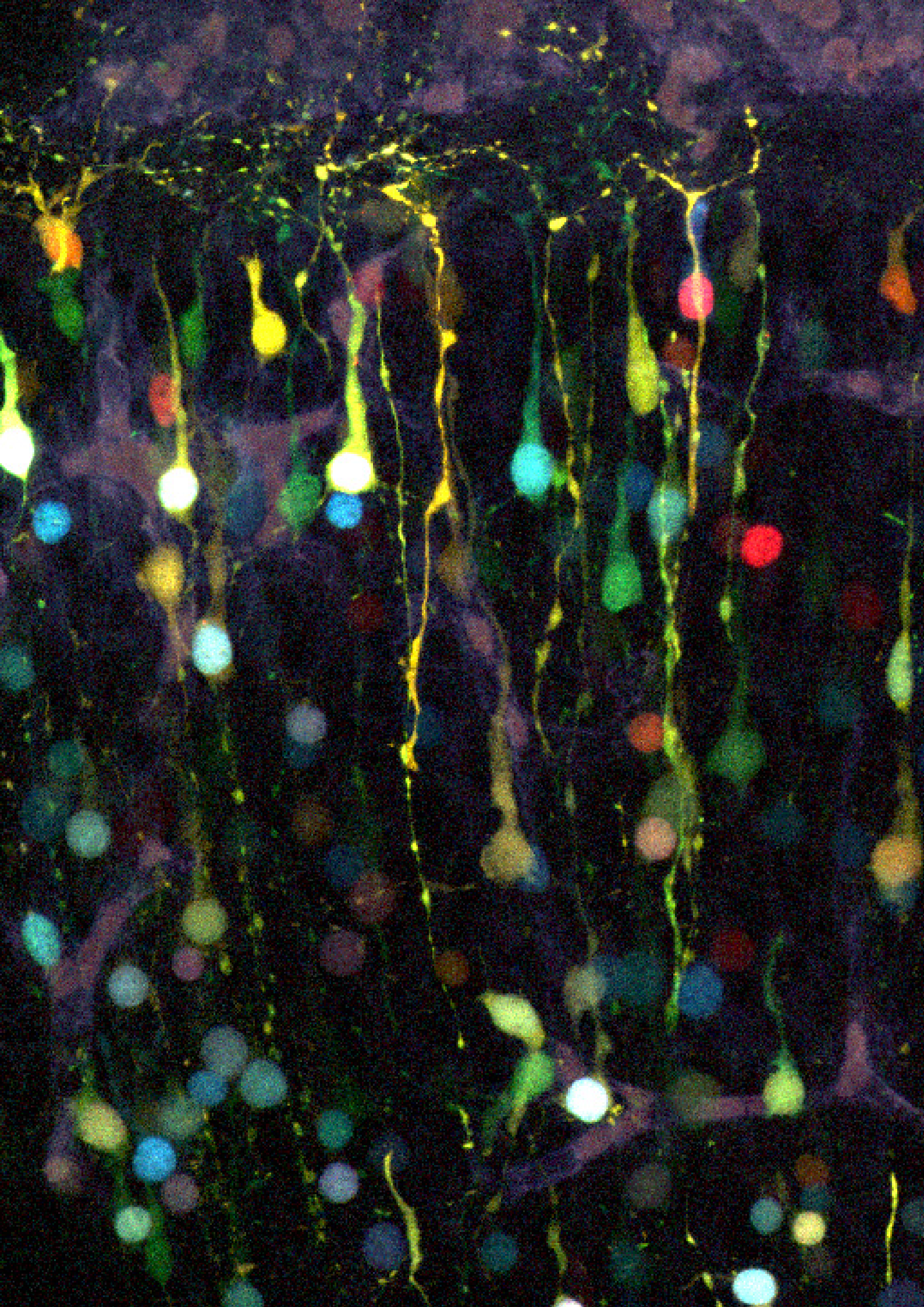

INTRODUCTION

Neural Stem cells

Neural stem cells (NSCs) are defined as cells that have the capability to self-renewal and to produce all the lineages present in the adult brain (Gage, 2000). Thus, cell diversity in the brain emerges as a result of NSCs specification progression into restricted neural progenitor cells (NPCs). Thus, NPCs have a limited fate, exhibiting reduced potential of differentiation and proliferation (Temple, 2001). Major cell types of mammalian brain, neurons, astrocytes, oligodendrocytes and NG2 cells, derived from progenitors that originally arise from the neural plate (neuroectoderm) in the early embryo. In parallel, other cell types with distinct origins colonize the brain at early embryonic stages, as microglia (mesoderm) and blood vessels (endoderm). In the developing brain, neuroepithelial cells (NECs) divide rapidly and symmetrically to give rise to radial glial cells (RGCs). The main difference between RGCs and NECs is that NECs form a pseudostratificated layer while RGCs are presented in a multilayered scenario. RGCs produce all major cell types (lineages) of the brain, and are often referred as NSCs of the developing brain (Guo et al., 2013). Thus RGCs can either symmetrically proliferate to maintain the pool of stem progenitors, or asymmetrically divide to generate transit-amplifying progenitors (TAPs) or neurons and glial cells (Götz & Huttner, 2005). Regarding to the inner-out pattern, lower-layers cortical neurons are the first to be generated while neurons from later developmental stages are situated above (Figure. 1). Later on, RGCs produce glial cells through intermediate progenitors or astrocytes by direct transformation. Throughout

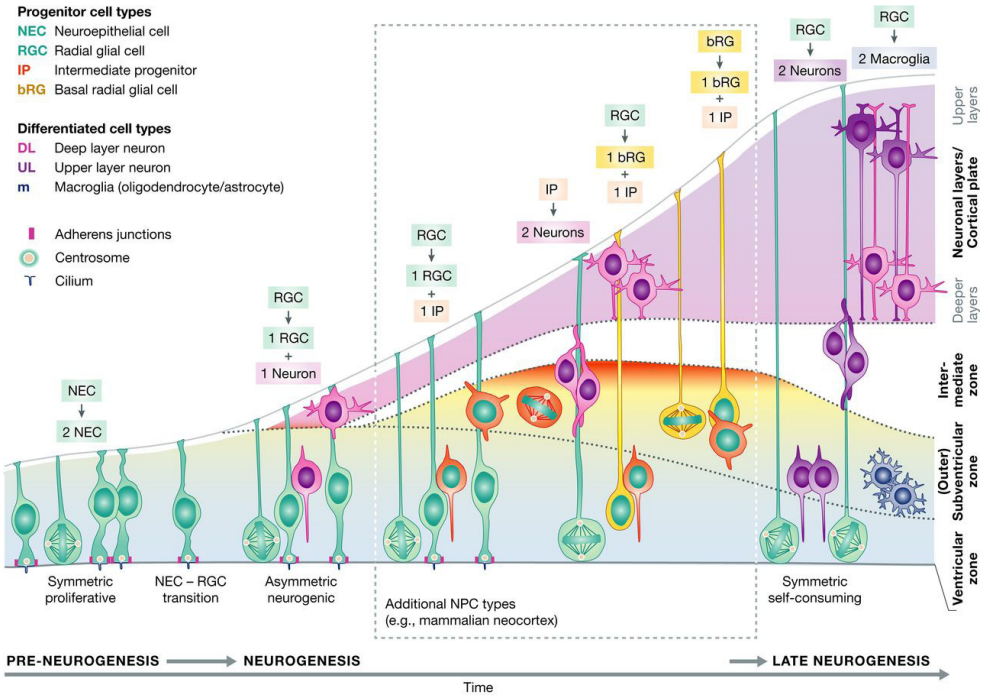

Figure 1. Overview of neurogenesis and gliogenesis in the embryonic brain. Cell progression from embryonic to postnatal stages is shown from left to right. Principal types of NSCs and NPCs and their progeny are specified by different colors. Self-renewal, symmetric or asymmetric divisions or cell differentiation are included in the scheme. Self-renewing neuroepithelial cells lining the ventricles are transformed into radial glial cells. Radial glia cells generate some neurons through asymmetric divisions as well as intermediate progenitors committed to neuronal or glial lineages. Abbreviations are specified in the box. (Paridaen & Huttner, 2014).

development, cell lineage progression starts with neurogenesis, followed by astrogenesis and finally oligodendrogenesis which continues thought perinatal stages (see Kriegstein &

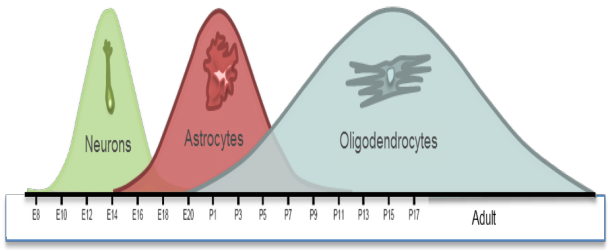

Figure 2. Developmental sequence of neuronal and glial lineages. The specification of the different neuronal and glial lineages takes places in overlapping temporal waves. In rodents, neurogenesis peaks at embryonic day 14, while astrogenesis and oligodendrogenesis do at perinatal stages. The generation of interneurons starts during embryonic life and continues postnatally restricted to the olfactory bulb and the dentate gyrus. Adapted from (Wang & Bordey, 2008).

Alvarez-Buylla, 2009 for review) (Figure. 2). This whole process of lineage specification and ultimately the loss of progenitor potential are regulated by intrinsic changes in gene expression, but it is also determined by the interaction with environmental and developmental cues. Further, the switch from neurogenesis to gliogenesis is determined by a competition between downstream transcription factors and growth factors signaling pathways (Sauvageot & Stiles, 2002; Martynoga et al., 2012;). Different patterning genes generated boundaries that determine the identity and fate of the neural progenitors grouped into diverse domains lining the ventricular surface (Rowitch & Kriegstein, 2010). RGCs are considered the major progenitor cell type throughout the central nervous system (Malatesta et al., 2003; Kriegstein & Noctor, 2004). However, new subtypes of NPCs populated subventricular surface (SVZ), as apical or basal RGCs or apical and subapical intermediate progenitors (IPCs) (for review see De Juan Romero & Borrell, 2015). This neural progenitor diversity goes further in the case of neuronal lineages, even considering the presence of different precursors comprised either with upper- or lower-layers cortical neurons (Franco & Müller, 2013). In addition, RGCs form a miscellaneous cell population within and across specific brain regions, displaying a region-specific gene expression that suggest a specific role in a regionalization of the developing nervous system (Kriegstein & Götz, 2003). Nowadays, this neurogenic pool of progenitors is considered as a heterogeneous cell population, encompassing multiple progenitors types, either with stem cell properties or more restricted capabilities (Franco & Müller, 2013). Different possibilities included multi-potential precursors/progenitors (named NSCs with the capability to give rise to all brain lineages), bi-potential precursors/progenitors (capable of generate two lineages) or committed progenitors, capable to produce one neural cell type (Figure. 3). This

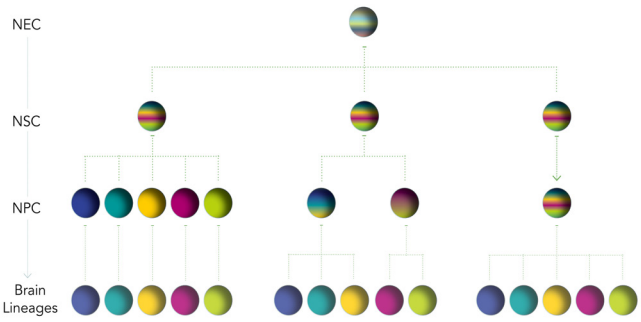

Figure 3. Lineage progression and progenitor commitment. Through embryonic development progenitors acquire sequential committed stages. Pluripotent neuroepithelial cells (NECs) self-renewal to generate neural stem cells (NSCs). Then, different progenitors types give rise to all adult brain lineages. Multipotent, pluripotent, bi-potent or committed neural progenitors (NPCs), with diverse lineage potentials cohabit the subventricular surface.

regional identity of specific neuronal progenitors has been also described for glial lineages, in which progenitors undelaying different domains produce glial cells restricted to a specific region (Bayraktar et al., 2015; Garcia-Marques and Lopez-Mascaraque, 2016). Taken together, the key role of development determining adult neural heterogeneity is starting to be pointed.

Olfactory system

The olfactory system is an excellent model for understanding general principles about how the brain processes information and also for elucidating the formation of neural circuits. Moreover, it is one of the two main pathways where neurogenesis appear in adulthood, it is a consistent system for understanding the basic principles of neuroscience. The incorporation of new cellular elements to the olfactory bulb (OB) occurs during development and even during adulthood (Altman, 1966, 1969; Mackay-Sim and Kittel, 1991; Luskin, 1993; Lois and Alvarez-Buylla, 1994). This plastic process is the result of the combination of cellular contributions from both the telencephalic subventricular zone and the olfactory placode/epithelium (De Carlos et al., 1995; Blanchart et al., 2011), where olfactory sensory neurons (OSNs) undergo continuous lifelong turnover. Analysis of the olfactory system and its cellular components provide important insights into neural mechanisms.

In mammals, olfaction starts in the nose, where inhaled odorant molecules contact with the main olfactory epithelium (OE) within the nasal cavity (Figure. 4A). The OE is a pseudostratified neuroepithelium comprised by supporting or sustentacular cells, two population of basal cells (horizontal and globose basal cells) in addition to mature and immature OSNs. OSNs are bipolar cells with dendrites extending into the nasal cavity and axons projecting into the brain. Each OSN has a single dendritic process

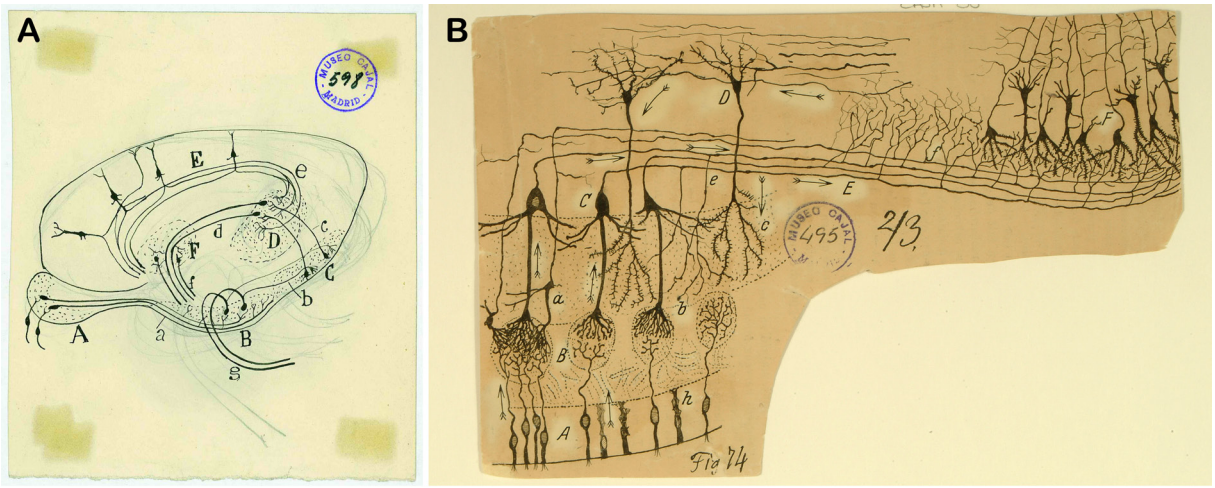

Figure 4. Olfactory circuit through Cajal's view. A. Reproduction of an original Cajal cartoon of the olfactory system (published in Figueres-Oñate et al., 2014, Cajal Legacy, Instituto Cajal, CSIC,Madrid, Spain). **B.** Cajal's diagram outlining the circuitry and the trajectory of the nerve impulse (arrows). (A) Bipolar cells of the olfactory mucosa. (B) Olfactory glomeruli. (C) Mitral cells. (D) Grains. (E) External root (lateral olfactory tract). (F) Olfactory cortex. (a) Small tufted cell; (b) main dendrite of a mitral cell; (c) terminal dendritic tuft of a granule cell; (e) recurrent dendritic collaterals of a mitral cell; (g) surface triangular cells of the olfactory cortex; (h) epithelial cells of the nasal mucosa (Ramón y Cajal, 1894).

with several olfactory cilia branched into the mucus lining the nasal cavity, thus make them the unique neurons in the organism that are in direct contact with the environment. At the other bipolar end, the OSN has unbranched axon that projects to the OB, structure in the forebrain that serves as the first relay of olfactory information, located in the mice at the most rostral/apical part of the telencephalon. Thus, these neurons are the first participants in the olfactory pathway, expressing in their membranes particular receptors to recognize different olfactory stimuli. In mice, there are about five million OSNs, and each OSN typically expresses only one of the approximately 1300 olfactory receptor genes (Zhang & Firestein, 2002), the largest gene family in the entire mammalian genome. These chemosensory receptors are proteins with seven transmembrane domains coupled with G-proteins that bind the odorants. The OSNs expressing the same olfactory receptor gene are randomly distributed within the nasal cavity, but their axons selectively converge to only 1–4 of the 1600–1800 OB glomeruli. Nevertheless, an odor is the result of the combination of numerous molecules recognized by different receptors (for review see Mombaerts et al., 1996).

Then, an olfactory stimulus begins with the activation of OSN when an odorant binds to its specific receptor. OSNs are the responsible to transduce chemical information into electric signals. Olfactory information impulse reaches the brain precisely in discrete spherical structures called glomeruli which cover the entire OB to contact dendrites of the OB projection neurons: mitral/tufted cells. Axons of mitral/tufted cells project their axons to the olfactory cortex forming the lateral olfactory tract (LOT). The olfactory cortex is a phylogenetically old cortical structure compound by three layers. The direct axonal input from mitral and some tufted cells into the olfactory cortex, makes this system as the unique sensory pathway without a thalamic relay (for review see López-Mascaraque & de Castro, 2002; 2016) (Figure. 4B). However, although much is known about how odors are represented at the level of olfactory bulb, the nature of odor representations in the piriform cortex is still poorly understood (for review see Bekkers and Suzuki, 2013).

Altogether, just with two synapses of mitral/tufted cells, either in the piriform cortex or other olfactory nucleus, olfactory information is processed. Among other several areas, olfactory cortex includes the olfactory tubercle, piriform cortex, amygdala, and entorhinal cortex. The olfactory information is then further transmitted to the thalamus, hypothalamus or hippocampus. Thus, olfaction is the unique sensory information that arise to the cortex prior to thalamic processing.

Olfactory bulb cytoarchitecture

The OB has a well-defined laminar structure and it is formed by projection neurons (mitral cells and some tufted cells), interneurons (periglomerular cells, external tufted cells, short axon cells, granule cells, Van Gehuchten cells and Blanes cells) and glial cells (astrocytes, oligodendrocytes, olfactory ensheathing cells, NG2 and microglia). Those cells are distributed into the following OB layers (B): the olfactory nerve layer (ONL), glomerular layer (GL), the

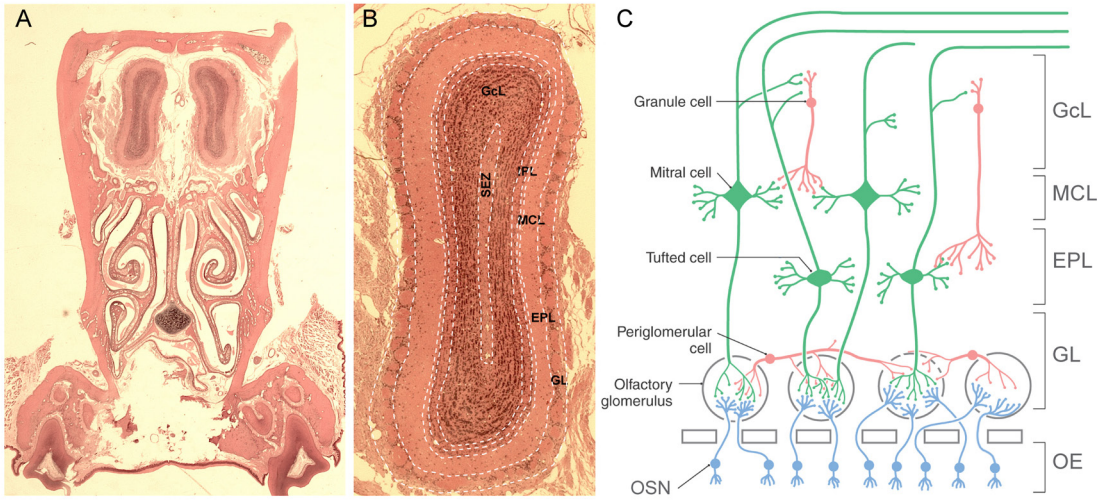

Figure 5. Layers and cell distribution in the Olfactory bulb. A-B. Representative images of hematoxylin-eosin stained adult coronal olfactory bulbs and epithelium (A) and olfactory bulb layers (B). From outside to inside: GL, Glomerular layer; EPL, External plexiform layer; MCL, Mitral cells layer; IPL, Inner plexiform layer; GcL, Grains and white matter layer; SEZ, Subependimal zone. **C.** Schematic drawing of the olfactory bulb, showing the laminar organization and the major cell types: Olfactory sensory neurons (ONL) are shown in blue, projection neurons in green and interneurons in red. Modified from Simpson&Sweazey, 2015.

external plexiform layer (EPL), the mitral cell layer (MCL), the internal plexiform layer (IPL) and the granule cell layer (GcL). The innermost part of the olfactory bulb, the subependymal zone (SEZ). Regarding to cell types colonizing each layer (Figure 5C), SEZ contains progenitor cells. The ONL is formed by the unbranched axons from the OSNs. This layer also contains an interesting population exclusively restricted to the olfactory system, the olfactory ensheathing cells (OEC, Valverde & López-Mascaraque, 1991) that ensheath hundreds of axons. Next stratum is the GL, formed by olfactory glomeruli, where OSNs transmit sensory information to mitral and tufted cells. Those glomeruli are surrounded by local juxtaglomerular neurons where periglomerular cells form the largest population in addition to external tufted cells. Below the glomeruli, the EPL is formed by middle tufted cells and inhibitory interneurons known as Van Gehuchten cells along with the lateral dendrites of mitral/tufted cells and apical dendritic processes of some superficial granular cells. Next layer is the MCL, composed by mitral cells. Mitral cell bodies form a regular single row and owe their name to their appearance. They are the principal output cells of the OB and are characterized in most mammals by a single apical dendrite that cross the EPL to branch into the glomerulus. Mitral cells are one of the projection neurons, whose entire development terminates at postnatal stages (Blanchart et al., 2006). Within the glomeruli, mitral cells interact and receive inputs from their vicinity through synaptic contacts with different periglomerular and granule cells. Mitral cells are the bridge connecting directly the periphery with higher integrative structures (reviewed in Gire et al., 2013). Below the MCL layer, the IPL is populated by most axon collaterals of mitral/tufted cells, while the GcL contains granule cells and different types of short-axon cells. The granule cells are small ovoid cells extending dendrites apically into the EPL and short secondary dendrites

confined to the GcL. These cells showed no evidence of axons (Golgi, 1875). The different subpopulations of these interneurons have been classified regarding to morphological/ spatial basis, molecular or physiological features (Price and Powell, 1970; Schneider and Macrides, 1978; López-Mascaraque et al., 1986; Crespo et al., 2001; McQuiston and Katz, 2001; Kosaka and Kosaka, 2005). Besides, the two main OB inhibitory interneuron types already described by Cajal have a significant role in the olfactory processing: periglomerular cells mediate lateral inhibition at the level of the glomeruli (Aungst et al., 2003), while granule cells mediate dendrodendritic inhibition onto the lateral collaterals of mitral cells (Isaacson and Strowbridge, 1998; Schoppa et al., 1998).

Neuroglia in the olfactory bulb

While neuronal cell types comprising the OB have been deeply characterized, glial cells have not been included in those analyses. The main types of glial cells as astrocytes, oligodendrocytes or NG2 cells are present in the OB (Figueres-Oñate et al., 2014). Initially, the olfactory astroglia was defined as a syncytium, but recent studies are finally shedding light to a further network specialization (Houades et al., 2008). Moreover, as we refer above, OECs are a specific type of glial cells localized in the ONL. During development, OECs coexist with astrocytes as part of the migratory mass and they maintain certain progenitor characteristics (Murdoch and Roskams, 2008; Blanchart et al., 2011; Blanchart and López-Mascaraque, 2011) Doucette, 1990; Murdoch & Roskams, 2008; Schwarting, Gridley, & Henion, 2007). Those cells among others, are the responsible of the permissibility within the olfactory bulb to OSNs axons growing during development and adulthood, being a key component of the ability of the OE to continually regenerate.

Furthermore, the origin of OB glial cells is still on progress. Fist of all, most studies focused their analysis and further classification of OB glial population on morphological (de Castro, 1920; Valverde & Lopez-Mascaraque, 1991) and immunohistochemical (Bailey & Shipley, 1993; Chiu & Greer, 1996; Emsley & Macklis, 2006; Jimenez et al., 2004) cell characteristics. Astrocytic markers, GFAP and S100, are highly expressed in the OB (Emsley & Macklis, 2006), as well as oligodendroglial markers as Olig2, PDGFR, MBP, CNPase, APC or NG2 (Maria Figueres-Oñate & López-Mascaraque, 2016). It is also important to note the distinct morphological and molecular specificity role of astrocytes throughout the SVZ-RMS-OB pathway (García-Marqués et al., 2010) within the glial populations. Further, astrocytes in the OB do not just play an insulating or supporting role, but they are also an active part of the sensory integration in the olfactory glomeruli, interacting with their neuronal counterparts, in a glomerulus-specific manner (Roux et al., 2011). Moreover, although the ontogeny and heterogeneity those glial cell populations within the OB is starting to be explored (García-Marqués et al., 2014; García-Marqués & López-Mascaraque, 2016), some studies pointed the endogenous source of OB oligodendrocytes (Spassky et al., 2001; Figueres-Oñate & López-Mascaraque, 2016).

Briefly, a better understanding of glial

cells generation from embryonic progenitors and the factors controlling their proliferation, migration, and integration into OB neural circuits is crucial. Moreover, it is also essential to use clonal analysis to further address the intra-bulbar heterogeneity including both neuronal and glial lineages and their physiological implications.

Adult Neurogenesis in the OB

Unlike other brain structures, the OB is not a simple relay nucleus, but a center for information processing and storage. "Once development is over, the growth and regeneration of axons and dendrites are irrevocably dried up. In the adult brains the nervous pathways are fixed, finished, immutable. Everything can die, nothing can regenerate itself. It belongs to the science of the future to change, if possible, this cruel decree" (Ramón y Cajal, 1913). Cajal missed one of the most important characteristics of the olfactory bulb: the cell turnover. However, the idea that new neurons could be generated in adult brains and incorporated in preexistent circuits was unreliable on that time. "Nature has given us a limited amount of brain cells. Here is a capital, large or small, that nobody can increase as the neuron is unable to multiply" (Ramón y Cajal, 1931). Nevertheless, adult neurogenesis is some of the most important brain discoveries of the last century opening new debate about the function and integration of these cells into the established system (Altman, 1962, 1969).

Thus, neurogenesis persists into adulthood in many vertebrates including humans. In addition to the olfactory epithelium the adult mammalian brain contains two major neurogenic niches: the subgranular zone of the hippocampal dentate gyrus and the subventricular zone (SVZ, also named subependimal zone, SEZ) lining the walls of the lateral ventricles. In this work, we focused on the largest germinal niche in the adult mammalian

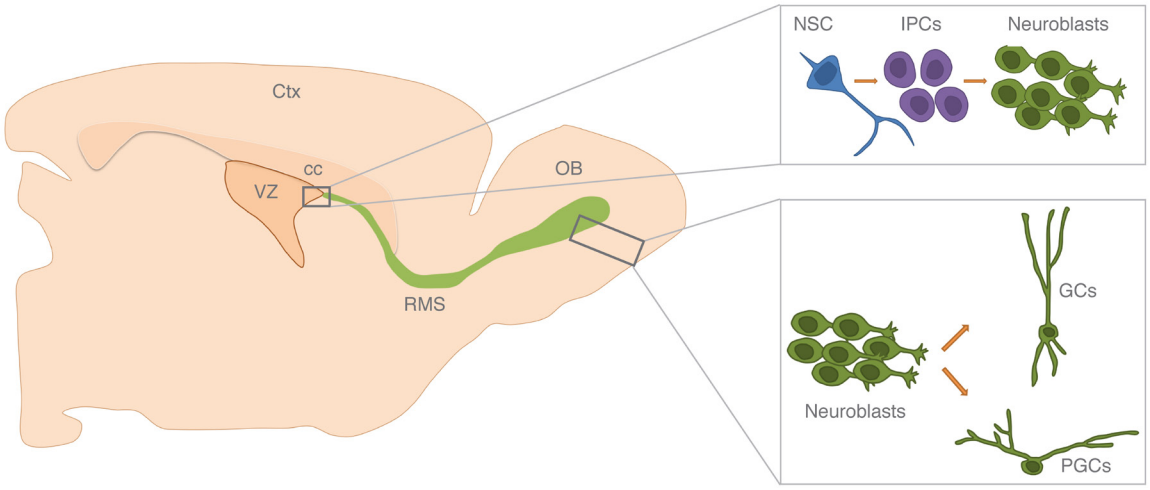

Figure 6. Adult neurogenesis in the Subventricular Zone. Named neural stem cells (NSC) reside in the lateral ventricular zone (VZ) of adult mice, and give rise to neuroblast through transit amplifying progenitors or intermediate progenitors (IPCs). Young neurons travel large distances along the rostral migratory stream (RMS) until reach the olfactory bulb (OB) where they mature and differentiate into granular (GCs) and periglomerular (PGCs) interneurons. *Ctx. Cortex. Cc. Corpus callosum.*

brain, the neurogenic niche surrounding the ventricular surface, where astrocyte-like cells (B cells) divide to produce neuroblasts via intermediate progenitors (Figure 6). These neuroblasts migrate along the rostral migratory stream to the OB, where they differentiate into either granular or periglomerular interneurons (Luskin, 1998; Doetsch et al., 1999; Alvarez-Buylla and Garcia-Verdugo, 2002).

The glial nature of those adult progenitors is evident, suggesting that RGCs directly transform into adult progenitors that persist in the adult SVZ (Merkle et al., 2004). Moreover, some evidences point that adult ventricular progenitors derive from embryonic precursors located in the same region (Kohwi et al., 2007; Fuentealba et al., 2015), although a mixture of NPCs from different areas takes place at perinatal stages in the adult SVZ (Willaime-Morawek et al., 2006; Young et al., 2007). Furthermore, postnatal SVZ progenitors proliferate and give rise to multilineage precursors demonstrated both in vivo (Ganat et al., 2006; Gotz et al., 2007) or in vitro (Laywell et al., 2000). Although some authors report that neurons and glial cells are produced from those multipotent progenitors at adult stages (Ventura & Goldman, 2007), the in vivo generation of different neural lineages from the same progenitor remains unresolved (Dimou & Götz, 2014). In another in vitro approach, Ortega et al (Ortega et al., 2013) suggested that astrocytes and interneurons share common progenitors while the oligodendroglial lineage is independent from those other two. Thus, the stem properties of those adult precursors at physiological conditions still has been partially elucidated and has to be proved.

Adult SVZ Neurogenic niche

The main particularity of the SVZ neurogenic niche is that newly generated cells had to migrate long distances to reach its final position: the olfactory bulb. Those adult progenitors, also named neural stem cells or B1 cells, generate transit-amplifying progenitors (TAPs, or classically C-cells) that divide up to 3 times in the neurogenic niche before to differentiate into neuroblast (NBs) or A cells, comprised to the neuronal lineage (Ponti et al., 2013). Those neuroblasts tangentially migrate to the OB along the rostral migratory stream (RMS). NBs in the RMS retain their ability to proliferate (Smith & Luskin, 1998; Poon et al., 2010), but once they reach to the OB, NBs begin to radially migrate until their final position to be integrated into the preexisting neural olfactory circuit (Belluzzi et al., 2003; Carleton et al., 2003), replacing granular and periglomerular cells in the OB (Imayoshi et al., 2008). This radial migration is mediated by different signals as ephrins, neural cell adhesion molecule (NCAM) or reelin (Lledo & Saghatelyan, 2005). Young neurons are positioned either within the GcL or/ and the GL where they completely differentiate. Following arrival and maturation in the OB, almost 50% of newborn neurons are eliminated from the bulbar circuit within 45 days from birth, in an activity dependent manner (Petreanu & Alvarez-Buylla, 2002). During the maturation process, odor input is essential to achieve the correct integration within established olfactory pathway (Ma, Kim, Ming, & Song, 2009). Moreover, adult neurogenesis is narrowly

associated to odorant inputs (Bonzano et al., 2016). Thus, an exposure to an enriched odor increases de number of new born olfactory neurons, improving odor memory (Rochefort et al., 2002). Odor discrimination learning likewise increase the number of new neurons generation (Alonso et al., 2006). Besides, the survival of neuroblast which are going to be integrated into preexisting circuits, its also mediated by the odorant exposure (Yamaguchi & Mori, 2005). Moreover, the dynamic neurogenic process in adult mice is highly regulated by multiple factors closely interrelated in all their proliferation steps: cell cycle, differentiation, migration, and programmed cell death. Besides, programed cell death is the last step in controlling adult neurogenesis. Indeed, the half of NPCs and new neurons undergo cell death to remove unessential cells in all the neurogenic processes. Programed cell death occurs either in the neurogenic niche, in migrating neuroblast (Kim et al., 2007) or in maturation of new neurons. Interestingly, persisting neurons survive up to 1 year (Winner et al., 2002). However, it is really difficult to determine programed cell death implication in physiological neurogenesis in vivo (reviewed by Ryu et al., 2016).

The particular attributes of the neurogenic niche enable a balance of quiescent and active precursors in those micro-domains. Indeed, the particular dispositions of adult neural progenitors facilitate the comprehensive regulation of the neurogenic niche (Figure 7). The balance between quiescent and active adult progenitors is highly regulated by cerebrospinal fluid (CSF), which flows in the ventricular cavity, and it is in close contact with ependymal cells

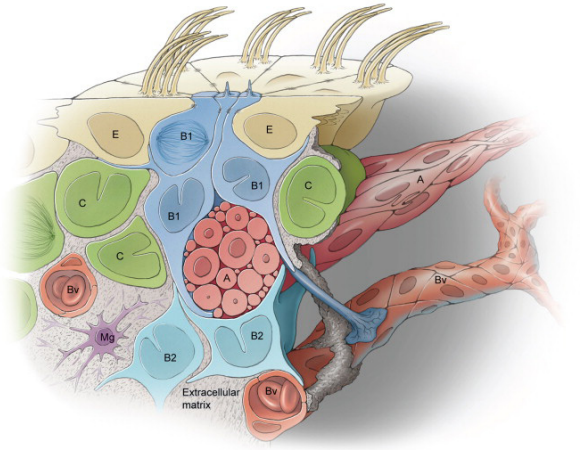

Figure 7. Cytoarchitecture of the adult neurogenic niche. Adult neural progenitors (also type B1 cells, in blue) display an apical primary cilium in contact with the ventricular cavity and the cerebrospinal fluid flow. Multiciliated ependymal cells (E, in beige) form pinwheel-like structures around the apical processes of type B1cells. These cells extend a basal process that contacts blood vessels (Bv, shown in brown). Cells with astrocytic characteristics but do not contact the ventricle are part of the niche (B2, in lighter blue). Transit-amplifying type C cells (in green) are found close to NPCs cells or in adjacent to blood vessels. Chains of migrating neuroblasts (A, in red) are also in close contact to their progenitors. From Ihrie & Álvarez-Buylla, 2011.

and NPCs apical processes. Ependymal cells surround those adult progenitors in peculiar conformations named pinwheels in which several Ecells surround NPCs apical processes (Mirzadeh et al., 2008). Moreover, this apical membrane, in contact with the CSF, may be involved in symmetrical division of radial glial cells (Kosodo et al., 2004). Additionally, since the basal processes of NPCs are in close contact with blood vessels, perivascular signals are involved in the instruction of cell genesis and fate in the adult brain (Goldman & Chen, 2011). All together, CSF and vasculature signals are closely correlated with cell proliferation or quiescence (Porlan et al., 2013).

Moreover, in addition to NPCs other GFAP cells with no stem properties populate the ventricular niche playing important roles in the

neurogenic process (for review see Gengatharan et al., 2016). Calcium signaling between those astrocytes from the niche seems to be important to maintain the neural progenitor cells niche (Lacar et al., 2011). Further, GABA signaling also modulates the activity of NPC in the SVZ, although it is released by neuroblasts as a feedback mechanism to control NPC proliferation (Liu et al., 2005). On the other hand, migratory chains are coated by astrocytes, with different properties from those of other cortical locations, which facilitate NBs movement to the OB (García-Marqués et al., 2010). In addition, these particular characteristics of astrocytes evolving neuroblasts in the RMS have been also reported in other glial lineages, as microglia. Is has been addressed that the microglia of the SVZ and the RMS had a particular phenotype that supports NBs migration (Ribeiro Xavier et al., 2015). The functional implication of those glial cells surrounding the RMS can go much further since it has being demonstrated that in the hippocampus astrocytes communicate with far neurons modulating the properties of newly generated interneurons (Rouach, 2009).

Remarkably, the proliferative capacity of NPCs decreases with age. First evidences are morphological changes in the cytoarchitecture of the ventricular niche, leading the main proliferative capability to the dorso-lateral ventricular surface (Conover & Shook, 2011) and a disruption of the SVZ-RMS axis (Mobley et al., 2013). Moreover, aging subventricular zone decreases its proliferative activity around a 70%, addressing some NSC niche consuming (Capilla-Gonzalez et al., 2015). There is an evident reduction in the population of NBs and TAPs (Luo et al., 2006), as well as in the NPCs population (Ahlenius et al., 2009). Besides, some evidences report a deregulation of NPCs cell cycle machinery in 6-months young adults (Daynac et al., 2016).

Adult neurogenesis in other brain niches

The presence of NSCs and neurogenesis in the adult mammalian central nervous system changed the view of the plasticity and function of the brain. Even in almost all mammals new neurons are generated in the olfactory system and in the hippocampus, the situation in the human brain varies (Figure 8) (Magnusson & Frisén, 2016). We know that around 700 hundred of neurons are daily generated in the adult hippocampus of humans (Spalding et al., 2013), being this neurogenesis much more prominent than in rodents. Nevertheless, SVZ/RMS appears to not be a source of newborn neurons to the human OB throughout adulthood (Sanai et al., 2004, 2007, 2011; Curtis et al., 2007; Whitman and Greer, 2009; Bergmann et al., 2012). Conversely, there are other niches in the human brain, as the striatum (Ernst et al., 2014), 3er ventricle (Cheng, 2013; Rojczyk-Gołebiewska et al., 2014), cerebellum and thalamus (Ryu et al., 2016) where cell turnover occurs throughout adult live. Further, in both temporal/frontal cortex and amygdala from patients undergoing brain resection due to epilepsy, trauma, or dysplasia have been isolated multipotent progenitors (Arsenijevic et al., 2001). Back to rodents, some studies reported newly incorporation of neurons in non-neurogenic niches using BrdU/DCX immunolabelling (Shapiro et al., 2009).

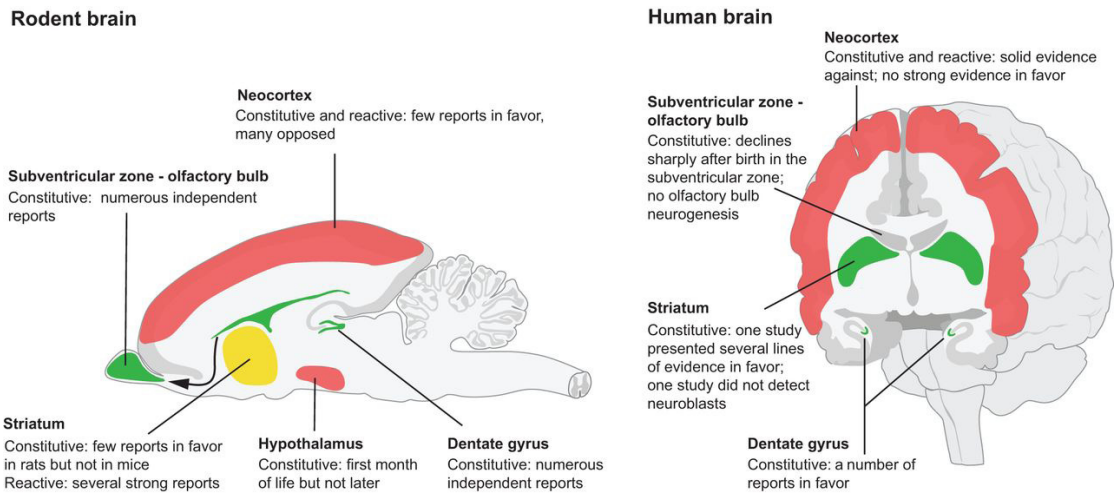

Figure 8. Adult neurogenesis in different regions of the adult rodent and human brains. The neurogenic capability in mice (left) and human (right) brains are represented by different colors. Green areas indicate regions where neurogenesis takes place throughout life; yellow color mark regions with adult neurogenesis mostly in response to injuries and the red colored regions are the brain areas with no strong evidence for adult neurogenesis (Magnusson & Frisén, 2016).

Moreover, the lateral striatum of the Guinea Pig contains neuronal progenitors, likely of astrocytic nature, that are quiescent at birth but become transiently activated around weaning (Luzzati et al., 2014). In addition, local activation of parenchymal progenitors can be produced in response to stroke or inflammation in the adult mice (Nato et al., 2015). However, the production of those cells under physiological conditions still to be further studied. In that line, cortical astrocytes can become neurogenic in vitro when isolated from the lessoned neocortex (Buffo et al., 2008) or in vivo after overexpression of specific transcription factors (Niu et al., 2013). In the same vein, some NG2 cells, responsible for the generation of mature oligodendrocytes (Rhodes et al., 2006) remain undifferentiated and homogenously distributed thought adult brain. NG2 cells are also pointed to present the potential to generate a wide variety of cell types including astrocytes, but also oligodendrocytes and neurons, both in vitro and in vivo (Belachew et al., 2003; Baracskay et al., 2007). However, the stem capabilities of these cells and the abilities to generate neurons in vivo still highly debated (reviewed in Nishiyama et al., 2009; Richardson et al., 2011). Anyhow, induced reprograming by different transcription factors of those parenchymal glial cells, either astrocytes or NG2 cells, is a hot topic in Neuroscience nowadays (Gascón et al., 2016; Smith et al., 2016).

Progenitor potential and cell heterogeneity

Adult SVZ contains progenitors that give rise to different GABAergic, dopaminergic and glutamatergic interneurons types in the OB throughout live (Batista-Brito et al., 2008; Brill et al., 2009; Lledo et al., 2006; Young et al., 2007). Moreover, these newly generated cells become granule or periglomerular interneurons in the OB. In fact, neurogenic niche covers several microdomains of the ventricular walls comprising the pallium, subpallium and septum, as well as

the RMS (Azim et al., 2012). Additionally, spatial patterning within SVZ progenitors indicates that different interneuron subtypes are linked to different domains of the adult neurogenic niche (Merkle et al., 2007). Thus, the heterogeneity of SVZ progenitors underlay different phenotypes of OB interneurons (Fiorelli et al., 2015). Moreover, the link between specific regional walls of the SVZ and the generation of different granular or periglomerular cell subtypes is one of the current hot-topics in adult neurogenesis (Merkle et al., 2007, 2014; Figueres-Oñate & López-Mascaraque, 2016). NPCs of the dorsal part of the lateral ventricles are mostly committed to both superficial granule cells and tyrosine hydroxylase (TH) periglomerular cells, whereas ventral NPCs produce both deep granular cells and calbindin (CB) periglomerular cells. On the other hand, calretinin (CR) granular and periglomerular cells are derived from medial SVZ progenitors (Figure 9A). In addition, some morphologically subtypes of interneurons located between superficial GcL and EPL derived from progenitors located in the most ventral part of the rostral SVZ (Merkle et al., 2014). This progenitor heterogeneity and regionalization in the adult ventricular surface is suggested to be maintained due to the combination of transcription factors and morphogens (Ihrie et al., 2011). The specific embryonic origin of this regional arrangement of the adult SVZ remains unexplored, although the association to embryonic territories and maintenance of the expression of specific set of transcription factors has been suggested

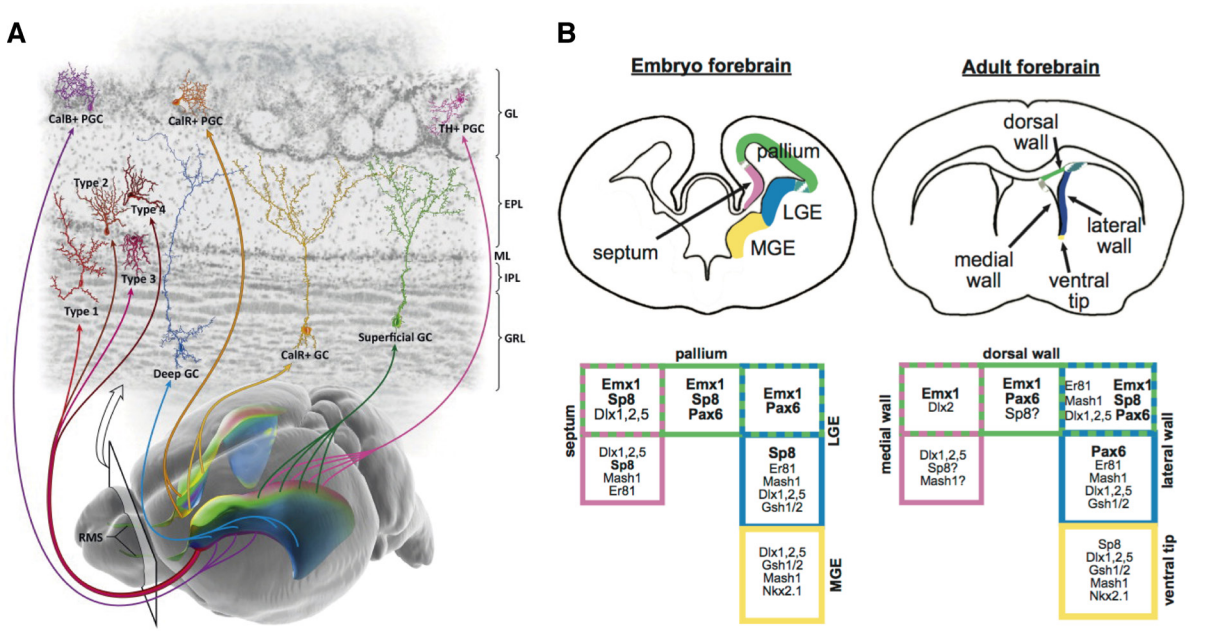

Figure 9. Heterogeneity of the neurogenic niche. A. Regional organization of subventricular zone neural progenitors. 3D view of the adult mouse brain with colored lateral ventricles to indicate the regional organization of the neurogenic niche. The top section is a coronal view of the olfactory bulb indicating the different types of generated interneurons: granular cells (GC) [green: superficial; yellow: calretinin (CalR) superficial; blue: deep], periglomerular cells [pink: tyrosine hydroxylase (TH); orange: calretinin (CalR); purple: calbindin (CalB)] and novel subtypes (Type 1–4) of interneurons derived from the most anterior SVZ. CalB, calbindin; CalR, calretinin; TH, tyrosine hydroxylase; PGC, periglomerular cell; GC, granule cell; GL, glomerular layer; EPL, external plexiform layer; ML, mitral cell layer; IPL, internal plexiform layer; GRL, granular layer (Lim & Alvarez-Buylla, 2014) **B.** Transcription factor expression in the developing and adult forebrain germinal zones. Germinal zones labeled with different colors according to transcription factors expressed either in the embryonic or adult brain. MGE, Medial ganglionic eminence; LGE, lateral ganglionic eminence. From (Alvarez-Buylla et al., 2008)

(Alvarez-Buylla et al., 2008; Fiorelli et al., 2015). However, even in the adult brain most olfactory interneurons are generated from NPCs dispersed from the whole ventricular wall, during embryonic development they arise from lateral ganglionic eminence progenitors (Toresson and Campbell, 2001; Wichterle et al., 2001). In both, adult and embryonic SVZ different transcription factors are expressed in the same domains of the ventricular walls (Figure 9B): 1) pallial markers (Emx1, Pax6, Tbr2, Tbr1, Neurog2) in the most dorsal part; 2) subpallial markers (Dlx1/2/5, Gsx1/2 (Gsh1/2), Mash1 (Ascl1), Nkx2.1, Nkx6.2) in lateral part and 3) septal markers (Zic1/3) (Hack et al., 2005; Kohwi et al., 2007; Waclaw et al., 2009; Young et al., 2007; López-Júarez et al., 2013; Azim et al., 2014). In addition, the lack of specific subtypes of interneurons in the adult OB was reported in mice deficient in some of those transcription factors (Kohwi et al., 2005). Thus, SVZ heterogeneity seems to stem from its embryonic origin (Long et al., 2007). Further, in addition to this adult NPCs ventricular heterogeneity, a different distribution of neurogenic hotspots along the neurogenic niche was reported by analyzing the lateral ventricular surface by wholemounts preparations (Azim et al., 2012; Mirzadeh et al., 2008).

On the other hand, single-cell transcriptome analyses technology reveals new data of cell heterogeneity, addressing the variability of gene expression within the neurogenic niche whether in active NPCs or quiescent NPCs (Codega et al., 2014)., at physiological conditions or after brain insults (Beckervordersandforth et al., 2010; Codega et al., 2014; Llorens-Bobadilla et al., 2015).

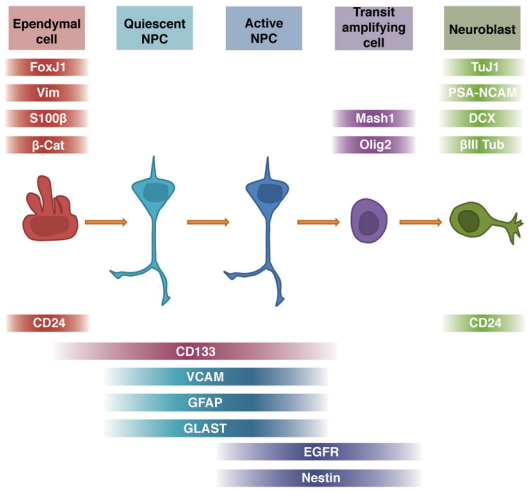

Figure 10. Molecular markers in the neurogenic niche. Cells cohabiting in the adult ventricular surface are highlighted in different colors. Molecular markers expressed by these cells are represented by the same color. The expression of most markers in different cell types makes more difficult the identification of cell populations.

However, the identity and cell dynamics of NPCs in these reports is mostly assessed considering the whole population of ventricular progenitors that express different specific molecular/immunohistochemical markers. However, NPC populations with apparently similar morphological and molecular identities exhibit variable levels of self-renewal and differentiation capacity. Likely, cell diversity should be based on single progenitors potential rather than NPCs pools, aiming the requirement of finer analyses at individual cell level. Moreover, the lineage transition between NPCs and its progeny accomplished a gradual cell maturation, probably co-expressing different molecular markers in different cell types (Figure 10). Thus, none single molecular marker can unambiguously define separate populations. Neural Stem cells have been classically defined as GFAP+ expressing cells in the adult brain with a particular morphology (Imura et al., 2003), but

this protein is also expressed by general astrocyte populations (Nolte et al., 2001). Further, CD133 (or prominin1) is a transmembrane glycoprotein present in the cilia of the ventricular surface related to NSC in the adult niche (Mirzadeh et al., 2008) but also to ependymal cells (Coskun et al., 2008). Hence, markers used to identify NSCs populations are also expressed by neuroblasts, as occurs with the CD24 expression mostly overlapped within distinct populations. Nestin is another marker of aNSCs maintained in TAPs (Gengatharan et al., 2016). Moreover, cell location could also influence in the properties of the cells expressing the same markers (Pfenninger et al., 2011).

Altogether, the isolation and clear identification of cells by molecular markers present some shortcomings that make difficult the isolation of single cell populations. Accordingly, clonal analysis and lineage tracing became crucial in neural stem cell biology (Gao et al., 2014; Calzolari et al., 2015).

Lineage tracing

Lineage cell tracing define the origin, fate and behavior of cells in a specific tissue or organism. In the brain, lineage tracing allow the identification and tracking of the progeny of a single neural progenitor. The determination of lineages and study of the clonal relationships within cohabiting cells in the adult brain is an important question in Neuroscience (for review see Kretzschmar & Watt, 2012). Whether the cell heterogeneity of adult brains is ontogenically determined and if so which are the physiological implications is currently one of the hottest questions in the field. Labeling all progeny of a specific progenitor cell or population of cells is a central tool of developmental biology, revealing patterns of progenitor proliferation, migration, and differentiation. Due to the huge heterogeneity within progenitors pool, clonal analysis is particularly important for stem cell biology. This concept arise at the end of the 19th century with the studies of Whitman and collaborators in leech embryos (Whitman, 1887) and still been a subject undergoing intense study nowadays. Different methodologies were used to address cell lineages in the brain. On of the main advances in lineage tracing was to trace the whole lineage tree in the nematode C.elegans (Sulston et al., 1983) though time-lapse microscopy (http://www.wormatlas.org/celllineages.html). Other approaches also used direct observation to determine lineage progression in mammals, by isolating progenitor cells and tracing lineages trees of their descendants (Temple, 1989; Ortega et al., 2011). However, the isolation of cells from its endogenous environment to obtain the recordings could be a drawback. Otherwise, when the in vivo direct observation is not viable, p.e. because the lack of visibility through the tissue, some lineages approaches have been carried out with chemical staining dyes. Subsequently, cell labeling was achieved by incorporating a chromogen to an enzymatic reaction. However, fluorescent "vital dyes" to label cells and trace their progeny, soon displaced preexistent methods. The principal advantage of fluorescent reporters versus other genetic markers is their easily in vivo application and the needless of tissue processing for observation. Initially, some of the widely fluorescent dyes

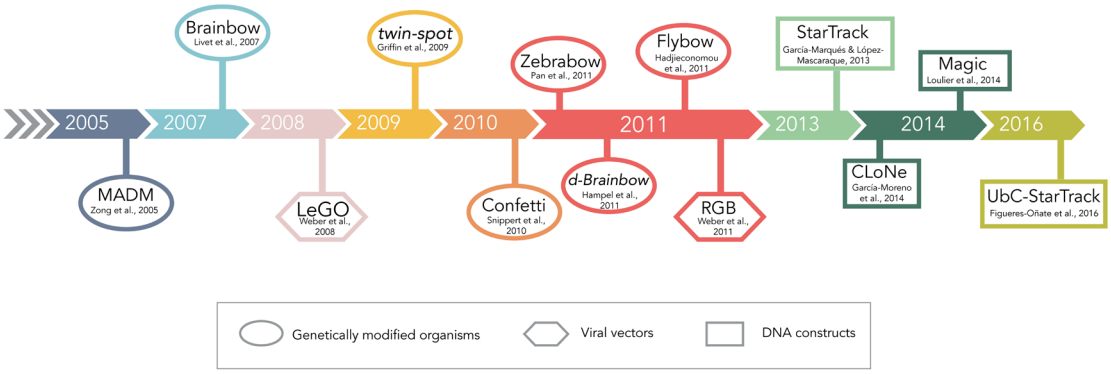

Figure 11. Multicolor lineage methods. Timeline presenting most relevant approaches using a combination of fluorescent reporters for fate mapping or lineage tracing. Depending on designed strategy, each method is enclosed either by a circle (for genetically modified organisms as mice, zebrafish or drosophila), a square (for constructs transfected by viral particles) or a hexagon (DNA constructs encoding the different fluorescent reporters).

used were Fast Blue (cytoplasmic marker) and Diamidino Yellow (nuclear marker) that allowed retrograde labeling of groups of cells and could be simultaneously injected to observe double labeling in single cells. Moreover, lipophilic carbocyanine fluorescent dyes, as DiI and DiO, used in vivo and in fixed tissue, has been used for anterograde and retrograde neuronal tracing (Honig and Hume, 1986, 1989) and allowed the detailed visualization of the cell morphology.

Later on, the discovery of the green fluorescent protein (GFP) (Chalfie et al., 1994) or -galactosidase encoded by the LacZ gene (Son et al., 1996), overtook the use of dyes for lineage tracing. Those reporter genes were injected into different brain structures and either transfected by lipofection (Holt et al., 1990), electroporation (Itasaki et al., 1999), or infected by viral particles (Luskin et al., 1988). In fact, retroviruses were largely used to trace cell lineages (Levison et al., 1993; Noctor et al., 2001; Zerlin et al., 2004). Reducing the amount of virus in each injection allowed to trace single progenitor cells to perform clonal analyses (Yu et al., 2009). Reporter genes introduced by viral vectors are integrated into host cells and transposed to all their progeny. Indeed, this method was refined for clonal analysis through the development of retroviral libraries in which each virus contains a reporter gene and specific sequences recognizable by PCR (Golden et al., 1995). Nevertheless, limitations of retrovirus labeling include epigenetic silencing or no transfection in quiescent or not mitotic cells (Petit et al., 2005). Otherwise, transplantation of cells coming from genetically modified organisms is a method also employed to trace cell lineages (Lois & Alvarez-Buylla, 1994; Merkle et al., 2007). However, one of the highest disadvantages with transplanted cells is that grafted cells may not behave as they do in physiological conditions (Watt & Jensen, 2009). Chimeric mice, generated from a tetraparental embryo, allowed determining the origin of many structures in the body (reviewed in Le Douarin, 2005). Alternatively, DNA replication that occurs prior to cell division produces somatic mutations that do not lead phenotypic effects. Therefore, DNA somatic mutations accumulated in the cells that can give important information about lineages trees (Salipante & Horwitz, 2006).

The idea of tracking cells from their progenitors to their final fate destination arose together with the development of some genetic tools, making the permanent cell labeling feasible. In particular, Cre-loxP recombination system was determinant to address questions about progeny (Sauer, 1987). Later, and inducible version of this technology was included in transgenic mice greatly expanding the possibilities of cellular studies involving genetic modifications (Feil et al., 1997). Genetically modified mice including inducible-Cre recombination have been used for in vivo fate mapping of neural progenitors (Dhaliwal & Lagace, 2011). Low doses of tamoxifen were applied to determine cell lineages in inducible Cre-transgenic lines expressing fluorescent proteins under specific cell types promoters (Magavi et al., 2012; Gao et al., 2014). However, since these approaches label a small number of clonally related cells, they are not entirely appropriate to analyze inter/intra-clonal relationships. Depending on the type of lineage study, different transgenic mice encoding fluorescent protein under different promoters have been generated reporting different problems/advantages for certain uses (Lacar et al., 2010). The employment of transgenic mice and the large variety of fluorescent reporters, arose the idea of the use of combinatorial expression of different fluorescent protein to trace sibling cells (Figure 11). First, three different fluorescent reporters were combined in order to stain neurons individually (Feng et al., 2000). But undoubtedly the greatest impact method in the field of fluorescent proteins has been Brainbow technology (Livet et al., 2007), which still presenting improved versions (Snippert et al., 2010; Cai et al., 2013). The principle of this technology is to create transgenic organisms that include fluorescent proteins expressed after Cre mediated recombination. This method produce stunning colorful images with high detailed morphologies of labeled cells, placing it as a very effective method for cell mapping but not for lineage tracing. Either this method was first design for mice, combinatorial use of fluorescent proteins has been remodeled to fate mapping in Drosophila melanogaster (Hadjieconomou et al., 2011; Hampel et al., 2011; Kanca et al., 2014) or Zebrafish (Pan et al., 2011; Pan et al., 2013). Other clonal methods employed isolated recombination in stochastic cells involving different transgenic lines, as mosaic analysis with double markers (Zong et al., 2005; Gao et al., 2014). This technology has been also modified to D. melanogaster (Griffin et al., 2009). Moreover, lentivirus encoding different fluorescent reporters (red, green and blue) were also included in those multicolor cell tracing approaches (Weber et al., 2008; Weber et al., 2011). Besides, in the last years this technology has been modified to trace lineages from single cells in desired brain regions without the necessity of genetically modify organism. Those new approaches include DNA constructs encoding different fluorescent reporters, which are electroporated in the cells of interest, allowing to trace all the progeny form single cells (García-Marqués & López-Mascaraque, 2013; García-Moreno et al., 2014; Loulier et al., 2014). Thus expands the possibilities of lineage tracing regardless of the organism and lineage and enables studies of cell heterogeneity.

Nevertheless, these techniques rely on the combined expression of as many as four fluorescent reporters which are susceptible to epigenetic silencing deriving in clonal splitting or lumping errors. Moreover, to visualize the fluorescence in some of those transgenic mice immunostaining is mandatory (Calzolari et al., 2015), and this one of the principal limitations due to the lack of specific antibodies to each fluorescent protein. To this respect, our Lab developed a stochastic retrospective clonal analysis method, called StarTrack, that allows to trace the progeny of single cells (Garcia-Marques and López-Mascaraque, 2013). This method is based on the combination of different piggyBac transposon constructs through the combinatorial expression of 12 fluorescent reporters under the regulation of the GFAP promoter. Following in utero electroporation, stochastic expression of these fluorescent proteins produces inheritable marks that enable the long-term in vivo tracing of glial progenitor lineages (García-Marques and López-Mascaraque, 2013, 2016; García-Marques et al., 2015).

By combining the use of state-of-the-art approaches as cell type-specific optogenetic manipulations, single cell analysis, in utero electroporation, in vivo genetic fate mapping, cell ablation, live-cell imaging techniques, patch-clamp recordings and two-photon microscopy in vivo and in brain slice preparations can help understanding how lineage progression takes place in the brain. Additionally, lineage tracing might provide a further and more functional readout of the specific characteristics between clonally related cells derived from the same NPC. To this respect, sibling cells could share some molecular mechanism, resulting in a preferential electrical coupling in neurons located in different cortical areas (Yu et al., 2012). Besides, this type of analyses results in important advances on the underlying molecular mechanisms of lineage specification and the pathological basis of genetic disorders.

All this emerging knowledge in the field over the last years, beg us to understand this broad cell-heterogeneity found in adult brains. Our basic purpose was to understand how the different types of neural cells existent in the adult brain are generated during nervous system development. Then, we focused our study on cell diversity through their ontogenetic origin, using the mice olfactory bulb as experimental model.

OBJECTIVES

The main objective of this thesis work was to develop a method to perform broad clonal analyses of the adult progeny from single telencephalic neural progenitors. Specific aims were the following:

1. To characterize the expression pattern of integrable vs. non-integrable ubiquitous vectors

    a. Analyses of the cell progeny after *in utero* and postnatal plasmids electroporation.

    b. Comparison of the labeling in the different neural lineages after integrable vs. non-integrable ubiquitous vectors targeting.

2. To generate a ubiquitous genetic tool for lineage tracing and the identification of clonally related cells from all brain cell lineages.

    a. Generation of a mixture of plasmids under a ubiquitous promoter to target the cell progeny of single progenitors: UbC-StarTrack.

    b. To develop different strategies to achieve an inheritable and stable cell labeling.

    c. To test the feasibility of the method to label sibling cells from all the brain cell lineages.

3. To determine the origin of adult olfactory bulb interneurons and fate from ventricular progenitors.

    a. Analyses of the spatial distribution through the olfactory bulb cell layers of targeted cells after *in utero* and postnatal electroporations.

    b. Characterization of the cell phenotypes in the adult olfactory bulb after embryonic/postnatal progenitor targeting.

    c. Provide the regional origin of glial cells in adult olfactory bulb.

4. To perform a clonal analysis of sibling cells in the olfactory bulb: application of the UbC-StarTrack to the postnatal neurogenic niche.

    a. Distribution of sibling cells along the rostral migratory stream.

    b. Dispersion pattern and clonal properties of sibling olfactory interneurons after short and long term periods after UbC-StarTrack electroporation.

    c. Clonal analyses of targeted progenitors at the ventricular surface.

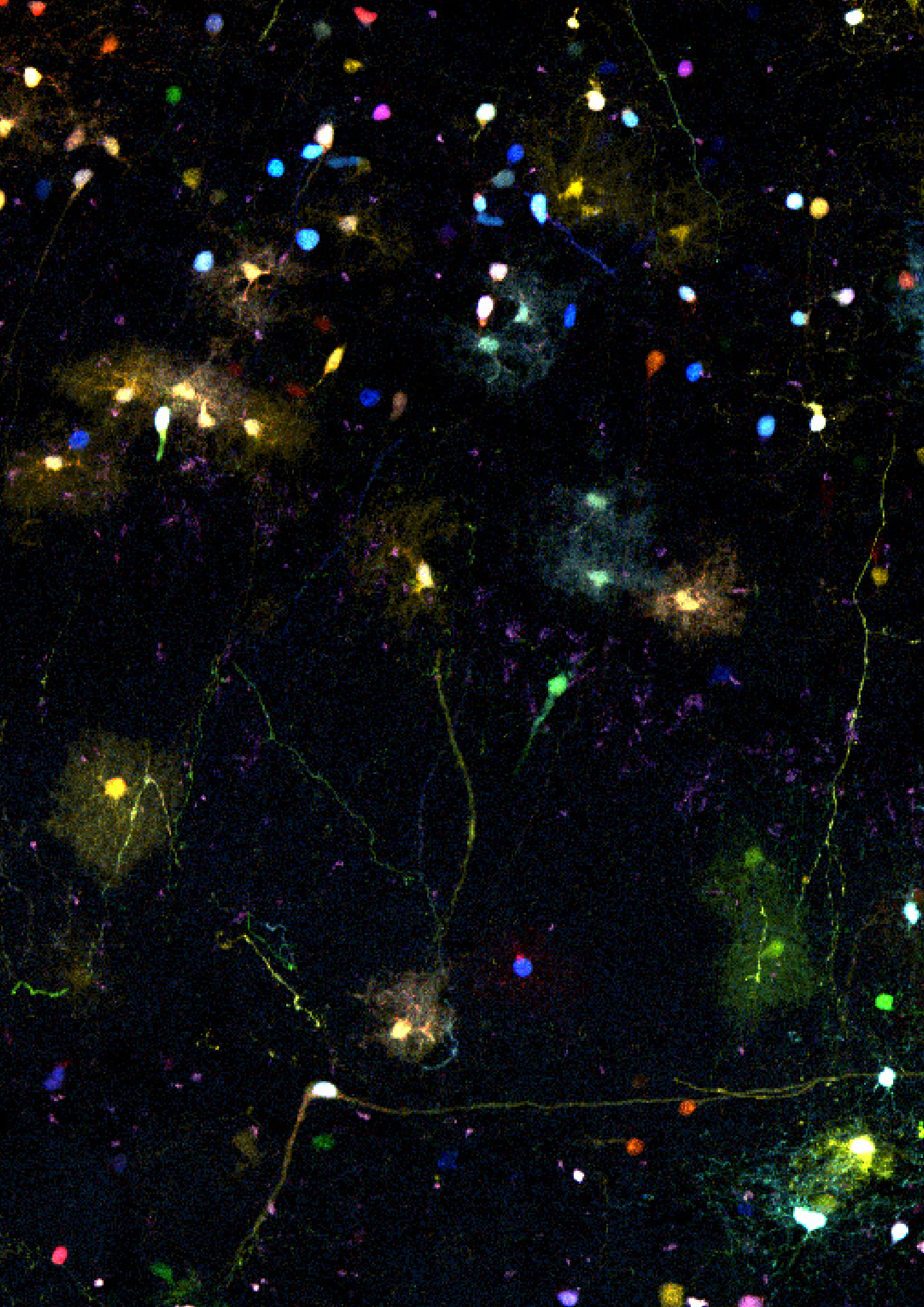

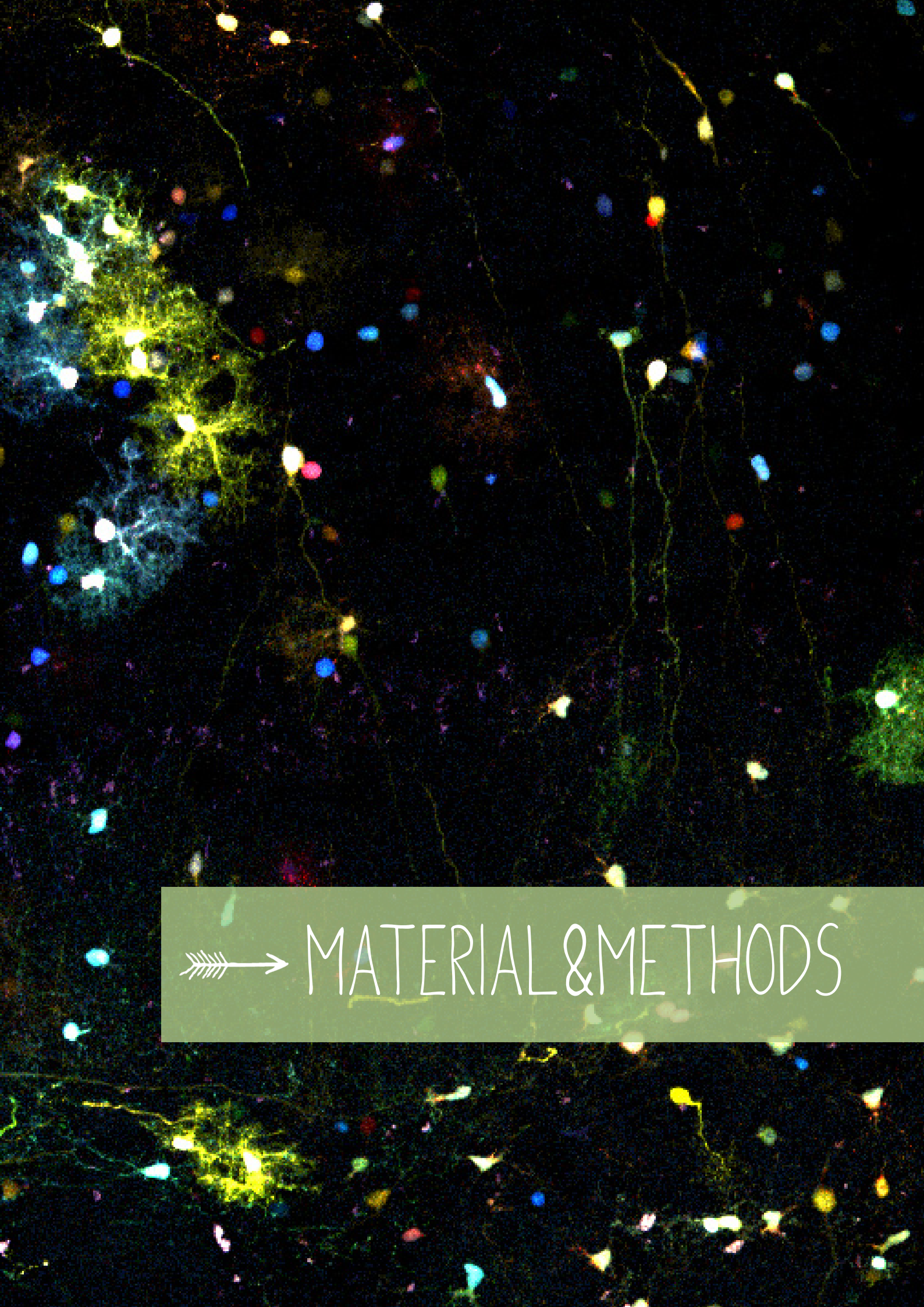

MATERIAL&METHODS

Animals

Wild type C57BL/6 mice were obtained from the Cajal Institute animal facility, and all the procedures were carried out in compliance with the ethical regulations on the use and welfare of experimental animals of the European Union (2010/63/EU) and the Spanish Ministry of Agriculture (RD 1201/2005 and L 32/2007). The CSIC Bioethical Committee approved all the animal protocols.

Mice gestation period lasts 19 days, considering the day on vaginal plug visualization as embryonic day (E) 0 and day of birth was designed as postnatal day (P) 0. In addition, mice from onwards P30 were considered an adult mouse. At least N=3 animals were used per experimental condition.

In Utero Electroporation (IUE)

Pregnant females were anesthetized at required embryonic dates with 4% isofluorane and maintained with 2-3%isofluorane/O2 inhalation. Then, mice were transferred to a sterile surgery area that includes a thermal plate at 37°C. Before surgery, mice were administered an antibiotic (enroflozacine, 5 mg/kg) and an anti-inflammatory NSAID analgesic (meloxicam, 300 µg/kg) subcutaneously. Uterine horns were exposed by laparotomy and plasmid mixture was injected into the brain embryos using glass micropipettes. Intraventricular lateral injections into E11-E12 brain embryos were guided by an ultrasound device (VeVo 770; VisualSonics), while embryos from E13 onwards were visualized by trans-illumination. Successful filling of the LV will be confirmed by fast green diffusion. Each embryo was hold between tweezer-type electrodes to deliver one or two trains of 5 square pulses of 50ms length with 950ms between each pulse. Applied voltages varied depending on the embryonic day (Table 1).

	E11	E12	E13	E14	E15	E16	E17	P0-P2
Voltage	28V	30V	33V	35V	37V	40V	43V	100V

Table 1. Applied voltages for *in utero* or postnatal mice brains electroporation.

After electroporation of all embryos, uterine horns were placed back into the abdominal cavity and the abdominal incision was sutured with absorbable polyglycolyc acid sutures while the skin incision with silk sutures. After cleaning the wound with saline and covering the area with povidone-iodine the animal was placed in a thermal blanket. Embryos were allowed to develop until the selected age for brain analyses.

Postnatal electroporation

Pups (P0/P1) were anesthetized by hypothermia and lateral ventricles were visualized by trans-illumination through a optical fiber. The selected StarTrack-mixture was injected into the ventricular cavity and electroconductive LEM Gel (DRV1800, MORETTI S.P.A.) was placed on both electrode paddles to avoid damaging

the pups and to achieve successful current flow. Five 100V electric pulses will be applied (50ms duration, 950ms intervals), with the positive electrode positioned in the dorso-lateral region to direct the negatively charged DNA to the subventricular zone. After the pulses, the pups will be placed on a thermal plate and after recovering they will be returned to their mother.

Tamoxifen administration

Tamoxifen (Tx, Sigma-Aldrich) was dissolved in corn oil (Sigma-Aldrich) at a final concentration of 20mg/ml and a single dose of 5 mg/40 gr body weight was administered. When analyzing embryos, Tx was administrated to pregnant females by intraperitoneal injection 24h post IUE, whereas working with pups, it was administered one day after the electroporation. Animals should be analyzed at least 2-3 days after Tx injection to allow the inhibition of non-integrated constructs.

BrdU procedure

5'Bromo-2'-deoxyuridine (BrdU, Roche) was solved into Saline 0,9% at a final concentration of 5mg/ml. It was intraperitoneally administered at a 50mg/kg body-weigh. To detect labeled cells, brain slices were placed into hydrochloric acid to denaturalize the DNA at 37° between 30-45 min. Then the slices were placed in borate buffer to neutralize the acid action and washed with 0.1%triton-phosfate buffer as in a regular immunofluorescence. The used anti-BrdU primary antibodies were anti-BrdU Rat (1:400, Bio-Rad), or Ms (1:500 Hybridoma Bank).

Tissue processing

Mice were analyzed at embryonic, postnatal and adult stages. When embryos were used for analysis, dams were anesthetized with pentobarbital, embryos extracted from uterine horns and they were fixed by transcardiac perfusion with 4% paraformaldehyde in 0.1 M phosphate buffer (PFA4%) and then post-fixed overnight in the same fixative. Postnatal mice were anesthetized by hypothermia (P0 to P6) or intraperitoneal injection of sodium pentobarbital (Dolethal, 40-50mg/Kg) from P6 onwards. Brains were fixed by transcardiac perfusion with PFA4% and then post-fixed overnight in the same fixative. For sectioning, brains were included into agarose and coronally/sagittally vibratome serially sectioned (50 -100 µm thick). For long-term storage, sections were mounted on a glass slide and coveslipped with Mowiol antifading mounting media and stored at 4°.

Immunohistochemical characterization

Molecular identity of labeled cells were characterized using immunohistological markers. Briefly, sections were permeabilized firs with 0.5% Triton-X in PBS (PBS-T) and then

with 0.1% PBS-T and incubated in blocking solution (5% normal goat serum (NGS) in 0.1% PBS-T). Sections were then incubated overnight with the selected antibodies in NGS5% at required concentrations (described in the material and methods detailed in each paper of the current thesis work). The following day, sections were washed with 0.1% PBS-T and primary antibodies were detected with appropriated conjugated secondary antibodies. After UbC-StarTrack electroporations, secondary antibodies were in all cases conjugated with the far-red fluorophore (1:1000, Alexa Fluor 633 or 647, Molecular Probes). For the immunofluorescences in tissue without electroporation secondary antibodies were either conjugated with a green fluorophore (1:1000, Alexa Fluor 488nm, Molecular Probes) or a red fluorochrome (1:1000, Alexa Fluor 488nm, Molecular Probes). Finally, the sections were mounted onto slides in PB/Glycerol (1:1) for a preliminary evaluation in the fluorescence microscope and selected sectios will be definitively coveslipped with Mowiol antifading mounting media and stored at 4º.

DNA vectors

Broadly, cloning strategies were developed as follows. Oligonucleotides were obtained from SIGMA-ALDRICH, PCR amplifications were performed by the molecular biology facility of the Instituto Cajal. PCR products were cloned using CloneJET PCR Cloning Kit (Fermentas) and cohesive restriction enzymes (Fermentas) in all cases. The Rapid DNA Ligation Kit (Fermentas) was used for ligations and the resulting products were transformed into E. coli JM107 bacteria using the "TransformAid" Bacterial Transformation Kit (Fermentas). All constructs generated in the current thesis are specifically detailed in the material and methods section of the corresponding publication.

Vector containing the hyperactive transposase of the PiggyBac system (hyPBase) was kindly provided by Prof. Bradley, while the pCAG-CreERT2 plasmid was a kind gift from Connie Cepko (Addgene #14797).

Cell transfection

HEK293 and OliNeu cells were cultured to validate the in vitro expression of the generated constructs. Briefly, 1.5-2·105 cells per well were cultured on polyornithine-plated 6-well plates maintained at 37 °C in an atmosphere of 5% CO2, and in DMEM (Invitrogen) supplemented with 10% fetal bovine serum (Sigma-Aldrich) and 0.5% penicillin/streptomycin (Invitrogen). Every 3-4 days the confluent cultures were passaged using 0.05% Trypsin-EDTA (Gibco). Transfection was performed by the calcium phosphate protocol. A maximal amount of 3µg of total DNA mixture was prepared for each 6-well. The fluorescent expression of the distinct generated UbC-StarTrack constructs was assessed 1 day after calcium phosphate transfection.

Electroporation of organotypic slices

E14 brains were embedding in low melting point agarose dissolved in 1X KREBS buffer and 300 µm vibratome slices were placed on polycarbonate membranes (Whatman) and cultured for 1-2 hours before electroporating them in MEM medium (LifeTechnologies). Prior to electroporation, membranes were placed in Neurobasal medium (LifeTechnologies) and the UbC-StarTrack plasmid mixture was then injected into the SVZ with a borosilicate glass filament. To avoid direct contact between the electrode and the slice, the membranes containing the slices were placed between a protective agarose support, the electrodes were placed in position and then, 2 pulses (voltage: 80mV, 5ms on/500ms off) were delivered to pass the reporters into the cells. Slices were analyzed after a 48-72h incubation at 37 °C in an atmosphere of 5% CO2 in DMEM.

Image acquisition

Fluorescent labeling was visualized under an epifluorescence microscope (Nikon, Eclipse E600) with the appropriate filter cubes (Semrock): UV-2A (FF01-334/40-25) Cerulean (FF01-405/10), GFP (FF01-473/10), YFP (FF01-520/15), mKO (FF01-540/15), mCherry (FF01-590/20) and Cy5 (FF02-628/40-25). Images were acquired on a Leica TCS-SP5 confocal microscope, capturing the different XFPs in separate channels. The wavelength of excitation (Ex) and emission (Em) for each XFP were (in nanometers, nm): mT-Sapphire (Ex: 405; Em: 520-535), mCerulean (Ex: 458; Em: 468-480), EGFP (Ex: 488; Em: 498-510), YFP (Ex: 514; Em: 525-535), mKO (Ex: 514; Em: 560-580), mCherry (Ex: 561; Em: 601-620), and Alexa 633 (Ex: 633; Em: 650-760). Confocal laser lines were in-between 25-40% in all cases and the maximum projection images will be created using confocal (LASAF Leica) and NIH-ImageJ software. Captured images were processed to equally adjust the contrast using Adobe Photoshop CS5 software.

Data analyses

For the different quantifications achieved in the current thesis work diverse software were used as Matlab (The Math Works Inc., USA), LASAF (Leica) and NIH-ImageJ. SigmaPlot 13 (Systat Software) was used to determine the statistical .

To analyze the clonally-related cells after UbC-StarTrack electroporation, images were analyzed with a custom macro integrated into ImageJ software (NIH). The critical step in the macro analysis will be to appropriately select labeled cells. A threshold for every image in each confocal channel was adjusted in order to create positive cell selection for each XFP. Background subtraction was employed before the threshold selection by applying a

smooth filter to improve cell signal selection. Then, a binary image was created including the labeled cells in each channel to generate the positive selections. A watershed filter was applied after the binary image to separate contiguous tagged cells and to analyze them as individual points. Once the selection had been performed, minimal fluorescence intensity was determined to consider all the values over it as positive fluorescent labeling. Subsequently, data were automatically organized in a table including maximal and minimal XFP intensity value for each labeled cell and its specific fluorescent expression for each of the six reporters. Thus, a color-code was assigned for each labeled cells, and them were ordered by those codes to assess the study of potential clonally related cells. Further analysis will be performed to determine sibling cells based on the fluorescence intensity ranges and the location of the fluorophore (nucleus or cytoplasm).

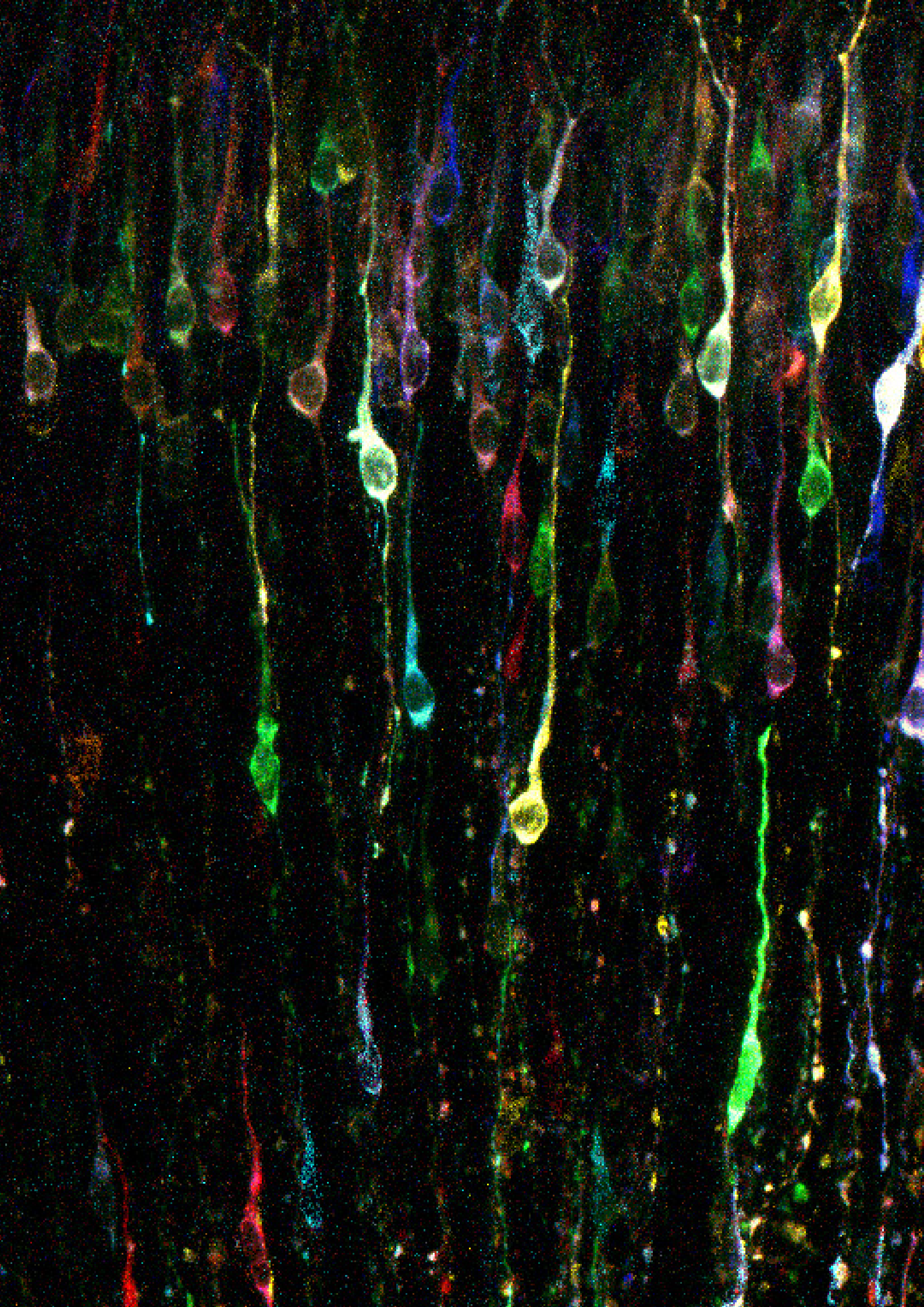


RESULTS

CHAPTER 1

Spatiotemporal analyses of neural lineages after embryonic and postnatal progenitor targeting combining different reporters. Figueres-Oñate, M., Garcia-Marques, J., Pedraza, M., De Carlos, J.A. and López-Mascaraque, L. (2015). Frontiers in Neuroscience, doi: 10.3389/fnins.2015.00087

In this work we performed a comparative analyses on the feasibility of integrable vs. non-integrable ubiquitous constructs, to better understand their fluorescent reporter expression after in vivo targeted electroporation in mice brains. To this end, we designed two gene constructs under the human Ubiquitin C (UbC) promoter: a piggyBac transposable plasmid and a non-integrable construct without terminal repeat in 3' region, impeding the genomic integration by the piggyBac transposase. To clearly distinguish between those two conformations each plasmid drives the expression of different fluorescent reporters. The integrable construct expressed the enhanced green fluorescent protein (EGFP) and the non-integrable expressed the mCherry fluorescent protein. We performed in utero and postnatal co-electroporations with these two constructs along with the transposase, to compare the labeled adult neural progeny. The results of those experiments are shown in the first paper included in this thesis work: "Spatiotemporal analyses of neural lineages after embryonic and postnatal progenitor targeting combining different reporters". Our data, highlighted the importance on the use of integrable vectors to track glial cell lineages or neuronal cells differentiated after a large number of divisions in the adult brain. In addition, the stable labeling of non-integrated vectors in cells generated shortly after the electroporation, alerted about the importance of the inhibition of those non-integrated constructs to perform color-based clonal analyses.

frontiers in Neuroscience

ORIGINAL RESEARCH
published: 17 March 2015
doi: 10.3389/fnins.2015.00087

Spatiotemporal analyses of neural lineages after embryonic and postnatal progenitor targeting combining different reporters

*Maria Figueres-Oñate, Jorge García-Marqués, Maria Pedraza, Juan Andrés De Carlos and Laura López-Mascaraque **

Instituto Cajal-Consejo Superior de Investigaciones Científicas, Department of Molecular, Cellular and Developmental Neurobiology, Madrid, Spain

Genetic lineage tracing with electroporation is one of the most powerful techniques to target neural progenitor cells and their progeny. However, the spatiotemporal relationship between neural progenitors and their final phenotype remain poorly understood. One critical factor to analyze the cell fate of progeny is reporter integration into the genome of transfected cells. To address this issue, we performed postnatal and *in utero* co-electroporations of different fluorescent reporters to label, in both cerebral cortex and olfactory bulb, the progeny of subventricular zone neural progenitors. By comparing fluorescent reporter expression in the adult cell progeny, we show a differential expression pattern within the same cell lineage, depending on electroporation stage and cell identity. Further, while neuronal lineages arise from many progenitors in proliferative zones after few divisions, glial lineages come from fewer progenitors that accomplish many cell divisions. Together, these data provide a useful guide to select a strategy to track the cell fate of a specific cell population and to address whether a different proliferative origin might be correlated with functional heterogeneity.

Keywords: neurogenesis, gliogenesis, cell fate, cell division, electroporation, neurons, glial cells

OPEN ACCESS

Edited by:
Jack M. Parent, University of Michigan, USA

Reviewed by:
Alfonso Represa, Institut de Neurobiologie de la Méditerranée, France
Joseph LoTurco, University of Connecticut, USA

****Correspondence:***
Laura López-Mascaraque, Instituto Cajal-Consejo Superior de Investigaciones Científicas, Department of Molecular, Cellular and Developmental Neurobiology, Avda. Dr. Arce, 37, 28002-Madrid, Spain
mascaraque@cajal.csic.es

Specialty section:
This article was submitted to Neurogenesis, a section of the journal Frontiers in Neuroscience

Received: *10 December 2014*
Accepted: *01 March 2015*
Published: *17 March 2015*

Citation:
Figueres-Oñate M, García-Marqués J, Pedraza M, De Carlos JA and López-Mascaraque L (2015) Spatiotemporal analyses of neural lineages after embryonic and postnatal progenitor targeting combining different reporters. Front. Neurosci. 9:87. doi: 10.3389/fnins.2015.00087

Introduction

Neural cells are originated from a complex mix of distinct progenitors, which are pluripotent stem cells with restricted differentiation potential. The first progenitor cells are a subset of non-committed neuroectodermal progenitors that become specified as neural progenitor cells (NPCs). Subsequently, NPCs undergo repeated symmetric divisions to self-renew while they divide asymmetrically to produce distinct neural and glial lineages at different time points. Those progenitors should maintain a balance between self-renewal and lineage commitment, becoming either neural stem cells or committed progenitors that undergo a limited number of divisions producing a lineage-restricted cell progeny. After an initial symmetrical amplification of the progenitor pool, radial glial cells (RGC) start to undergo asymmetrical divisions producing more restricted progenitors cells, including intermediate progenitor cells (see reviews by Götz and Huttner, 2005; Franco and Müller, 2013). RGCs differentiate at early developmental stages into neuron-committed progenitor cells and at later stages into glial-restricted precursors (Noctor et al., 2002; Anthony et al., 2004). Perinatally, some RGCs continue generating neurons and oligodendrocytes, while others RGCs transform into adult subventricular zone (SVZ) astrocytes, that differentiate to adult neural

stem cells (Kriegstein and Alvarez-Buylla, 2009). However, the precise relationship between neural progenitors and their commitment to each cell lineage is still largely unknown. Recent data indicates a role for the transcription factor Pax6 in regulating the orientation of cleavage plane that is crucial for symmetric vs. asymmetric cell divisions (Asami et al., 2011).

During NPCs life, it is difficult to differentiate between the clonal contribution of a particular cell in development, and its ongoing contribution in the adult. So far, several strategies for cell lineage analyses trace the development and cell progeny of NPCs. Different approaches and transgenic mice have been used to analyze either the cell division pattern or the progenitor cycle progression as FUCCI reporters (Sakaue-Sawano et al., 2008). Moreover, newly generated cells can be labeled by birth-dating methods, such as retrovirus infections, incorporation of thymidine analogs and transgenic mice (Imayoshi et al., 2011). Further, genetic and fate-mapping studies revealed the temporal and spatial origin of different neuronal populations. However, most of these approaches have technical limitations (Blanpain and Simons, 2013). Before attempting to interpret NPCs commitment, it is necessary to distinguish the fate of daughter cells or even to track, over long time periods, the progeny of a single cell. Thus, the lineage tracer should be retained permanently and transmitted to all progeny of the founder cell, and should not be spread to unrelated cells (Kretzschmar and Watt, 2012). DNA-mediated gene transfer by electroporation allows the permanent labeling of a particular neural cell population and its progeny. Lineage tracing with multicolor reporters can provide information on cell tracking, cell viability, cell function, and cell proliferation. However, depending on the selected gene vectors to clone the DNA fragments, transfected plasmids may be episomally transcribed or may be designed to be integrated into the host cell genome (Yoshida et al., 2010) allowing a long-term stable expression. Integration of reporter proteins in neural progenitors genome by co-electroporation of transposon vectors (Ding et al., 2005; Nakanishi et al., 2010), generates a specific and permanent color combination by random transposition, allowing the analyses of *in vivo* single cell progeny (García-Marqués and López-Mascaraque, 2012; García-Moreno et al., 2014; Loulier et al., 2014; Siddiqi et al., 2014).

Here, we undertake a comparative analysis of the labeled adult cell progeny by targeting neural progenitors after embryonic and postnatal co-electroporation of integrable and non-integrable constructs. Our results showed that the percentages of labeled cell types differed greatly depending on the construct. We highlighted the importance of the selected strategy to efficiently track the whole and specific cell progeny of neural progenitors.

Materials and Methods

Animals

Wild type C57BL/6 mice of either sex were raised at the Cajal Institute animal facility. All of the experiments were performed according to ethical regulations on the use and welfare of experimental animals of the European Union (2003/65/CE) and the Spanish Ministry of Agriculture (RD 1201/2005 and L 32/2007). Bioethical committee of CSIC approved these experimental procedures. Day of vaginal plug detection was defined as the first embryonic day 0 (E0) and the day of birth was defined as postnatal day 0 (P0).

Tissue Processing

Mice were analyzed in both embryonic and adult stages (considering adult stages from P30 onwards). Pups from P1 to P6 were anesthetized by hypothermia, whereas mice from P6 onwards were anesthetized with intraperitoneal injection of pentobarbital (40–50 mg/Kg body weight), and then perfused with 4% paraformaldehyde (PF). Brains were postfixed in PF overnight, and coronal or sagittal sections (50–100 μm) were serially obtained with a vibratome.

Expression Vectors

We used the piggyBac transposon integrable plasmid, pPB-UbC-EGFP, encoding the enhanced green fluorescent protein (EGFP) under the human ubiquitous Ubiquitin C (UbC) promoter, provided by Prof. Bradley (Yusa et al., 2009). This plasmid is flanked by two terminal repeats sequences (TRs) recognized by the piggyBac transposase (mPBase). The mPBase inserts the vector, including the reporter gene, directly into the genome of the transfected cell at TTAA repeat regions (**Figure 1A**, integrable). This allows the analyses of the entire cell progeny regardless of its mitotic activity. We also designed a new plasmid encoding mCherry fluorescent protein under the UbC promoter, using pPB-UbC-EGFP as the cloning vector. The region containing the EGFP and the 3′TRs was excised using the enzymes *BamHI/MluI*, to avoid the genomic insertion of the mPBase. Next, the region encoding mCherry protein, amplified from the StarTrack pPB-GFAP-mCherry (García-Marqués and López-Mascaraque, 2012), was cloned into the excised vector in the *BamHI/MluI* sites. Thereby, we generated a new non-integrable construct (**Figure 1A**, non-integrable) that will remain as episomal plasmid in the electroporated cells.

In Utero Electroporation (IUE)

IUE was performed as previously described (García-Marqués et al., 2014). Briefly, E13-E14 pregnant mice were anesthetized with isofluorane (Isova vet, Centauro), and placed in a thermic plate. The skin and the abdominal cavity were cut, opened, and the uterine horns exposed. The DNA mixture solution consisted of an equal amount of pPB-UbC-EGFP and UbC-mCherry plasmids, plus half the amount of mPBase and 0.1% Fast Green. The final concentration was 1 μg/μL, and 1 μl of the solution was injected into the lateral ventricle of each embryo by a pulled glass micropipette. After that, the head of each embryo was placed between 3 mm tweezer-type electrodes (Sonidel) and 5 electric pulses of 50 ms length were passed after 950 ms intervals using an electroporator. In all cases, the electroporated region was the ventricular zone in the dorso-lateral area (**Figure 1B**). The voltage varied depending on the embryonic day from 33 V at E13 to 35 V at E14. After electroporation, the uterus was repositioned and the abdominal cavity was sutured. Pregnant mice received a subcutaneous injection of both 5 mg/kg of the antibiotic enrofloxacine (Baytril; Bayer, Kiel, DE) and 300 μg/kg of the anti-inflammatory/analgesic meloxicam (Metacam; Boehringer

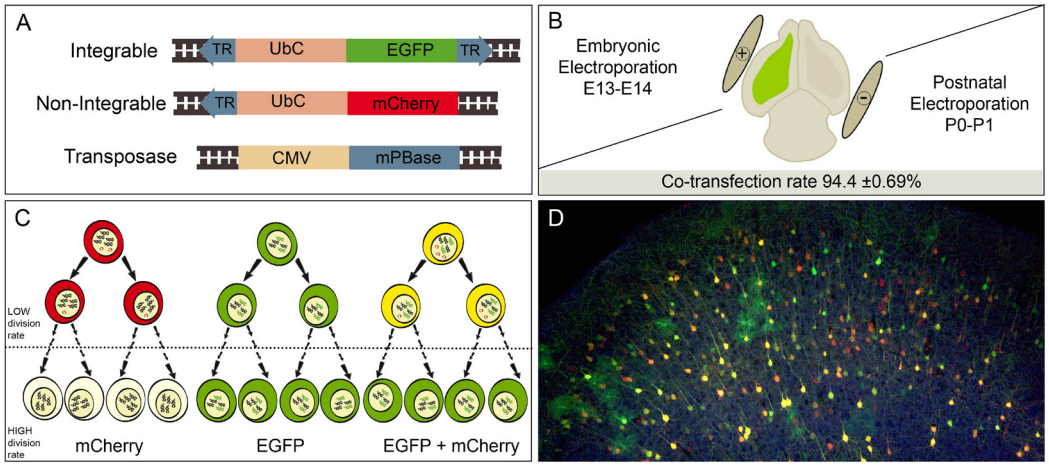

FIGURE 1 | *Experimental procedure*. (A) Simplified diagram of the designed constructs. Integrable construct contains an EGFP (enhanced green fluorescent protein) encoding region under the Ubiquitin C human gene (UbC) promoter. The transposase recognizes the terminal repeats sequences (TR, blue), cleaves and integrate flanked region into the host cell genome. Non-integrable construct encodes mCherry fluorescent protein under UbC promoter. Construct modified by removing the 3′ TR from the original vector. PiggyBac transposase (mPBase) under the control of the ubiquitous CMV promoter. **(B)** A mixture of the three constructs was injected (green color) and electroporated into the LV at either postnatal or embryonic stages. Positive and negative poles of the tweezer electrode were orientated to target the ventricular dorso-lateral area. The co-transfection rate of integrable and non-integrable constructs 2 dpi was 94.4 ± 0.69%. **(C)** Transfected cells expressed red, green or yellow fluorescence depending of reporter uptake (one or both reporters). Red expression will be lost by dilution of non-integrable plasmid in the recurrent dividing cells. Consequently, green integrable vector will be the unique label after several rounds of divisions. Dotted line means undetermined number of cell divisions. **(D)** Adult cortical labeled cells after embryonic co-electroporation of the three constructs, showing red, green and yellow cells.

Ingelheim) and embryos were allowed to continue developing until desired.

Postnatal Electroporation

Pups (P0/P1) were anesthetized by hypothermia and trans-illuminated under a cold light to facilitate the visualization of the lateral ventricles. The ventricular cavity was injected with 2 μl of the plasmid mix, and 5 electric pulses of 100 V were applied (50 ms each pulse, separated by 950 ms intervals). Electroconductive LEM Gel (DRV1800, MORETTI S.P.A.) was placed in both electrode paddles to avoid pups damage and get a successful current flow. The positive electrode was positioned to direct the negatively charged DNA. After the pulses, animals were reanimated and returned to the mother.

Immunohistochemistry

Electroporated labeled cells were identified by their morphological features and then confirmed by the expression of different molecular markers. The following primary antibodies were used: rabbit anti-Tbr1 (1:500, Chemicon AB9616) and mouse anti-NeuN (1:500, Chemicon MAB377) to classify neuronal cells; rabbit anti-PDGFRα (1:300, SantaCruz-338), mouse anti-S100β (1:300), rabbit anti-Olig2 (1:3000, Millipore), rat anti-MBP (1:1000, Abcam R7349) to identify glial lineages. In all cases the secondary antibodies were labeled with an infrared fluorochrome (1:1000, Alexa Fluor 633 or 647, Molecular Probes).

Image Processing

Fluorescent labeling was visualized using an epifluorescence microscope (Nikon, Eclipse E600) with the appropriate filter cubes: rhodamine (569–610 nm) and fluorescein (450–490 nm), to visualize mCherry and EGFP, respectively. Then, images were obtained on a Leica TCS-SP5 confocal microscope. Maximum projection images were created using confocal software (Leica LAS AF Software). Captured images were processed to equally adjust the contrast using Adobe Photoshop CS5 software.

Statistical Analysis

For quantification four coronal sections from $n = 4$ mice per age were imaged. Co-transfection efficiency, of both red and green fluorescent proteins, was calculated through the LAS AF software (Leica) in electroporated animals (IUE at E14), at 2 days post-IUE. Quantitative analysis of the expression of integrable and non-integrable constructs in the different neural populations was performed by manual selection of positive cells labeled by one or both constructs in the different neural populations. To determine the intensity for each fluorescent protein in every selected cell, data were obtained using customized routine designed in Matlab (The Math Works Inc., USA). Quantification of the number of labeled cells was performed in mice electroporated at embryonic (E14) and postnatal stages (P1). Short-term group was sacrificed 5 days after electroporation (P6) and the long-term group 1 month after (P30). To determine the statistical significance, One-Way analysis of

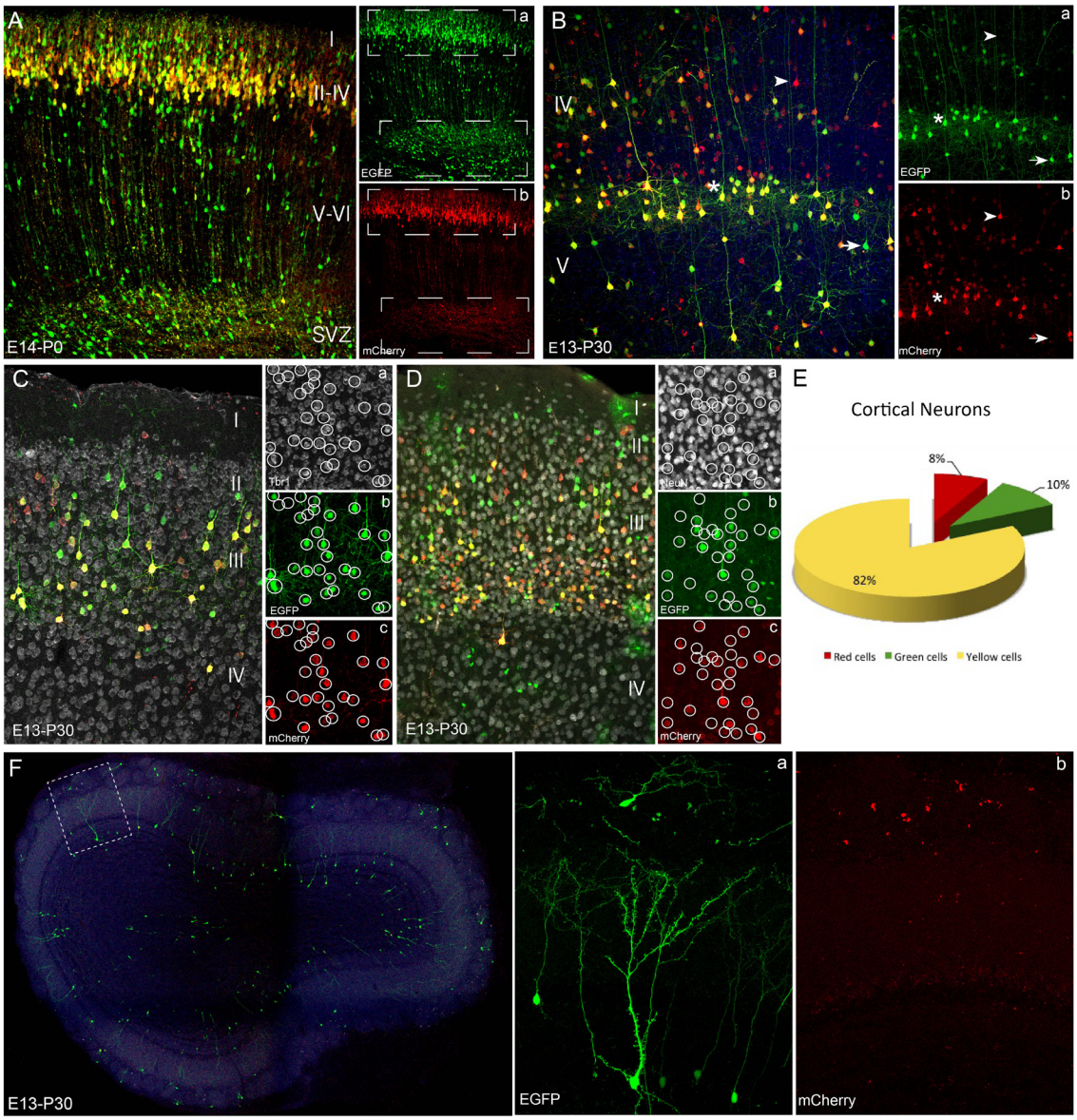

FIGURE 2 | Neuronal lineage after embryonic electroporation. (A) Cortical P0 cells transfected at E14. Neurons in layers II and IV expressed interchangeably red or green plasmids (upper box in **a,b**). Cells located close to subventricular zone lost the mCherry non-integrable vector. This proliferative zone mostly expressed the integrated plasmid (EGFP), because the mCherry-plasmid dilution through cell division rounds (lower box in **a,b**). **(B)** Adult (P30) cortical cells labeled after IUE at E13 expressed either green (arrow) or red (arrowhead) reporters. Yellow cells (asterisk) co-expressed both constructs. At adult stages non-integrable constructs maintained a stable cell expression. **(C,D)** IUE performed at E13 and analyzed at adult stages (P30). Tbr1- (**Ca**) and NeuN-positive cells (**Da**) revealed the neuronal fate of cortical neurons expressed both the integrated (green, **b**) and non-integrated (red, **c**) constructs. **(E)** Percentage of adult cortical neurons (IUE at E14, analysis P30, $n = 4$ animals, 4 sections per animal) expressing green- (9.6 ± 1.5%), red- (8.1 ± 1.5%) or both constructs (82.3 ± 1.6%). **(F)** Interneurons in the olfactory bulb after IUE at E13. Olfactory bulb transfected interneurons expressed only the green integrated construct **(a)**. Separate confocal channels demonstrate the lack of mCherry signal **(b)**. IUE: *In utero* electroporation.

variance (ANOVA) was performed by SigmaPlot 13 (Systat Software), and values were represented as the mean ± SEM. *Post-hoc* analysis was made by pairwise comparison procedures by Turkey's significance test. A confidence interval of 95% ($p < 0.05$) was required to considered values statistically significant.

Results

Neuronal Progeny after *In Utero* Electroporation of Genome-Integrable (EGFP) vs. Non-Integrable (mCherry) Plasmids

We used the piggyBac system to genetically label progenitor cells and their progeny with reporter fluorescent proteins under the ubiquitous UbC promoter. We compared labeled neural progeny after *in vivo* co-electroporation of the following three vectors (**Figure 1A**): (1) Integrable construct, encoding the green fluorescent protein (EGFP) flanked by transposase recognition sites (Terminal repeats, TRs), (2) Non-integrable construct encoding the fluorescent protein red fluorescent protein (mCherry) without TRs in 3′ region, and (3) the transposase of the piggyBac system (mPBase). In all cases, these three constructs were injected and co-electroporated targeting the dorso-lateral ventricular zone, at either embryonic or postnatal ages (**Figure 1B**). Cell progeny showed three different patterns of reporter protein expression: mCherry positive cells (red), EGFP positive cells (green) and cells expressing both reporters (yellow), depending on the uptake of one or both constructs into progenitors during electroporation. Red positive cells (expressing non-integrated sequence) will lose their label after multiple rounds of cell division, as a result of the dilution of the construct. Thus, the red non-integrable construct will not allow tracking the whole cell progeny. Red plasmid dilution will also occur in the case of yellow positive cells expressing both fluorescent reporters. In that case cells coming from yellow progenitors after divisions will only express the green integrated reporter (**Figure 1C**). On the other hand, green positive cells will maintain the label through all cell division rounds, allowing the complete cell progeny tracking. These three color-patterns were observed *in vivo* in electroporated cells as shown in **Figure 1D**. To precisely determine cell dilution by proliferation, we performed *in utero* co-electroporation (IUE) at different embryonic stages, with a co-transfection rate of 94.4 ± 0.69% ($n = 4$ mice, 4 slices per brain). At perinatal stages, cells transfected into the LV at E14, produced a large number of labeled neuronal cells (**Figure 2A**). Decomposition in separate channels (red and green, **Figures 2Aa,b**) clearly revealed that neurons located in upper layers expressed both the integrated and non-integrated sequences (upper boxes in **Figures 2Aa,b**). However, the majority of cells located close to the SVZ, as well as those cells ascending to cortical layers, only expressed the integrated green reporter (**Figures 2Aa,b**, lower boxes).

To examine whether these embryonic progenitor cells exhibited distinct cell fate potentials over time, the cell progeny analyses were also performed at mature cortical stages. At P30, cells transfected by IUE at E13 retained the expression of both reporters (**Figure 2B**): EGFP (integrated, **Figure 2Ba**) and mCherry (non-integrated, **Figure 2Bb**). Therefore, layer V cortical neurons exhibited red, green and yellow (combination of both reporters) fluorescence, indicating that the expression of non-integrated sequences remained stable over time in cells generated after a limited number of progenitor divisions. Immunohistochemical analysis was performed using the neuronal marker Tbr1 (T-box brain gene 1), expressed in adult pallial neurons of upper- and lower- cortical layers (**Figures 2Ca–c**), as well as the neuronal nuclei marker, NeuN (**Figures 2Da–c**). Both markers co-localized with green, red and yellow transfected cells verifying the neuronal lineage. To quantify the percentage of cells expressing one or both constructs we analyzed only those mice with IUE at E14 ($n = 4$, and 4 representative sections per animal), to avoid the dilution effect within the neuronal cortical layers. Analysis of the adult labeled cells showed that 82.3 ± 1.6% of the neuronal population expressed both constructs, 9.6 ± 1.5% expressed just the green while the red construct was only expressed in the 8.1 ± 1.5% of neurons (**Figure 2E**).

Additionally, after IUE of integrable and non-integrable plasmids in the dorso-lateral part of the embryonic ventricular zone, labeled cells were located in the adult olfactory bulb (OB), corresponding to interneurons originated at perinatal stages. Those labeled periglomerular and granule cells only expressed the green reporter protein (**Figure 2F**). The unique presence of green positive cells (**Figure 2Fa**), but not red cells (**Figure 2Fb**), clearly indicated that those SVZ progenitors underwent repeated divisions during embryonic stages before being differentiated into OB interneurons.

Expression of Reporter Genes in Neuronal Committed-Lineages after Postnatal Electroporation of Genome-Integrable (EGFP) vs. Non-Integrable (mCherry) Plasmids

To further individually explore the postnatal progeny of precursor cells, co-electroporation of the plasmid mixture was performed into the neonatal SVZ (**Figure 3**). Short-term expression analysis (P6, **Figures 3A–D,I**) revealed an equivalent expression of both integrable and non-integrable reporters. Labeled cells corresponding to either progenitor cells remained within the SVZ (**Figure 3B**), neuroblasts along the rostral migratory stream (RMS, **Figure 3C**) or incoming neuroblasts and immature interneurons within the OB (**Figure 3D**). Those interneurons mostly expressed both constructs after short-term survival times (yellow cells: 68.5 ± 1.5%). Equivalent expressions of both integrable (green cells: 19.6 ± 4.3%) and non-integrable (red cells: 11.9 ± 5%) reporters were determined after quantification analysis (**Figure 3I**). There were not significant differences between the percentage of labeled green and red cells after One-Way ANOVA analyses. Different expression pattern was observed at long-term survival analysis (P30, **Figures 3E–H,J**). In the SVZ, glial-like cells strongly co-expressed both plasmids (**Figure 3F**), suggesting that they did not undergo enough division rounds to lose the non-integrable plasmids. Cell expression of non-integrable (red) plasmids decreased along the RMS cells (**Figure 3G**) that mostly expressed the integrable EGFP plasmid. Besides, OB interneurons co-expressed both plasmids (**Figures 3H,J**; yellow cells: 42.1 ± 4.6%), but since in the RMS the neuroblasts were green labeled, those red positive cells in the OB probably corresponded to the first incoming OB interneurons. This was corroborated after the One-Way ANOVA analysis, showing a significant increment ($P < 0.001$) in the percentage of green OB interneurons in long-term experiments (**Figure 3K**). By contrast there were not significant differences in the percentage of red cells comparing short- and long-term experiments. Thus, those data provided

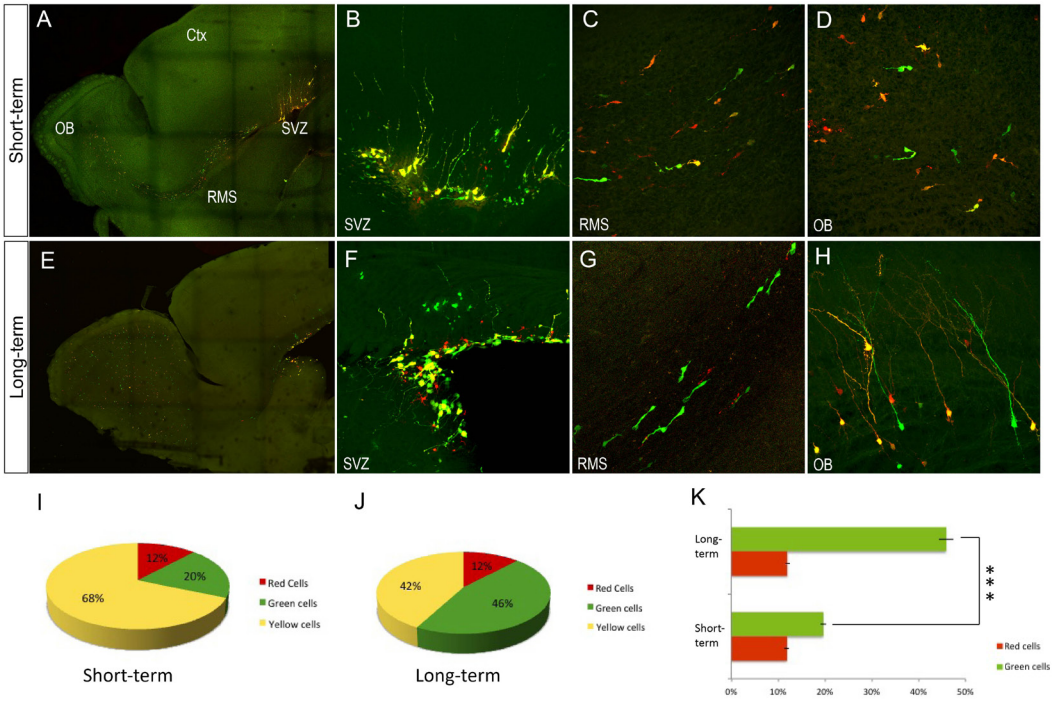

FIGURE 3 | Olfactory bulb interneurons after postnatal electroporation (P1). (A–D) P6 transfected cells expressed the integrated and non-integrated constructs interchangeably. **(B)** In the SVZ, transfected red and green cells showed glial morphology. **(C)** In the rostral migratory stream large cells labeled were directed to the olfactory bulb. **(D)** OB displayed a huge number of neuroblasts in the ependymal zone. **(E–H)** Adult transfected cells. **(F)** In the SVZ glial-like cells co-expressed both plasmids. **(G)** In the RMS migrating neuroblast mostly expressed just the EGFP plasmid (integrated). **(H)** Transfected OB cells co-expressed both constructs. Sagittal sections. **(I–K)** Quantitative analyses after postnatal electroporation (P1). **(I)** Short-term analyses after postnatal electroporation (P1 to P6) showed that OB interneurons mostly expressed both constructs: yellow cells, 68.5 ± 1.5%; green cells, 19.6 ± 4.3% and red cells, 11.9 ± 5%. **(J)** Long term survival times after postnatal electroporation (P1 to P30) showed the following distribution: yellow cells, 42.1 ± 4.6%; green cells, 45.9 ± 3.3% and red cells, 12 ± 3%. **(K)** Increase of green cells in long term analyses. One-Way ANOVA showed a high statistical significance lower that $P < 0.001$ Ctx, cortex; OB, Olfactory bulb; RMS, rostral migratory stream; SVZ, subventricular Zone.

insights into cell fate determination analyses of SVZ progenitor cells.

Tracking Glial Cell Progeny after Electroporation of Genome-Integrable (EGFP) vs. Non-Integrable (mCherry) Plasmids

After embryonic mixture co-electroporation, adult cortical neurons showed an equal expression of both plasmids (**Figure 4A**), whereas glial cells expressed predominantly the green plasmid. Those glial cells were located through upper cortical layers (**Figure 4Aa**), lower cortical layers and within the corpus callosum (**Figure 4Ab**). Those cells expressing just the green reporter protein (**Figures 4Bb,c**) of the integrable construct correspond to mature astrocytes since they co-expressed the S100β marker (**Figure 4Ba**). Thus, ventricular embryonic progenitors underwent a large number of divisions to produce those astrocytes. However, although most oligodendrocytes expressed the green fluorescent protein (integrated construct, **Figures 4Cb**, **Db**) some located within the white matter expressed also the non-integrable red construct (**Figures 4Cc,Dc**). Oligodendrocytic fate of labeled cells was detected by the oligodendrocyte transcription factor, Olig2, and myelin basic protein, MBP (**Figures 4Ca,Da**). PDGFRα positive cells (**Figures 4Ea**, **Fa**) mainly co-expressed the green integrable construct (**Figure 4Eb,c**), although in some cases both constructs were found in groups of PDGFRα positive cells (**Figures 4Fb,c**). Quantitative analysis of the expression of one or both reporter fluorescent proteins was performed separately in both astroglial and oligodendroglial populations. Only cells that displayed typical morphology were included into the analysis. Quantification of adult astrocytes percentage, after IUE at E14, revealed that 99.13 ± 0.19% expressed only the green construct. A low percentage of yellow astrocytes (0.8 ± 0.19%) were co-labeled (**Figure 4G**). No sections with astrocytes expressing only the red non-integrable constructs were found. Quantification of percentage of adult oligodendrocytes, IUE transfected at E14, showed that 93 ± 3.9% expressed just the green construct while 7 ± 3.9% expressed both green integrable and red non-integrable constructs (**Figure 4H**). No red expressing cells were found.

Electroporation of postnatal SVZ progenitors yielded glial cells after several weeks (**Figure 5**). Interestingly, those glial cells,

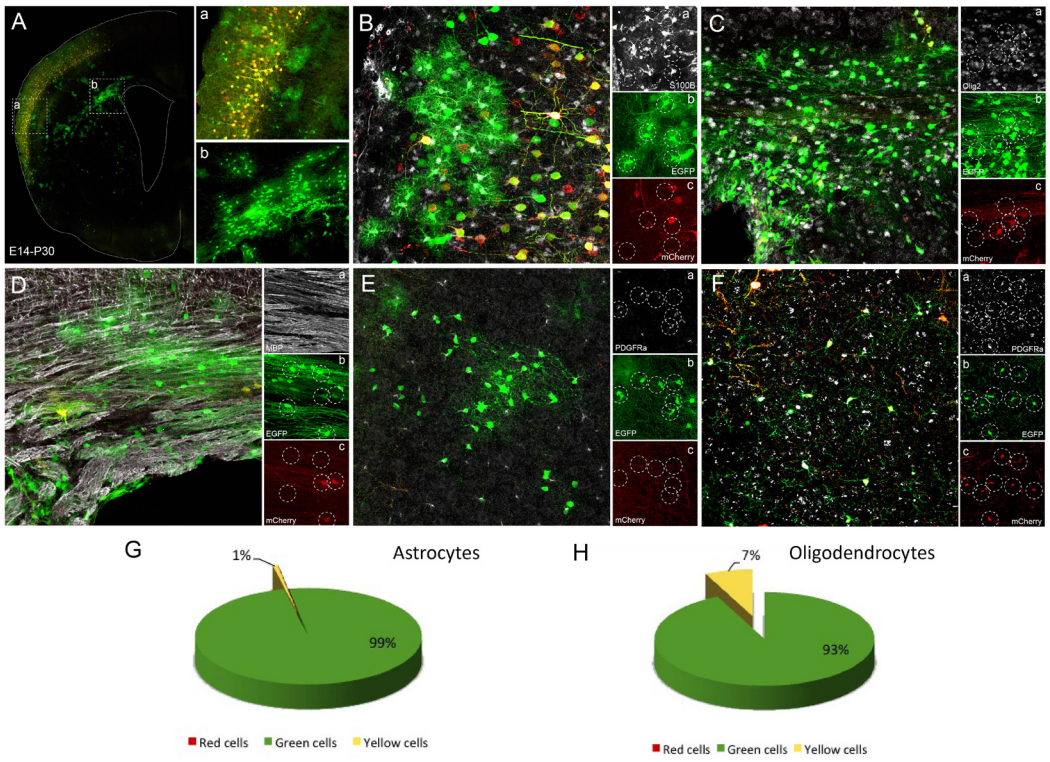

FIGURE 4 | Glial cells labeled after E14 *in utero* electroporation. (A) Coronal section showing a general view of adult transfected cortical cells. (**a**) High magnification of box a showing cortical neurons expressing both constructs while astroglial cells just expressed the integrable construct (green). (**b**) High magnification of lower cortical layers and white matter showing glial cells labeled with green reporter protein corresponding to integrable vector. **(B–F)** Immunohistochemistry to identify the phenotype of transfected labeled cells. **(B)** S100β positive cells **(a)** co-localized only with green transfected cells (integrable construct, **b**), but never with the non-integrable vector (red, **c**). **(C)** Olig2 positive cells **(a)** mostly colocalized with cells expressed the green reporter (integrable construct, **b**) whereas some olig2 positive cells co-expressed the non-integrable construct **(c)**. **(D)** MBP positive cells **(a)** colocalized with cells mostly expressing the integrable construct **(b)**, although some red cells were found **(c)**. **(E)** PDGFRα-positive cells (**a**, NG2 cells) colocalized with transfected cells expressing only the green integrated construct **(b,c)**. **(F)** PDGFRα positive cells **(a)** expressing the integrable and the non-integrable constructs (**b,c**). **(G)** Percentage of adult astrocytes (IUE at E14, analysis P30, $n = 4$ mice, 4 sections per animal) expressing green- (99.13 ± 0.19%) or both constructs (0.8 ± 0.19%). **(H)** 93 ± 3.9% of the adult oligodendroglial cells after IUE at E14 expressed just the green construct while 7 ± 3.9% expressed both constructs.

generated from postnatal precursors, expressed only the integrable construct at P30. After postnatal electroporation into the dorsolateral part of the neonatal SVZ (**Figure 5A**), glial cells were found in the white matter (**Figure 5B**) and within the gray matter both in lower cortical layers (**Figure 5C**) and the striatum (**Figure 5D**). Consequently those glial cells probably arose from SVZ progenitors after a long number of divisions.

Discussion

This work addresses, characterizes and compares the labeled adult cell progeny after postnatal and *in utero* electroporation of different fluorescent reporters. Long-term labeled cells were obtained by the use of the piggyBac transposon system in both cerebral cortex and SVZ-RMS-OB pathway, at embryonic and postnatal mice stages. This provides a useful guide to tracking the cell fate of a specific cell population.

Importance of the Reporter Gene Integration into the Host Genome

The use of piggyBac transposon system ensured the tracking of glial cell populations, which would not be possible without plasmid integration into the genome of transfected cells (García-Marqués and López-Mascaraque, 2012; García-Marqués et al., 2014). Otherwise, the non-integrable fluorescent reporter gene will be lost in successive cell divisions, and the fluorescence will be unequally inherited between daughter cells. Moreover, one of the main challenges faces by *in vivo* gene electroporation is the presence of non-integrable plasmids that remain in an episomal form (Sato et al., 2007). This is of particular relevance to track glial cell lineages or neuronal cells differentiated after a large number of divisions in the adult brain. Our findings indicated that transposable constructs (piggyBac transposon system) are required to achieve the complete integration into the host cell genome, allowing to track those lineages generated after several

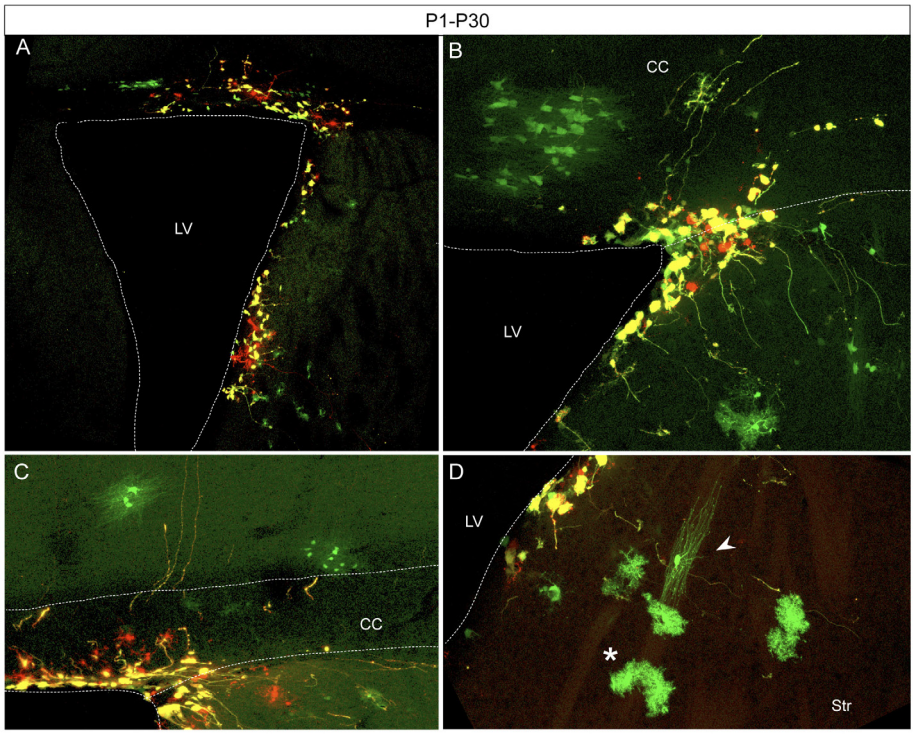

FIGURE 5 | Adult glial transfected cells after postnatal electroporation (P1) (A) Electroporation area showing targeted cells located in the dorso-lateral wall of the lateral ventricle. **(B–D)** Glial cells derived from SVZ progenitors expressed just the integrated construct (green) whereas remaining SVZ-cells highly co-expressed both constructs (yellow). Transfected cells with glial morphology located in the withe matter **(B)**, in lower cortical layers **(C)**, and in the striatum **(D)**. Typical morphologies of astrocytes (**D**, asterisk) and oligodendrocytes (**D**, arrowhead). CC, corpus callosum; LV, Lateral ventricle; Str, striatum.

rounds of divisions. Transfected progenitor cells with an integrable plasmid maintained long-term stable fluorescent reporter expression, while cells containing non-integrable plasmids lost their expression throughout sequential dilution of the reporter by successive cell divisions. Non-integrable plasmids will be only maintained in those cells with a reduced number of divisions. Accordingly, transposon systems have been used to avoid the plasmid dilution and to track all the cell progeny (Yoshida et al., 2010; Chen and LoTurco, 2012; Kita et al., 2013).

Biological Implication of Non-Integrable Plasmids

We evidenced the stable expression of non-integrable plasmids in differentiated cells, several months post-electroporation. Non-integrable plasmids were actively expressed in those cells, as previously reported in RNAi and gene expression analyses (Matsuda and Cepko, 2007; LoTurco et al., 2009). Moreover, the expression of non-integrable genomic constructs persisted in cells generated after a reduced number of divisions. This fact became interesting when the requirement is to label the first cell generation after overexpression/downregulation cell analyses. However, the presence of non-integrable reporter proteins will be negative for other studies such as clonal multicolor analysis from a single cell (García-Moreno et al., 2014; Loulier et al., 2014; Siddiqi et al., 2014). Those color-clonal methods are based on the genomic integration of stochastic combination of fluorescent proteins in each progenitor, maintained throughout the whole progeny. The permanent expression of non-integrated reporter fluorescent proteins in cells generated after few cell divisions will interfere with the specific code of colors of clonally related cells. However, those non-integrable plasmids do not interfere in the analyses of astroglial clones since they are diluted through multiple progenitor cell divisions (García-Marqués and López-Mascaraque, 2012; Martín-López et al., 2013; García-Marqués et al., 2014). This approach, besides to permit the cell tracing, can be extrapolated to other genetic strategies applied to low vs. high dividing cells.

In Vivo Cell Lineage Tracking Depends on the Electroporation Stage

The expression of integrable vs. non-integrable constructs for the same cell lineage was different depending on electroporation stage. Therefore, it is important the electroporation time point correlated with the lineage commitment of the progenitor.

Our cell fate lineage analysis of OB interneurons revealed different results based on whether the electroporation was

performed at embryonic or postnatal stages. SVZ produces neuroblasts that migrate to the OB and differentiate into interneurons throughout perinatal and postnatal life (Altman and Das, 1965; Lois and Alvarez-Buylla, 1994). We highlighted the requirement of the use of integrable constructs to target OB interneurons after IUE, since their OB progenitors undertake a large number of divisions before differentiating to that population (Miller and Gauthier, 2007; Kriegstein and Alvarez-Buylla, 2009). In fact, radial glia cells from the embryonic ventricular zone give rise to cortical cell types and intermediate progenitors before producing OB interneurons (Ming and Song, 2005). At postnatal ages, radial glia transforms into B-cells that first generate C-cells (intermediate progenitors) to finally differentiate into A-cells (neuroblasts) (Doetsch et al., 1997) accomplishing a huge amplification. Nevertheless, we detected that immature OB interneurons and RMS-neuroblasts co-expressed both integrable and non-integrable constructs 5 days after postnatal electroporation. It is not probable that those transfected cells were derived from a B-cell of the postnatal SVZ since lineage progression from B-cells to neuroblast takes in between 3 and 4 days (Ponti et al., 2013). Probably those cells came from the electroporation of advanced intermediate stages cells, such as C-cells or neuroblasts, with a reduced number of divisions to allow the dilution of non-integrate plasmid. Thus, electroporation age (embryonic or postnatal) was important since dilution of non-integrable constructs was related to the lineage-commitment of progenitors. In fact, when RMS- and OB-cells were analyzed 1 month after postnatal electroporation, the number of red cells (non-integrable plasmid) decreased in the RMS, indicating that new generated OB interneurons only expressed integrable plasmids. Indeed, the percentage of green (integrable construct) transfected OB interneurons highly increased at long-term analyses. Time-lapse studies of SVZ progenitors estimate that after the initial division of B1 cells, C cells divide three times and neuroblasts up to 2 times (Ponti et al., 2013). These data correlated with the lack of non-integrable construct in the RMS through time, since those neuroblasts came from SVZ progenitors that divided several times before attaining the neuronal fate. Other authors targeted OB interneurons after 21 days post-electroporation of non-integrable constructs (Fernández et al., 2011), while labeled SVZ- and RMS-cells were lost after 3–4 weeks of postnatal electroporation of non-integrable constructs (Lacar et al., 2010).

In Vivo Lineage Cell Tracking Ultimately Depends on the Cell Identity

Our data indicated that glial cells were mostly green labeled carrying the integrable plasmid either after embryonic or postnatal electroporation. For instance, all the astrocytes expressed only the green construct regardless the stage of electroporation, which provides additional information about the embryonic division pattern of astrocyte-committed lineage progenitors (for review: Wang and Bordey, 2008). According to the postnatal astrocyte generation, precursors of those cells arrive to the final destination and actively proliferate there (Ge et al., 2012). Thus, it is correlated with the lost of non-integrated reporter, due to the elevate rate of cell divisions exhibited in this glial lineage.

Even though, we showed some glial cell populations, as NG2 and oligodendrocytes, which expressed the non-integrable construct, only the integrable reporter labeled the majority. Indeed, our recent data revealed that NG2 cells, form clones comprised by various hundreds of cells in adult brain (García-Marqués et al., 2014). The expression of non-integrated reporters after embryonic electroporation could be explained due to the existence of two main sources (ventral and cortical) of oligodendrocyte progenitors (Kessaris et al., 2006; Richardson et al., 2006). Dorsal electroporated oligodendrocyte-committed progenitors, originated in ventral regions, produce mature oligodendrocytes after fewer divisions than those from cortical regions. That would result in the permanence of the non-integrable reporters. On the other hand, when transfected cells are non-committed progenitors (e.g., radial glia or intermediate progenitors) the oligodendrocytes would differentiate after a larger number of divisions, resulting in the loss of the red non-integrable construct. Our approach will be helpful to address whether a different proliferative origin might be correlated with functional heterogeneity.

Remarkably, after postnatal electroporation of the dorsolateral SVZ, transfected glial cells arranged in groups of a few cells, located throughout the gray matter (lower cortical layers and striatum) and white matter (corpus callosum). Those groups of cells, reduced in number, showed only the integrated green construct suggesting that they originated from amplified precursors, as intermediate progenitors. Furthermore, these electroporated progenitors give rise to interneurons and glial cells through multiple amplification of precursor, since most differentiate cells only expressed the green fluorescent protein. This suggests that the lineage determines the cell division pattern regardless of the progenitor stage, since glial cells are generated from multiple divisions, despite coming from postnatal glial lineage-committed progenitors.

Co-Electroporation of Integrable and Non-Integrable Plasmids as an Indirect Measure of Proliferative Potentials

Clonal studies with retroviral libraries (Levison et al., 1999; Zerlin et al., 2004) showed mixed glial clones originated from postnatal SVZ progenitors. Retroviruses are integrated into dividing cells at the injection site, providing information of the lineages that mitotic cells are going to produce, but not on other non-dividing progenitors lining the ventricle at the injection time. However, electroporation allows the tracking of the whole progeny of both quiescent and mitotic cells lining the ventricle at the electroporation time. Analyses of the SVZ, 30 days after postnatal electroporation, evidenced the presence of a huge number of SVZ labeled cells with a B cell morphology co-expressing both plasmids, since B-cells generated different cell types by asymmetric divisions (Rothenaigner et al., 2011). Probably, those cells remained un-dividing or "short-diving" within the SVZ as they highly expressed both fluorophores. Thus, those cells divided a limited number of times compared to the intermediate progenitors or neuroblasts, which is consistent with the presence of a large number of quiescent neural progenitors in the SVZ (Song et al., 2012).

All together, these results validate the comparison between integrated vs. non-integrated reporters as a method for an indirect measure of the proliferation rate. Comparative expression analyses after embryonic or postnatal co-electroporation in the cerebral cortex and in the SVZ-RMS-OB, showed that neuronal lineages arise from many progenitors in proliferative zones after few divisions. By contrast, glial lineages come from fewer progenitors that accomplish many cell divisions.

Concluding Remarks

The integration into the host genome of the reporter plasmids is required for a successful long-term lineage tracking of glial and OB interneurons generated from both dorso-lateral SVZ embryonic progenitors, as well as postnatal cell populations. Moreover, the use of integrable constructs allows the maintenance of cell labeling within the electroporated area, providing information about the origin of these differentiated cells, essential in ontogenetic and cell migration studies. The use of integrable and non-integrable plasmids is a valuable tool for further exploration of both quiescent cells and cell populations with a high division rate. Stable expression in both neuronal and glial lineages validates the method to track the dividing pattern potential for all brain areas and cell populations. Additionally, our data highlighted the importance of stable and persistent expression of non-integrable fluorescent reporters that remained in both cortical neurons generated at embryonic stages and throughout the postnatal SVZ-RMS-OB pathway. In addition, the comparison of differential expression of integrable and non-integrable plasmids might also be an indirect measure of the relative number of divisions before cell differentiation. Finally, the expression of non-integrated reporters vs. integrated allows studying the heterogeneity of neural populations originated from different proliferative rates.

Acknowledgments

We are grateful to Ana Bribián, Jose Luis Trejo for helpful comments on the manuscript; Daniel Gómez-Domínguez for statistical advice and Lucia Cordobés for technical assistance. This work was supported by research Grant BFU2013-48807-R from the Spanish Ministry of Economy and Competitiveness.

References

Altman, J., and Das, G. D. (1965). Post-natal origin of microneurones in the rat brain. *Nature* 207, 953–956. doi: 10.1038/207953a0

Anthony, T. E., Klein, C., Fishell, G., and Heintz, N. (2004). Radial glia serve as neuronal progenitors in all regions of the central nervous system. *Neuron* 41, 881–90. Available online at: http://www.ncbi.nlm.nih.gov/pubmed/15046721

Asami, M., Pilz, G. A., Ninkovic, J., Godinho, L., Schroeder, T., Huttner, W. B., et al. (2011). The role of Pax6 in regulating the orientation and mode of cell division of progenitors in the mouse cerebral cortex. *Development* 138, 5067–5078. doi: 10.1242/dev.074591

Blanpain, C., and Simons, B. D. (2013). Unravelling stem cell dynamics by lineage tracing. *Nat. Rev. Mol. Cell Biol.* 14, 489–502. doi: 10.1038/nrm3625

Chen, F., and LoTurco, J. (2012). A method for stable transgenesis of radial glia lineage in rat neocortex by piggyBac mediated transposition. *J. Neurosci. Methods* 207, 172–180. doi: 10.1016/j.jneumeth.2012.03.016

Ding, S., Wu, X., Li, G., Han, M., Zhuang, Y., and Xu, T. (2005). Efficient transposition of the piggyBac (PB) transposon in mammalian cells and mice. *Cell* 122, 473–483. doi: 10.1016/j.cell.2005.07.013

Doetsch, F., García-Verdugo, J. M., and Alvarez-Buylla, A. (1997). Cellular composition and three-dimensional organization of the subventricular germinal zone in the adult mammalian brain. *J. Neurosci.* 17, 5046–5061. Available online at: http://www.ncbi.nlm.nih.gov/pubmed/9185542

Fernández, M. E., Croce, S., Boutin, C., Cremer, H., and Raineteau, O. (2011). Targeted electroporation of defined lateral ventricular walls: a novel and rapid method to study fate specification during postnatal forebrain neurogenesis. *Neural Dev.* 6:13. doi: 10.1186/1749-8104-6-13

Franco, S. J., and Müller, U. (2013). Shaping our minds: stem and progenitor cell diversity in the mammalian neocortex. *Neuron* 77, 19–34. doi: 10.1016/j.neuron.2012.12.022

García-Marqués, J., and López-Mascaraque, L. (2012). Clonal identity determines astrocyte cortical heterogeneity. *Cereb. Cortex* 23, 1463–1472. doi: 10.1093/cercor/bhs134

García-Marqués, J., Núñez-Llaves, R., and López-Mascaraque, L. (2014). NG2-glia from pallial progenitors produce the largest clonal clusters of the brain: time frame of clonal generation in cortex and olfactory bulb. *J. Neurosci.* 34, 2305–2313. doi: 10.1523/JNEUROSCI.3060-13.2014

García-Moreno, F., Vasistha, N. A., Begbie, J., and Molnár, Z. (2014). CLoNe is a new method to target single progenitors and study their progeny in mouse and chick. *Development* 141, 1589–1598. doi: 10.1242/dev.105254

Ge, W. P., Miyawaki, A., Gage, F. H., Jan, Y. N., and Jan, L. Y. (2012). Local generation of glia is a major astrocyte source in postnatal cortex. *Nature* 484, 376–380. doi: 10.1038/nature10959

Götz, M., and Huttner, W. B. (2005). The cell biology of neurogenesis. *Nat. Rev. Mol. Cell Biol.* 6, 777–788. doi: 10.1038/nrm1739

Imayoshi, I., Sakamoto, M., and Kageyama, R. (2011). Genetic methods to identify and manipulate newly born neurons in the adult brain. *Front. Neurosci.* 5:64. doi: 10.3389/fnins.2011.00064

Kessaris, N., Fogarty, M., Iannarelli, P., Grist, M., Wegner, M., and Richardson, W. D. (2006). Competing waves of oligodendrocytes in the forebrain and postnatal elimination of an embryonic lineage. *Nat. Neurosci.* 9, 173–179. doi: 10.1038/nn1620

Kita, Y., Kawakami, K., Takahashi, Y., and Murakami, F. (2013). Development of cerebellar neurons and glias revealed by *in utero* electroporation: golgi-like labeling of cerebellar neurons and glias. *PLoS ONE* 8:e70091. doi: 10.1371/journal.pone.0070091

Kretzschmar, K., and Watt, F. M. (2012). Lineage tracing. *Cell* 148, 33–45. doi: 10.1016/j.cell.2012.01.002

Kriegstein, A., and Alvarez-Buylla, A. (2009). The glial nature of embryonic and adult neural stem cells. *Annu. Rev. Neurosci.* 32, 149–184. doi: 10.1146/annurev.neuro.051508.135600

Lacar, B., Young, S. Z., Platel, J.-C., and Bordey, A. (2010). Imaging and recording subventricular zone progenitor cells in live tissue of postnatal mice. *Proc. Natl. Acad. Sci. U.S.A.* 4, 1–16. doi: 10.3389/fnins.2010.00043

Levison, S. W., Young, G. M., and Goldman, J. E. (1999). Cycling cells in the adult rat neocortex preferentially generate oligodendroglia. *J. Neurosci. Res.* 57, 435–46. Available online at: http://www.ncbi.nlm.nih.gov/pubmed/10440893

Lois, C., and Alvarez-Buylla, A. (1994). Long-distance neuronal migration in the adult mammalian brain. *Science* 264, 1053–1224. doi: 10.1126/science.8178174

LoTurco, J., Manent, J.-B., and Sidiqi, F. (2009). New and improved tools for *in utero* electroporation studies of developing cerebral cortex. *Cereb. Cortex* 19(Suppl. 1), 20–25. doi: 10.1093/cercor/bhp033

Loulier, K., Barry, R., Mahou, P., Le Franc, Y., Supatto, W., Matho, K. S., et al. (2014). Multiplex cell and lineage tracking with combinatorial labels. *Neuron* 81, 505–520. doi: 10.1016/j.neuron.2013.12.016

Martín-López, E., García-Marques, J., Núñez-Llaves, R., and López-Mascaraque, L. (2013). Clonal astrocytic response to cortical injury. *PLoS ONE* 8:e74039. doi: 10.1371/journal.pone.0074039

Matsuda, T., and Cepko, C. L. (2007). Controlled expression of transgenes introduced by *in vivo* electroporation. *Proc. Natl. Acad. Sci. U.S.A.* 104, 1027–1032. doi: 10.1073/pnas.0610155104

Miller, F. D., and Gauthier, A. S. (2007). Timing is everything: making neurons versus glia in the developing cortex. *Neuron* 54, 357–369. doi: 10.1016/j.neuron.2007.04.019

Ming, G., and Song, H. (2005). Adult neurogenesis in the mammalian central nervous system. *Annu. Rev. Neurosci.* 28, 223–250. doi: 10.1146/annurev.neuro.28.051804.101459

Nakanishi, H., Higuchi, Y., Kawakami, S., Yamashita, F., and Hashida, M. (2010). piggyBac transposon-mediated long-term gene expression in mice. *Mol. Ther.* 18, 707–714. doi: 10.1038/mt.2009.302

Noctor, S. C., Flint, A. C., Weissman, T. A., Wong, W. S., Clinton, B. K., and Kriegstein, A. R. (2002). Dividing precursor cells of the embryonic cortical ventricular zone have morphological and molecular characteristics of radial glia. *J. Neurosci.* 22, 3161–3173.

Ponti, G., Obernier, K., Guinto, C., Jose, L., Bonfanti, L., and Alvarez-Buylla, A. (2013). Cell cycle and lineage progression of neural progenitors in the ventricular-subventricular zones of adult mice. *Proc. Natl. Acad. Sci. U.S.A.* 110, E1045–E1054. doi: 10.1073/pnas.1219563110

Richardson, W. D., Kessaris, N., and Pringle, N. (2006). Oligodendrocyte wars. *Nat. Rev. Neurosci.* 7, 11–18. doi: 10.1038/nrn1826

Rothenaigner, I., Krecsmarik, M., Hayes, J. A., Bahn, B., Lepier, A., Fortin, G., et al. (2011). Clonal analysis by distinct viral vectors identifies bona fide neural stem cells in the adult zebrafish telencephalon and characterizes their division properties and fate. *Development* 138, 1459–1469. doi: 10.1242/dev.058156

Sakaue-Sawano, A., Kurokawa, H., Morimura, T., Hanyu, A., Hama, H., Osawa, H., et al. (2008). Visualizing spatiotemporal dynamics of multicellular cell-cycle progression. *Cell* 132, 487–498. doi: 10.1016/j.cell.2007.12.033

Sato, Y., Kasai, T., Nakagawa, S., Tanabe, K., Watanabe, T., Kawakami, K., et al. (2007). Stable integration and conditional expression of electroporated transgenes in chicken embryos. *Dev. Biol.* 305, 616–624. doi: 10.1016/j.ydbio.2007.01.043

Siddiqi, F., Chen, F., Aron, A. W., Fiondella, C. G., Patel, K., and LoTurco, J. (2014). Fate mapping by piggybac transposase reveals that neocortical GLAST+ progenitors generate more astrocytes than Nestin+ progenitors in rat neocortex. *Cereb. Cortex* 24, 508–520 doi: 10.1093/cercor/bhs332

Song, J., Zhong, C., Bonaguidi, M. A., Sun, G. J., Hsu, D., Gu, Y., et al. (2012). Neuronal circuitry mechanism regulating adult quiescent neural stem-cell fate decision. *Nature* 489, 150–154. doi: 10.1038/nature11306

Wang, D. D., and Bordey, A. (2008). The astrocyte odyssey. *Prog. Neurobiol.* 86, 342–367. doi: 10.1016/j.pneurobio.2008.09.015

Yoshida, A., Yamaguchi, Y., Nonomura, K., Kawakami, K., Takahashi, Y., and Miura, M. (2010). Simultaneous expression of different transgenes in neurons and glia by combining *in utero* electroporation with the Tol2 transposon-mediated gene transfer system. *Genes Cells* 15, 501–512. doi: 10.1111/j.1365-2443.2010.01397.x

Yusa, K., Rad, R., Takeda, J., and Bradley, A. (2009). Generation of transgene-free induced pluripotent mouse stem cells by the piggyBac transposon. *Nat. Methods* 6, 363–369. doi: 10.1038/nmeth.1323

Zerlin, M., Milosevic, A., and Goldman, J. E. (2004). Glial progenitors of the neonatal subventricular zone differentiate asynchronously, leading to spatial dispersion of glial clones and to the persistence of immature glia in the adult mammalian CNS. *Dev. Biol.* 270, 200–213. doi: 10.1016/j.ydbio.2004.02.024

Conflict of Interest Statement: The authors declare that the research was conducted in the absence of any commercial or financial relationships that could be construed as a potential conflict of interest.

CHAPTER 2

UbC-StarTrack, a clonal method to target the entire progeny of individual progenitors. Figueres-Oñate, M., Garcia-Marques, J. and López-Mascaraque, L. (2016). *Scientific Reports doi.10.1038/srep33896 (In Press).*

Once we tested the behavior of ubiquitous constructs, we had the tools to design the Ubiquitous-StarTrack clonal methodology. The principle of this clonal method is the permanence of the same color-code combination in single progenitors and their progeny, independently of their lineages. Sibling cells acquire the progenitor fluorescent combination, regardless of the mitotic activity or the fate of generated cells. Therefore, our previous data comparing the labeled populations with integrable vs. non-integrable fluorescent reporters were important in the design of the present approach for two reasons. First, to obtain labeling in populations generated after a long number of divisions, the ubiquitous constructions should include piggyBac integrable regions. Second, the non-integrated constructs by the piggyBac transposase should be inhibited to maintain the same color-combination in the entire cell progeny, avoiding the interference with the clonal color combinations. Consequently, sibling cells are just defined by the color code provided by the genomic integrated fluorescent reporters. To address this issue we incorporated the Cre-LoxP strategy. A tamoxifen inducible Cre was used to inhibit the non-genomic integrated constructs by the piggyBac transposase, resulting in a stable and heritable clonal labeling for all sibling cells.

The generation of the UbC-StarTrack approach is presented in the second publication included in this thesis work "UbC-StarTrack, a clonal method to target the entire progeny of individual progenitors". One of the most remarkable potentials of this approach is the high number of theoretical color combinations obtained after the electroporation of the six different fluorescent proteins expressed either in the cell nucleus or in the cytoplasm. Those twelve constructs were successfully tested either in vitro, ex vivo or in vivo. Moreover, an in vivo analysis of the fluorophores revealed the concurrence of fluorescent reporters expression, intensity ranges and frequency of the different combinations. Altogether, UbC-StarTrack is a clonal method that can help to answer many questions in the field of stem cell biology.

De: SciRep.Production@nature.com
Fecha: 8 de septiembre de 2016, 19:04:49 CEST
Para: mascaraque@cajal.csic.es
Asunto: A proof of SREP article SREP33896

Dear Dr Laura Lopez-Mascaraque,

Your article proof has been submitted for correction. We will contact you should we have any further questions.

The publication date for your article will be scheduled at the end of the production process, 4 working days prior to the article going online. We will contact you with further information at this point.

If your press office is planning to send out a press release for your work we do ask that they don't send anything out until we have confirmed a publication and embargo time with the corresponding author on your paper. For any queries regarding press releases, please contact press@nature.com.

Scientific Reports Production
Scirep.Production@nature.com

SCIENTIFIC REPORTS

OPEN

UbC-*StarTrack*, a clonal method to target the entire progeny of individual progenitors

Received: 31 May 2016
Accepted: 05 September 2016
Published: xx xx xxxx

María Figueres-Oñate, Jorge García-Marqués† & Laura López-Mascaraque

Clonal cell analysis defines the potential of single cells and the diversity they can produce. To achieve this, we have developed a novel adaptation of the genetic tracing strategy, UbC-*StarTrack*, which attributes a specific and unique color-code to single neural precursors, allowing all their progeny to be tracked. We used integrable fluorescent reporters driven by a ubiquitous promoter in PiggyBac-based vectors to achieve inheritable and stable clonal cell labeling. In addition, coupling this to an inducible Cre-LoxP system avoids the expression of non-integrated reporters. To assess the utility of this system, we first analyzed images of combinatorial expression of fluorescent reporters in transfected cells and their progeny. We also validated the efficiency of the UbC-*StarTrack* to trace cell lineages through *in vivo*, *in vitro* and *ex vivo* strategies. Finally, progenitors located in the lateral ventricles were targeted at embryonic or postnatal stages to determine the diversity of neurons and glia they produce, and their clonal relationships. In this way we demonstrate that *UbC-StarTrack* can be used to identify all the progeny of a single cell and that it can be employed in a wide range of contexts.

In the brain, groups of clonally related cells are responsible for forming all the adult neural circuits. Thus, clonal analys1is of single cells is a powerful means to understand how neural cells acquire their identity and functional differences. There is currently much controversy regarding the commitment and heterogeneity of neural progenitors. Classical theory considered the radial glia as the main neural stem cell capable to generating all neural cell types[1]. More recently, other neural progenitors are thought to be committed to certain cell lineages and to generate distinct neural progeny at specific developmental times[2]. Thus, it is crucial to understand the broad heterogeneity of progenitor pool and to be able to distinguish the progeny of an individual progenitor from the rest of the cells in the brain.

Retroviral vectors carrying a single reporter gene were able to show that radial glia cells are indeed a common progenitor for both glial and neuronal cells[3]. In addition, this tool has been also used to elucidate clonal relationships between neurons[4]. Other clonal methods employed isolated recombination in stochastic cells involving different transgenic lines, as mosaic analysis with double markers[5,6]. However, since these approaches label a small number of clonally related cells, they are not entirely appropriate to analyze inter/intra-clonal relationships. To perform larger and more reliable clonal analyses, libraries of tagged retroviruses have been designed[7]. Alternatively, other approaches to identify clonally-related cells rely on somatic mutations during the DNA replication, associated with cell division[8], or on genetic multicolored cell labeling using either transgenic animals or infection with fluorescent lentivirus[9–11]. Recently, multicolor non-viral PiggyBac transposon mediated genomic integration has proved to be a very useful tool to define progeny at the single cell level[12–14] Indeed, we previously designed the *StarTrack* strategy in order to study clonally related astroglial cells that are derived from single progenitors using the hGFAP promoter[15,16]. Here we present a novel adaptation of that system, UbC-*StarTrack*, to perform clonal analysis and tracing of neural cell types derived from single progenitors. Unlike other lineage approaches, our ubiquitous lineage-tracing method avoids the expression of non-integrated copies of electroporated plasmids, taking advantage of the Cre-lox strategy to achieve unequivocal labeling of the entire progeny of single progenitors. Indeed, the strategy behind this method represents an exciting tool for other areas in the field of biomedicine, avoiding the use of genetically engineered mouse models.

Instituto Cajal, CSIC, Madrid, Spain. †Present address: HHMI, Janelia Research Campus, VA, USA. Correspondence and requests for materials should be addressed to L.L.-M. (email: mascaraque@cajal.csic.es)

Results

UbC-*StarTrack* multicolor labeling for single-cell clonal tracking. UbC-*StarTrack* is based on the combination of six different fluorescent reporter proteins (XFPs) cloned into integrable, floxed and ubiquitous constructs (Ubiquitin C, UbC): mT-Sapphire, a UV-excitable monomeric GFP mutant XFP with a large stokes shift; mCerulean, the brightest monomeric fluorescent cyan protein; EGFP, a weak dimer enhanced green fluorescent protein; YFP, weak dimer yellow fluorescent protein widely used; Kusabira Orange (mKO), the brightest orange monomer; mCherry, a photostable red monomer. The appropriate spectral separation of these fluorophores allows the independent confocal acquisition of photostable XFPs with minimal overlap (Fig. 1A). These XFPs were designed to be expressed in the cytoplasm, either in the absence of any specific cell signaling (Fig. 1B) or by fusing the microtubule associated TAU protein to the different XFP constructs to facilitate cell identification (UbC-TAU·*StarTrack*: Fig. 1C). In order to obtain more diversity of clonal markers and further increase the possible combinatorial events in a single cell, the XFPs were also fused to histone H2B to promote their nuclear expression (UbC-H2B·*StarTrack*: Fig. 1D). To achieve heritable and stable labeling of the cell progeny, co-electroporation of two additional constructs was necessary, these expressing the hyperactive transposase of the PiggyBac system (hyPBase) and Cre-recombinase fused to a tamoxifen-inducible mutated estrogen receptor ($CreER^{T2}$, Fig. 1E). To attain efficient expression in all neural types, ubiquitous promoters drove the expression of both the hyPBase and Cre enzymes. As such, a mixture of these fluorescent constructs can be co-electroporated and stochastically integrated into each progenitor, generating unique color codes.

Stable and heritable targeting strategy. Regarding the division pattern of transfected progenitor, non-integrated constructs might gradually be diluted by successive cell divisions or may be episomally maintained, affecting the clonal code of single-cell progeny. Glial cells divide repeatedly before their final differentiation, leading to the dilution of episomal plasmids reflecting just the fluorescence of integrated constructs. However, electroporated progenitors committed to the neuronal lineage undergo few cell divisions and thus, little dilution of episomal plasmids will occur, interfering with the clonal analysis[17]. To obtain a stable clonal mark, XFPs were cloned within an integrable region flanked by two terminal repeats (TRs) that are recognized by the PiggyBac transposase (Fig. 1F, purple arrows). In addition, to perform an indubitable clonal cell analysis, we inhibited the potential residual episomal plasmids (the copies not integrated by the transposase) using the tamoxifen (Tx) inducible Cre-Lox system. The Cre-recombinase recognizes and cleaves the region flanked by two LoxP-sites strategically inserted into the UbC-*StarTrack* constructs. After Tx administration, Cre cleaves the fluorescent reporter genes flanked by the LoxP-sites in the episomal copies that have not been integrated into the genome (Fig. 1G). When hyPBase driven integration does occur, one LoxP site flanking the XFP is deleted (Fig. 1F) to ensure that $CreER^{T2}$ does not affect the expression of the XFPs incorporated into the host genome.

The efficiency by which the Cre-LoxP strategy prevents the labeling of non-genomic constructs was tested by *in utero* co-electroporation (IUE) of $CreER^{T2}$ in the presence and absence of hyPBase. In addition, a ubiquitous EGFP plasmid (UbC-$EGFP^{flox}$) flanked by LoxP sites and a ubiquitous non-floxed and non-integrable mCherry encoding plasmid (UbC-mCherry) were co-electroporated. The UbC-mCherry plasmid was used as a control vector given that it is not integrated into the genome by hyPBase and $CreER^{T2}$ does not inhibit it. After IUE of UbC-$EGFP^{flox}$, UbC-mCherry and $CreER^{T2}$ alone, without hyPBase, the plasmids remained as episomal copies. As such, when Tx was not administered, green and red fluorescence was evident in neurons but not in glial cells (Fig. 1H), whereas Tx administration resulted in the lack of green fluorescent labeled cells. Thus, tamoxifen induction of $CreER^{T2}$ prevented the UbC-$EGFP^{flox}$ expression (Fig. 1I).

Finally, the UbC-$EGFP^{flox}$, UbC-mCherry, hyPBase and $CreER^{T2}$ constructs were co-electroporated to confirm that $CreER^{T2}$ activation had no effect on the normal EGFP expression after integration. Ten days after Tx induction, cells with a glial morphology that expressed GFP but not RFP were evident in the corpus callosum of adult brains (Fig. 1J), corroborating hyPBase activity. The presence of green labeled cells (Fig. 1J) in cortical layers indicated that tamoxifen-activated $CreER^{T2}$ had no effect on the expression of integrated UbC-$EGFP^{flox}$ constructs, only on the episomal copies (Fig. 1I). Thus, after IUE of UbC-*StarTrack* mixtures and subsequent Tx administration, the fluorophores used were stable and lineage tracing could be performed over either short (4 days post-IUE: Fig. 1K) or longer periods (8 months post-IUE: Fig. 1L).

UbC-StarTrack *in vitro* and *ex vivo*. To *in vitro* analyze the transfection capability and stability of the different UbC-*StarTrack* variants (Fig. 1B–D) a mixture containing the six XFPs of each group was co-transfected into cultured HEK cells (Fig. 2A–D). Fluorescent reporters signal from each UbC-*StarTrack* mixture were analyzed one-day post-transfection. UbC-*StarTrack* and UbC-TAU·*StarTrack* constructs were uniformly expressed in the cell cytoplasm (Fig. 2A,B). By contrast, UbC-H2B·*StarTrack* reporter gene expression was exclusively expressed in the cell nucleus (Fig. 2C), contributing to the clonal cell identity but without providing morphological information about any cell type. Thus, the six different variant XFP constructs were brightly and stable *in vitro* expressed in the appropriate cell location. Transfections combining different sets of constructs were performed to confirm their co-expression in the same cell at the accurate cell compartment. Moreover, suitable transfection of the different DNA mixtures was obtained in the oligodendroglial precursors cell line Oli-Neu (data not shown).

Each UbC-*StarTrack* construct that expressed a XFP was electroporated into HEK cells independently, to determine the minimal spectrum separation with the confocal acquisition parameters employed. Their spectra led to the ordering of the fluorophores as mT-Sapphire, mCerulean, EGFP, YFP, mKO and mCherry, and they were successfully excited with five different confocal laser lines: 405, 456, 488, 514 and 561 nm. To avoid spectral overlap, emission wavelengths were chosen as close as possible to the peak spectrum, with a range of 10 nm for each XFP. When acquired individually, the electroporated XFPs gave a fluorescent signal in the channel

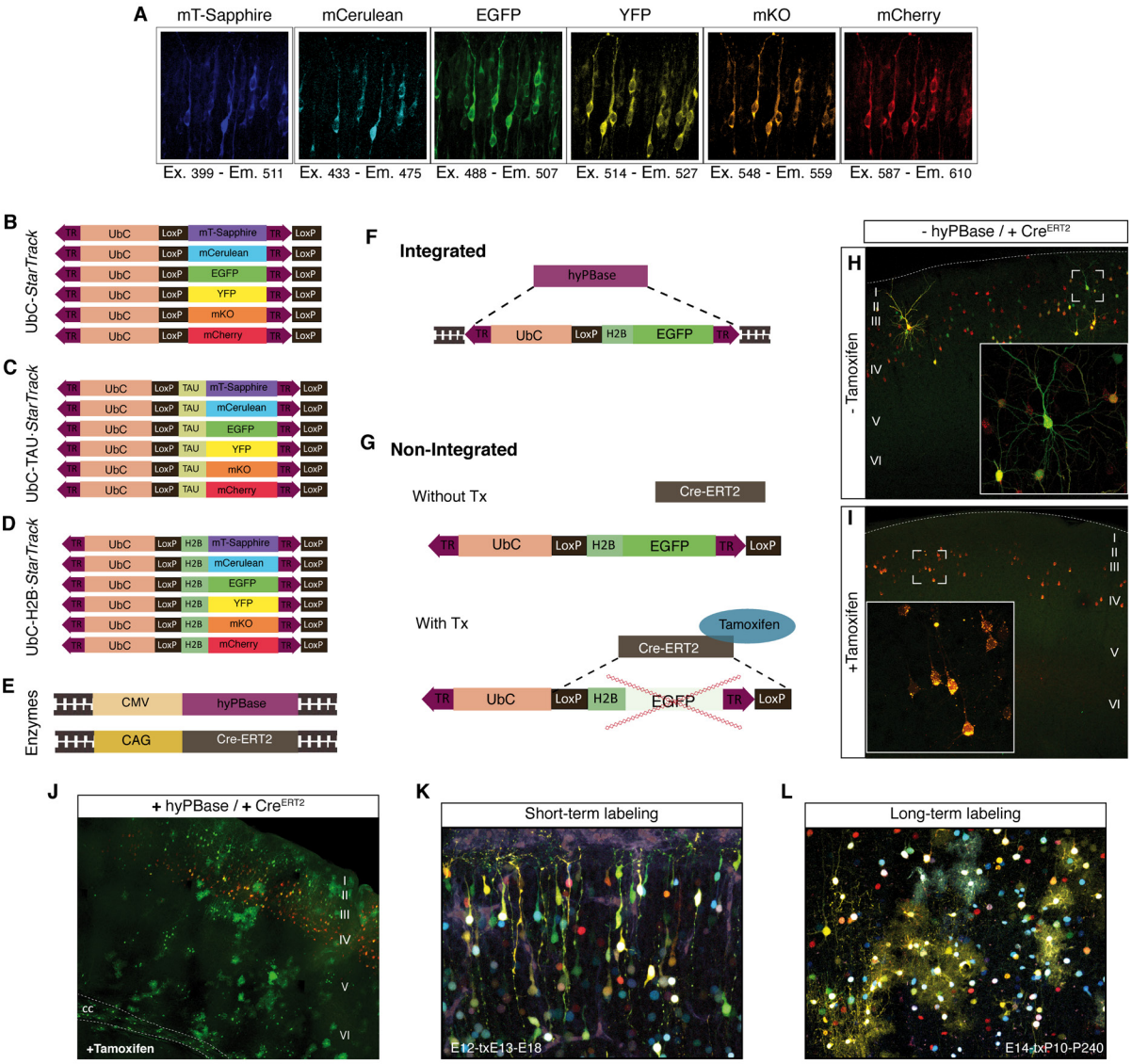

Figure 1. UbC-*StarTrack* design. (**A**) Fluorescent reporters: mT-Sapphire, mCerulean, Enhanced green fluorescent protein (EGFP), Yellow fluorescent protein (YFP), monomeric Kusabira Orange (mKO) and mCherry. Spectral profiles for the single fluorophores: Ex, Major excitation peak; Em, Major emission peak. (**B**) Scheme of the six ubiquitous constructs with the different fluorescent proteins expressed in the cytoplasm: UbC-*StarTrack*. (**C**) Scheme of the six constructs with the different TAU-fluorescent fusion proteins: UbC-TAU·StarTrack. (**D**) Scheme of the six ubiquitous constructs encoding the different H2B-fluorescent fusion proteins: UbC-H2B·StarTrack. (**E**) Hyperactive version of the PiggyBac transposase (hyPBase) and an inducible Cre recombinase (Cre-ER^{T2}) were added to the UbC-*StarTrack* electroporation mixture. Ubiquitous promoters drove the expression of both constructs. (**F**) hyPBase introduces several copies of constructs into the cell genome after electroporation. (**G**) Cre recombinase activated by tamoxifen (Tx) deletes the episomal copies of vectors (not integrated by the transposase). (**H**) IUE (E14) of UbC-EGFP^{flox}, UbC-Cherry and CreER^{T2} in the absence of the transposase (hyPBase). Without Tx administration, brains processed at P20 displayed green and red-labeled cells. (**I**) IUE (E14) of UbC-EGFP^{flox}, UbC-Cherry and CreER^{T2} in the absence of transposase (hyPBase). After Tx administration, there were no traces of the GFP protein in brains processed at P20. CreER^{T2} activation by Tx successfully inhibits floxed non-integrated constructs. (**J**) Co-electroporation of CreER^{T2}, UbC-EGFP^{flox} and UbC-mCherry in the presence of the hyPBase. Genomic integration of EGFP floxed plasmids permanently labels cells with a high rate of division. Green cells, corresponding to glial lineages located within the corpus callosum (cc) and cortical areas. (**K**) Short term labeling following Tx administration one day after IUE (E12) of the UbC-TAU·*StarTrack* mixture and analyzing the brains five days later. (**L**) After UbC-*StarTrack* and UbC-H2B·*StarTrack* IUE (E12), fluorescent reporters remained brightly expressed 8 months later (P240) having administered Tx to pups at P10.

designated to each particular fluorophore (Fig. 2D), and each of the XFPs provided separate fluorescent signals, with the exception of YFP. Indeed, complete spectral separation between YFP and mKO was not possible under the confocal laser conditions employed.

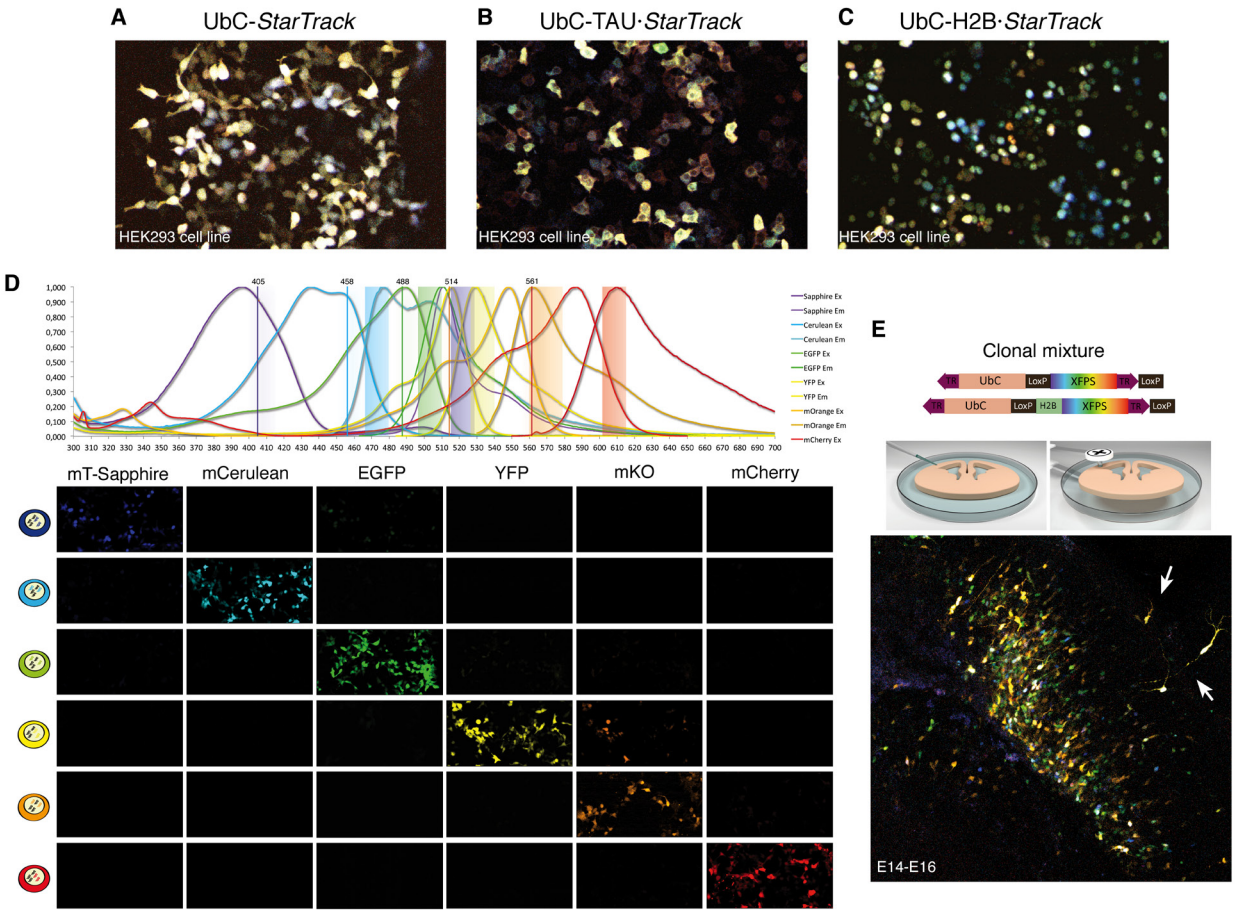

Figure 2. ***In vitro*** **and** ***ex vivo*** **transfection of the UbC-StarTrack variants.** (**A–C**) Newly generated UbC-*StarTrack* (A), UbC-TAU·*StarTrack* (**B**) and UbC-H2B·*StarTrack* (**C**) constructs were transfected to HEK cells *in vitro* and fluorescent signals were acquired 1 day after transfection. (**D**) Fluorescent spectra of the different fluorescent reporters under the specific confocal acquisition settings. Each fluorescent protein was electroporated individually and its expression was recorded in all confocal channels. Fluorescent expression was only acquired in the designated channel, except for YFP that displayed weak fluorescence in the mKO confocal channel. (**E**) UbC-*StarTrack* and UbC-H2B·*StarTrack* were suitable to perform *ex vivo* clonal analyses after electroporation of the ubiquitous mixture into E14 brain slices since labeled cells migrated out of the area electroporated after 2 days in culture (arrows). *3D-draw provided by Lluis Fortes-Marco.*

To further determine the viability and stability of these constructs for *ex vivo* experiments, we co-transfected the six UbC-*StarTrack* and the UbC-H2B·*StarTrack* variants into the subventricular zone (SVZ) of embryonic brain slices. After 48h, labeled cells were located within the SVZ, and clonal cells were dispersed throughout the lower cortical layers (Fig. 2E), while some cells appeared to be migrating to other cortical layers (Fig. 2E, arrows).

In vivo **analysis of UbC-*StarTrack*.** *Exploring combinatorial possibilities of UbC-StarTrack.* The UbC-*StarTrack* strategy appeared to be a powerful tool to accurately define individual clones, since there are about four thousand theoretical combinations of the 12 fluorescent constructs. To analyze the combinatorial capacity of the XFPs *in vivo*, images from five different IUE animals were analyzed at adult stages (Fig. 3). Since we sought to analyze the combinatorial color possibilities of the construct mixture and the prevalence of XFPs, mice were subjected to IUE on different developmental days from E11 to E14. Adult brains were analyzed with an ImageJ macro designed for this purpose, evaluating 4–6 mosaic images of electroporated areas from each animal. The XFP combinations in 6,690 cells from 5 different animals were analyzed, and clones with a large number of sibling cells (>40) were ruled out in order to prevent clone-size producing a bias in the combinatorial analysis.

Initially, we set out to elucidate the variation in the fluorescence intensity of each fluorophore. The ImageJ macro allowed the minimum threshold values of the fluorescence to be identified, avoiding the inclusion of background noise as a false positive signal in the analysis. Intensity values from 8-bit images were stored in the range 0 to 255 (Fig. 3A) and after sampling the images, the lowest intensity considered to be XFP expression was >20. The XFP with the broadest distribution was mT-Sapphire, exhibiting the widest range of values, while the maximum intensity from the images analyzed corresponded to YFP. The XFP with the lowest fluorescence intensity was mCerulean, with a maximum value of 156, and it was followed by mKO at 178 (Fig. 3A). Both XFPs (mCerulean and mKO) were expressed in an intensity range of 20–50 in more than the 50% of positive cells. In terms of the

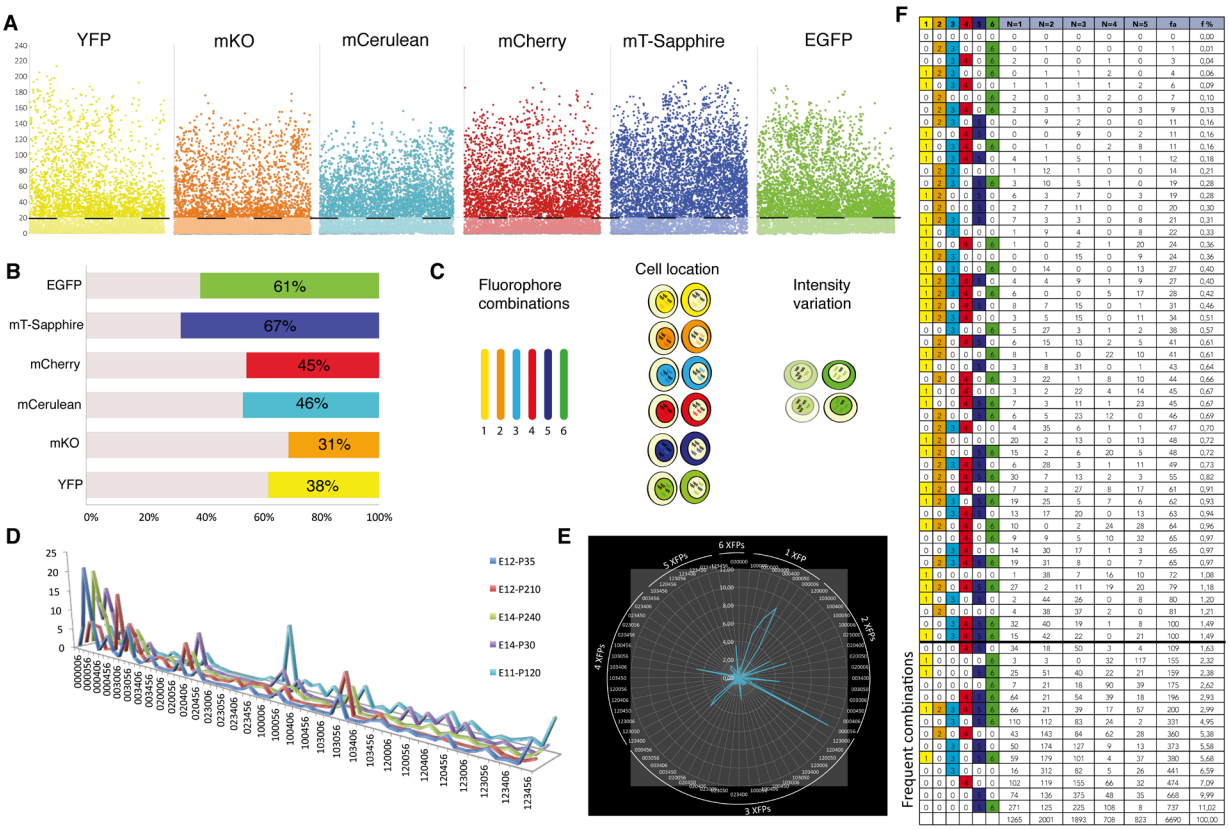

Figure 3. Image analyses of transfected cells. (**A**) Intensity of selected fluorescent reporters within a range of 0–255 in cells analyzed from 8-bit images; a value > 20 was considered to be positive. (**B**) Proportion of positive cells for each fluorescent protein among the 6,690 analyzed (N = 5). (**C**) Combinatorial analysis of the six fluorescent reporters results in 64 possible combinations. Fluorophore location (nuclear vs. cytoplasmic) increases the number of theoretical combinations to 4,096. Since sibling cells must express the fluorophore in the same range of intensity, by simply considering two different groups of intensity the theoretical combinations ascend exponentially to more than 16 million. (**D**) Relative peaks of fluorescent reporter combinations in each individual animal (n = 5). (**E**) Frequency values combining one, two, three, four, five or six fluorophores in the cells analyzed (n = 6,690). (**F**) Raw data analyses showing fluorophore combination per animal. Frequent combinations (at the bottom of the table) were those that less accurately defined sibling cells.

proportion of cells analyzed that expressed each fluorophore, mT-Sapphire and EGFP were the XFPs most often detected (Fig. 3B), expressed by more than 60% of the 6,690 cells analyzed with a signal. Conversely, mKO was expressed by the lowest number of positive cells, only 30% of those with a fluorescent signal.

We then examined the combinatorial events of the six fluorophores expressed in those 6,690 analyzed cells. Our macro translated these combinations into a six number code, indicating a positive (> = 20) or negative (<20) signal for each fluorophore (Fig. 3C). The order of XFPs in the color code was determined by the confocal acquisition parameters (1-YFP; 2-mKO; 3-mCerulean; 4-mCherry; 5-mTsaphire; 6-EGFP; 0-represented absence of a fluorescent signal). Just considering the six XFPs, UbC-*StarTrack* provided 64 combinations, although the scope of the method was wider as the fluorophores could be located in either the nucleus or cytoplasm, ascending the number of theoretical combinations to 4,096. Moreover, as hyPBase integrates a variable number of plasmid copies, fluorophore intensity was another parameter that should remain within a similar range among sibling cells, exponentially increasing the possible number of combinations. The color-code frequency was performed analyzing the number of times that each 64 possible combination appeared within the macro data. The maximal peak of each combination differed between animals, corroborating the stochastically assignation of color-codes (Fig. 3D). Besides, ordering the codes by linking one, two, three, four, five or the six fluorophores, produced different peaks in specific combinations, the bulk clustered in in combinations of one or two XFPs (Fig. 3E). As hyPBase integrates a variable number of constructs, each combination theoretically has the same probability of being present, yet some combinations were more prevalent than others. Since we analyzed 64 possible fluorophore combinations, a relative frequency around 1.56% indicated equal probability, although 14 combinations of fluorophores had a higher probability than this (Fig. 3F). Single fluorophores or associations of fluorophores with similar spectra (e.g., mCherry-mKO or mT-Sapphire-EGFP) were the most frequent color combinations. The blending of the six XFPs was also very recurrent. Thus, less probable color codes were better candidates to define sibling cells than those with higher probabilities.

In vivo co-electroporation of UbC-StarTrack. Cell dispersion analyses of the different UbC-*StarTrack* mixtures were performed *in vivo* at both at embryonic and adult stages (Fig. 4A). After IUE of the UbC-TAU·*StarTrack* mixture (Fig. 1C), labeling appeared in both radial glial cells and SVZ progenitors at perinatal stages. Moreover, transfected immature neurons were located in upper and lower cortical layers (Fig. 4B). At adult stages, TAU-fused fluorescent protein was expressed accurately in both neuronal (Fig. 4C, arrowheads) and glial lineages (Fig. 4C, asterisks). Five months after IUE, large glial cell clusters comprised of sibling cells were recognizable by the expression of the same combination of XFPs (Fig. 4D,E). Cells were morphologically identified as either cortical NG2 cells (Fig. 4D) or white matter oligodendrocytes (Fig. 4E). Thus, TAU-fused fluorescent protein proved to be a good option to track and morphologically identify cells. After UbC-*StarTrack* IUE (Fig. 1B), the cytoplasmic expression of XFPs allowed different cell morphologies to be characterized (Fig. 4F,G). At perinatal stages, radial glia cells with their processes contacting the pial surface were evident morphologically and immature neurons occupied upper and lower cortical layers (Fig. 4F), whereas both neurons (Fig. 4G, arrowhead) and glial cells (Fig. 4G, asterisks) were successfully tracked at adult stages. Nuclear constructs (UbC-H2B·*StarTrack*: Fig. 1D) were designed to increase the number of fluorescent labels, resulting in larger combinations of fluorophores to ensure clonal coding. IUE of the plasmid mixture did not allow the morphological identification of cells at either perinatal (Fig. 4H) or adult stages (Fig. 4I). Thus, to elucidate the theoretical increment of XFP combinations necessary for clonal analyses, UbC-H2B·*StarTrack* was combined with either UbC-*StarTrack* or UbC-TAU·*StarTrack*. Co-electroporation of nuclear plasmids with the UbC-TAU·*StarTrack* resulted in a reduction in the TAU-fused fluorescent protein signal (Fig. 4J). Since the nuclear fluorescence was much brighter than the intensity of TAU fluorescence, the confocal conditions limited adequate signal acquisition of both reporters. By contrast, co-electroporation of UbC-*StarTrack* and UbC-H2B·*StarTrack* resulted in successful expression of both reporters, maintaining the cytoplasmic label along with the valuable information provided by the nuclear marker (Fig. 4K). As such, this latter combination was the strategy selected to further define clonally-related cells. Moreover, ubiquitous constructs were co-electroporated with the GFAP-*StarTrack* constructs[15], in order to probe the extended potential and applications of this tool, combining different expression vectors under the control of different promoters (Fig. 4L).

UbC-StarTrack to target different cell lineages in distinct brain areas. The IUE of nuclear and cytoplasmic UbC-*StarTrack* mixtures allowed glial and neuronal lineages to be tracked. Sibling cells were defined by the same composition of fluorophores, both in the same cell location and range of intensity (Fig. 5). Cells were identified as neurons, astrocytes, oligodendrocytes and NG2 cells according to morphological criteria, and using immunohistochemistry for specific cell type markers (data not shown). To identify clonally-related cells, we performed a qualitative cell analysis based on the color combination and fluorophore cell location (nuclear or cytoplasmic). Different UbC-*StarTrack* labeled cortical clones were easily recognizable by their different fluorescent reporter combinations (Fig. 5Aa). To assess the color-code of each clonal cell, the expression of every fluorophore was individually analyzed (Fig. 5Aa1–4). Then, to further address the clonal cell identity, we quantified the fluorophore intensity in each cell with the same color-code (Fig. 5B–F). These parameters were necessary to accurately define a clone. Since the first cell generated after IUE were neurons, the inhibition of non-integrated plasmids was critical to obtain the same clonal code for all the neuronal progeny. Neurons expressing the same nuclear and/or cytoplasmic combination of fluorophores in the same range of intensity clearly maintained clonal relationships (Fig. 5B). Indeed, it was possible to observe two nearby cells that were not clonally related (blue and green labels in Fig. 5B), since they differed in terms of the YFP, mKO and mCherry fluorescent proteins locations (nuclear and cytoplasmic vs. only cytoplasmic). Moreover, in this case fluorophore intensity variation between sibling neurons was up to 40-points (Fig. 5B, graph).

While clonally related sister neurons were arranged sparsely and rarely grouped in the same domain (Fig. 5B), glial clones produced a variable number of densely arranged cell clusters depending on the cell lineage (Fig. 5C–E). As such, UbC-*StarTrack* allowed the identification of various clones from different glial lineages, even when were located close together (Fig. 5A,C). The number of clonally related sibling astrocytes (Fig. 5C) was lower than that of oligodendrocytes and NG2 cells (Fig. 5A,D,E). After we defined the fluorophore composition of adult labeled cells, the intensity values established their clonal identity. For example, two different astrocyte clones in Fig. 5C (blue and yellow numbered clones) were discriminated by both fluorophore expression and intensity values (Fig. 5C, graph). Besides, UbC-*StarTrack* allowed to trace the oligodendroglial lineage (Fig. 5D). Large numbers of sibling oligodendrocytes were located within the corpus callosum in adult brains (Fig. 5D). Following IUE with the clonal mixture, NG2 sibling cells formed huge clones throughout adult olfactory bulb layers (Fig. 5E), as described previously with *StarTrack*[16]. In those cases, cell clones were clearly defined not only by color-codes but intensity values (Fig. 5D,E, graphs). Interestingly, the relationship between fluorophores and intensities was likewise maintained within mixed clones formed by cells from different lineages (Fig. 5F). At perinatal stages, immature astrocytes and neurons were clonally-related with the same color-codes and fluorophores intensity values (Fig. 5F yellow and green clones). We highlighted that fluorophore intensity variation was less than 150 points within analyzed sibling cells, independently of their lineage. This demonstrated certain variation in the clonal behavior of neuronal and glial populations and indeed within glial populations, the astrocyte clones were smaller than those of NG2 cells or oligodendrocytes.

UbC-*StarTrack* and UbC-H2B·*StarTrack* co-electroporation (Fig. 6A) tracked neural populations located in diverse brain areas depending on both the orientation of the electrodes and the embryonic stage of targeted progenitors (Fig. 6B–F). Adult neurons were located in their corresponding cortical layers, after E13 electroporation with the positive electrode oriented towards the dorsal pallium (Fig. 6B). Otherwise, glial clones occupied several cortical layers, corpus callosum and SVZ (Fig. 6Ba,b). To trace cell lineages in the adult piriform cortex (Fig. 6C), IUE was performed before E12, placing the electrodes laterally to target the lateral cortical stream. Either neurons or glial cells were labeled in this cortex (Fig. 6Ca). Different extracortical brain areas were labeled after IUE at

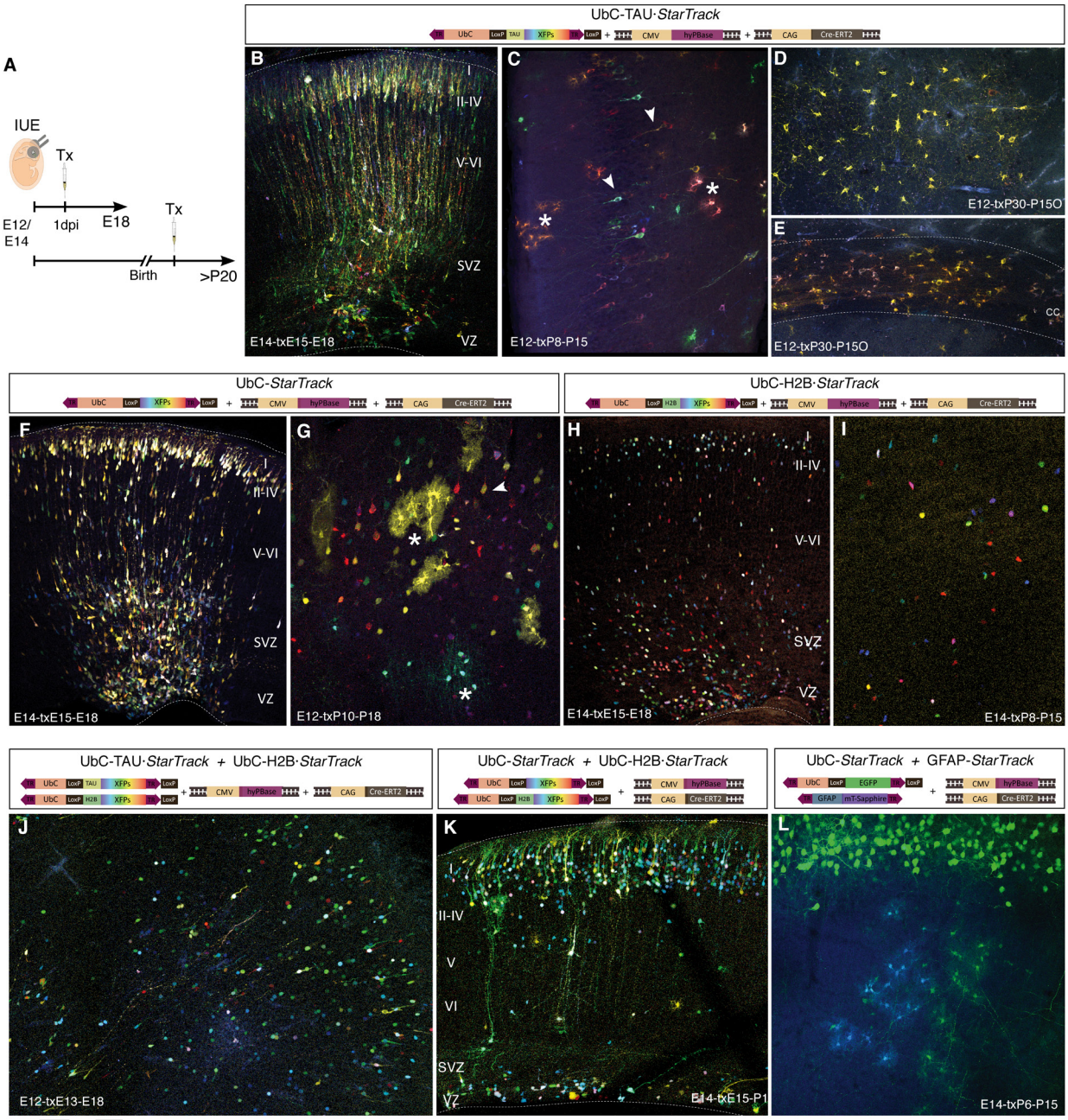

Figure 4. ***In vivo*** **co-electroporation of the UbC-*StarTrack* mixtures.** (**A**) Scheme of the procedure. After IUE, tamoxifen (Tx) was administrated either the day after electroporation for perinatal studies or at perinatal stages for brain analyses at adult stages. (**B–C**) IUE of the UbC-TAU·*StarTrack* mixture. (**B**) At E18, immature neurons and radial glial cells were labeled by TAU constructs after Tx administration one day following IUE (E14). (**C**) IUE (E12), Tx (P8), brain analysis (P15): Labeled cells in the piriform cortex with neuronal (arrowheads) and glial (asterisk) morphologies. (**D–E**) IUE (E12), Tx (P30), brain analysis (P150). Large clones of NG2 glial cells occupying several cortical areas (**D**) and oligodendrocytes within the corpus callosum (cc, **E**). (**F–G**) UbC-*StarTrack* mixture. (**F**) IUE (E14), Tx (E15), brain analysis (E18). Cytoplasmic labeling determines the cell fate. (**G**) IUE (E12), Tx (P10), brain analysis (P18). Mature neuronal (arrowhead) and glial (asterisks) cells were identified morphologically. (**H–I**) Nuclear UbC-H2B·*StarTrack* mixture labeled only the cell nucleus without providing information regarding cell identity. (**H**) IUE (E14), Tx (E15), brain analysis (E18). Labeled cells indicated the distribution (as in **B**,**F**) but not the cell phenotype. (**I**) IUE (E14), Tx (P8), brain analysis (P15): labeled cells validated the stable expression of those constructs. (**J**) IUE (E12), Tx (E13), brain analysis (E18): combination of the cytoplasmic, UbC-TAU·*StarTrack* and nuclear UbC-H2B·*StarTrack* mixtures. (**K**) IUE (E14), Tx (E15), brain analysis (P1). Co-electroporation of the non-specific cytoplasmic, UbC-*StarTrack* and nuclear UbC-H2B·*StarTrack* mixtures is the best plasmid combination to track sibling cells. (**L**) IUE (E14), Tx (P6), brain analysis (P15). Each ubiquitous-*StarTrack* plasmid could be used individually and/or in combination with other plasmids. Vector expressing mT-Sapphire driven by the GFAP promoter was co-electroporated with the Ubiquitous vector expressing EGFP.

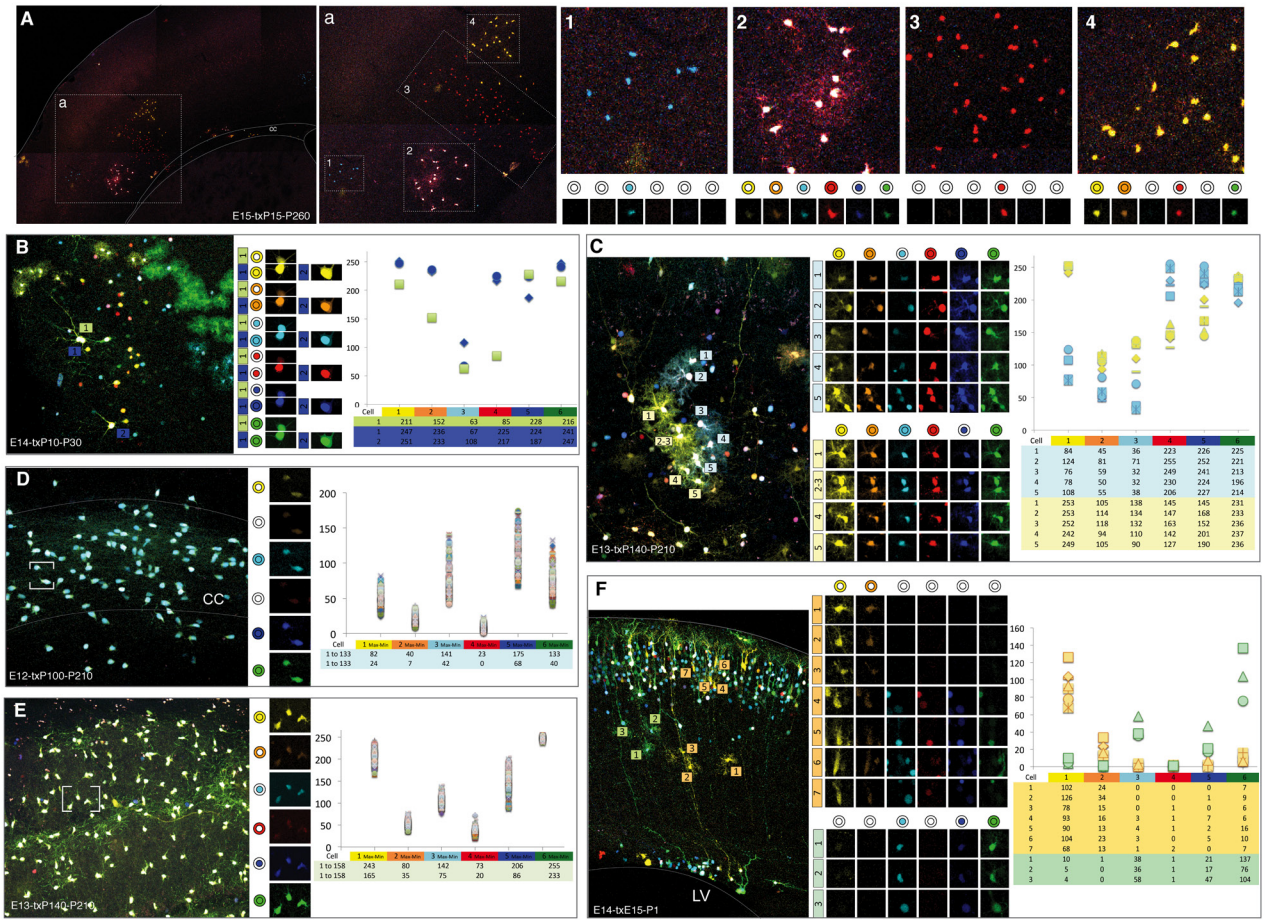

Figure 5. Clonally-related cells from different lineages targeted by IUE of the UbC-*StarTrack* + UbC-H2B·StarTrack. (**A**) Qualitative cell analysis based on the color combination and fluorophore cell location (nuclear or cytoplasmic). (a) UbC-StarTrack labeled cortical clones numbered from 1 to 4. (1–4) Different clonal color-codes detailed by the expression of each fluorescent reporter ordered as: YFP, mKO, mCerulean, mCherry, mT-Sapphire and EGFP. (**B**) Neuronal clone dispersed throughout the cerebral cortex after IUE (E14), Tx (P10) and brain analysis (P30). Fluorescent reporter expression showed one cell (1-green) not clonally-related with the blue clone. Intensity values for each cell are represented on the graph colored and numbered accordingly with their clonal color identity (green or blue). (**C**) Sibling adult astrocytes were located in tighter domains after IUE (E13), Tx (P140), brain analysis (P210). Intensity values for each fluorescent reporter is graphically represented for individual cells of two clones (blue and yellow) comprising five cells each one. (**D**) Oligodendrocytes within the corpus callosum (cc) formed large clusters of clonally related cells after IUE (E12), Tx (P100), brain analysis (P210). Color-code and intensity values for each of the 133 clonally-related cells are dotted in the graph. Both, maximum and minimum intensity values for each fluorescent reporter are detailed in the table. (**E**) NG2 cells occupying several olfactory bulb layers. IUE (E12), Tx (P140), brain analysis (P210). Specific color-code and fluorescent cell intensity for each reporter is represented in the graph. Both, maximum and minimum intensity values of the 158 clonally-related cells are arranged in the table. (**F**) P1 labeled cortical neurons in the dense cortical plate and radial glia cells connecting with the pial surface after IUE (E14) and Tx (E15). Two mixed cell clones formed by immature astrocytes and neurons (orange and green). Note the color-code for the seven clonally-related orange cells and the three green cells. Intensity values for each fluorescent reporter are presented in the graph.

E13. Positioning the electrodes towards the more rostral area allowed clonal analyses and lineage tracing to be performed in the olfactory bulb (Fig. 6D). However, by injecting the plasmid mixture into the third ventricle and placing the paddles either laterally or ventrally, cells were targeted in the hippocampus (Fig. 6E) and hypothalamus (Fig. 6F) respectively. Thus, the UbC-*StarTrack* strategy allowed several brain regions to be targeted raising enormous possibilities for lineage-tracing studies.

Discussion

We developed UbC-*StarTrack* to track and compare different clonal populations from the same or different lineages. This tool represents an efficient approach to track the progeny of neural progenitors in diverse brain areas from embryonic to adult stages, irrespective of their mitotic activity. Using UbC-*StarTrack*, precise identification at the single cell level could be achieved through the stochastic genome integration of six different XFPs expressed in specific cell compartments (nucleus and cytoplasm). This produced a unique color code for each parental cell

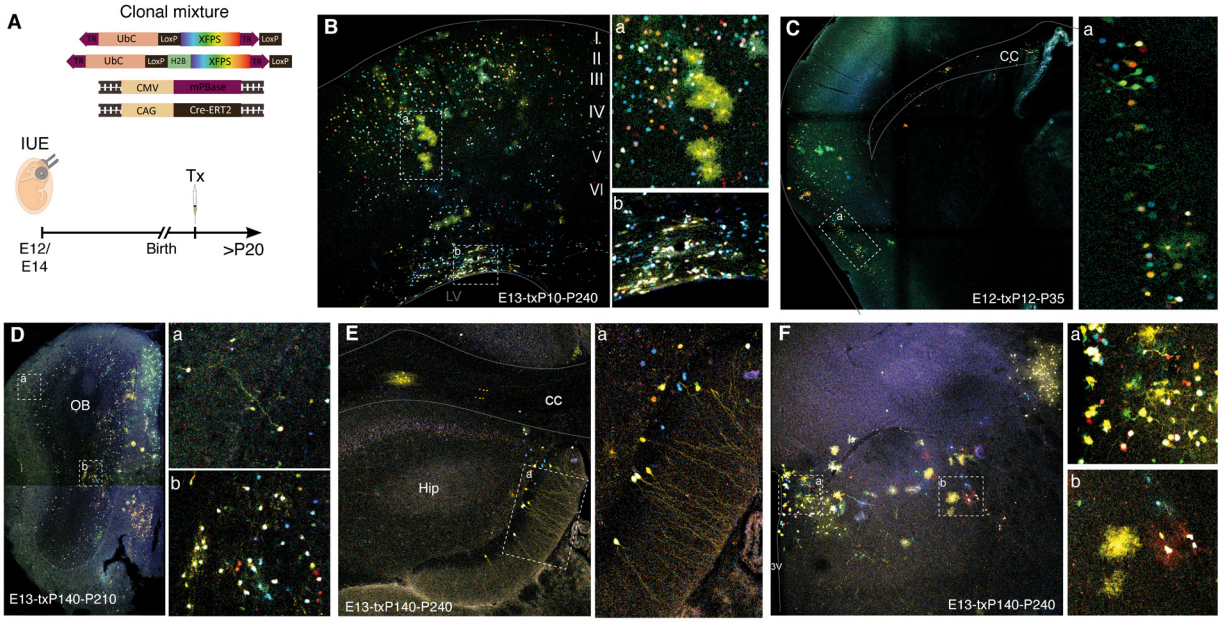

Figure 6. Cell targeting in different brain locations with UbC-*StarTrack* + UbC-H2B·StarTrack. (**A**) Different brain regions targeted after *in utero* co-electroporation of the UbC-*StarTrack* and UbC-H2B·StarTrack mixtures. (**B**) Adult labeled neuronal and glial cells located in the cerebral cortex (a) and within the SVZ (b). IUE (E13), Tx (P10), brain analysis (P240). (**C**) Piriform cortex labeled after IUE at E12, placing the electrodes towards the lateral cortical stream. Glial and neuronal lineages labeled in piriform cortex (a). IUE (E12), Tx (P12), brain analysis (P35). (**D**-**F**) Targeting extracortical brain areas: (**D**) olfactory bulb (IUE E13, Tx P140, OB analyses P210); (**E**) hippocampus (IUE E13, Tx P140, analyses P240); (**F**) hypothalamus (IUE E13, Tx P140, analyses P240). cc, Corpus callosum; LV, Lateral Ventricle; OB, Olfactory bulb; Hip, hippocampus; 3 V, third ventricle.

and its descendants, allowing neurons and/or different glial cells from single-fate restricted, bi-and tri-potent precursors to be identified.

The enormous cell heterogeneity of the adult brain will not be totally understood without specific studies to analyze all the progeny of single cells. Transcriptome analyses[18] or somatic mutations during development[19,20] have proven to be powerful approaches to determine the nature of different neural populations or to establish lineage cell relationships, respectively. Similarly, retroviral vectors have classically been used for tracing cell lineage but since cells must be in cycle for them to integrate stably, the quiescent state of some neural progenitors means they are ineffective to track some populations. More recently, cell lineage approaches have been developed that are based on the probability of labeling by sporadic isolated genomic recombination e.g., in presence of low Tx doses[6,21]. However, it is not absolutely clear that the cells labeled by these approaches are from just one progenitor or whether they are from different progenitors that are found nearby in the same region. Moreover, these approaches rely on labeling few cells, impeding further intra-clonal studies to define any physiological and functional relationships.

We previously used the PiggyBac system for long-term clonal tracking of the glial lineage in different brain regions[22–24]. The PiggyBac transposase specifically inserts a sequence into the genome of transfected cells that contains two terminal repeat regions at 5′-TTAA-3′ sites[25], which in the case of UbC-*StarTrack* included a reporter gene. Here we employed a hyperactive version of the mPBase (hyPBase) that integrates a variable number of transposable copies into the genome at a 10-fold higher transposition rate (9 copies on average), without compromising genomic integrity[26,27]. Nevertheless, some electroporated constructs will be transfected into progenitor cells but not integrated into the genome by the hyPBase. Furthermore, the permanent and stable expression of non-integrated constructs in cells that divide little after electroporation has been reported[17], highlighting the relevance of those non-integrated constructs in clonal methods based on multicolor codes where the combination of different XFPs reflects the progeny of a single cell. Unlike other lineage approaches[12,13], episomal plasmids must be inhibited to establish a unique color code for the entire progeny of a single cell. Indeed, non-integrated or episomal plasmids can generate alterations in the fluorescent clonal code of sibling cells, impeding the accurate analysis of these lineages. To overcome these limitations and to achieve a unique ID for the progeny of an individual cell, we used a Cre-LoxP recombination strategy to silence the expression of non-integrated reporters[28]. Our system was improved by using a tamoxifen-inducible Cre recombinase[29]. Thus, co-electroporation of the UbC-*StarTrack* constructs resolved both the issues related to integration and the inhibition of non-integrated constructs in order to produce a reliable clonal signal in all the progeny, irrespective of the lineage or time of electroporation. To analyze early-generated cell lineages, the tamoxifen administration should be performed 1dpe to accurate label all the cells from single progenitors with the same color-code.

Regarding the evaluation of the clonal markers, the theoretical number of possible combinations after the co-electroporation of both UbC-*StarTrack* and UbC-H2B·*StarTrack* mixtures ascends to more than four thousand. In fact, UbC-*StarTrack* is the clonal method with the widest range of XFPs, expanding the clonal combinations to allow accurate identification of sibling neural cells. While other approaches used Red-Green-Blue reporters[13,30] or four fluorophores[12], our clonal method was based on the expression of six different reporters. These XFPs were selected on the basis of their photostability and brightness[31], without requiring immuno-tagging as other clonal approaches[32]. To corroborate the hypothetical UbC-*StarTrack* potential, we estimated the XFP combinations produced in cells from different IUE brains. In terms of individual fluorophore expression, mKO, YFP or Cerulean could be detected in 30–40% of the cells analyzed, indicating they are useful XFPs for the purpose. The less frequent XFPs were relevant as the clones that expressed these reporters are reliable because of their lower probability. Conversely, prevalent XFPs like EGFP or mT-Sapphire are less informative to define cell clones but they are necessary to increase the number of possible combinations and they contribute to defining less probable combinations. According to the data obtained from more than 6,000 cells, some fluorophore combinations accurately define clones and others, as single-fluorophore expression, do not.

Given the high levels of DNA transposition of the PiggyBac transposase[33], the distinct intensities of the XFP reporters detected for individual cells were important to define clones. While reporter intensity might vary in function of acquisition conditions, neither the confocal laser intensity nor the range emitted by the laser changed within the animals. Only the gain, line/frame average and the offset could be modified when initializing the acquisition of a new animal. Once defined, these parameters were maintained for the acquisition of the whole brain. Moreover, intensity values within cells with the same color-codes did not vary more than 150 points. Together, this information should be taken into consideration when defining sibling cells with UbC-*StarTrack*: fluorophore combination, fluorophore location within the cell and fluorophore intensity.

To achieve the study of all neural cells we used UbC promoter, which drives consistent expression in different cell types[34] and in our hands, it allowed relationships to be established between sibling cells in all neural populations, making comparisons within or between lineages effortless. Our transposon-based genomic approach enabled us to track the entire progeny, which is not possible with previous methods due to the many cell divisions prior to differentiation[35,36]. There were two main differences between glial and neuronal lineages after UbC-*StarTrack* IUE: clonal cell dispersion and the number of cells per clone. Regarding clonal dispersion, sibling neurons were more scattered than glial cells since neurons often migrate to their final position far from their site of birth[37]. After targeting E12 progenitors, neuronal clones are comprised of less than 10 sibling neurons[6], while clonally related-glial cells were located in adjacent domains since these cells actively divide at their final position[38]. Regarding cell number, glial clones form clusters of 5 to 20 cells in the case of astrocytes, and of more than 400 cells in the case of NG2 cells[39]. UbC-*StarTrack* tracked large oligodendrocyte clones that were recognizable by their morphology and due to their position in the adult corpus callosum. Thus, the distribution of clonally related cells and their cell number was related to their cell lineage.

Together, these data demonstrate the use of this approach to efficiently track the entire progeny of specific single progenitors. Besides being an efficient method for lineage analysis, UbC-*StarTrack* is also a versatile method that is finely tuned and adapted to a broad number of specific variables regarding cell fate tracking. Indeed, we generated 18 ubiquitous, bright and stable XFPs, which can be readily combined with other expression vectors. Moreover, this approach could be adapted to analyze any cell lineage by using appropriate promoters in order to simultaneously track different populations. Moreover, genetically engineered mouse models can be combined with the UbC-*StarTrack* constructs, providing additional information. Indeed, in transgenic mice containing any XFP the loss of a specific fluorescent UbC-*StarTrack* construct will provide significant information. Our floxed constructs are suitable to track clonal related lineages, even in Tx inducible transgenic mice lines. In fact, using such transgenic mice, Tx administration will activate the conditional gene while the non-integrated UbC-*StarTrack* constructs will be inhibited, overcoming the need for the CreER^{T2} plasmid electroporation. Moreover, *in vitro* or *ex vivo* clonal analysis using a wide range of primary cultures could be performed.

Finally, UbC-*StarTrack* will undoubtedly be a useful tool to understand the fundamental events in cancer biology, serving to address the lineage heterogeneity within primary tumors or metastatic niches, to track cancer stem cells and their progeny, and to study the precursor-progeny relationships within tumorigenic cells. Another important area, in which our method could add important information is that of neural disease, providing information as to how cell clonality may be involved in the recovery from injury[40], or the specific role of clonally related cells in developmental or neurodegenerative brain disorders.

Methods

Animals. Wild type C57BL/6 mice from the Cajal Institute animal facility were treated according to the European Union guidelines on the use and welfare of experimental animals (2010/63/EU) and those of the Spanish Ministry of Agriculture (RD 1201/2005 and L 32/2007). Performed experimental approaches were approved by the Cajal Institute, CSIC Animal Experimentation Ethics Committees and the Community of Madrid (Ref.PROEX 44/14). The day of detection of the vaginal plug was defined as the first embryonic day (E0) and the day of birth as postnatal day 0 (P0).

Wild type C57BL/6 mice from the Cajal Institute animal facility were treated according to the European Union guidelines on the use and welfare of experimental animals (2010/63/EU) and those of the Spanish Ministry of Agriculture (RD 1201/2005 and L 32/2007). The CSIC Bioethical Committee approved all the procedures used here. The day of detection of the vaginal plug was defined as the first embryonic day (E0) and the day of birth as postnatal day 0 (P0).

Construct generation. Oligonucleotides were obtained from SIGMA-ALDRICH, and the PCR products obtained with these were cloned using *CloneJET PCR Cloning Kit* (Fermentas) and cohesive restriction enzymes

(Fermentas) in all cases. The Rapid DNA Ligation Kit (FERMENTAS) was used for ligations and the resulting products were transformed into *E. coli* JM107 bacteria using the "*TransformAid*" Bacterial Transformation Kit (Fermentas).

To generate UbC-*StarTrack*, we employed a PiggyBac plasmid encoding the enhanced green fluorescent protein (EGFP) under the control of ubiquitous human Ubiquitin C (UbC) gene promoter, pPB-UbC-EGFP (Yusa *et al.* 2009). Initially, a cloning vector containing the LoxP sites (34 bp) and a multiple cloning site (MCS) was generated. The resulting plasmid, pPB-UbC-MCS^{flox} was used successively to clone the XFPs: mT-Sapphire, mCerulean, yellow fluorescent protein (YFP), EGFP, monomeric Kusabira Orange (mKO), and mCherry. The XFPs were amplified by PCR from the pPB-GFAP-XFPs *StarTrack* constructs (García-Marqués-López-Mascaraque, 2013), and the floxed and integrable plasmids expressing six different XFPs were developed, named UbC-*StarTrack*. The sequence encoding histone h2B (H2B) was amplified by PCR using the pPB-GFAP-XFPs *StarTrack* constructs as a template and they were fused to each fluorescent protein in the UbC-*StarTrack* constructs: UbC-H2B·*StarTrack*. Moreover, the Tau protein was amplified from the P3-IRES-tauEGFP plasmid (Adgene #15643) and fused to the different XFPs, generating the UbC-TAU·*StarTrack* constructs. All the constructs were sequenced to assess the efficiency of cloning.

The vector containing the hyperactive transposase of the PiggyBac system (hyPBase) was kindly provided by Prof. Bradley, while the pCAG-CreER^{T2} plasmid was a kind gift from Connie Cepko (Addgene #14797). A non-integrable plasmid encoding mCherry under the UbC promoter (UbC-mCherry) was used as a control of electroporation (Figueres-Oñate *et al.*[17]).

HEK 293 transfected cells. HEK293 cells were cultured to validate the *in vitro* expression of the constructs generated. Briefly, 1.5–2·10^5 cells per well were cultured on polyornithine-plated 6-well plates maintained at 37 °C in an atmosphere of 5% CO_2, and in DMEM (Invitrogen) supplemented with 10% fetal bovine serum (Sigma-Aldrich) and 0.5% penicillin/streptomycin (Invitrogen). Transfection was performed either with the calcium phosphate method or with the commercial transfection reagent TurboFect (Life Technologies). In both cases, a total amount of 3 μgr from the DNA mixture was administrated to each well. The expression of the newly generated constructs was assessed 1 day after transfection. To long-term clonal experiments, cells were passaged every 3–4 days the confluent cultures using 0.05% Trypsin-EDTA (Gibco).

Electroporation of organotypic slices. After embedding E14 brains in low melting point agarose dissolved in 1X KREBS buffer, 300 μm slices were placed on polycarbonate membranes (Whatman) placed in KREBS medium. UbC-*StarTrack* plasmid mixture was then injected into the SVZ with a borosilicate glass filament. To avoid direct contact of the electrode with the slice, the membranes containing the slices were placed between a protective agarose support, the electrodes were placed in position and then, 2 pulses (voltage: 80 mV, 5 ms on/500 ms off) were delivered to pass the reporters into the cells. After electroporation, membranes containing brain slices were cultured 1 hour in MEM medium (Life Technologies) and then were placed in Neurobasal medium (LifeTechnologies) for long-term cultures. Slices were analyzed after 48–72 h incubation at 37 °C in an atmosphere of 5% CO2 in Neurobasal.

In utero electroporation (IUE). IUE was performed as described previously (Figueres-Oñate *et al.*[17]). Briefly, E11 to E15 pregnant mice were anesthetized with 1.5% isofluorane/O2 inhalation and their uterine horns were exposed by midline laparotomy. Intraventricular lateral injections into E11-E12 brain embryos were guided by an ultrasound device (VeVo 770; VisualSonics) and embryos from E13 onwards were visualized by trans-illumination. Five consecutive electric square wave pulses (from 28 V, E11 to 37 V, E15; 50 ms duration) were applied to each embryo, after which the uterine horns were replaced into the abdominal cavity. Dams were placed in clean cage to recover and they were monitored closely.

Tamoxifen administration. Tamoxifen (Tx, Sigma-Aldrich) was dissolved in corn oil (Sigma-Aldrich) at a concentration of 20 mg/ml and a single dose of 5 mg/40 gr body weight was administered. When analyzing embryos, Tx was administrated to pregnant females by intraperitoneal injection 24 h post IUE, whereas to analyze adult mice it was administered at perinatal stages.

Tissue processing. Mice were analyzed at embryonic, postnatal and adult stages. When embryos were used for analysis, the dams were sacrificed, the embryos were extracted from uterine horns and they were then decapitated. Postnatal mice were anesthetized by hypothermia (P1 to P6) or intraperitoneal injection of sodium pentobarbital (Dolethal, 40–50 mg/Kg: from P6 onwards), their brain was fixed by transcardiac perfusion with 4% paraformaldehyde in 0.1 M phosphate buffer and then post-fixed overnight in the same fixative. Coronal/sagittal serial vibratome sections (50–100 μm thick) were then obtained.

Image processing and data analyses. Fluorescent labeling was visualized under an epifluorescence microscope (Nikon, Eclipse E600) with the appropriate filter cubes (Semrock): UV-2A (FF01-334/40-25) Cerulean (FF01-405/10), GFP (FF01-473/10), YFP (FF01-520/15), mKO (FF01-540/15), mCherry (FF01-590/20) and Cy5 (FF02-628/40-25). Images were acquired on a Leica TCS-SP5 confocal microscope, capturing the different XFPs in separate channels. The wavelength of excitation (Ex) and emission (Em) for each XFP were (in nanometers, nm): mT-Sapphire (Ex: 405; Em: 520–535), mCerulean (Ex: 458; Em: 468–480), EGFP (Ex: 488; Em: 498–510), YFP (Ex: 514; Em: 525–535), mKO (Ex: 514; Em: 560–580), mCherry (Ex: 561; Em: 601–620), and Alexa 633 (Ex: 633; Em: 650–760). Confocal laser lines were in-between 25–40% in all cases and the maximum projection images were created using confocal (LASAF Leica) and NIH-ImageJ software.

The imaging data was analyzed with a custom macro integrated into ImageJ (NIH). The critical step in the macro analysis was to appropriately select the labeled cells for which the threshold for every image in each

confocal channel was adjusted in order to create positive cell selection for each XFP. Background subtraction was employed before the threshold selection by applying a smooth filter to improve cell signal selection and a binary image was then created to generate the selection. A watershed filter was applied after the binary image to separate contiguous tagged cells and to analyze them as individual points. Once the selection had been performed, minimal fluorescence intensity was considered as a positive value. Subsequently, the data were automatically organized in a table indicating the maximal and minimal XFP intensity value for each labeled cell and its specific color code represented in the potential clonally related cells. Further analysis was performed to determine sibling cells based on the fluorescence intensity ranges and the location of the fluorophore (nucleus or cytoplasm).

References

1. Kriegstein, A. & Alvarez-Buylla, A. The glial nature of embryonic and adult neural stem cells. *Annu. Rev. Neurosci.* **32,** 149–84 (2009).
2. Franco, S. J. & Müller, U. Shaping our minds: stem and progenitor cell diversity in the mammalian neocortex. *Neuron* **77,** 19–34 (2013).
3. Noctor, S. C., Flint, a C., Weissman, T. a., Dammerman, R. S. & Kriegstein, a R. Neurons derived from radial glial cells establish radial units in neocortex. *Nature* **409,** 714–20 (2001).
4. Yu, Y.-C., Bultje, R. S., Wang, X. & Shi, S.-H. Specific synapses develop preferentially among sister excitatory neurons in the neocortex. *Nature* **458,** 501–4 (2009).
5. Zong, H., Espinosa, J. S., Su, H. H., Muzumdar, M. D. & Luo, L. Mosaic analysis with double markers in mice. *Cell* **121,** 479–92 (2005).
6. Gao, P. *et al.* Deterministic Progenitor Behavior and Unitary Production of Neurons in the Neocortex. *Cell* **159,** 775–788 (2014).
7. Golden, J. a, Fields-Berry, S. C. & Cepko, C. L. Construction and characterization of a highly complex retroviral library for lineage analysis. *Proc. Natl. Acad. Sci. USA* **92,** 5704–8 (1995).
8. Salipante, S. J. & Horwitz, M. S. Phylogenetic fate mapping. *Proc. Natl. Acad. Sci. USA* **103,** 5448–5453 (2006).
9. Livet, J. *et al.* Transgenic strategies for combinatorial expression of fluorescent proteins in the nervous system. *Nature* **450,** 56–62 (2007).
10. Hadjieconomou, D. *et al.* Flybow: genetic multicolor cell labeling for neural circuit analysis in Drosophila melanogaster. *Nat. Methods* **8,** 260–6 (2011).
11. Weber, K. *et al.* RGB marking facilitates multicolor clonal cell tracking. *Nat. Med*. doi: 10.1038/nm.2338 (2011).
12. García-Moreno, F., Vasistha, N. a, Begbie, J. & Molnár, Z. CLoNe is a new method to target single progenitors and study their progeny in mouse and chick. *Development* **141,** 1589–98 (2014).
13. Loulier, K. *et al.* Multiplex cell and lineage tracking with combinatorial labels. *Neuron* **81,** 505–20 (2014).
14. Siddiqi, F. *et al.* Fate Mapping by PiggyBac Transposase Reveals That Neocortical GLAST+ Progenitors Generate More Astrocytes Than Nestin+ Progenitors in Rat Neocortex. *Cereb. Cortex* **24,** 508–520 (2014).
15. García-Marqués, J. & López-Mascaraque, L. Clonal Identity Determines Astrocyte Cortical Heterogeneity. *Cereb. Cortex* **23,** 1463–1472 (2013).
16. García-Marqués, J., Núñez-Llaves, R. & López-Mascaraque, L. NG2-glia from pallial progenitors produce the largest clonal clusters of the brain: time frame of clonal generation in cortex and olfactory bulb. *J. Neurosci.* **34,** 2305–13 (2014).
17. Figueres-Oñate, M., García-Marqués, J., Pedraza, M., De Carlos, J. A. & López-Mascaraque, L. Spatiotemporal analyses of neural lineages after embryonic and postnatal progenitor targeting combining different reporters. *Front. Neurosci.* **9,** 1–11 (2015).
18. Cahoy, J. D. *et al.* A Transcriptome Database for Astrocytes, Neurons, and Oligodendrocytes: A New Resource for Understanding Brain Development and Function. *J. Neurosci.* **28,** 264–278 (2008).
19. Carlson, C. A. *et al.* Decoding cell lineage from acquired mutations using arbitrary deep sequencing. *Nat. Methods* **9,** 15–19 (2012).
20. Evrony, G. D. *et al.* Cell Lineage Analysis in Human Brain Using Endogenous Retroelements. *Neuron* **85,** 49–59 (2015).
21. Magavi, S., Friedmann, D., Banks, G., Stolfi, A. & Lois, C. Coincident generation of pyramidal neurons and protoplasmic astrocytes in neocortical columns. *J. Neurosci.* **32,** 4762–72 (2012).
22. Parmigiani, E. *et al.* Heterogeneity and Bipotency of Astroglial-Like Cerebellar Progenitors along the Interneuron and Glial Lineages. *J. Neurosci.* **35,** 7388–7402 (2015).
23. García-Marqués, J. & López-Mascaraque, L. Clonal Mapping of Astrocytes in the Olfactory Bulb and Rostral Migratory Stream. *Cereb. Cortex* bhw071, doi: 10.1093/cercor/bhw071 (2016).
24. Figueres-Oñate, M. & López-Mascaraque, L. Adult Olfactory Bulb Interneuron Phenotypes Identified by Targeting Embryonic and Postnatal Neural Progenitors. *Front. Neurosci.* **10,** 1–12 (2016).
25. Wang, H. H., Fraser, M. J. & Cary, L. C. Transposon mutagenesis of baculoviruses: analysis of TFP3 lepidopteran transposon insertions at the FP locus of nuclear polyhedrosis viruses. *Gene* **81,** 97–108 (1989).
26. Woltjen, K. *et al.* piggyBac transposition reprograms fibroblasts to induced pluripotent stem cells. *Nature* **458,** 766–70 (2009).
27. Yusa, K., Zhou, L., Li, M. A., Bradley, A. & Craig, N. L. A hyperactive piggyBac transposase for mammalian applications. *Proc. Natl. Acad. Sci. USA* **108,** 1531–6 (2011).
28. Sternberg, N. & Hamilton, D. Bacteriophage Pl Site-specific Recombination. *J. Mol. Biol.* **4,** 467–486 (1981).
29. Matsuda, T. & Cepko, C. L. Controlled expression of transgenes introduced by *in vivo* electroporation. *Proc. Natl. Acad. Sci. USA* **104,** 1027–32 (2007).
30. Gomez-Nicola, D., Riecken, K., Fehse, B. & Perry, V. H. *In-vivo* RGB marking and multicolour single-cell tracking in the adult brain. *Sci. Rep.* 1–10, doi: 10.1038/srep07520 (2014).
31. Shaner, N. C., Steinbach, P. A. & Tsien, R. Y. A guide to choosing fluorescent proteins. *Nat. Methods* **2,** 905–909 (2005).
32. Calzolari, F. *et al.* Fast clonal expansion and limited neural stem cell self-renewal in the adult subependymal zone. *Nat. Neurosci.* **18,** 490–492 (2015).
33. Ding, S. *et al.* Efficient transposition of the piggyBac (PB) transposon in mammalian cells and mice. *Cell* **122,** 473–83 (2005).
34. Lois, C., Hong, E. J., Pease, S., Brown, E. J. & Baltimore, D. Germline transmission and tissue-specific expression of transgenes delivered by lentiviral vectors. *Science* **295,** 868–72 (2002).
35. Lacar, B., Young, S. Z., Platel, J.-C. & Bordey, A. Imaging and recording subventricular zone progenitor cells in live tissue of postnatal mice. *Front. Neurosci.* **4,** 1–16 (2010).
36. Kita, Y., Kawakami, K., Takahashi, Y. & Murakami, F. Development of cerebellar neurons and glias revealed by in utero electroporation: Golgi-like labeling of cerebellar neurons and glias. *PLoS One* **8,** e70091 (2013).
37. Kriegstein, A. R. & Noctor, S. C. Patterns of neuronal migration in the embryonic cortex. *Trends Neurosci.* **27,** 392–9 (2004).
38. Ge, W.-P., Miyawaki, A., Gage, F. H., Jan, Y. N. & Jan, L. Y. Local generation of glia is a major astrocyte source in postnatal cortex. *Nature* **484,** 376–80 (2012).
39. Bribián, a., Figueres-Oñate, M., Martín-López, E. & López-Mascaraque, L. Decoding astrocyte heterogeneity: New tools for clonal analysis. *Neuroscience* **323,** (2016).
40. Martín-López, E., García-Marques, J., Núñez-Llaves, R. & López-Mascaraque, L. Clonal astrocytic response to cortical injury. *PLoS One* **8,** e74039 (2013).

Acknowledgements

We are very grateful to Carmen Hernandez and Belen Garcia from the Imaging and Microscopy Facility of the Institute Cajal, for support with ImageJ macro design. We would like to thank Emilio Tejera for technical assistance, Lluis Fortes-Marco for 3D drawing, all the members of the López-Mascaraque's laboratory for critically reading the manuscript and Mark Sefton for editorial assistance. This work was supported by research Grant BFU2013-48807-R from the Spanish Ministry of Economy and Competitiveness.

Author Contributions

M.F.-O. participated in experimental design, performed experiments, analyzed data, and prepared the manuscript. J.G.-M. participated in experimental design and revised the manuscript. L.L.-M. was responsible for conceptual design, writing the paper and obtained funding.

Additional Information

Competing financial interests: The authors declare no competing financial interests.

How to cite this article: Figueres-Oñate, M. *et al.* UbC-*StarTrack,* a clonal method to target the entire progeny of individual progenitors. *Sci. Rep.* **6**, 33896; doi: 10.1038/srep33896 (2016).

CHAPTER 3

Adult Olfactory Bulb Interneuron Phenotypes Identified by Targeting Embryonic and Postnatal Neural Progenitors. Figueres-Oñate, M and López-Mascaraque, L. (2016). *Frontiers in Neuroscience,* doi: 10.3389/fnins.2016.00194.

The olfactory pathway is an excellent model to study cell heterogeneity and fate of distinct progenitors. The constant incorporation of neurons into the olfactory bulb throughout adult life, makes this pathway as a perfect neurogenic experimental model. In the adult mice brain remains two main neurogenic regions that still producing neurons throughout life. One is the hippocampal area and other the ventricular surface of the lateral ventricles, which provide neurons to the olfactory bulb. In the ventricular surface neural progenitors divide to produce neuroblasts through transit amplifying progenitors. Those neuroblasts migrate, along the rostral migratory stream (RMS), to the olfactory bulb where they differentiate into granular or periglomerular cells. In this work, we performed a broad analysis of the fate of progenitors lining the ventricular surface targeted at either embryonic or postnatal ages. The results were published as "Adult Olfactory Bulb Interneuron Phenotypes Identified by Targeting Embryonic and Postnatal Neural Progenitors". We showed the expression pattern of neuronal and glial markers in the olfactory bulb after targeted electroporation of embryonic (E13-E15) and postnatal (P1) stem cell compartments using a transposable construct expressing the EGFP under the ubiquitous UbC promoter. Our results showed that the age of the mice and the electrode placement were critical for the targeting of different cell lineages in the OB, particularly for glial lineages and projection neurons. Glial progenitors were only targeted in the olfactory bulb (OB) when performing electroporations in the intrabulbar ependymal zone at embryonic stages. Targeted glial cells from different lineages were identified by their colocalization with astrocytic, oligodendrocytic or NG2 immunomarkers. Moreover, embryonic or postnatal dorso-lateral ventricular NPCs, produced interneurons that where similarly distributed in all the OB layers, with the majority disposition of targeted interneurons in the granular cell layer. Finally, a wide immunomarkers battery allowed to describe the fate of different labeled interneurons in the adult olfactory bulbs.

frontiers in Neuroscience

ORIGINAL RESEARCH
published: 09 May 2016
doi: 10.3389/fnins.2016.00194

Adult Olfactory Bulb Interneuron Phenotypes Identified by Targeting Embryonic and Postnatal Neural Progenitors

*Maria Figueres-Oñate and Laura López-Mascaraque **

Molecular, Cellular, and Developmental Neurobiology, Instituto Cajal, Consejo Superior de Investigaciones Científicas, Madrid, Spain

Neurons are generated during embryonic development and in adulthood, although adult neurogenesis is restricted to two main brain regions, the hippocampus and olfactory bulb. The subventricular zone (SVZ) of the lateral ventricles generates neural stem/progenitor cells that continually provide the olfactory bulb (OB) with new granule or periglomerular neurons, cells that arrive from the SVZ via the rostral migratory stream. The continued neurogenesis and the adequate integration of these newly generated interneurons is essential to maintain homeostasis in the olfactory bulb, where the differentiation of these cells into specific neural cell types is strongly influenced by temporal cues. Therefore, identifying the critical features that control the generation of adult OB interneurons at either pre- or post-natal stages is important to understand the dynamic contribution of neural stem cells. Here, we used *in utero* and neonatal SVZ electroporation along with a transposase-mediated stable integration plasmid, in order to track interneurons and glial lineages in the OB. These plasmids are valuable tools to study the development of OB interneurons from embryonic and post-natal SVZ progenitors. Accordingly, we examined the location and identity of the adult progeny of embryonic and post-natally transfected progenitors by examining neurochemical markers in the adult OB. These data reveal the different cell types in the olfactory bulb that are generated in function of age and different electroporation conditions.

Keywords: *in utero* electroporation, postnatal neurogenesis, postnatal electroporation, periglomerular, lineage tracing

OPEN ACCESS

Edited by:
Jack M. Parent,
University of Michigan, USA

Reviewed by:
Benedikt Berninger,
University Medical Center of the Johannes Gutenberg University Mainz, Germany
Harold Cremer,
Centre National de la Recherche Scientifique, France

****Correspondence:***
Laura López-Mascaraque
mascaraque@cajal.csic.es

Specialty section:
This article was submitted to Neurogenesis, a section of the journal Frontiers in Neuroscience

Received: *06 January 2016*
Accepted: *20 April 2016*
Published: *09 May 2016*

Citation:
Figueres-Oñate M and López-Mascaraque L (2016) Adult Olfactory Bulb Interneuron Phenotypes Identified by Targeting Embryonic and Postnatal Neural Progenitors. Front. Neurosci. 10:194. doi: 10.3389/fnins.2016.00194

INTRODUCTION

In 1962, Joseph Altman revealed that tritiated thymidine could be incorporated into some neurons (based on their appearance under light microscopy) in the rat hippocampus (Altman, 1962; Altman and Das, 1965) and in the olfactory bulb (Altman, 1969). Electron microscopy confirmed the generation of neurons postnatally (Kaplan and Hinds, 1977; Bayer, 1983), a process that involves cell proliferation, neuronal differentiation, and integration into existing neural circuits. Newly generated cells originate in the SVZ of the lateral ventricle, which develops from the residual progenitors of the lateral ganglionic eminence (LGE) at embryonic stages (Bayer et al., 1994; Wichterle et al., 2001; Young et al., 2007). These develop into quite diverse interneurons (Price and Powell, 1970; Pinching and Powell, 1971), characterized morphologically and by their location,

firing pattern and immunomarkers. Most of these newly generated interneurons are GABAergic granule cells (GCs: >90%), with a minority differentiating into periglomerular cells (PGCs: Altman, 1969; Luskin, 1993; Lois and Alvarez-Buylla, 1994). To date, PGCs have been characterized either as GABAergic, dopaminergic (Kosaka et al., 1998; Bagley et al., 2007; Batista-Brito et al., 2008), or as a subset of glutamatergic excitatory juxtaglomerular interneurons (Brill et al., 2009; Winpenny et al., 2011). All these PGCs can be incorporated into neural circuits during adulthood, albeit at a lower proportion than granular cells (De Marchis et al., 2007; Whitman and Greer, 2007). The identity of both granule and PGCs is regulated both spatially and temporally (Merkle et al., 2007; Sequerra, 2014; Fuentealba et al., 2015). Moreover, the heterogeneity among newly generated cells is determined in function of their location within the SVZ, defining whether they become granule cells or periglomerular interneurons. Neural progenitor cells (NPCs) in the dorsal adult SVZ give rise to superficial GCs, CR^+ cells, and periglomerular TH^+ cells, whereas the lateral and ventral regions generate mostly deep GCs and periglomerular $Calbindin^+$ cells (for a review, see Fiorelli et al., 2015). In addition, the diversity of olfactory bulb (OB) interneurons is also determined by their temporal origin (De Marchis et al., 2007). TH+ and Calbindin+ (PGCs) production are generated principally during embryogenesis and their production declines postnatally, when $Calretinin^+$ GCs and PGC generation increases (Batista-Brito et al., 2008). Specific subpopulations of adult newborn OB cells have also been characterized based on progenitor domains (Merkle et al., 2007, 2014). Adult born GCs have been classified into five different groups based on their maturational states (Petreanu and Alvarez-Buylla, 2002) and new subtypes are still being described (Merkle et al., 2014).

In order to fully capture the heterogeneity among the OB interneurons generated in the adult, embryonic, or postnatal cells were targeted by electroporation with a ubiquitous transposable vector expressing the enhanced green fluorescent protein (eGFP). Our data reveals this tool to be a powerful means to visualize the specific cell fate of different embryonic and postnatal progenitors in function of their age and on the placement of the electrodes for electroporation. Thus, in this analysis we are able to correlate, lineages, and cell dispersion within the different OB layers as a function of those parameters.

MATERIALS AND METHODS

Animals

Wild type C57BL/6 mice were obtained from the Cajal Institute animal facility, and the day the vaginal plug was detected was considered as the first embryonic day (E0) and day of birth as postnatal day 0 (P0). All procedures were carried out in compliance with the ethical regulations on the use and welfare of experimental animals of the European Union (2010/63/EU) and the Spanish Ministry of Agriculture (RD 1201/2005 and L 32/2007), and the CSIC's bioethical committee approved all the animal protocols. At least $N = 3$ animals were used per experimental condition.

Transposable Vectors

The pPB-UbC-eGFP integrable plasmid containing eGFP under the control of the human ubiquitous Ubiquitin C (UbC) promoter was used here (Yusa et al., 2009; Figueres-Oñate et al., 2015). The genomic integration of this construct was mediated by co-electroporation with a vector containing a hyperactive transposase of the PiggyBac system (hyPBase), kindly provided by Prof. Bradley (Yusa et al., 2011).

In utero Electroporation (IUE)

Briefly, E13 or E15 pregnant mice were anesthetized with 2% isofluorane (Isova vet, Centauro), which was maintained with 1.5% isofluorane/O_2 inhalation, and the mice were placed on a thermal plate at 37°C during the surgery. Before making the peritoneal excision, the mice were administered an antibiotic, enrofloxacin (5 mg/kg: Baytril Bayer), and an anti-inflammatory agent, meloxicam (300 μg/kg: VITA Laboratories). The uterine horns were exposed by midline laparotomy and the embryos maintained humid with physiological saline. Embryos were visualized by trans-illumination and up to 1 μl of the plasmid mixture was injected through a pulled glass capillary into the lateral ventricle of each embryo. The DNA mixture was comprised of the pPB-UbC-eGFP construct and hyPBase in a 3:1 ratio (1–2 μg/ml final concentration), with 0.1% Fast Green (SIGMA). Five consecutive electric square wave pulses (33 or 37 V, 50 ms duration, 950 ms interval) were then applied with 3 mm tweezer-type electrodes (Sonidel). Subsequently, the uterine horns were returned to the abdomen, and the abdominal muscle and skin were sutured. The mice were allowed to recover at 37°C with oxygen administration.

Postnatal Electroporation

Pups (P0/P1) were anesthetized by hypothermia and placed under a cold light to facilitate visualization of the lateral ventricles by trans-illumination. The DNA mixture (see above) was injected into the ventricular cavity and electroconductive LEM Gel (DRV1800, MORETTI S.P.A.) was placed on both electrode paddles to avoid damaging the pups and to achieve successful current flow. Five 100 V electric pulses were applied (50 ms duration, 950 ms intervals), with the positive electrode positioned in the dorso-lateral region to direct the negatively charged DNA to the subventricular zone. After the pulses, the pups were placed on a thermal plate and when they had recovered, they were returned to their mother.

Tissue Processing

Brains were analyzed at adult stages (from P25 onwards). Mice were deeply anesthetized by intraperitoneal injection of sodium pentobarbital (Dolethal, 40–50 mg/kg) and they were transcardially perfused with 4% paraformaldehyde (PFA). The brains were post-fixed in PFA overnight at 4°C and 50 μm thick free-floating coronal or sagittal vibratome sections were obtained.

Immunohistochemistry

To identify the phenotypes of the olfactory bulb cell population, we studied the immunohistochemical labeling of neuronal and

glial antibodies. Sections were permeabilized with 0.1% Triton-X in PBS (PBS-T), blocked with 5% normal goat serum (NGS) and then they were incubated with the primary antibodies (see **Table 1**). The following day, the sections were washed and subsequently incubated with the appropriate conjugated secondary antibodies: red fluorophore (1:1000, Alexa Fluor 568 nm, Molecular Probes) or an infrared fluorochrome (1:1000, Alexa Fluor 633 or 647 Molecular Probes).

Imaging Processing

Green fluorescent labeling was examined under an epifluorescence microscope (Nikon, Eclipse E600) with the fluorescein filter cube (450–490 nm, Semrock). Immunohistochemical labeling was observed with the red and far-red filter cubes: rhodamine (569–610 nm) and Cy5 (628–640 nm). The final images were acquired on a Leica TCS-SP5 confocal microscope adjusting the settings so that there was no spectral overlap: eGFP (Ex: 488; Em: 498–550), Alexa 568 (Ex: 561; Em: 575–620), and Alexa 633/647 (Ex: 633; Em: 645–740). Confocal laser lines were used in-between 25 and 40% in all cases.

The maximum projection images were created using the confocal software (LASAF Leica) and other software, such as NIH-ImageJ software. Captured images were processed to adjust the contrast and brightness equally using Adobe Photoshop CS5 software.

Quantitative Analysis

After image acquisition the distribution of the OB cells after either postnatal or *in utero* electroporation was analyzed with ImageJ software. First, images were converted to 8-bits and to facilitate the analyses of both the cell's morphology and layer localization, ICA Lut was applied. Cells were counted using the Cell Counter plug-in analysis tool of the Image J software, analyzing four P25-30 mice animals per group (IUE or postnatal electroporation). Up to 1875 OB cells were counted following postnatal electroporation and 926 cells from the *in utero* electroporated animals. The somata area of DCX positive cells was analyzed with the ImageJ software (60 cells within the granular cell layer and 40 within the subependymal zone). Statistical analyses were performed with SigmaPlot 13 (Systat Software) and the values were represented as the mean ± SEM. *T*-tests were performed to determine the significance between different groups, or with the Mann-Whitney Rank Sum Test when the normality test failed. A confidence interval of 95% ($p < 0.05$) was required to considered values statistically significant.

RESULTS

Histochemical Phenotypes of Neural Olfactory Bulb Cells

To establish the profile of neurochemical markers expressed by OB interneurons, first we performed an immunohistochemical study for a battery of markers (**Table 1** and Supplementary Figures S1, S2). Both neuronal and glial markers were used to determine the heterogeneity of cell phenotypes from the glomerular layer (GL), external plexiform layer (EPL), mitral layer (ML), internal plexiform layer (IPL), granular cell layer (GCL) to the subependymal zone (SEZ; Supplementary

TABLE 1 | Primary antibodies used for the immunohistochemical analysis of newly generated cells in the adult olfactory bulb.

Antibody	Abbreviations	USE	SP.	Source
Adenomatous Polyposis Coli	APC/CC-1	1:200	MS	Calbiochem (OP80)
Calbindin	CB	1:500	Rb	Abcam (Ab11426)
Calretinin	CR	1:500	Rb	Abcam (Ab702)
2′,3′-Cyclic-nucleotide 3′phosphodiesterase	CNPase	1:200	Ms	Covance (SMI-91R)
Doublecortin	DCX	1:500	Rb	Cell signaling (4604)
DOPA decarboxylase	DDC	1:500	Rb	Abcam (Ab3905)
Gamma-Aminobutyric acid	GABA	1:500	Rb	Sigma (A2052)
Glutamate decarboxylase 67	GAD67	1:500	Ms	Millipore (MAB5406)
Glial fibrillary acidic protein	GFAP	1:1000	Ms	Millipore (MAB3402)
Myelin Basic Protein	MBP	1:500	Rat	Serotec (MCA409S)
Neuronal Nuclei	NeuN	1:500	Ms	Millipore (MAB377)
Neuron-glial antigen 2	NG2	1:500	Ms	Millipore (AB5320)
Oligodentrocyte transcription factor 2	Olig2	1:2000	Rb	Millipore (AB9610)
Alpha-type platelet-derived growth factor receptor	PDGFRα	1:300	Rb	Santa Cruz (C-20) (sc-338)
Parvalbumin	PV	1:500	Rb	Swant (PV-25)
Reelin	Reel	1:500	Ms	Millipore (MAB5364)
S100 calcium binding protein beta	S100β	1:300	Ms	Abcam (Ab66028)
Somatostatin	SOM/SST	1:500	Rb	Millipore (AB5494)
T-box, brain, 1	Tbr1	1:500	Rb	Abcam (AB31940)
T-box, brain, 2	Tbr2	1:500	Rb	Abcam (Ab23345)
Tyrosine hydroxylase	TH	1:500	Rb	Millipore (AB152)

Figure S1A). Calbindin (CB, Supplementary Figure S1B) immunoreactive cells appeared predominantly in both the GL and the external plexiform layer (EPL). However, tyrosine hydroxylase (TH) was exclusively expressed by a subset of PGCs (Supplementary Figure S1C). Calretinin (CR, Supplementary Figure S1D) immunolabeling was restricted to periglomerular and granular cells, while Parvalbumin$^+$ cells (PV, Supplementary Figure S1E) were located throughout the EPL and occasionally in the external granular cell layer (eGCL). Few somatostatin (SOM) interneurons were found in the EPL (Supplementary Figure S1F), while dopa decarboxylase (DDC) was expressed by a large number of periglomerular and granular cells (Supplementary Figure S1G). All the interneurons were generally labeled for either GABA (Supplementary Figure S1H) or GAD67 (Supplementary Figure S1I). The microtubule-associated protein doublecortin (DCX), that plays an important role in neuronal migration, labeled neuroblasts within the SEZ and throughout the GCL (Supplementary Figure S1J). The extracellular protein reelin was mainly detected around mitral cells but also, around some tufted and periglomerular cells (Supplementary Figure S1K). Interestingly, the regulatory T-box brain 1 and 2 genes (Tbr1 and Tbr2) were expressed by a few glutamatergic periglomerular OB cells. Indeed, while both were expressed at the same OB location, Tbr2 labeled a few more cells (Supplementary Figure S1L) than Tbr1 (Supplementary Figure S1M) as described previously (Winpenny et al., 2011). To tag all the neurons in the OB we used the marker of neuronal nuclei, NeuN, which was mostly expressed in the GCL and the mitral cell layer in the OB (Supplementary Figure S1N). As a large number of neurons, mostly in the GL, did not express NeuN, we assessed the neurochemical identity of NeuN by double staining with CB (Supplementary Figure S1O) and CR (Supplementary Figure S1P). Although most CB$^+$ cells in the GL did not express NeuN, both antibodies co-stained a population of GL neurons, (arrowheads in Supplementary Figure S1O magnification). Only a few cells were dual stained for CR and NeuN in the GCL (arrowheads in Supplementary Figure S1P magnification). To further address the phenotype of the cells expressing NeuN, dual NeuN, and DCX labeling was assessed, the later an early neural marker (Supplementary Figure S1Q). While most DCX cells concentrated in the SEZ, both markers co-localized in a subset of GCL cells close to the SEZ (arrowheads in Supplementary Figure S1Q magnification), indicating an overlap of those immunomarkers. Finally, to better understand the distribution of the mature interneurons and the neuroblasts migrating along the SVZ-RMS-OB pathway, double immunostaining with CR-DCX was performed. DCX positive cells were confined to the RMS and the SEZ, while CR$^+$ cells were located in the eGCL and GL, regions with weaker DCX labeling (Supplementary Figure S1R).

The distribution of glial cells in the OB was studied with markers for astrocytes (GFAP and S100β proteins), NG2 cells (antibodies against NG2 and PDGFRα), and oligodendrocytes (Olig2, MBP, APC, and CNPase). GFAP-positive cells were located throughout the OB layers except for the EPL, mostly concentrating in the SEZ (Supplementary Figure S2A). NG2 stained cells were homogeneously distributed throughout all the OB layers (Supplementary Figure S2B) and Olig2 immunoreactivity was equally widespread along the SVZ-RMS-OB pathway (Supplementary Figure S2C). Finally, CNPase expression was restricted to myelinating oligodendrocytes (Supplementary Figure S2D). Dual immunofluorescence for Olig2 and APC (Supplementary Figure S2E) indicated that the vast majority of APC$^+$ cells co-expressed Olig2 (arrowheads in Supplementary Figure S2E magnifications), although since Olig2 is a marker for the complete oligodendroglial lineage and APC only labels myelinating oligodendrocytes, not all cells with Olig2 expressed the APC marker (asterisks in Supplementary Figure S2E magnifications). Olig2 and MBP did not co-localize (Supplementary Figure S2F) as their expression in oligodendrocytes differs considerably: Olig2 labels the nucleus while MBP is found in myelin sheaths. Finally, we also analyzed the co-expression of oligodendroglial and astroglial lineages with the combinations of the S100β-Olig2 (Supplementary Figure S2G) and GFAP-PDGFRα (Supplementary Figure S2H) markers. S100β and Olig2 were expressed in different cell populations (asterisks in Supplementary Figure S2G magnifications), although the S100β astrocytic marker co-localized with some Olig2$^+$ oligodendrocytes (arrowheads in Supplementary Figure S2E magnifications). By contrast, the GFAP and PDGFRα immunomarkers (Supplementary Figure S2H) did not co-localize along the SVZ-RMS-OB pathway (Supplementary Figure S2Ha magnification). In fact, GFAP was expressed strongly within the RMS (Supplementary Figure S2Hb magnification) while PDGFRα maintained a uniform cell density through this migratory channel.

Tracking Different Olfactory Bulb Cell Lineages with Different Electroporation Conditions

We followed the cell progeny in the OB by targeting neural progenitors using *in utero* or postnatal electroporation of the following vectors: a plasmid ubiquitously expressing eGFP flanked by two terminal repeat sequences (TRs); the PiggyBac transposase (mPBase). The mPBase transposase integrates the vector including the reporter gene directly into the genome of the transfected cell (**Figure 1A**), allowing the entire progeny of a single cell to be analyzed, regardless of its mitotic activity. To label the different OB populations, IUE was performed (E13–E15) varying electrode positions and with distinct orientations along rostro-caudal axis. Interestingly, neural populations labeled were located at different positions in the OB depending on the embryonic area electroporated. First, IUE was performed at E15 to target progenitors from the dorso-lateral area of the ventricular surface (**Figure 1B**). Analyzing brains 30 days post-electroporation (dpe), labeled cells corresponding to glial and neuronal lineages were located within the dorsal cortex (**Figure 1Ba**). After electroporation on E15, neurons were located within cortical layers II-III, whilst glial cells were widespread throughout cerebral cortex (**Figure 1Ba′**). Moreover, neuronal precursors and labeled oligodendrocytes were located within the corpus callosum, near to the ventricular surface (**Figure 1Ba″**). Furthermore, a large population of labeled neurons was also

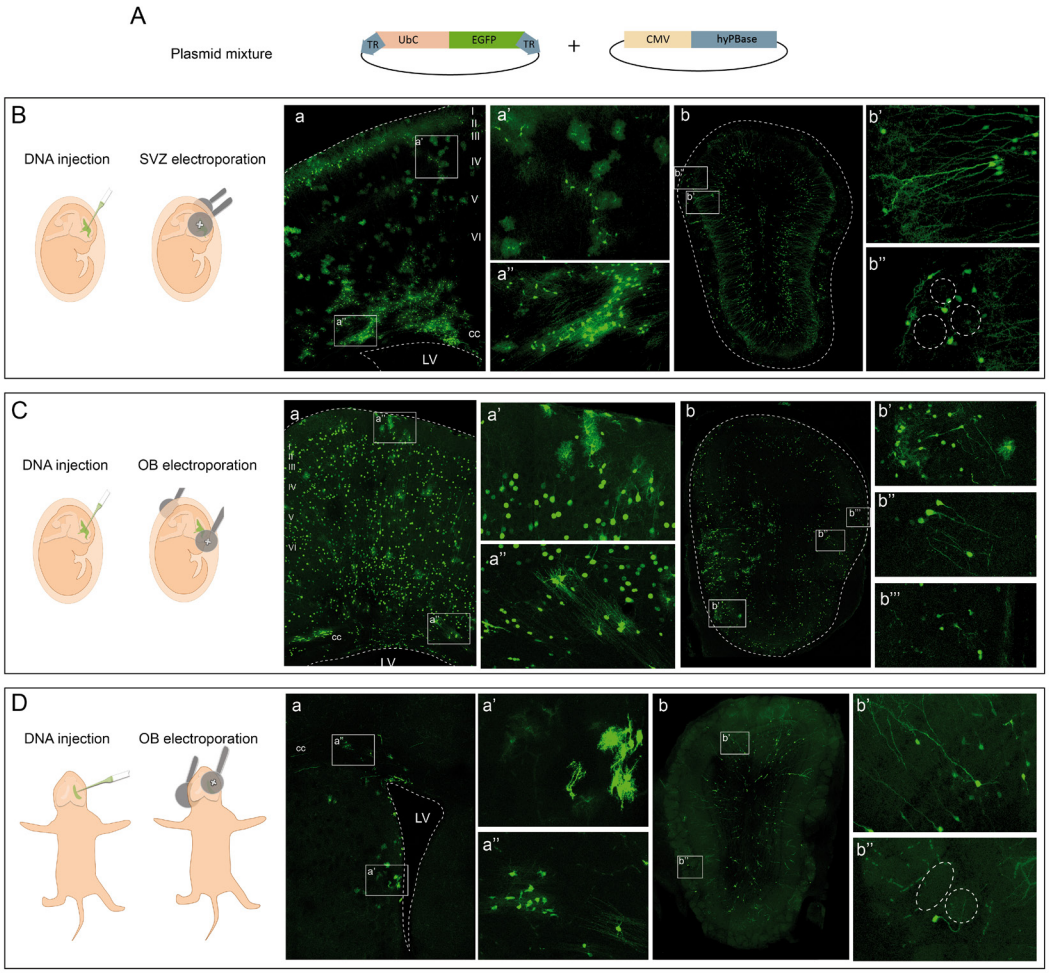

FIGURE 1 | Targeting cells in the olfactory bulb by electroporation. (A) *In vivo* electroporation after ventricular injection of a plasmid mixture containing an integrable vector expressing the eGFP reporter and the transposase of the PiggyBac system. **(B)** Dorso-lateral *in utero* electroporation (IUE) after injection of the plasmid mixture into the lateral ventricles. **(a)** Transfected cells occupying several layers of the cerebral cortex and the corpus callosum (cc) in adult mice. In particular, glial cells with different morphologies are shown, astrocytes in **(a′)** and oligodendrocytes in **(a″)**. After IUE of the subventricular zone (SVZ) OB cells were found in the OB **(b)** corresponding to granular **(b′)** and periglomerular **(b″)** phenotypes. **(C)** Rostral IUE after injection of the plasmid mixture into the lateral ventricles labeled cells in the cerebral cortex **(a)**. Neurons were widespread throughout the cerebral cortex, as were astrocytes **(a′)**. Cells corresponding to oligodendrocytes were positioned in the cc **(a″)**. Cells in the OB **(b)** with a glial **(b′)** and neuronal morphology corresponding to granular **(b″)** and periglomerular cells **(b‴)**. **(D)** Postnatal (P1) electroporation of dorso-lateral SVZ-progenitors. Labeled cells were surrounding the ventricular surface **(a)** with astroglial **(a′)** and oligodendroglial **(a″)** morphologies. In the OB **(b)** cells with a neuronal phenotype were situated in the granular **(b′)** and glomerular **(b″)** layers.

evident in the OB (**Figure 1Bb**). Transfected neurons were widespread along the rostro-caudal and ventro-lateral OB axis at 30 dpe, mostly located within the GCL (**Figure 1Bb′**) and GL (**Figure 1Bb″**). Remarkably, no glial cells were detected in the OB when performing dorso-lateral electroporations.

To assess the potentiality of progenitors at the OB ventricular surface, E13 IUE was performed directing the electrodes to the most rostral part of the LV (**Figure 1C**). At adult stages (30 dpe), labeled cells were distributed within the cerebral cortex of E13 electroporated brains (**Figure 1Ca**), with neurons distributed within layers II-VI of the cerebral cortex and glial cells also occupying several cortical areas (**Figure 1Ca′**). Progenitors remained labeled in the SVZ, as well as recognizable oligodendroglial cells (**Figure 1Ca″**). In contrast to dorso-lateral electroporation, labeled glia, and neurons were evident in the OB (**Figure 1Cb**). Thus, OB glial cells were produced by progenitors from the rostral part of the ventricular surface (**Figure 1Cb′**) but not by dorso-lateral progenitors after *in utero* electroporation (**Figure 1Bb**). The identity of the OB glia was addressed by studying different markers, corroborating the presence of astrocytes through the co-localization of eGFP with GFAP (Supplementary Figure S3A) and S100β (Supplementary

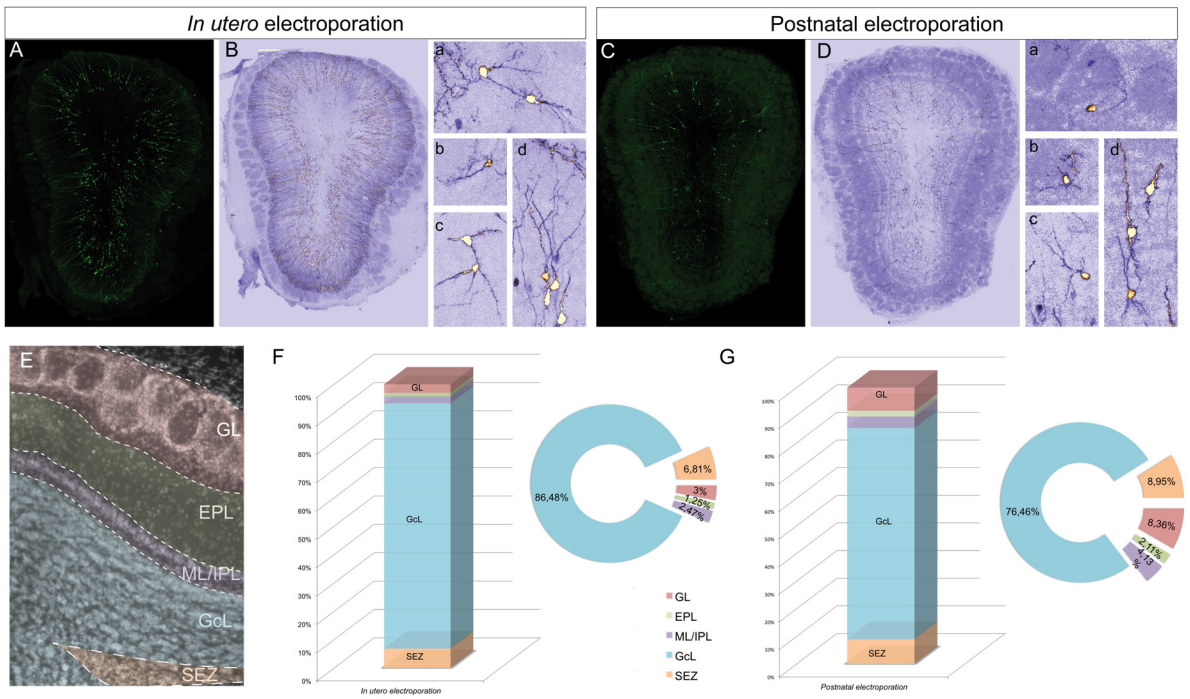

FIGURE 2 | Distribution of electroporated cells within the OB. The percentage of electroporated cells occupying different layers of the OB was studied after electroporation at E15 IUE or P1. **(A)** Representative coronal section of a P30 animal electroporated at E15. **(B)** To quantify the distribution the images were analyzed with ICA Lut (ImageJ software). Representative morphologies of periglomerular **(Ba)** and granular **(Bb–d)** electroporated cells. **(C)** Representative slice of a P30 OB after P1 electroporation. **(D)** Different cell morphologies and dispersion analysis was performed by applying the ICA Lut. Particular morphologies of periglomerular **(Da,b)** and granular **(Db–d)** electroporated cells are showed. **(E)** Different layers of analyzed OB: GL, glomerular layer; EPL, external plexiform layer; ML/IPL, mitral and internal plexiform layer; GCL, granular cell layer; SEZ, subependymal zone. **(F,G)** The percentage of P30 labeled cells after E15 IUE (1875 cells in 4 animals) and P1 electroporation (926 cells in 4 different animals) are shown in **(F,G)**, respectively.

Figure S3B). The oligodendroglial lineage was identified by either Olig2 (Supplementary Figure S3C) or PDGFRα (Supplementary Figure S3D), and electroporated cells that co-expressed both were present in the adult OB after such electroporations. Moreover, granular (**Figure 1Cb″**) and periglomerular cells (**Figure 1Cb‴**) were also labeled in the GCL and GL of the adult OB. Regarding their distribution, it is important to note that glial cells were located only within a lateral region of the OB, while neurons were broadly dispersed across the whole OB. Thus, neurons and glia generated from embryonic progenitors appear to have a different distribution pattern. Labeled SVZ progenitors remained at the adult ventricular surface (**Figure 1Ca″**), suggesting that some interneurons may still originate from these SVZ-transfected progenitors in the adult brain.

Finally, to specifically analyze the postnatal contribution of SVZ progenitors to the OB, we performed postnatal (P1) electroporations positioning the electrodes in the dorso-lateral region (**Figure 1D**). Transfected progenitors were evident in the dorso-lateral area of the ventricular surface of adult brains (30 dpe: **Figure 1Da**). Moreover, glial cells surrounded the electroporated area near the ventricular surface, with astrocytes (**Figure 1Da′**) and oligodendrocytes (**Figure 1Da″**) readily recognized. Targeting postnatal progenitors in the dorso-lateral region labeled interneurons in the OB (**Figure 1Db**). These postnatally labeled interneurons were mostly GCs located in the GCL (**Figure 1Db′**) and PGCs surrounding the glomeruli (**Figure 1Db″**).

Cell Phenotypes after Embryonic and Postnatal Electroporation

To assess the distribution and heterogeneity among the eGFP-transfected cells after *in utero* or postnatal electroporation, the cell dispersion within the OB layers was quantified at P30 (**Figure 2**). To focus exclusively on the extrabulbar origin of OB interneurons, only dorso-lateral electroporations of the SVZ were studied, examining a total of four animals with similar electroporations for both analyses (**Figures 2A,C**). A gross morphological analysis with ICA Lut (ImageJ) distinguished different arbor morphologies (**Figures 2B,D**) mainly associated with the glomerular (**Figures 2Ba,b**,**2Da,b**) and granule cell (**Figures 2Bc,d,2Dc,d**) layers. Glomerular cells have oval or round-shaped cell bodies, giving rise to a spiny apical dendritic tree that arborizes within the glomerulus (**Figures 2Ba,b,2Da,b**). However, most cells were overwhelmingly restricted to the GCL and they had dendritic arbors with a characteristic GC

morphology (**Figures 2Bc,d,2Dc,d**). We also quantified the percentage of electroporated cells in each layer of the OB after *in utero* or neonatal electroporation. Cells were arranged into five groups regarding their position within the GL, EPL, ML/IPL, GCL, or SEZ (**Figure 2E**). In general, eGFP-positive cells were similarly distributed after *in utero* or postnatal electroporation (**Figures 2F,G**). The proportion of the adult labeled cells in the different OB layers was quantified following *in utero* ($n = 4$ animals, 1875 eGFP-adult cells) and P1 ($n = 4$ animals, 926 eGFP-adult cells) electroporation. The vast majority of cells were located within the GCL (IUE 86.48 ± 0.59 and 76.46 ± 3.2% postnatal electroporation), with E15 and P1 electroporated animals displaying fewer labeled cells in the EPL (IUE: 1.25 ± 0.18% and P1: 2.11 ± 0.31%) and ML/IPL (IUE: 2.47 ± 0.32% and P1: 4.13 ± 0.96%). Thus, no significant differences were found in the layer distribution of the labeled cells between IUE and postnatal electroporation. However, the percentage of labeled cells in the GL was significantly different between E15 and P1 electroporated animals (*t*-test, $P = 0.022$), with more labeled cells in the GL of postnatal electroporated animals (8.36 ± 1.65%) than in electroporated embryos (3 ± 0.22%).

To address the heterogeneity of the cells generated by targeted progenitors we analyzed the neurochemical markers expressed by labeled cells within the OB (**Figure 3**). As our specific aim was to analyze interneurons that contribute to the olfactory bulb from an extra bulbar origin throughout life, electroporation was performed to target the dorso-lateral SVZ in either embryos (**Figure 1B**) or postnatal (**Figure 1D**) mice. The eGFP expressing cells analyzed in P30 mice represented a heterogeneous population of interneurons that expressed CR (**Figures 3A,B**), CB (**Figures 3C,D**), TH (**Figures 3E,F**), DDC (**Figures 3G,H**) and DCX (**Figures 3I,J**), yet not reelin (**Figures 4A,B**) or glial markers (**Figures 4C–J**).

According to the literature, the dorso-lateral area targeted is the origin of TH positive PGCs and thus, after electroporation, labeled cells were distributed in the glomerular area of the OB (**Figures 2F,G**). The number of $EGFP^+$ periglomerular cells was significantly higher in postnatal electroporated animals. However, the vast majority of eGFP-labeled cells were located within the GCL and SEZ as electroporation was directed toward the most dorso-lateral ventricular zones. In the OB, the labeled cells corresponded to a highly heterogeneous population, as reflected by the co-expression of the selected neuronal markers (arrowheads in **Figures 2A–H** magnifications), although interestingly in low numbers. The distribution of the labeled cells did not significantly vary after embryonic or postnatal electroporation, excluding PGCs. Regarding to the maturation of targeted cells, eGFP-DCX cells were found within the SEZ layer after either embryonic or postnatal electroporation (**Figures 3I,J** arrowheads). There were significant differences in the soma size of DCX positive cells in the SEZ (white region in Figure S4A) and GCL (pink area in Figure S4A), the former representing significantly smaller cells within the SEZ (mean 23.02 ± 0.89 μm^2, Supplementary Figure S4B) than those in the GCL (mean 51.97 ± 1.12 μm^2, Supplementary Figure S4C: Mann–Whitney test, $P < 0.001$, Supplementary Figure S4D). This suggests some maturation of the SEZ output when it reaches its final destination. In addition, after E15 IUE eGFP-DCX positive cells at P30 were found either near the SEZ, in the inner GCL, in the outer GCL or in the GL, reflecting the wide distribution of immature cells at the stages analyzed (Supplementary Figures S4E–G).

After IUE and postnatal electroporation transfected cells were rarely located in the EPL (IUE 1.25 ± 0.18 and 2.11 ± 0.31% postnatal electroporation) where PV and SOM are expressed widely. Moreover, the few eGFP-labeled cells in this layer did not express either PV (arrowheads in **Figures 3K,L** magnification) or SOM (arrowheads in **Figures 3M,N** magnification). We also performed reelin immunostaining to verify that no projection neurons were targeted (**Figures 4A,B**). Since mitral cells are generated between E10 and E13, with a peak of genesis at E11 (Blanchart et al., 2006), no eGFP-positive mitral cells were detected when IUE was performed at E15, as shown by reelin expression (**Figures 4A,B**). As expected, eGFP did not co-localize with any of the glial markers analyzed (S100β, **Figures 4C,D**; PDGFRα, **Figures 4E,F**; GFAP, **Figures 4G,H**; Olig2, **Figures 4I,J**) as electroporation did not target progenitors within the olfactory ventricle (**Figure 1C**).

DISCUSSION

This study addressed the distribution and neurochemical identity of adult OB interneurons targeted at either embryonic or postnatal ages with a ubiquitously expressed transposable reporter vector encoding eGFP. Through this approach, a stable tag is introduced into the genome of targeted progenitor cells that is inherited by all their progeny (Figueres-Oñate et al., 2015). Our results showed that the age of the mice and the electrode placement was critical for the targeting of different cell lineages in the OB, particularly for glial lineages and projection neurons. Moreover, the targeted cells represented a heterogeneous population of interneurons, both in animals electroporated as embryos or postnatally. The distribution of the progeny of either embryonic or postnatal dorso-lateral progenitors was similar in all the OB layers, except in the glomerular area where more PGCs were labeled by postnatal electroporation.

A Comparison of Embryonic and Postnatal OB Interneuron Generation

We previously reported that after *in vivo* embryonic electroporation of SVZ progenitors, several labeled OB interneurons undergo rounds of cell divisions before they differentiate (Figueres-Oñate et al., 2015). The progenitors of these interneurons were present in the SVZ at embryonic stages and the embryonic time at which the different OB populations of projection neurons and interneurons are generated has been addressed through *in utero* electroporation (Chen and LoTurco, 2012; Imamura and Greer, 2013, 2014; Siddiqi et al., 2014). OB interneurons originate from E13 progenitors located in the sub-pallium, specifically in the LGE (Wichterle et al., 2001; Kohwi et al., 2007). These LGE progenitors later distribute along the ventricular surface and some of them become adult neural stem cells, this destiny being specified before E15 (Fuentealba

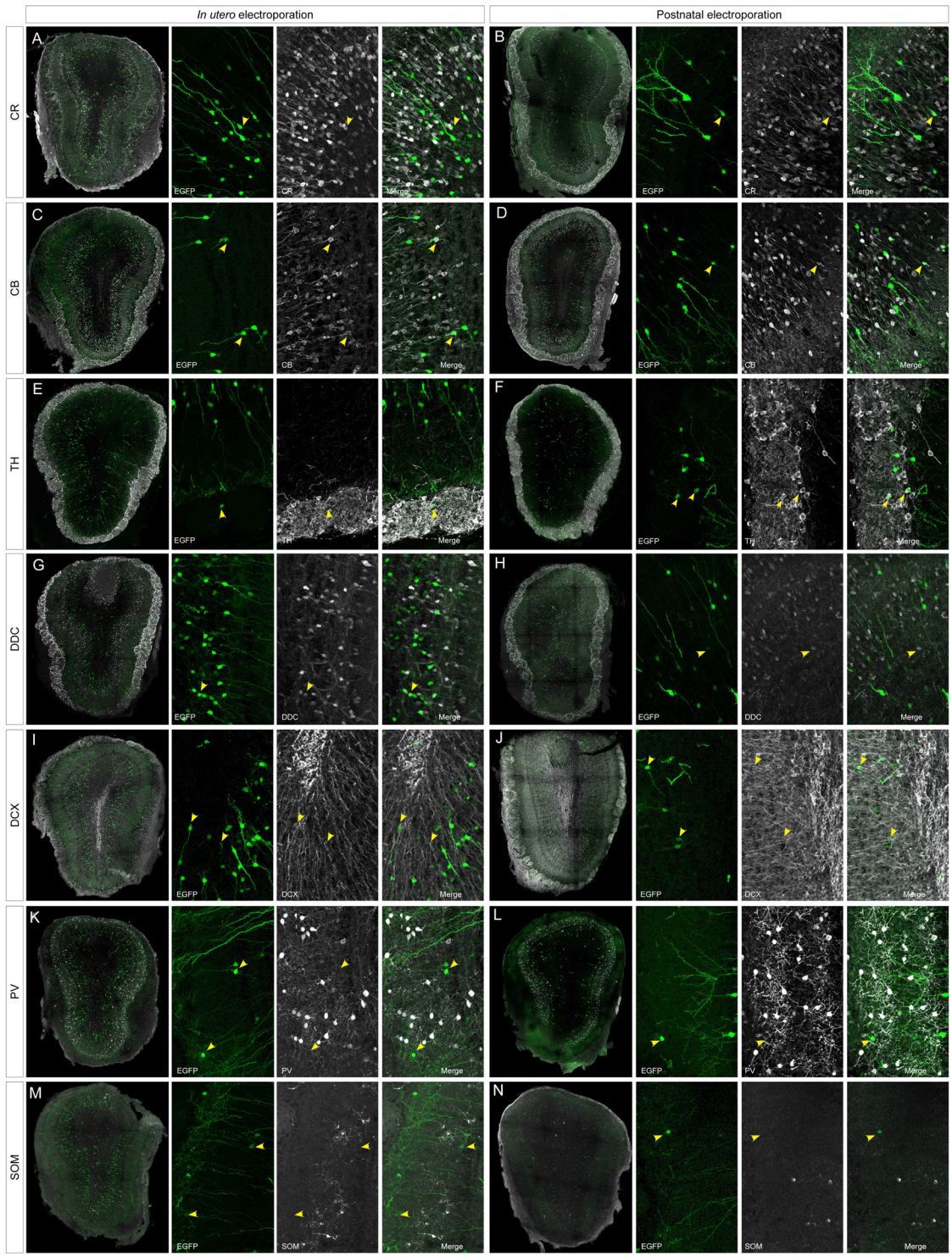

FIGURE 3 | Neuronal immunolabeling after IUE (E15) or postnatal (P1) electroporation. At P30, EGFP labeled cells immunostained for: CR, calretinin **(A,B)**; CB, calbindin **(C,D)**; TH, tyrosine hydroxylase **(E,F)**; DDC, dopa decarboxylase **(G,H)**; DCX, doublecortin **(I,J)**. Arrowheads in magnifications show targeted cells that co-express the respective markers. **(K–N)** After IUE or postnatal electroporation, analyzed cells targeted in the OB (arrowheads in **K,L**) did not contain parvalbumin (PV, arrowheads in **K,L** magnifications) or somatostatin (SOM, arrowheads in **M,N** magnifications).

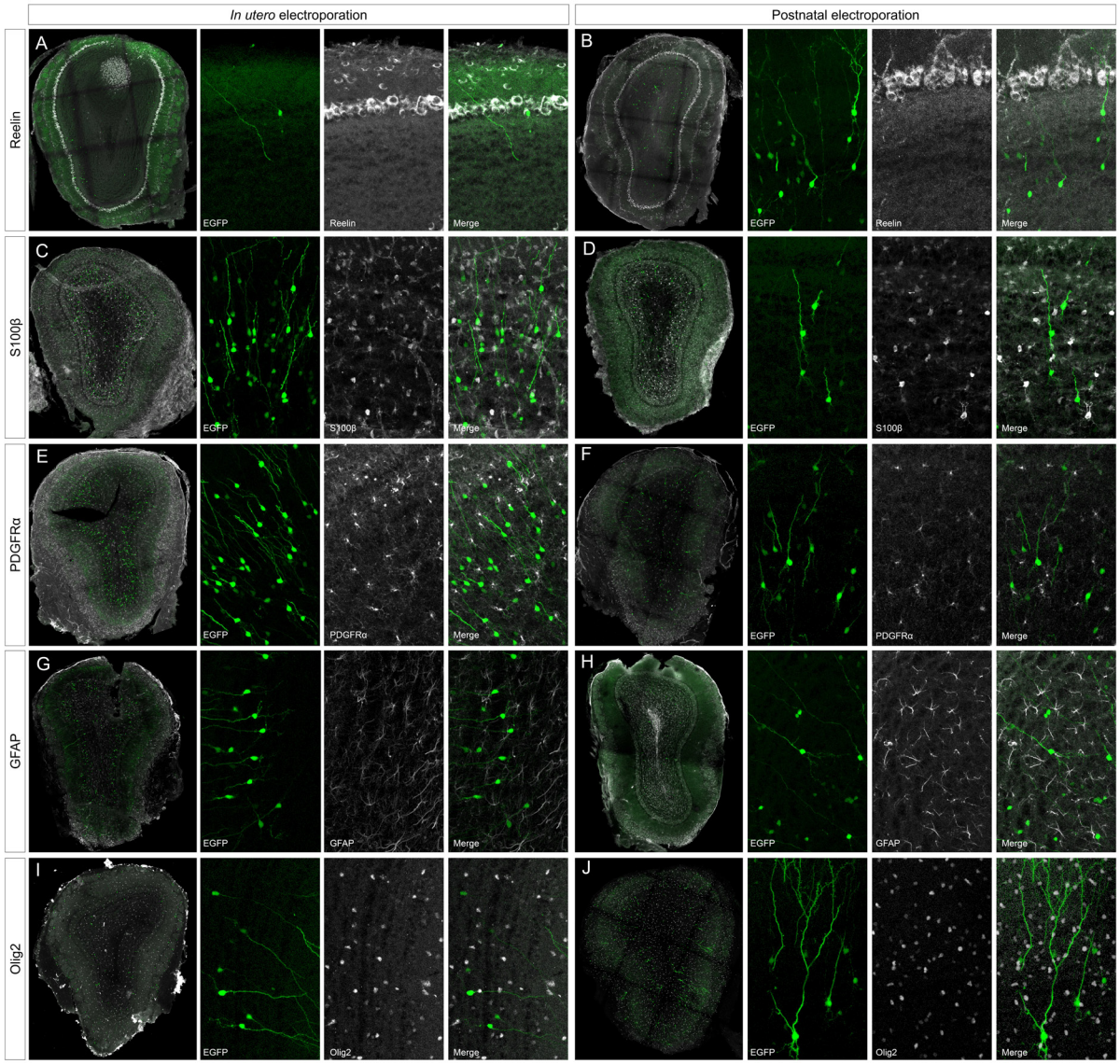

FIGURE 4 | Negative immunomarkers after IUE or postnatal electroporations. (A,B) After E15 or P1 electroporation, adult targeted cells (P30) did not express reelin (reel). **(C–J)** The analyzed glial markers, S100β **(C,D)**, PDGFRα **(E,F)**, GFAP **(G,H)**, or Olig2 **(I,J)**, did not co-localized with P30 EGFP^{+} cells. Thus, neither projection nor glial cells were targeted after electroporation of the dorso-lateral progenitors from the ventricular zone at embryonic or postnatal stages.

et al., 2015). Accordingly, our dorso-lateral electroporation at E15 labeled SVZ progenitors that were already compromised to establish certain OB interneuron subtypes. The temporal pattern of interneuron generation from embryonic to postnatal stages has been studied by tracing the lineages derived from specific progenitors in transgenic mice (Calzolari et al., 2015). In this way it became clear that different OB interneuron populations are generated from DLX1/2 progenitors at different times (Batista-Brito et al., 2008). Different adult new-born subpopulations are generated at different ages, the most heterogeneous being generated around the time of the animal's birth, when olfactory sensation begins (Brann and Firestein, 2014). For example, CB-positive PGCs are preferentially generated during the early postnatal period, whereas CR and TH neurons are mainly produced later in life (De Marchis et al., 2007). To measure the potential differences between OB interneurons generated at postnatal or embryonic ages, we used *in utero* and postnatal electroporation. However, at P30 there were no significant differences between the populations of transfected cells after dorso-lateral embryonic or postnatal

electroporation. The postnatal generation of specific granular or periglomerular interneuron subpopulations that originate from specific Pax6, Tbr2, 5HT3, or Neurog2 progenitors has previously been studied in the OB (Kohwi et al., 2005; Inta et al., 2008; Brill et al., 2009; Winpenny et al., 2011). Two weeks after postnatal electroporation at the ventricular surface, OB cells that were labeled expressed markers of interneurons and they were electrically excitable (Chesler et al., 2008). Moreover, the heterogeneity and specific regionalization of these interneurons in the OB can be addressed changing the orientation of the electrodes (Fernández et al., 2011). Thus, the SVZ represents a heterogeneous pool of neural progenitors at both embryonic or postnatal stages, highlighting that a correlation exists between OB neuron-type and SVZ regionalization (Hack et al., 2005; Merkle et al., 2007).

With regards location, our data showed that there were few transfected cells within the EPL and ML/IPL, the vast majority occupying either the most external or internal part of the granular cell layer. The increase in the proportion of transfected PGCs after postnatal electroporation may be related to the precise location of the SVZ progenitors that differentially contribute to distinct types of periglomerular interneurons (Lledo et al., 2008).

Targeted Cells Do Not Co-Localize with a Large Number of Markers

Our data show that newborn cells represent a heterogeneous population, since the transfected eGFP-cells expressed most of the markers analyzed. Actually, the large variety of markers for newly generated cells contrasts with the lower number of newborn cells expressing each when compared with the total number of eGFP transfected cells. In fact, after virus infection (Merkle et al., 2007), *in utero* electroporation (Fernández et al., 2011), or tamoxifen administration in transgenic mice (Batista-Brito et al., 2008), the percentages of labeled GCs that express immunohistochemical markers is also really low. Those different approaches to label adult newborn cells in the OB established that the percentage of CR and CB expressing neurons in the GCL is no more than 20% (Bagley et al., 2007). However, the percentage of positive CR cells in relation to the total population of cells in the GCL of the adult OB is around 10% (Parrish-Aungst et al., 2007). Therefore, despite the large diversity of markers used there are relatively few newly generated cells with regards the total proportion of those cells types in the OB. In this respect, and due to the lack of markers, new cells occupying the internal part of the granular layer were described by their morphology, layering, and origin (Merkle et al., 2014). This highlights the need for new markers to define these populations of newborn interneurons that are generated in the OB throughout adulthood.

Another possibility is that those cells remained immature at the time of analysis (P30), although newly generated cells display electrical properties 2 weeks after postnatal electroporation (Chesler et al., 2008). Similarly, Tbr1-Tbr2 expression is evident in dopaminergic cells 21 days after labeling (Winpenny et al., 2011). In other studies the immunochemical nature of OB interneurons arising from ventricular-targeted progenitors can be defined 15–30 days post progenitor targeting (Fernández et al., 2011; de Chevigny et al., 2012; Merkle et al., 2014). Otherwise, we found labeled cells that expressed immature markers like DCX at 20 dpe, widely spread across the OB, although there were too few to assume that analyzed cells did not express mature markers because they were undifferentiated. Moreover, our dual immunohistochemistry studies using markers of mature (NeuN, CB, CR) and immature (DCX) cells showed some overlap within these populations, indicating a gradual maturation of these cells.

Ontogeny of Glial Cells in the Olfactory Bulb

We recently analyzed the clonal dispersion and migratory routes of NG2 cells in the OB (García-Marqués et al., 2014) using the StarTrack method (García-Marqués and López-Mascaraque, 2013). We also described the large heterogeneity within the glial lineages in the OB (Figueres-Oñate et al., 2014; García-Marqués and López-Mascaraque, 2016) and cerebral cortex (Bribián et al., 2016). However, the origin of glial cells in the OB is not as well understood as that of neurons. Most studies describe the glial populations in the OB through their morphology (De Castro, 1920; Valverde and Lopez-Mascaraque, 1991) or using immunohistochemical markers (Bailey and Shipley, 1993; Chiu and Greer, 1996; Emsley and MacKlis, 2006), while the origin and heterogeneity this lineage within the OB is still unclear. A general analysis of the GFAP and S100β expression throughout the brain showed a high density of astrocytes in the OB (Emsley and MacKlis, 2006) and thus, considering OB astrocytes in functional studies is important to understand the specific role of glial cells in the SVZ-RMS-OB pathway (García-Marqués et al., 2010). Moreover, our data show that after postnatal or embryonic electroporation of the dorso-lateral part of the lateral ventricles there was no labeled glial cells within the OB. However, we could trace glial lineages in the OB, such as astrocytes, oligodendrocytes, and Ng2 cells after performing electroporations at E13 directed to the most rostral part of the lateral ventricles. Thus, these glial cells would appear to come from progenitors located within the OB. In addition, the distribution of glial cells within the OB in just one lateral region suggests that they may be generated following the radial glial processes, as in the cortex (García-Marqués and López-Mascaraque, 2013).

In summary, a better understanding of the neural cells generated in adulthood and the factors that control their proliferation, migration, and integration into neural circuits is crucial. Moreover, it is also essential to use clonal analysis so that single progenitor cells can be labeled and their progeny tracked in order to match progenitor cells to specific neural populations in the adult OB, including glial lineages.

AUTHOR CONTRIBUTIONS

LM, Conceived and designed the experiments, writing the paper and obtained funding. MF, help in the design of the study, performed the experiments and writing the paper.

ACKNOWLEDGMENTS

This work was supported by research Grant BFU2013-48807-R from the Spanish Ministry of Economy and Competitiveness. We thank Dr. Mark Sefton for helpful editorial assistance.

SUPPLEMENTARY MATERIAL

The Supplementary Material for this article can be found online at: http://journal.frontiersin.org/article/10.3389/fnins.2016.00194

REFERENCES

Altman, J. (1962). Are new neurons formed in the brains of adult mammals? *Science* 135, 1127–1128. doi: 10.1126/science.135.3509.1127

Altman, J. (1969). Autoradiographic and histological studies of postnatal neurogenesis. IV. Cell proliferation and migration in the anterior forebrain, with special reference to persisting neurogenesis in the olfactory bulb. *J. Comp. Neurol.* 137, 433–457. doi: 10.1002/cne.901370404

Altman, J., and Das, G. D. (1965). Post-natal origin of microneurones in the rat brain. *Nature* 207, 953–956. doi: 10.1038/207953a0

Bagley, J., LaRocca, G., Jimenez, D. A., and Urban, N. N. (2007). Adult neurogenesis and specific replacement of interneuron subtypes in the mouse main olfactory bulb. *BMC Neurosci.* 8:92. doi: 10.1186/1471-2202-8-92

Bailey, M. S., and Shipley, M. T. (1993). Astrocyte subtypes in the rat olfactory bulb: morphological heterogeneity and differential laminar distribution. *J. Comp. Neurol.* 328, 501–526. doi: 10.1002/cne.903280405

Batista-Brito, R., Close, J., Machold, R., and Fishell, G. (2008). The distinct temporal origins of olfactory bulb interneuron subtypes. *J. Neurosci.* 28, 3966–3975. doi: 10.1523/JNEUROSCI.5625-07.2008

Bayer, S. (1983). 3H-thymidine-radiographic studies of neurogenesis in the rat olfactory bulb. *Exp. Brain Res.* 50, 329–340. doi: 10.1007/bf00239197

Bayer, S. A., Zhang, X., Russo, R. J., and Altman, J. (1994). Three-dimensional reconstructions of the developing forebrain in rat embryos. *Neuroimage* 1, 296–307. doi: 10.1006/nimg.1994.1014

Blanchart, A., De Carlos, J. A., and López-Mascaraque, L. (2006). Time frame of mitral cell development. *J. Comp. Neurol.* 543, 529–543. doi: 10.1002/cne.20941

Brann, J. H., and Firestein, S. J. (2014). A lifetime of neurogenesis in the olfactory system. *Front. Neurosci.* 8:182. doi: 10.3389/fnins.2014.00182

Bribián, A., Figueres-Oñate, M., Martín-López, E., and López-Mascaraque, L. (2016). Decoding astrocyte heterogeneity: new tools for clonal analysis. *Neuroscience* 323, 10–19. doi: 10.1016/j.neuroscience.2015.04.036

Brill, M. S., Ninkovic, J., Winpenny, E., Hodge, R. D., Ozen, I., Yang, R., et al. (2009). Adult generation of glutamatergic olfactory bulb interneurons. *Nat. Neurosci.* 12, 1524–1533. doi: 10.1038/nn.2416

Calzolari, F., Michel, J., Baumgart, E. V., Theis, F., Götz, M., and Ninkovic, J. (2015). Fast clonal expansion and limited neural stem cell self-renewal in the adult subependymal zone. *Nat. Neurosci.* 18, 490–492. doi: 10.1038/nn.3963

Chen, F., and LoTurco, J. (2012). A method for stable transgenesis of radial glia lineage in rat neocortex by piggyBac mediated transposition. *J. Neurosci. Methods* 207, 172–180. doi: 10.1016/j.jneumeth.2012.03.016

Chesler, A. T., Le Pichon, C. E., Brann, J. H., Araneda, R. C., Zou, D.-J., and Firestein, S. (2008). Selective gene expression by postnatal electroporation during olfactory interneuron neurogenesis. *PLoS ONE* 3:e1517. doi: 10.1371/journal.pone.0001517

Chiu, K., and Greer, C. A. (1996). Immunocytochemical analyses of astrocyte development in the olfactory bulb. *Dev. Brain Res.* 95, 28–37. doi: 10.1016/0165-3806(96)00055-7

De Castro, F. (1920). Estudios sobre la neuroglia de la corteza cerebral del hombre y de los animales. *Trab. Lab. Invest. Biol.* 18, 1–35.

de Chevigny, A., Core, N., Follert, P., Wild, S., Bosio, A., Yoshikawa, K., et al. (2012). Dynamic expression of the pro-dopaminergic transcription factors Pax6 and Dlx2 during postnatal olfactory bulb neurogenesis. *Front. Cell Neurosci.* 6:6. doi: 10.3389/fncel.2012.00006

De Marchis, S., Bovetti, S., Carletti, B., Hsieh, Y. C., Garzotto, D., Peretto, P., et al. (2007). Generation of distinct types of periglomerular olfactory bulb interneurons during development and in adult mice: implication for intrinsic properties of the subventricular zone progenitor population. *J. Neurosci.* 27, 657–664. doi: 10.1523/JNEUROSCI.2870-06.2007

Emsley, J. G., and MacKlis, J. D. (2006). Astroglial heterogeneity closely reflects the neuronal-defined anatomy of the adult murine CNS. *Neuron Glia Biol.* 2, 175–186. doi: 10.1017/S1740925X06000202

Fernández, M. E., Croce, S., Boutin, C., Cremer, H., and Raineteau, O. (2011). Targeted electroporation of defined lateral ventricular walls: a novel and rapid method to study fate specification during postnatal forebrain neurogenesis. *Neural Dev.* 6:13. doi: 10.1186/1749-8104-6-13

Figueres-Oñate, M., García-Marqués, J., Pedraza, M., De Carlos, J. A., and López-Mascaraque, L. (2015). Spatiotemporal analyses of neural lineages after embryonic and postnatal progenitor targeting combining different reporters. *Front. Neurosci.* 9:87. doi: 10.3389/fnins.2015.00087

Figueres-Oñate, M., Gutiérrez, Y., and López-Mascaraque, L. (2014). Unraveling Cajal's view of the olfactory system. *Front. Neuroanat.* 8:55. doi: 10.3389/fnana.2014.00055

Fiorelli, R., Azim, K., Fischer, B., and Raineteau, O. (2015). Adding a spatial dimension to postnatal ventricular-subventricular zone neurogenesis. *Development* 142, 2109–2120. doi: 10.1242/dev.119966

Fuentealba, L. C., Rompani, S. B., Parraguez, J. I., Obernier, K., Romero, R., Cepko, C. L., et al. (2015). Embryonic origin of postnatal neural stem cells. *Cell* 161, 1644–1655. doi: 10.1016/j.cell.2015.05.041

García-Marqués, J., De Carlos, J. A., Greer, C. A, and López-Mascaraque, L. (2010). Different astroglia permissivity controls the migration of olfactory bulb interneuron precursors. *Glia* 58, 218–230. doi: 10.1002/glia.20918

García-Marqués, J., and López-Mascaraque, L. (2013). Clonal identity determines astrocyte cortical heterogeneity. *Cereb. Cortex* 23, 1463–1472. doi: 10.1093/cercor/bhs134

García-Marqués, J., and López-Mascaraque, L. (2016). Clonal mapping of astrocytes in the olfactory bulb and rostral migratory stream. *Cereb. Cortex.* [Epub ahead of print].

García-Marqués, J., Núñez-Llaves, R., and López-Mascaraque, L. (2014). NG2-glia from pallial progenitors produce the largest clonal clusters of the brain: time frame of clonal generation in cortex and olfactory bulb. *J. Neurosci.* 34, 2305–2313. doi: 10.1523/JNEUROSCI.3060-13.2014

Hack, M. A., Saghatelyan, A., de Chevigny, A., Pfeifer, A., Ashery-Padan, R., Lledo, P.-M., et al. (2005). Neuronal fate determinants of adult olfactory bulb neurogenesis. *Nat. Neurosci.* 8, 865–872. doi: 10.1038/nn1479

Imamura, F., and Greer, C. A. (2013). Pax6 regulates Tbr1 and Tbr2 expressions in olfactory bulb mitral cells. *Mol. Cell. Neurosci.* 54, 58–70. doi: 10.1016/j.mcn.2013.01.002

Imamura, F., and Greer, C. A. (2014). Segregated labeling of olfactory bulb projection neurons based on their birthdates. *Eur. J. Neurosci.* 41, 1–10. doi: 10.1111/ejn.12784

Inta, D., Alfonso, J., von Engelhardt, J., Kreuzberg, M. M., Meyer, A. H., van Hooft, J., et al. (2008). Neurogenesis and widespread forebrain migration of distinct GABAergic neurons from the postnatal subventricular zone. *Proc. Natl. Acad. Sci. U.S.A.* 105, 20994–20999. doi: 10.1073/pnas.0807059105

Kaplan, M. S., and Hinds, J. W. (1977). Neurogenesis in the adult rat: electron microscopic analysis of light radioautographs. *Science* 197, 1092–1094 doi: 10.1126/science.887941

Kohwi, M., Osumi, N., Rubenstein, J. L. R., and Alvarez-Buylla, A. (2005). Pax6 is required for making specific subpopulations of granule and periglomerular neurons in the olfactory bulb. *J. Neurosci.* 25, 6997–7003. doi: 10.1523/JNEUROSCI.1435-05.2005

Kohwi, M., Petryniak, M. A., Long, J. E., Ekker, M., Obata, K., Yanagawa, Y., et al. (2007). A subpopulation of olfactory bulb GABAergic interneurons is derived from Emx1- and Dlx5/6-expressing progenitors. *J. Neurosci.* 27, 6878–6891. doi: 10.1523/JNEUROSCI.0254-07.2007

Kosaka, K., Toida, K., Aika, Y., and Kosaka, T. (1998). How simple is the organization of the olfactory glomerulus?: the heterogeneity of so-called periglomerular cells. *Neurosci. Res.* 30, 101–110. doi: 10.1016/S0168-0102(98)00002-9

Lledo, P.-M., Merkle, F. T., and Alvarez-Buylla, A. (2008). Origin and function of olfactory bulb interneuron diversity. *Trends Neurosci.* 31, 392–400. doi: 10.1016/j.tins.2008.05.006

Lois, C., and Alvarez-Buylla, A. (1994). Long-distance neuronal migration in the adult mammalian brain. *Science* 264, 1145–1148. doi: 10.1126/science.8178174

Luskin, M. B. (1993). Restricted proliferation and migration of postnatally generated neurons derived from the forebrain subventricular zone. *Neuron* 11, 173–189. doi: 10.1016/0896-6273(93)90281-U

Merkle, F. T., Fuentealba, L. C., Sanders, T. A., Magno, L., Kessaris, N., and Alvarez-Buylla, A. (2014). Adult neural stem cells in distinct microdomains generate previously unknown interneuron types. *Nat. Neurosci.* 17, 207–214. doi: 10.1038/nn.3610

Merkle, F. T., Mirzadeh, Z., and Alvarez-Buylla, A. (2007). Mosaic organization of neural stem cells in the adult brain. *Science* 317, 381–384. doi: 10.1126/science.1144914

Parrish-Aungst, S., Shipley, M. T., Erdelyi, F., Szabo, G., and Puche, A. C. (2007). Quantitative analysis of neuronal diversity in the mouse olfactory bulb. *J. Comp. Neurol.* 501, 825–836. doi: 10.1002/cne.21205

Petreanu, L., and Alvarez-Buylla, A. (2002). Maturation and death of adult-born olfactory bulb granule neurons: role of olfaction. *J. Neurosci.* 22, 6106–6113.

Pinching, A. J., and Powell, T. P. S. (1971). The neuropil of the glomeruli of the olfactory bulb. *J. Cell Sci.* 9, 347–377.

Price, J. L., and Powell, T. P. (1970). The synaptology of the granule cells of the olfactory bulb. *J. Cell Sci. 7*, 125–155.

Sequerra, E. B. (2014). Subventricular zone progenitors in time and space: generating neuronal diversity. *Front. Cell. Neurosci.* 8:434. doi: 10.3389/fncel.2014.00434

Siddiqi, F., Chen, F., Aron, A. W., Fiondella, C. G., Patel, K., and LoTurco, J. (2014). Fate mapping by piggybac transposase reveals that neocortical GLAST+ progenitors generate more astrocytes than Nestin+ progenitors in rat neocortex. *Cereb. Cortex* 24, 508–520. doi: 10.1093/cercor/bhs332

Valverde, F., and Lopez-Mascaraque, L. (1991). Neuroglial arrangements in the olfactory glomeruli of the hedgehog. *J. Comp. Neurol.* 307, 658–674.

Whitman, M. C., and Greer, C. A. (2007). Adult-generated neurons exhibit diverse developmental fates. *Dev. Neurobiol.* 67, 1079–1093. doi: 10.1002/dneu.20389

Wichterle, H., Turnbull, D. H., Nery, S., Fishell, G., and Alvarez-Buylla, A. (2001). *In utero* fate mapping reveals distinct migratory pathways and fates of neurons born in the mammalian basal forebrain. *Development* 128, 3759–3771.

Winpenny, E., Lebel-Potter, M., Fernandez, M. E., Brill, M. S., Götz, M., Guillemot, F., et al. (2011). Sequential generation of olfactory bulb glutamatergic neurons by Neurog2-expressing precursor cells. *Neural Dev.* 6:12. doi: 10.1186/1749-8104-6-12

Young, K. M., Fogarty, M., Kessaris, N., and Richardson, W. D. (2007). Subventricular zone stem cells are heterogeneous with respect to their embryonic origins and neurogenic fates in the adult olfactory bulb. *J. Neurosci.* 27, 8286–8296. doi: 10.1523/JNEUROSCI.0476-07.2007

Yusa, K., Rad, R., Takeda, J., and Bradley, A. (2009). Generation of transgene-free induced pluripotent mouse stem cells by the piggyBac transposon. *Nat. Methods* 6, 363–369. doi: 10.1038/nmeth.1323

Yusa, K., Zhou, L., Li, M. A., Bradley, A., and Craig, N. L. (2011). A hyperactive piggyBac transposase for mammalian applications. *Proc. Natl. Acad. Sci. U.S.A.* 108, 1531–1536. doi: 10.1073/pnas.1008322108

Conflict of Interest Statement: The authors declare that the research was conducted in the absence of any commercial or financial relationships that could be construed as a potential conflict of interest.

frontiers

Supplementary Figures

Adult olfactory bulb interneuron phenotypes identified by targeting embryonic and postnatal neural progenitors

Maria Figueres-Oñate & Laura López-Mascaraque*

*Correspondence: mascaraque@cajal.csic.es

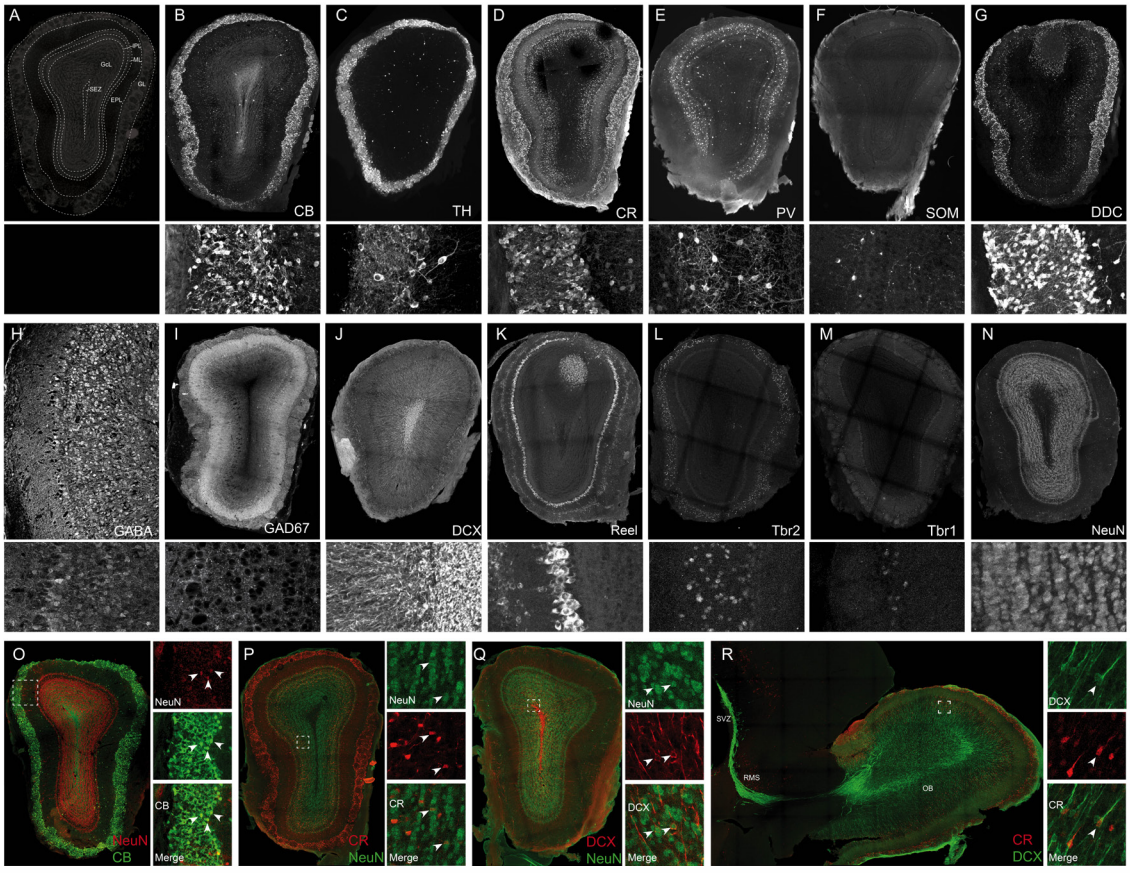

Supplementary Figure S1. Expression of different neuronal markers in the olfactory bulb. (A) Coronal section of the OB indicating the different layers. From inside-out, subependymal zone (SEZ), granular cell layer (GCL), internal plexiform layer (IPL), mitral cell layer (ML), external plexiform layer (EPL) and glomerular layer (GL). (B-N) Expression of the following protein markers within the OB: calbindin (CB, B), tyrosine hydroxylase (TH, C), calretinin (CR, D), parvalbumin (PV, E), somatostatin (SOM, F), dopa decarboxylase (DDC, G), GABA (H), GAD67 (I), doublecortin (DCX, J), reelin (Reel, K), Tbr2 (L), Tbr1 (M), neuronal nuclei (NeuN, N). (O-R) Dual immunohistochemistry for NeuN and CB (O), NeuN and CR (P), NeuN and DCX (Q) and CR-DCX (R). Arrowheads point to cells co-expressing both markers and asterisks to single labeled cells: SVZ, Subventricular Zone; RMS, Rostral migratory stream; OB, Olfactory bulb.

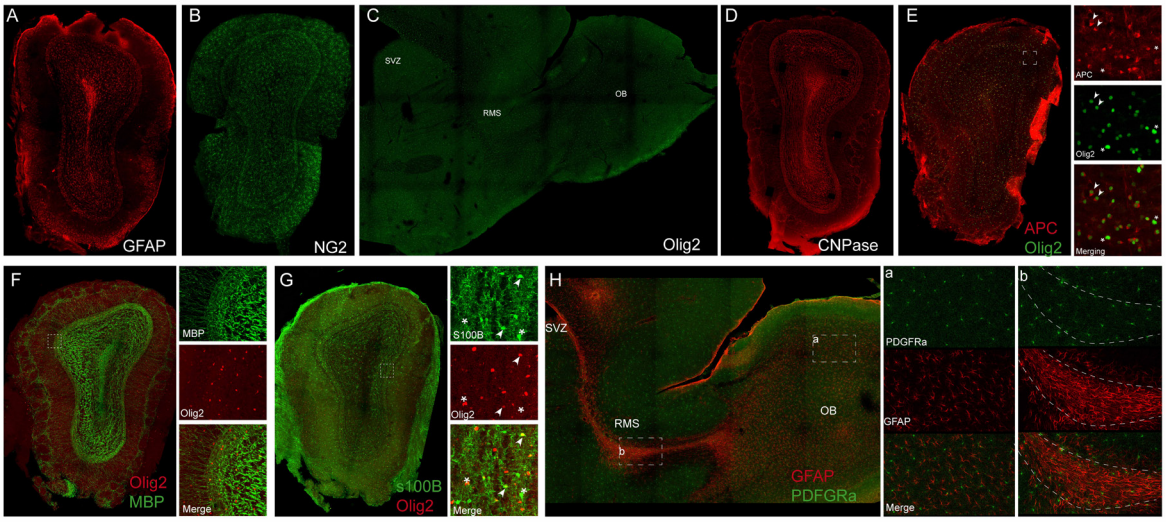

Supplementary Figure S2. Distribution of glial cells in the olfactory bulb. (A) Glial fibrillary acidic protein (GFAP) for astrocytes. (B) NG2-cells or polydendrocytes labeled with the Neuron-glial antigen 2 (NG2). (C) Olig2, the oligodendrocyte transcription factor 2 labels cells of the oligodendroglial lineage. Mature oligodendrocytes targeted either with CNPase (D) or co-labeled with APC-Olig2 (E, arrowheads). Olig2 targeted some cells from the oligodendroglial lineage that were not positive for APC (arrowheads, E). Co-localization of Olig2 with other mature oligodendrocyte markers, like MPB, was not clear (F). S100β and Olig2 co-localized in some cells (arrowheads, G) while the vast majority were from different cell populations (asterisks, G). GFAP and PDGFRα labeled different populations without overlapping (H). PDGFRα was homogeneously distributed in the SVZ-RMS-OB pathway, while GFAP was expressed strongly within the RMS and SEZ (H, a-b): SVZ, Subventricular Zone; RMS, Rostral migratory stream; OB, Olfactory bulb.

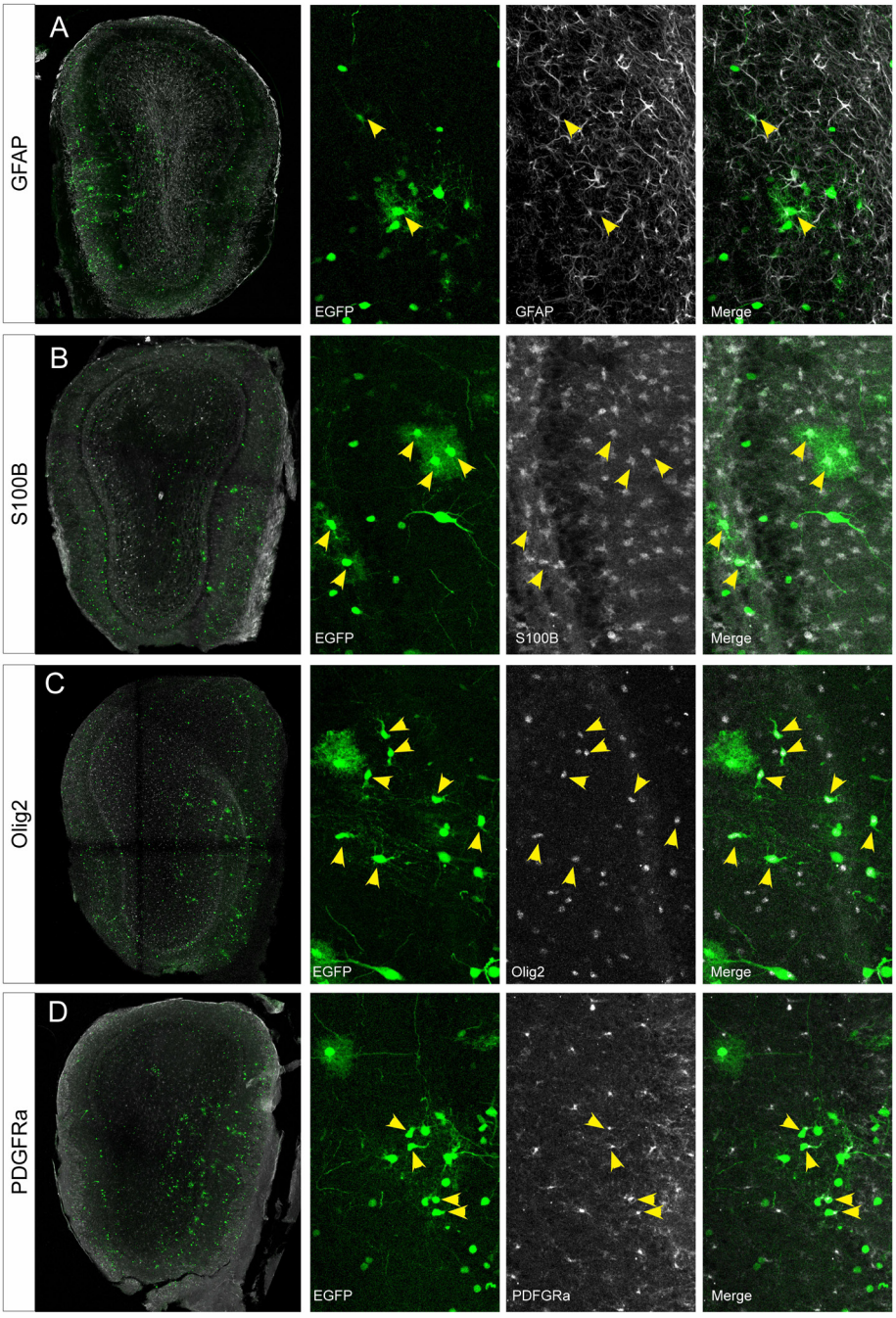

Supplementary Figure S3: Immunolabeling of different glial markers after IUE (E13) directed to the rostral ventricular surface. After electroporation of the most rostral part of the lateral ventricles at E13, glial cells were labeled in the OB 30 dpe. Arrowheads showed eGFP positive cells stained with the astrocyte marker GFAP (A). The astrocyte lineage was also assessed by staining with S100β (arrowheads, B). Oligodendroglial cells were also targeted by electroporation as witnessed with Olig2 (arrowheads, C) and PDGFRα (arrowheads, D).

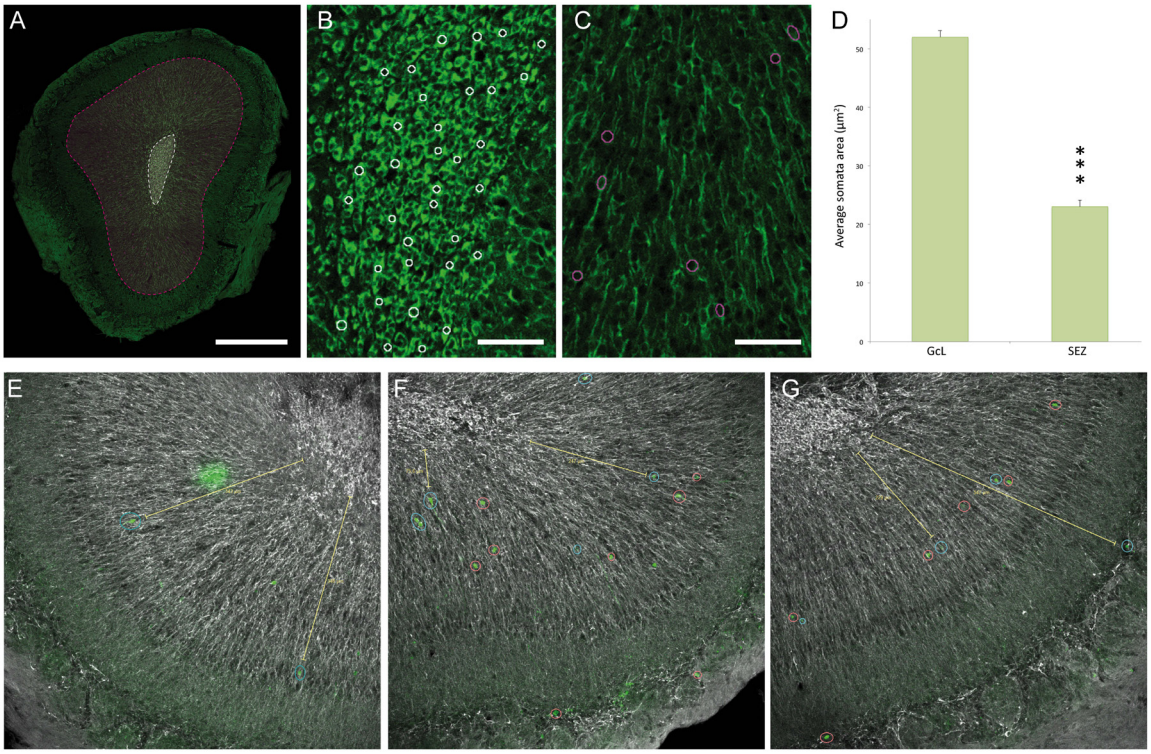

Supplementary Figure S4: Doublecortin immunolabeling. A representative coronal section of a P30 OB was selected to analyze the somata area of DCX positive cells (A). The area of the labeled cells was measured within the GCL (pink area in A) and the SEZ (white area in A). Somata of DCX positive cells were selected and counted in the SEZ (as shown in B, n=46) and GCL (C, n=60). Significant differences were seen when comparing the average somata size of labeled cells from the GCL (51.97±1.12 µm^2) and SEZ (23.02 ± 0.89 µm^2) (D). After electroporation at E15, some eGFP positive cells were also positive for DCX (blue circles in E-G) and the distance from the SEZ was determined in microns. Double stained cells were located in either the outer GCL (343-348 µm from the SEZ, E), close to the SEZ (75.6 µm from the SEZ, F) or surrounding the glomeruli (547 µm from the SEZ, G). Electroporated cells negative for DCX immunolabeling are indicated by a red circle. Scale bar 500 µm in A, and 50 µm in B,C.

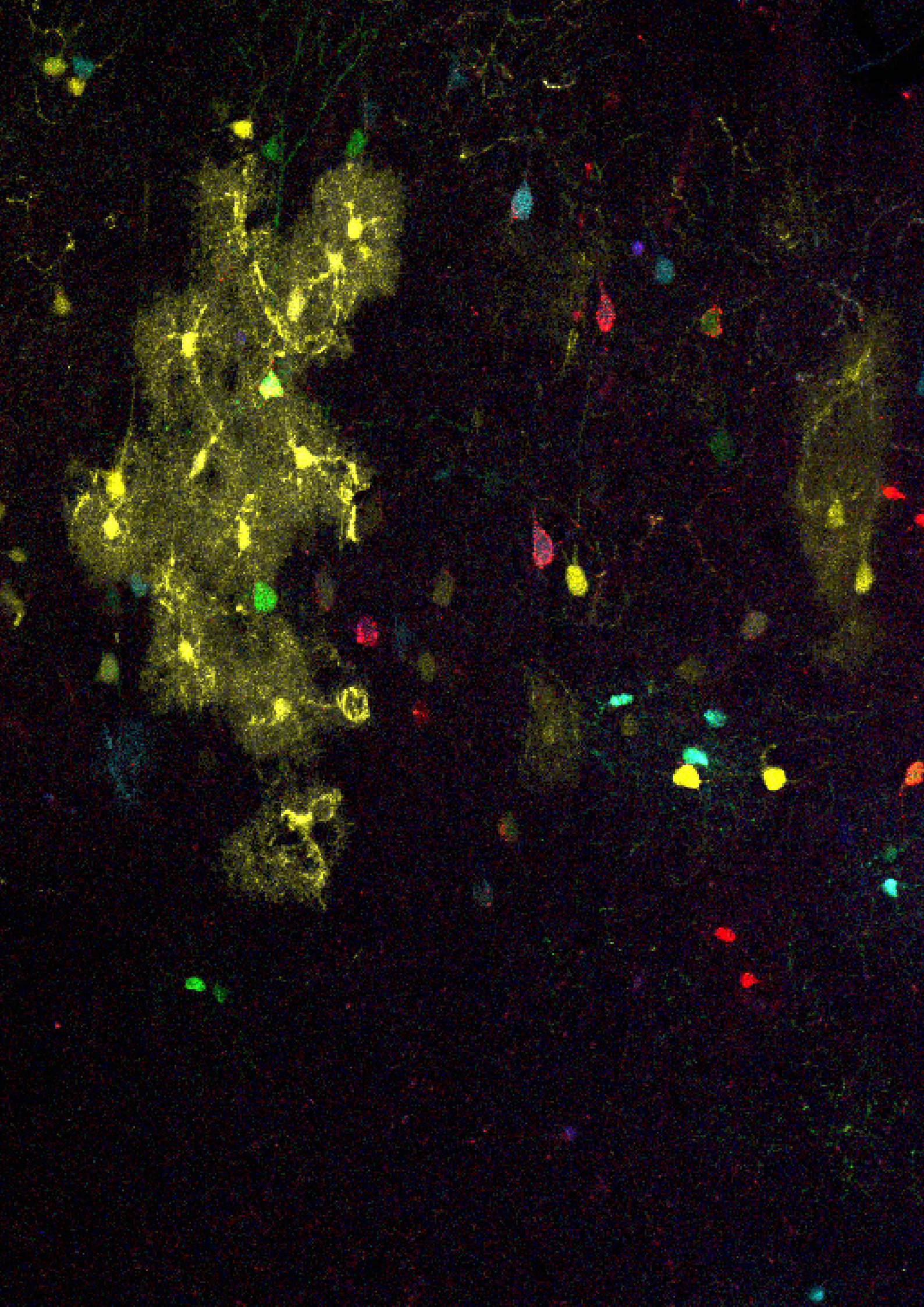

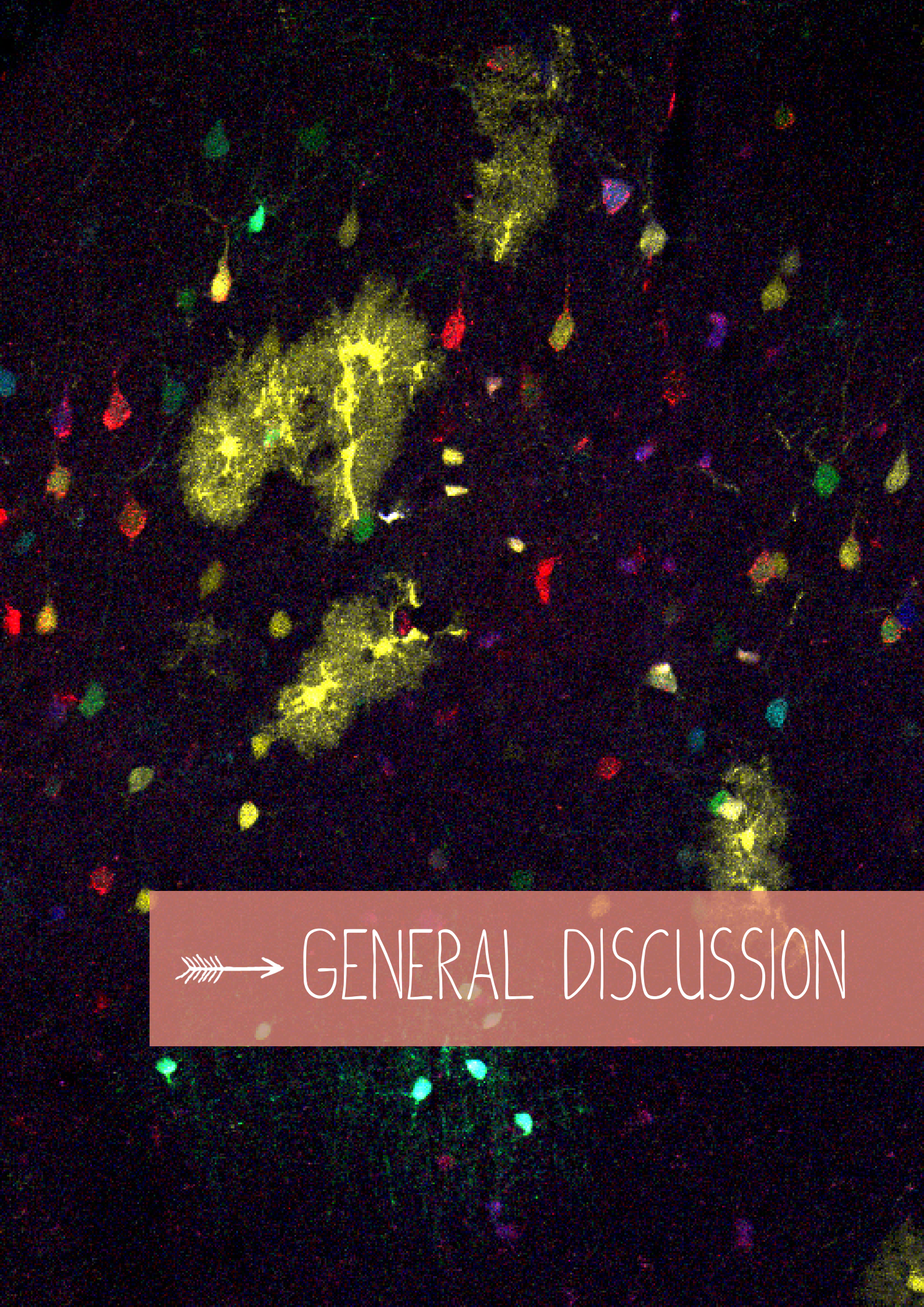

GENERAL DISCUSSION

The main aim of this Thesis project was to draw the clonal progeny of single progenitors in order to understand their nature and fate. To insight clonal relationships between the different brain lineage, we designed a strategy enable us to identify both neuronal and glial clones derived from single progenitors, the UbC-StarTrack. Analyses of clonal dispersion in the adult brain revealed specific clonal distribution patterns and the existence of clonal arrangements in specific domains. Moreover, the identification of the cell progeny revealed specific relationships between the ontogenetic origin of different neural cell types with their final heterogeneous morphologies and functions.

First, we performed a comparative analysis of the labeled adult cell progeny after postnatal and in utero electroporation of integrable vs. non-integrable fluorescent reporters. We conclude that the integration of reporter constructs into the genome is required for a successful long-term lineage tracking of glial and OB interneurons generated from both dorso-lateral SVZ embryonic and postnatal progenitors. Moreover, the use of integrable constructs allowed to preserve the cell labeling within the electroporated area, providing information about the origin of mature labeled cells, , which could be essential for ontogenic and cell migraton analyses. As regard, transposon systems have been used to avoid plasmid dilution and to stably track the cell progenies (Yoshida et al., 2010; Chen & LoTurco, 2012; Kita et al., 2013). Cell fate lineage analysis of OB interneurons revealed different results depending the embryonic or postnatal electroporation. We highlighted the necessity to use the integrable constructs in order to target OB interneurons after IUE, since OB progenitors undertake a large number of divisions before to be committed to this population (Miller & Gauthier, 2007; Kriegstein & Alvarez-Buylla, 2009). Indeed, labeled SVZ- and RMS-cells were lost after 3-4 weeks of postnatal electroporation of non-integrable constructs (Lacar et al., 2010). Additionally, our data highlighted the importance of stable and persistent expression of non-integrable fluorescent reporters that remained in cortical neurons generated at embryonic stages and postnatal SVZ-RMS-OB pathway cells. To this respect, the use of integrable and non-integrable plasmids is a valuable tool for further exploration of both quiescent cells (Song et al., 2012) and cell populations with a high division rate, due to dilution of non-integrated constructs through cell divisions (Sato et al., 2007). In addition, the stable expression of non-integrated reporters vs. integrated allows studying the heterogeneity of neural populations originated from different proliferative rates. Finally, differences in the labeling of integrated vs. non-integrated constructs, was intimately related to cell identity. Thus, our data indicated that glial cells were mostly green labeled, carrying only the integrable plasmid, either after embryonic or postnatal electroporation.

Once collected the information about the behavior of ubiquitous transposable vs. non-transposable vectors, we carried out a novel adaptation of the StarTrack methodology, named UbC-StarTrack. It was designed to perform clonal analysis and tracing of neural cell types derived from single progenitors. To ensure stable and inheritable cell labeling of all

clonally related cells, we employed the piggyBac system. The transposase of the piggyBac system (mPBase) integrates a variable number of copies into the genome (9 copies on average; Woltjen et al., 2009), here we used a hyperactive version (hyPBase) that has a 10-fold higher transposition rate without compromising genomic integrity (Yusa et al., 2011). Moreover, unlike other multicolor lineage approaches, our transposable ubiquitous lineage-tracing method avoids the expression of non-integrated copies of electroporated plasmids, taking advantage of the Cre-lox strategy (Sternberg & Hamilton, 1981). This allows an invariable and unalterable labeling of the entire progeny of single progenitors, regardless of mitotic activity. Additionally, our clonal method was based on the expression of six different reporters while other approaches used three (Gomez-Nicola et al., 2014; Loulier et al., 2014) or four fluorophores (Snippert et al., 2010; García-Moreno et al., 2014). Our six XFPs were selected on the basis of their photostability and brightness (Shaner et al., 2005), without requiring immunotagging. Those fluorescent reporters expressed in the cell nucleus and cytoplasm, increasing theoretical combinations of the method up to four thousand. We analyzed the frequency of fluorophore combinations along with the variation of intensity within sibling cells, determining that brightness values of specific color-codes did not vary more than 150 points between clonally-related cells. Thus, to define sibling cells with UbC-StarTrack it is important the following parameters: fluorophore combination, fluorophore cell location and fluorophore intensity. Therefore, UbC-StarTrack is positioned as the multicolor approach with the highest number of potential combinations. To achieve the study of neural cells from all brain lineages, we used UbC promoter, which drives consistent expression in different cell types (Lois et al., 2002). This ubiquitous promoter allowed to establish clonal relationships between sibling cells from different neural populations, making comparisons within or between lineages effortless. Regarding clonal dispersion, sibling neurons were more scattered than glial cells, that could be related to the their distinct proliferation pattern. Thus, astrocyte and oligodendrocyte precursors reach to their final destination, actively proliferate and undergo differentiation into mature cells during perinatal stages (Miron et al., 2011; Ge et al., 2012). However, most neurons migrate long distances to their final position, far from their birth-site (Kriegstein & Noctor, 2004). The enormous cell heterogeneity of the adult brain will not be totally understood without specific studies to analyze all the progeny of single cells. Indeed, the strategy behind this method represents an exciting tool for other areas in the field of biomedicine, avoiding the use of genetically engineered mouse models.

Next, we focused on the olfactory pathway targeting embryonic or postnatal progenitors to fully capture the heterogeneity among the adult OB interneurons. We co-electroporated a ubiquitous transposable piggyBac vector expressing the enhanced green fluorescent protein (EGFP) and a construct encoding for the hyPBase. Our data revealed that age of progenitors targeting and electrode placement was critical to trace different cell lineages in the OB, particularly for glial lineages and projection neurons. To this

respect, we provided evidences of the specific generation of OB glial cells from endogenous embryonic bulbar ependymal zone progenitors. In addition, our Lab added valuable results to the glial ontogeny and heterogeneity within the OB. Thus, we recently analyzed the clonal dispersion and migratory routes of NG2 cells in the OB (Garcia-Marques et al., 2014) using the StarTrack method (García-Marqués & López-Mascaraque, 2013). We also described the large heterogeneity within the glial lineages in the OB (Figueres-Oñate et al., 2014) and cerebral cortex (Bribián et al., 2015). Moreover, our data show an unilateral distribution of glial cells within the OB, suggesting a similar radial migration of glial cells as showed in the cortex (García-Marqués & López-Mascaraque, 2013). In addition, a deeper clonally analyses of the astrocytic lineage within the different OB layer was recently described (García-Marqués & López-Mascaraque, 2016). Interestingly, we showed that labeled cells in the OB, after targeting progenitors of the dorso-lateral ventricular surface, never co-localized with glial immune-markers. Therefore, electroporation appears to be a powerful means to visualize the specific cell fate of different embryonic and postnatal progenitors (Imamura and Greer, 2013, 2014; Chen and LoTurco, 2012; Siddiqi et al., 2014). Likewise, in this study we analyzed lineages and dispersion of targeted cells throughout the different OB layers depending on targete progenitors. Labeled interneurons co-localized with most of the interneuronal immunomarkers after targeting dorsolateral progenitors at embryonic or postnatal electroporation. Consequently, targeted cells represented a heterogeneous population of interneurons (De Marchis et al., 2007; Batista-Brito et al., 2008). This raises the interesting question whether adult NPCs inherit regional specification from embryonic progenitors and whether they share lineage with embryonic progenitors. OB interneurons originated from E13 progenitors located in the subpallium, specifically in the LGE (Wichterle et al., 2001; Kohwi et al., 2007). These LGE progenitors later distribute along the ventricular surface and some of them become adult neural stem cells, this destiny being specified before E15 (Fuentealba et al., 2015). Accordingly, dorso-lateral electroporation at E15 labeled SVZ progenitors that were already compromised to establish certain OB interneuron subtypes. To this respect, our results show a similar distribution of labeled cells within OB layers from either embryonic or postnatal dorso-lateral progenitor electroporation, except in the glomerular area where more PGCs were labeled by postnatal electroporation. All together, a better understanding of cells generated in adulthood and the factors that control their proliferation, migration and integration into neural circuits is crucial. Moreover, it is also essential to perform a clonal analysis from single progenitor to track their progeny in order to match progenitor cells to specific neural populations in the adult OB, including glial lineages.

After confirming the feasibility of the UbC-StarTrack method and to explore the high heterogeneity within the SVZ-RMS-OB pathway, we sought to validate it by addressing some relevant questions. One important question in Neuroscience is the cell potential of adult neural progenitors, since the analysis of lineage

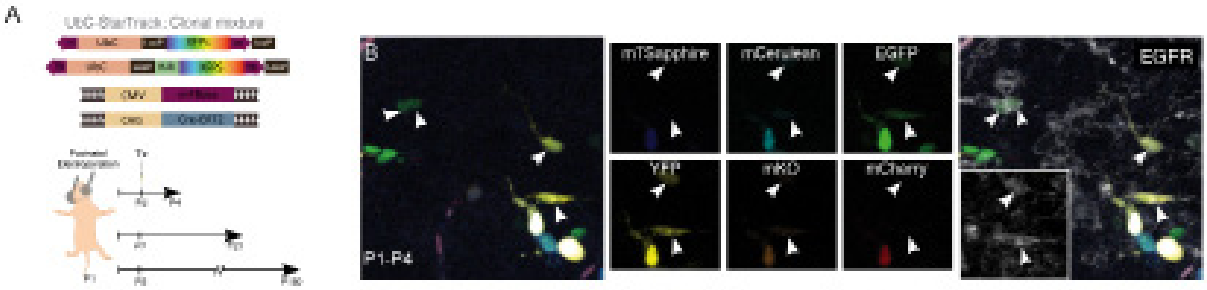

Figure 12. UbC-StarTrack for analyzing adult neurogenesis. A. Experimental procedure. The clonal mark was achieved by the electroporation of the UbC-StarTrack mixture. Postnatal electroporation was performed at P1. Tamoxifen was administrated 24hours post-electroporation to stable label the cell progenies. Mice were analyzed either at short-times (P4), young adults (P21) or adult mice (P180). **B.** At short-times sibling clusters of labeled cells co-localized with EGFR (arrowheads), immunomarker for active NPCs and transit amplifying progenitors.

segregation during postnatal neurogenesis has not been sufficiently addressed because technical difficulties. The term adult NSC, involves both cell renewal and pluripotency. Thus, a authentic adult NSC should have the capability to give rise to all the different lineages in the adult brain. However, both in vitro analyses (Ortega et al., 2013) and unpublished results from our group do not corroborate the stem cell nature of these progenitors. In fact, some evidences point that those adult progenitors could give rise to all cell lineages in vitro (Reynolds & Weiss, 1996; Ortega et al., 2011) and in vivo (Kempermann et al., 1997; Menn et al., 2006; Sohn et al., 2015) but the in vivo multipotent capacity is still controversial. Lineage analyses of the adult ventricular surface are biased, since the proper identification of neural stem cells involve the following issues. As regard, to address the different populations of progenitors, the use of transgenic mice carrying fluorescent expression under a determinate promoter could have lumping or splitting errors, analyzing only a small subpopulation of desired cells or including cells that are not under study. Moreover, single-cell analysis are based on isolation after molecular markers tagging usually including CD133+(prominin1) (Mirzadeh et al., 2008; Beckervordersandforth et al., 2010; Codega et al., 2014; Llorens-Bobadilla et al., 2015) although only the 29% of the GFAP+/Bcells of the lateral ventricular surface express CD133 (Mirzadeh et al., 2008) and it is also expressed by ependymal cells (Coskun et al., 2008). To isolate NSCs, most of the studies removed cells form the lateral wall of the ventricles and the results are mainly extrapolated to all neurogenic ventricular walls. However, the progenitor behavior and cell commitment is dependent of the specific region where they are positioned (Merkle et al., 2014). So far, most progenitor analyses are highly influenced by the experimental approach, with the consequent loss of information about the pool of progenitors lining the ventricles of adult rodents. Altogether, direct evidences supporting the presence of NSC capable of both self-renewal and multilineage differentiation at the clonal level is still missing in vivo. With the UbC-StarTrack method we can perform unbiased studies from neural progenitors located just in the desired ventricular surface at specific time points.

At this respect, our ongoing project aims to demonstrate the viability and potential applications of the UbC-StarTrack method. We

specifically perform a clonal analysis of the postnatal potential of individual progenitor cells and their dispersion patterns of clonally-related cells in the adult olfactory bulb. After targeting perinatal progenitors (P1) with a UbC-StarTrack mixture injection into the ventricular surface and posterior dorsolateral electroporation (Figure 12A), single NPCs were stochastically labeled with specific color-codes combinations that were maintained within their cell progenies, revealing their cell identity by immunohistochemistry (Figure 12B). At later postnatal stages (P20-P30) UbC-StarTrack labeled cells exhibited different morphologies at the ventricular surface (Figure 13A). These neural progenitor-like cells presented either thicker proximal dendrites (Figure 13Aa,b) or cells with filopodia (Figure 13Ac) that characterized immature morphologies. In the RMS sibling neuroblasts (Figure 13B) migrated in small clusters along the migratory pathway (Circles in Figure 13B). Finally, in the olfactory bulb clonally-related neurons were mainly located within the same OB layers, although distributed throughout the dorso-ventral and medio-lateral axes (Figure 13C). Remarkably, 6 months after postnatal electroporation sibling interneurons in the OB formed clones composed by less than 20 cells (Figure 14A). The clonal cell dispersion was related to the clone size; clones containing higher number of cells occupying broader domains in the rostro-caudal OB axis. Moreover, the bulk of analyzed sibling cells were restricted to the same OB layer (Figure 14B), although extended along the dorso-

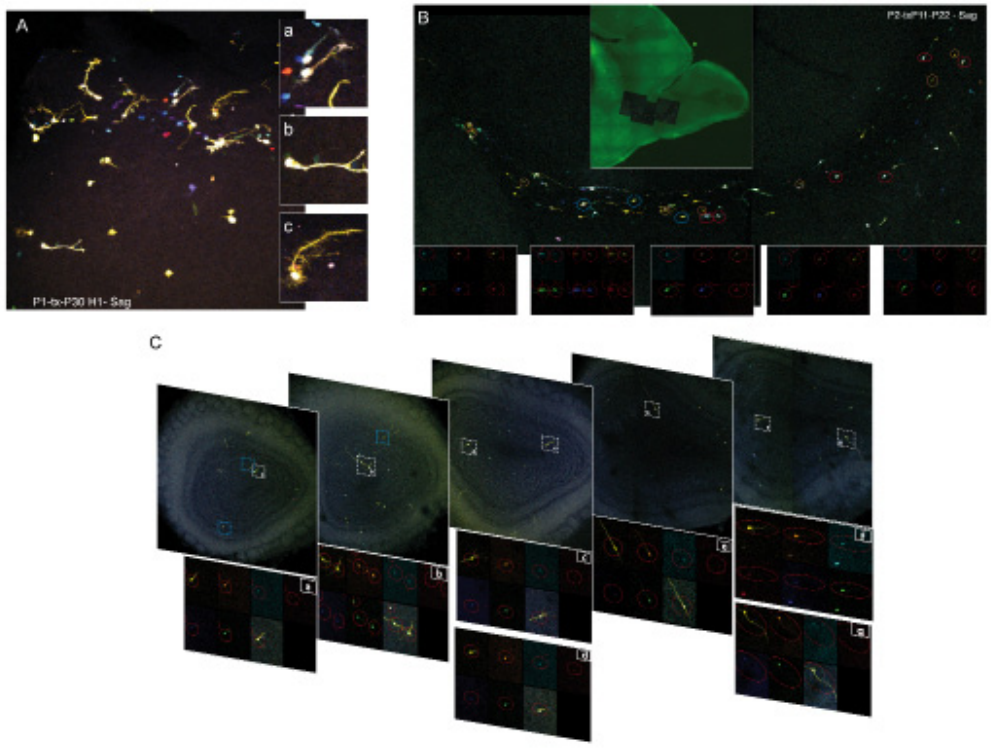

Figure 13. Distribution of sibling cells in young adults. A. Different morphologies of labeled cells observed lining the ventricles, either immature (a,b) or branched (c). **B.** Rostral migratory stream at P1. Sibling cells were circled by the same color. Small clusters were found in this migratory chain. The specific color-code for sibling red-circled neuroblast is detailed in channel magnifications at the bottom. **C.** Serial coronal sections of a P21 OB. Sibling cells were framed with the same colors. The color-code for sibling white-framed young neurons was detailed in channel magnifications at the bottom of each coronal section.

ventral and medio-lateral axes. In particular, clonal analyses revealed that targeted postnatal SVZ progenitor cells mostly generated specific interneuron types in the OB located in the OB granular cell layer according with previous work (Figueres-Oñate & López-Mascaraque, 2016). It is interesting to mention that none sibling cells were located at the ventricular surface six months after electroporation, suggesting progenitors consuming. Interestingly, other clonal studies of adult neurogenesis show that active NSCs are exhausted in few months (Calzolari et al., 2015). Interestingly, our data evidenced cell clones consisted in striatal astrocytes and granular cells in the OB suggesting the presence of SVZ bipotential progenitors. Further, both cell dispersion pattern and the number of cells comprising a clone was different depending on the glial or neuronal nature of sibling cells. Clonally related oligodendroglial- and NG2-cells formed bigger clones (Garcia-Marques et al., 2014), compared to astrocytes or interneurons although with a narrow cell distribution compared to interneurons (Figure 14C). Moreover, astrocytic clones showed a reduction in the clonal size compared to progenitors targeted at embryonic stages (García-Marqués & López-Mascaraque, 2013, 2016) (Figure 14D). Thus, we validate the UbC-StarTrack for the determination of single cell progeny. The overlapping of immunomarkers presented in the different populations of the neurogenic

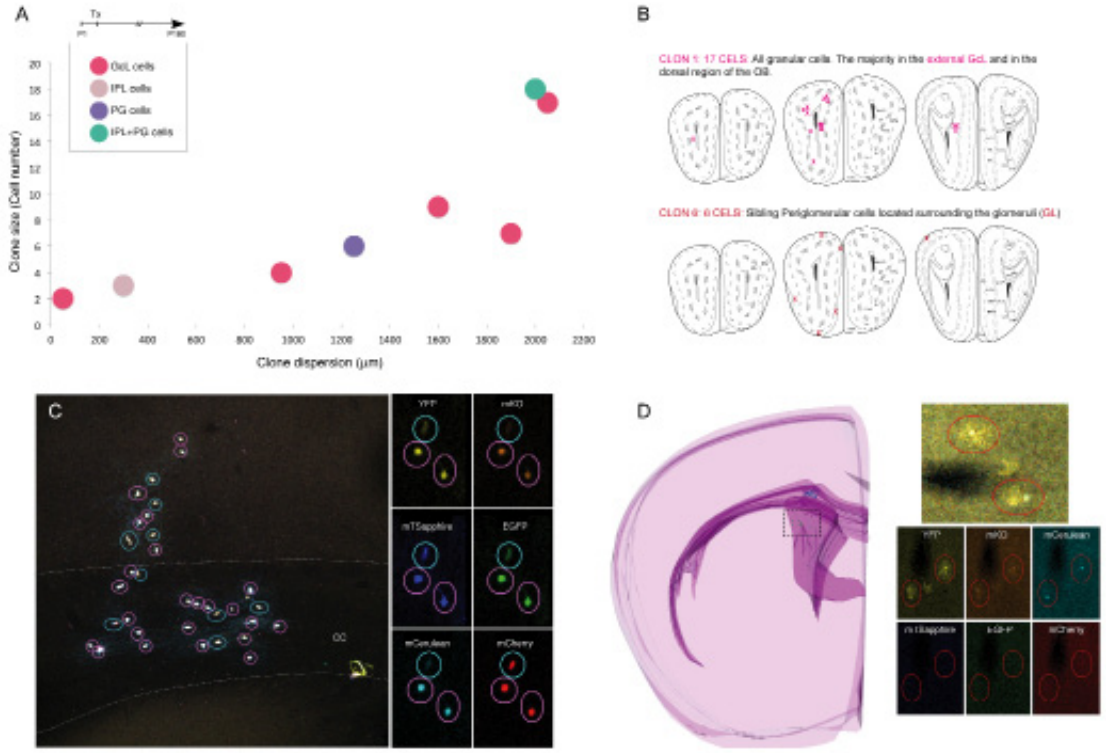

Figure 14. Distribution of sibling cells in 6month adults. A. At P180 sibling cells were more scattered in adult OB regarding to clone size. Colored spots represent the layer disposition of sibling cells. **B.** Two examples of sibling interneurons either distributed throughout the granular cell layer (GcL) or the glomerular layer (GL) in P180 OBs. **C.** Distribution of two clones of oligodendrocytes (blue or magenta circled) within the corpus callosum (cc) and the cerebral cortex showed after P1 postnatal electroporation. The specific color-code for each clone is specify in magnifications. **D.** Sibling astrocytes located in the ventricular surface or in the striatum surrounding a blood vessel at P180 after P1 electroporation. The specific color-code for each clone is specify in magnifications.

niche, points the UbC-StarTrack as an accurate method to address the fate of ventricular NPCs. Moreover, its ubiquitously expression allows lineage tracing regardless the genes or markers expressed by the cell of interest.

Consequently, the identity and potential of adult progenitors can provide insights into how cell diversity is generated in the adult brain as well as to understand the adult NPCs. Finally, our studies revealed a degree of heterogeneity among adult neural progenitors, which provide insights into how we could use these neural progenitors to more effectively generate specific cell types for brain repair.

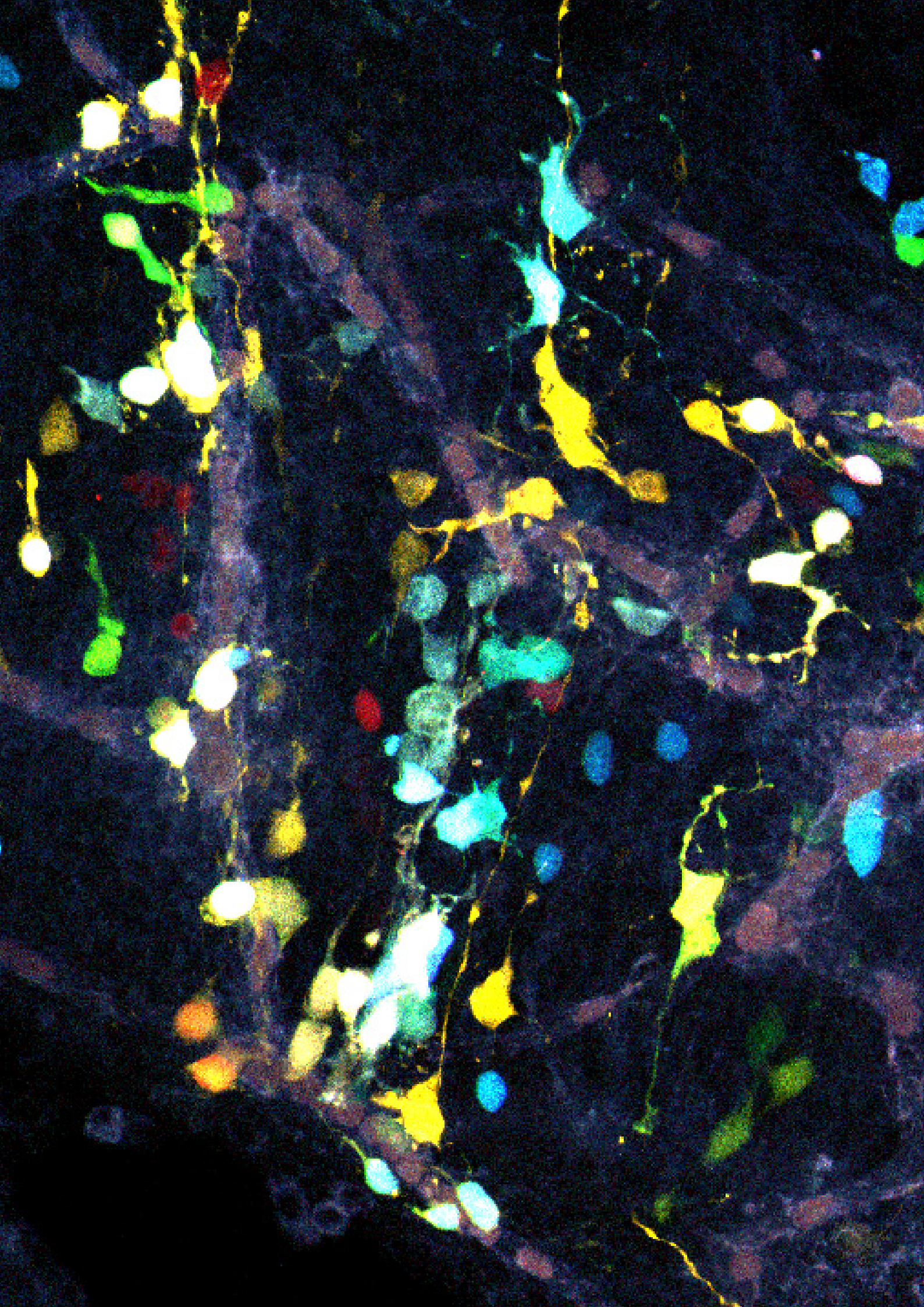

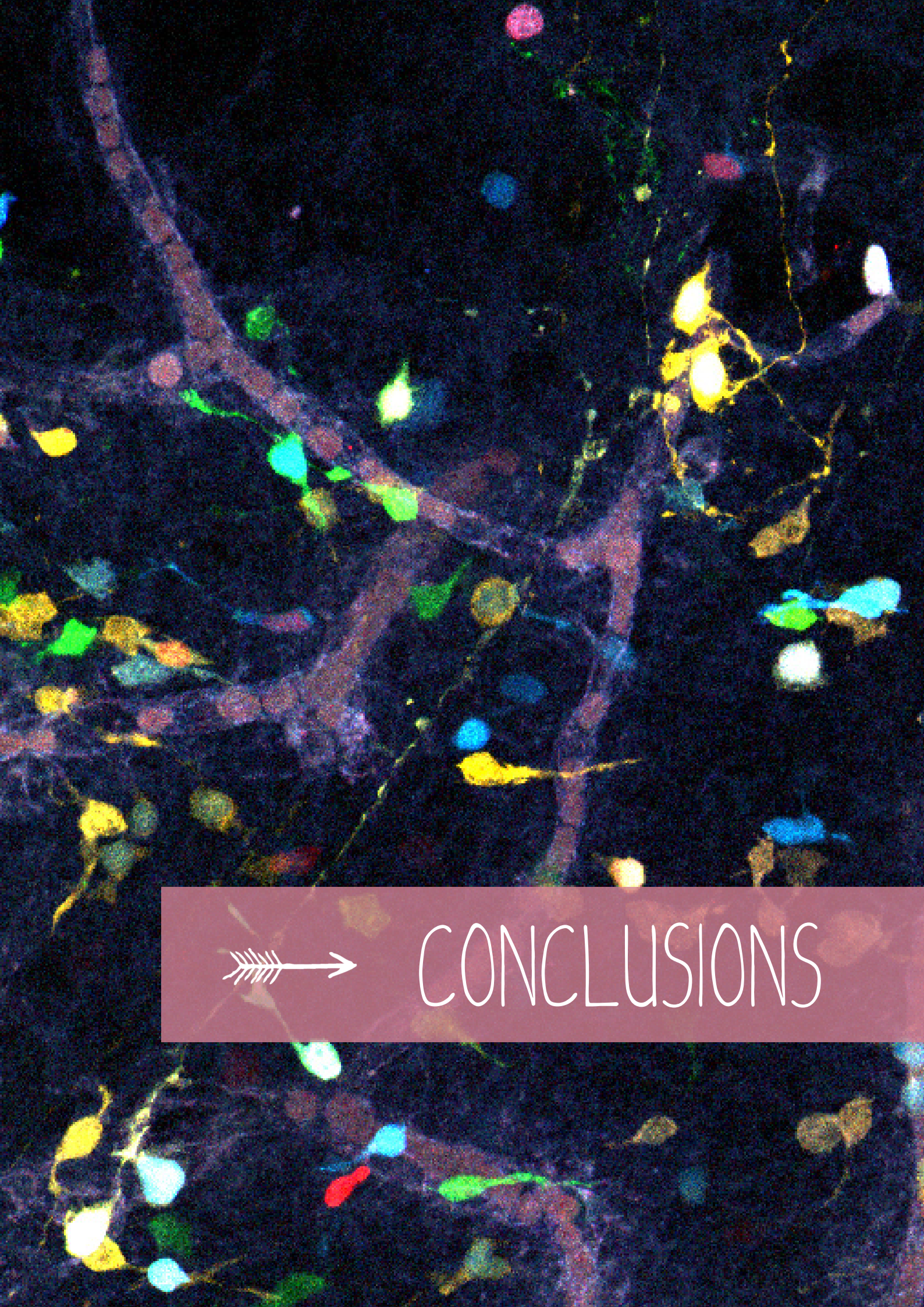

CONCLUSIONS

This thesis represents a major step forward in understanding cell lineage relationships, not only in the brain research but also in other relevant biomedical areas. The following conclusions can be drawn from this thesis:

1. UbC-StarTrack is a versatile clonal method, revealed as a powerful tool to track the whole cell progeny of single cells, independently of the cell lineage, proliferative rate or brain region.

2. UbC-StarTrack can be used for clonal studies either in vivo, in vitro or ex vivo, not only in Neuroscience but also in different fields of biomedical research

3. The genomic integration of constructs is crucial for clonal analysis in order to label all the cell progeny of actively dividing progenitors.

4. The inhibition of episomal plasmids is a critical step to obtain a unique color code for the entire progeny coming from a single cell.

5. The validation of this clonal method provides a useful guide to select a precise strategy that efficiently tracks the entire specific progeny of single cell.

6. Postnatal and embryonic dorso-lateral ventricular progenitors produce a vast heterogeneity of olfactory bulb interneurons. These cells are similarly distributed within the olfactory bulb layers with an increment of periglomerular interneurons after postnatal progenitors targeting.

7. Sibling olfactory bulb interneurons labeled after postnatal targeting of dorso-lateral ventricular surface progenitors are widely distributed along the rostro-caudal axis of the olfactory bulb, although they are limited to the same layer.

8. Within the olfactory bulb, subpopulations of glial cells are generated by endogenous/ ependymal olfactory bulb progenitors but not by the subventricular.

El trabajo presentado en esta tesis doctoral constituye un paso hacia delante en el conocimiento sobre las relaciones entre distintos linajes celulares, aplicable no tan solo al campo de la Neurociencia básica y desordenes patológicos del cerebro, sino también a otras áreas relevantes de la Biología, como cáncer o estudios de células madre.

Las principales conclusiones de esta Tesis Doctoral son las siguientes:

1. UbC-StarTrack se presenta como un versátil y potente método, idóneo para trazar toda la descendencia de células únicas, independientemente de su linaje, tasa de proliferación o región cerebral que habiten.

2. Se ha demostrado que UbC-StarTrack puede ser usado en estudios de análisis clonal tanto in vivo, in vitro o ex vivo, aplicable no tan solo en el campo de la Neurociencia sino también en otras áreas biomédicas.

3. La integración genómica de los constructos electroporados es una condición decisiva en los métodos el análisis clonal, sobretodo para permitir el marcaje de toda la descendencia de progenitores con una alta tasa de proliferación.

4. La inhibición de los plásmidos no integrados por la transposasa del sistema PiggyBac tras la electroporación, es muy importante para la obtención de un código de color inalterable para toda las células derivadas de un mismo progenitor.

5. La validación del método presentada, proporciona una útil guía para la selección de una adecuada estrategia en cada caso experimental concreto para trazar eficientemente los linajes procedentes de las células marcadas.

6. Los progenitores tanto postnatales como embrionarios situados en la zona dorso-lateral del ventrículo lateral, producen una gran heterogeneidad de interneuronas situadas el bulbo olfativo. Ambos progenitores generan células distribuidas de manera similar entre las distintas capas del bulbo olfativo, con tan sólo un incremento de la proporción de interneuronas periglomerulares después de marcar progenitores postnatales.

7. Las interneuronas hermanas generadas a partir de progenitores perinatales presentan una amplia dispersión en el eje rostro-caudal del bulbo olfativo, aunque todas las interneuronas pertenecientes a un mismo clon se posicionan la misma capa del bulbo olfativo.

8. En el bulbo olfativo, ciertas subpoblaciones de células gliales son generadas por progenitores localizados en la propia zona ependimaria del bulbo olfativo en estadios embrionarios, y no a partir de progenitores embrionarios de la zona ventricular adyacente al ventrículo lateral.

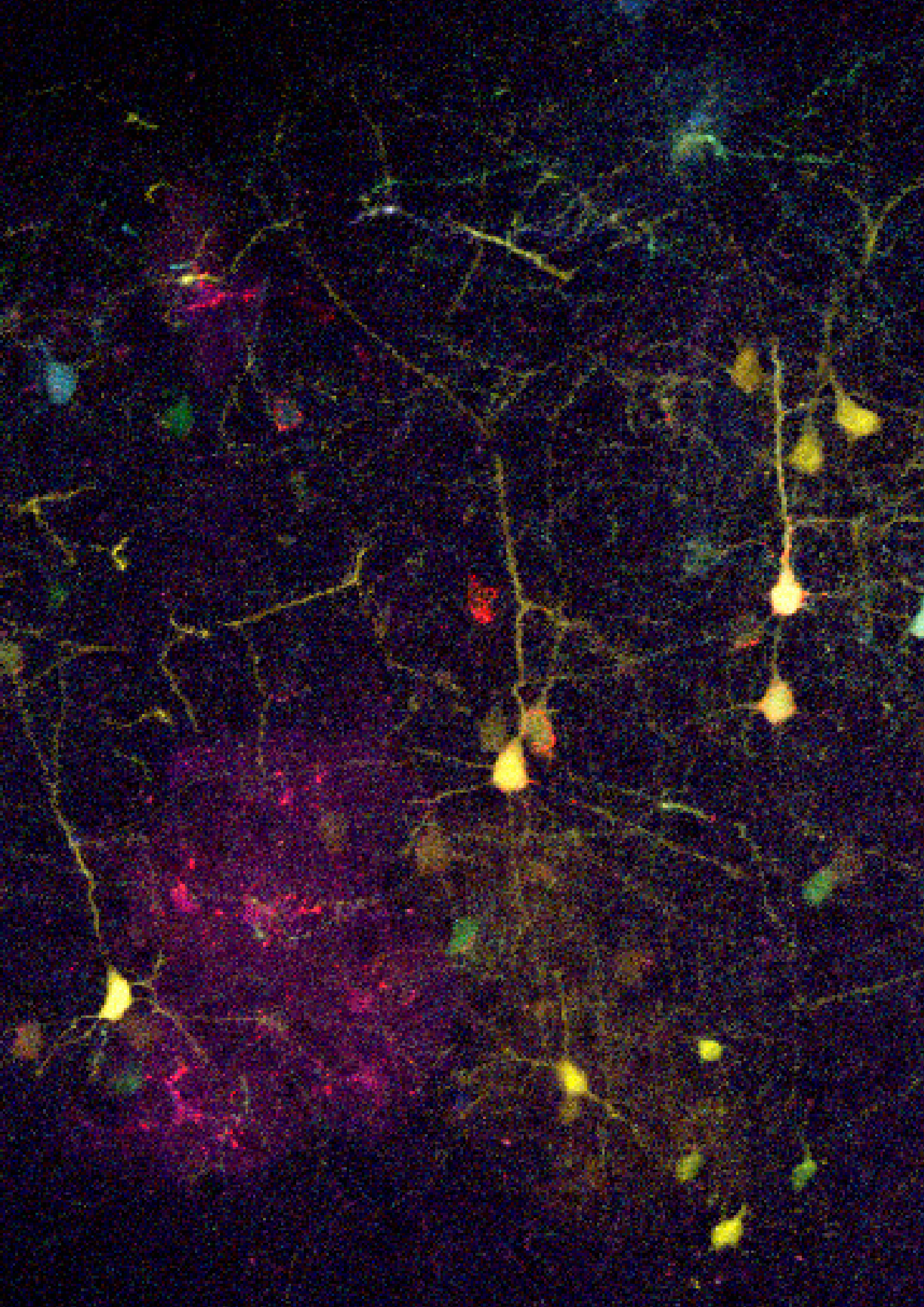

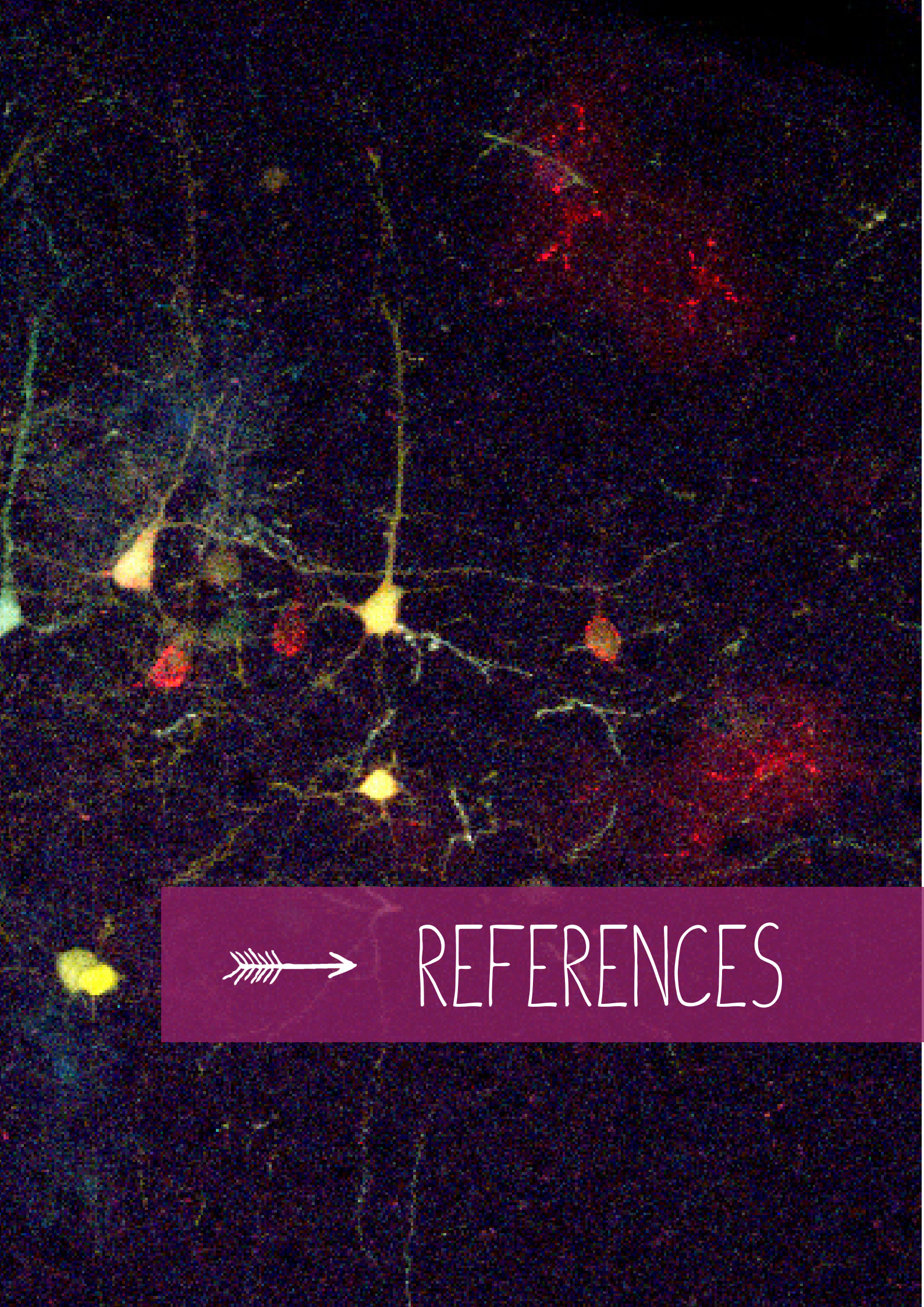

REFERENCES

Ahlenius, H., Visan, V., Kokaia, M., Lindvall, O., & Kokaia, Z. (2009). Neural stem and progenitor cells retain their potential for proliferation and differentiation into functional neurons despite lower number in aged brain. The Journal of Neuroscience : The Official Journal of the Society for Neuroscience, 29(14), 4408–19. http://doi.org/10.1523/JNEUROSCI.6003-08.2009

Alonso, M., Viollet, C., Gabellec, M. M., Meas-Yedid, V., Olivo-Marin, J. C., & Lledo, P. M. (2006). Olfactory discrimination learning increases the survival of adult-born neurons in the olfactory bulb. J Neurosci, 26(41), 10508–10513. http://doi.org/10.1523/JNEUROSCI.2633-06.2006

Altman, J. (1962). Are new neurons formed in the brains of adult mammals? Science (New York, N.Y.), 135(3509), 1127–8.

Altman, J. (1966). Proliferation and migration of undifferentiated precursor cells in the rat during postnatal gliogenesis. Experimental Neurology, 16(3), 263–78.

Altman, J. (1969). Autoradiographic and histological studies of postnatal neurogenesis. IV. Cell proliferation and migration in the anterior forebrain, with special reference to persisting neurogenesis in the olfactory bulb. The Journal of Comparative Neurology, 137(4), 433–57. http://doi.org/10.1002/cne.901370404

Alvarez-Buylla, A., & Garcia-Verdugo, J. M. (2002). Neurogenesis in adult subventricular zone. The Journal of Neuroscience : The Official Journal of the Society for Neuroscience, 22(3), 629–34.

Alvarez-Buylla, A., Kohwi, M., Nguyen, T. M., & Merkle, F. (2008). The Heterogeneity of Adult Neural Stem Cells and the Emerging Complexity of Their Niche The Heterogeneity of Adult Neural Stem Cells and the Emerging Complexity of Their Niche. Cold Spring Harbor Symposia on Quantitative Biology, LXXIII, 357–365. http://doi.org/10.1101/sqb.2008.73.019

Arsenijevic, Y., Villemure, J. G., Brunet, J. F., Bloch, J. J., Deglon, N., Kostic, C., … Aebischer, P. (2001). Isolation of multipotent neural precursors residing in the cortex of the adult human brain. Experimental Neurology, 170(1), 48–62. http://doi.org/10.1006/exnr.2001.7691

Arwert, E. N., Lal, R., Quist, S., Rosewell, I., van Rooijen, N., & Watt, F. M. (2010). Tumor formation initiated by nondividing epidermal cells via an inflammatory infiltrate. Proceedings of the National Academy of Sciences of the United States of America, 107(46), 19903–19908. http://doi.org/10.1073/pnas.1007404107

Aungst, J. L., Heyward, P. M., Puche, a C., Karnup, S. V, Hayar, a, Szabo, G., & Shipley, M. T. (2003). Centre-surround inhibition among olfactory bulb glomeruli. Nature, 426(6967), 623–9. http://doi.org/10.1038/nature02185

Azim, K., Fiorelli, R., Zweifel, S., Hurtado-Chong, A., Yoshikawa, K., Slomianka, L., & Raineteau, O. (2012). 3-Dimensional Examination of the Adult Mouse Subventricular Zone Reveals Lineage-Specific Microdomains. PLoS ONE, 7(11). http://doi.org/10.1371/journal.pone.0049087

Azim, K., Rivera, A., Raineteau, O., & Butt, A. M. (2014). GSK3?? regulates oligodendrogenesis in the dorsal microdomain of the subventricular zone via Wnt-??-catenin signaling. Glia, 62(5), 778–789. http://doi.org/10.1002/glia.22641

Bailey, M. S., & Shipley, M. T. (1993). Astrocyte subtypes in the rat olfactory bulb: Morphological heterogeneity and differential laminar distribution. Journal of Comparative Neurology, 328(4), 501–526. http://doi.org/10.1002/cne.903280405

Baracskay, K., Kidd, G., Miller, R., & Trapp, B. (2007). NG2-Positive Cells Generate A2B5-Positive Oligodendrocyte Precursor Cells. Glia, 55, 1001–1001. http://doi.org/10.1002/glia.20519

Batista-Brito, R., Close, J., Machold, R., & Fishell, G. (2008). The distinct temporal origins of olfactory bulb interneuron subtypes. The Journal of Neuroscience : The Official Journal of the Society for Neuroscience, 28(15), 3966–75. http://doi.org/10.1523/JNEUROSCI.5625-07.2008

Bayraktar, O. A., Fuentealba, L. C., Alvarez-Buylla, A., & Rowitch, D. H. (2015). Astrocyte development and heterogeneity. Cold Spring Harbor Perspectives in Biology, 7(1). http://doi.org/10.1101/cshperspect.a020362

Beckervordersandforth, R., Tripathi, P., Ninkovic, J., Bayam, E., Lepier, A., Stempfhuber, B., … G??tz, M. (2010). In vivo fate mapping and expression analysis reveals molecular hallmarks of prospectively isolated adult neural stem cells. Cell Stem Cell, 7(6), 744–758. http://doi.org/10.1016/j.stem.2010.11.017

Bekkers, J. M., & Suzuki, N. (2013). Neurons and circuits for odor processing in the piriform cortex. Trends in Neurosciences, 36(7), 429–38. http://doi.org/10.1016/j.tins.2013.04.005

Belachew, S., Chittajallu, R., Aguirre, A., Yuan, X., Kirby, M., Anderson, S., & Gallo, V. (2003). Postnatal NG2 proteoglycan-expressing progenitor cells are intrinsically multipotent and generate functional neurons. The Journal of Cell Biology, 161(1), 169–86. http://doi.org/10.1083/jcb.200210110

Belluzzi, O., Benedusi, M., Ackman, J., & LoTurco, J. J. (2003). Electrophysiological differentiation of new neurons in the olfactory bulb. The Journal of Neuroscience : The Official Journal of the Society for Neuroscience, 23(32), 10411–10418. http://doi.org/10.1371/journal.pone.0037742

Bergmann, O., Liebl, J., Bernard, S., Alkass, K., Yeung, M. S. Y., Steier, P., … Fris??n, J. (2012). The Age of Olfactory Bulb Neurons in Humans. Neuron, 74(4), 634–639. http://doi.org/10.1016/j.neuron.2012.03.030

Blanchart, A., Carlos, J. A. de, & López-Mascaraque, L. (2006). Time Frame of Mitral Cell Development. The Journal of Comparative Neurology, 543(October 2005), 529–543. http://doi.org/10.1002/cne

Blanchart, A., & López-Mascaraque, L. (2011). From the periphery to the brain: Wiring the olfactory system. Translational Neuroscience, 2(4), 293–309. http://doi.org/10.2478/s13380-011-0038-x

Blanchart, a., Martín-López, E., De Carlos, J. a., & López-Mascaraque, L. (2011). Peripheral contributions to olfactory bulb cell populations (migrations towards the olfactory bulb). Glia, 59(2), 278–292. http://doi.org/10.1002/glia.21100

Bonzano, S., Bovetti, S., Gendusa, C., Peretto, P., & Marchis, S. De. (2016). Adult born olfactory bulb dopaminergic interneurons: molecular determinants and experience-dependent plasticity, 10(May), 1–8. http://doi.org/10.3389/fnins.2016.00189

Brill, M. S., Ninkovic, J., Winpenny, E., Hodge, R. D., Ozen, I., Yang, R., … Götz, M. (2009). Adult generation of glutamatergic olfactory bulb interneurons. Nature Neuroscience, 12(12), 1524–33. http://doi.org/10.1038/nn.2416

Buffo, A., Rite, I., Tripathi, P., Lepier, A., Colak, D., Horn, A.-P., … Götz, M. (2008). Origin and progeny of reactive gliosis: A source of multipotent cells in the injured brain. Proceedings of the National Academy of Sciences of the United States of America, 105(9), 3581–6. http://doi.org/10.1073/pnas.0709002105

Cai, D., Cohen, K. B., Luo, T., Lichtman, J. W., & Sanes, J. R. (2013). Improved tools for the Brainbow toolbox. Nature Methods, 10(6), 540–7. http://doi.org/10.1038/nmeth.2450

Calzolari, F., Michel, J., Baumgart, E. V., Theis, F., Götz, M., & Ninkovic, J. (2015a). Fast clonal expansion and limited neural stem cell self-renewal in the adult subependymal zone. Nature Neuroscience, 18(4), 490–492. http://doi.org/10.1038/nn.3963

Calzolari, F., Michel, J., Baumgart, E. V., Theis, F., Götz, M., & Ninkovic, J. (2015b). Fast clonal expansion and limited neural stem cell self-renewal in the adult subependymal zone. Nature Neuroscience, 18(4), 490–492. http://doi.org/10.1038/nn.3963

Capilla-Gonzalez, V., Herranz-Pérez, V., & García-Verdugo, J. M. (2015). The aged brain: genesis and fate of residual progenitor cells in the subventricular zone. Frontiers in Cellular Neuroscience, 9(September), 365. http://doi.org/10.3389/fncel.2015.00365

Carleton, A., Petrenanu, L., Lansford, R., Alvarez-Buylla, A., & Lledo, P.-M. (2003). Becoming a new neuron in the adult OB. Nature Neuroscience, 6(5), 507–518.

Chalfie, M., Tu, Y., Euskirchen, G., Ward, W., & Prasher, D. (1994). Green fluorescent protein as a marker gene expression. Science, 263(February), 802–805. Retrieved from http://www.ncbi.nlm.nih.gov/pubmed/18051416

Chen, F., & LoTurco, J. (2012). A method for stable transgenesis of radial glia lineage in rat neocortex by piggyBac mediated transposition. Journal of Neuroscience Methods, 207(2), 172–80. http://doi.org/10.1016/j.jneumeth.2012.03.016

Cheng, M.-F. (2013). Hypothalamic neurogenesis in the adult brain. Frontiers in Neuroendocrinology, 34(3), 167–78. http://doi.org/10.1016/j.yfrne.2013.05.001

Chiu, K., & Greer, C. a. (1996). Immunocytochemical analyses of astrocyte development in the olfactory bulb. Brain Research. Developmental Brain Research, 95(1), 28–37. Retrieved from http://www.ncbi.nlm.nih.gov/pubmed/8873973

Codega, P., Silva-Vargas, V., Paul, A., Maldonado-Soto, A. R., DeLeo, A. M., Pastrana, E., & Doetsch, F. (2014). Prospective Identification and Purification of Quiescent Adult Neural Stem Cells from Their In Vivo Niche. Neuron, 82(3), 545–559. http://doi.org/10.1016/j.neuron.2014.02.039

Conover, J. C., & Shook, B. A. (2011). Aging of the Subventricular Zone Neural Stem Cell Niche. Aging and Disease, 2(1), 49–63.

Coskun, V., Wu, H., Blanchi, B., Tsao, S., Kim, K., Zhao, J., … Sun, Y. E. (2008). CD133+ neural stem cells in the ependyma of mammalian postnatal forebrain. Proceedings of the National Academy of Sciences of

the United States of America, 105(3), 1026–31. http://doi.org/10.1073/pnas.0710000105

Crespo, C., Blasco-Ibáñez, J. M., Marqués-Marí, A. I., & Martínez-Guijarro, F. J. (2001). Parvalbumin-containing interneurons do not innervate granule cells in the olfactory bulb. Neuroreport, 12(11), 2553–6.

Daynac, M., Morizur, L., Chicheportiche, A., Mouthon, M.-A., & Boussin, F. D. (2016). Age-related neurogenesis decline in the subventricular zone is associated with specific cell cycle regulation changes in activated neural stem cells. Scientific Reports, 6(November 2015), 21505. http://doi.org/10.1038/srep21505

De Carlos, J. A., L??pez-Mascaraque, L., & Valverde, F. (1995). The telencephalic vesicles are innervated by olfactory placode-derived cells: a possible mechanism to induce neocortical development. Neuroscience, 68(4), 1167–1178. http://doi.org/10.1016/0306-4522(95)00199-S

De Carlos, J. A., López-Mascaraque, L., & Valverde, F. (1996). Early olfactory fiber projections and cell migration into the rat telencephalon. International Journal of Developmental Neuroscience : The Official Journal of the International Society for Developmental Neuroscience, 14(7–8), 853–66.

De Castro, F. (1920). Estudios sobre la neuroglia de la corteza cerebral del hombre y de los animales. Trabajos Del Labratorio de Investigaciones Biológicas, XVIII.

De Castro, F. and López-Mascaraque, L. 2016. Olfactory system embryonic development. Kaufman's Atlas of Mouse Development Supplement, Elsevier, pp. 275-281.

De Juan Romero, C., & Borrell, V. (2015). Coevolution of radial glial cells and the cerebral cortex. Glia, 63(8), 1303–1319. http://doi.org/10.1002/glia.22827

De Marchis, S., Bovetti, S., Carletti, B., Hsieh, Y.-C., Garzotto, D., Peretto, P., … Rossi, F. (2007). Generation of distinct types of periglomerular olfactory bulb interneurons during development and in adult mice: implication for intrinsic properties of the subventricular zone progenitor population. The Journal of Neuroscience : The Official Journal of the Society for Neuroscience, 27(3), 657–64. http://doi.org/10.1523/JNEUROSCI.2870-06.2007

Dhaliwal, J., & Lagace, D. C. (2011). Visualization and genetic manipulation of adult neurogenesis using transgenic mice. European Journal of Neuroscience, 33(6), 1025–1036. http://doi.org/10.1111/j.1460-9568.2011.07600.x

Dimou, L., & Götz, M. (2014). Glial Cells as Progenitors and Stem Cells: New Roles in the Healthy and Diseased Brain. Physiological Reviews, 94(3), 709–737. http://doi.org/10.1152/physrev.00036.2013

Doetsch, F., Caillé, I., Lim, D. A., Garcia-Verdugo, J. M., & Alvarez-Buylla, A. (1999). Subventricular zone astrocytes are neural stem cells in the adult mammalian brain. Cell, 97(6), 703–16.

Doucette, R. (1989). Development of the nerve fiber layer in the olfactory bulb of mouse embryos. The Journal of Comparative Neurology, 285(4), 514–27. http://doi.org/10.1002/cne.902850407

Doucette, R. (1990). Glial influences on axonal growth in the primary olfactory system. Glia, 3(6), 433–49. http://doi.org/10.1002/glia.440030602

Emsley, J. G., & Macklis, J. D. (2006). Astroglial heterogeneity closely reflects the neuronal-defined anatomy of the adult murine CNS. Neuron Glia Biology, 2(3), 175. http://doi.org/10.1017/S1740925X06000202

Ernst, A., Alkass, K., Bernard, S., Salehpour, M., Perl, S., Tisdale, J., … Frisén, J. (2014). Neurogenesis in the striatum of the adult human brain. Cell, 156(5), 1072–83. http://doi.org/10.1016/j.cell.2014.01.044

Feil, R., Wagner, J., Metzger, D., & Chambon, P. (1997). Regulation of Cre recombinase activity by mutated estrogen receptor ligand-binding domains. Biochemical and Biophysical Research Communications, 237(3), 752–7. http://doi.org/10.1006/bbrc.1997.7124

Feng, G., Mellor, R. H., Bernstein, M., Keller-peck, C., Nguyen, Q. T., Wallace, M., … Sanes, J. R. (2000). Imaging Neuronal Subsets in Transgenic Mice Expressing Multiple Spectral Variants of GFP. Neuron, 28, 41–51.

Figueres-Oñate, M., Gutiérrez, Y., & López-Mascaraque, L. (2014). Unraveling Cajal's view of the olfactory system. Frontiers in Neuroanatomy, 8(July), 1–12. http://doi.org/10.3389/fnana.2014.00055

Figueres-Oñate, M., & López-Mascaraque, L. (2016). Adult Olfactory Bulb Interneuron Phenotypes Identified by Targeting Embryonic and Postnatal Neural Progenitors. Frontiers in Neuroscience, 10(May), 1–12. http://doi.org/10.3389/fnins.2016.00194

Fiorelli, R., Azim, K., Fischer, B., & Raineteau, O. (2015). Adding a spatial dimension to postnatal ventricular-subventricular zone neurogenesis. Development, 142(12), 2109–2120. http://doi.org/10.1242/dev.119966

Franco, S. J., & Müller, U. (2013). Shaping our minds: stem and progenitor cell diversity in the mammalian neocortex. Neuron, 77(1), 19–34. http://doi.org/10.1016/j.neuron.2012.12.022

Fuentealba, L. C., Rompani, S. B., Parraguez, J. I., Obernier, K., Romero, R., Cepko, C. L., & Alvarez-Buylla, A. (2015). Embryonic Origin of Postnatal Neural Stem Cells. Cell, 161(7), 1644–1655. http://doi.org/10.1016/j.cell.2015.05.041

Gage, F. H. (2000). Mammalian Neural Stem Cells. Science, 287(5457), 1433–1438. http://doi.org/10.1126/science.287.5457.1433

Ganat, Y. M., Silbereis, J., Cave, C., Ngu, H., Anderson, G. M., Ohkubo, Y., … Vaccarino, F. M. (2006). Early postnatal astroglial cells produce multilineage precursors and neural stem cells in vivo. The Journal of Neuroscience : The Official Journal of the Society for Neuroscience, 26(33), 8609–21. http://doi.org/10.1523/JNEUROSCI.2532-06.2006

Gao, P., Postiglione, M. P., Krieger, T. G., Hernandez, L., Wang, C., Han, Z., … Shi, S.-H. (2014). Deterministic Progenitor Behavior and Unitary Production of Neurons in the Neocortex. Cell, 159(4), 775–788. http://doi.org/10.1016/j.cell.2014.10.027

García-Marqués, J., De Carlos, J. a, Greer, C. a, & López-Mascaraque, L. (2010). Different astroglia permissivity controls the migration of olfactory bulb interneuron precursors. Glia, 58(2), 218–30. http://doi.org/10.1002/glia.20918

García-Marqués, J., & López-Mascaraque, L. (2013).

Clonal Identity Determines Astrocyte Cortical Heterogeneity. Cerebral Cortex, 23(6), 1463–1472. http://doi.org/10.1093/cercor/bhs134

García-Marqués, J., & López-Mascaraque, L. (2016). Clonal Mapping of Astrocytes in the Olfactory Bulb and Rostral Migratory Stream. Cerebral Cortex (New York, N.Y. : 1991), bhw071. http://doi.org/10.1093/cercor/bhw071

Garcia-Marques, J., Nunez-Llaves, R., & Lopez-Mascaraque, L. (2014). NG2-Glia from Pallial Progenitors Produce the Largest Clonal Clusters of the Brain: Time Frame of Clonal Generation in Cortex and Olfactory Bulb. Journal of Neuroscience, 34(6), 2305–2313. http://doi.org/10.1523/JNEUROSCI.3060-13.2014

García-Marqués, J., Núñez-Llaves, R., & López-Mascaraque, L. (2014). NG2-glia from pallial progenitors produce the largest clonal clusters of the brain: time frame of clonal generation in cortex and olfactory bulb. The Journal of Neuroscience : The Official Journal of the Society for Neuroscience, 34(6), 2305–13. http://doi.org/10.1523/JNEUROSCI.3060-13.2014

García-Moreno, F., Vasistha, N. a, Begbie, J., & Molnár, Z. (2014). CLoNe is a new method to target single progenitors and study their progeny in mouse and chick. Development (Cambridge, England), 141(7), 1589–98. http://doi.org/10.1242/dev.105254

Gascón, S., Murenu, E., Masserdotti, G., Ortega, F., Russo, G. L., Petrik, D., … Götz, M. (2016). Identification and Successful Negotiation of a Metabolic Checkpoint in Direct Neuronal Reprogramming. Cell Stem Cell, 18(3), 396–409. http://doi.org/10.1016/j.stem.2015.12.003

Ge, W.-P., Miyawaki, A., Gage, F. H., Jan, Y. N., & Jan, L. Y. (2012). Local generation of glia is a major astrocyte source in postnatal cortex. Nature, 484(7394), 376–80. http://doi.org/10.1038/nature10959

Ge, W. P., & Jia, J. M. (2016). Local production of astrocytes in the cerebral cortex. Neuroscience, 323, 3–9. http://doi.org/10.1016/j.neuroscience.2015.08.057

Gengatharan, A., Bammann, R. R., & Saghatelyan, A. (2016). The Role of Astrocytes in the Generation, Migration, and Integration of New Neurons in the Adult Olfactory Bulb. Frontiers in Neuroscience, 10(April), 1–8. http://doi.org/10.3389/fnins.2016.00149

Gire, D. H., Restrepo, D., Sejnowski, T. J., Greer, C., De Carlos, J. a, & Lopez-Mascaraque, L. (2013). Temporal processing in the olfactory system: can we see a smell? Neuron, 78(3), 416–32. http://doi.org/10.1016/j.neuron.2013.04.033

Golden, J. a, Fields-Berry, S. C., & Cepko, C. L. (1995). Construction and characterization of a highly complex retroviral library for lineage analysis. Proceedings of the National Academy of Sciences of the United States of America, 92(12), 5704–8. Retrieved from http://www.pubmedcentral.nih.gov/articlerender.fcgi?artid=41765&tool=pmcentrez&rendertype=abstract

Goldman, S. a, & Chen, Z. (2011). Perivascular instruction of cell genesis and fate in the adult brain. Nature Neuroscience, 14(11), 1382–9. http://doi.org/10.1038/nn.2963

Golgi, C. (1875). Sulla fina struttura dei bulbi olfactorii. Rivista Sperimentale Di Freniatria E Medicina Legale, 1, 66–78.

Gomez-Nicola, D., Riecken, K., Fehse, B., & Perry, V. H. (2014). In-vivo RGB marking and multicolour single-cell tracking in the adult brain. Scientific Reports, 1–10. http://doi.org/10.1038/srep07520

Götz, M., & Huttner, W. B. (2005). The cell biology of neurogenesis. Nature Reviews. Molecular Cell Biology, 6(10), 777–88. http://doi.org/10.1038/nrm1739

Griffin, R., Sustar, A., Bonvin, M., Binari, R., del Valle Rodriguez, A., Hohl, A. M., … Perrimon, N. (2009). The twin spot generator for differential Drosophila lineage analysis. Nature Methods, 6(8), 600–602. http://doi.org/10.1038/nmeth.1349

Guo, C., Eckler, M. J., McKenna, W. L., McKinsey, G. L., Rubenstein, J. L. R., & Chen, B. (2013). Fezf2 expression identifies a multipotent progenitor for neocortical projection neurons, astrocytes, and oligodendrocytes. Neuron, 80(5), 1167–1174. http://doi.org/10.1016/j.neuron.2013.09.037

Hack, M. a, Saghatelyan, A., de Chevigny, A., Pfeifer, A., Ashery-Padan, R., Lledo, P.-M., & Götz, M. (2005). Neuronal fate determinants of adult olfactory bulb neurogenesis. Nature Neuroscience, 8(7), 865–872. http://doi.org/10.1038/nn1479

Hadjieconomou, D., Rotkopf, S., Alexandre, C., Bell, D. M., Dickson, B. J., & Salecker, I. (2011). Flybow: genetic multicolor cell labeling for neural circuit analysis in Drosophila melanogaster. Nature Methods, 8(3), 260–6. http://doi.org/10.1038/nmeth.1567

Hampel, S., Chung, P., McKellar, C. E., Hall, D., Looger, L. L., & Simpson, J. H. (2011). Drosophila Brainbow: a recombinase-based fluorescence labeling technique to subdivide neural expression patterns. Nature Methods, 8(3), 253–9. http://doi.org/10.1038/nmeth.1566

Holt, C. E., Garlick, N., & Cornel, E. (1990). Lipofection of cDNAs in the embryonic vertebrate central nervous system. Neuron, 4(2), 203–214. http://doi.org/10.1016/0896-6273(90)90095-W

Houades, V., Koulakoff, A., Ezan, P., Seif, I., & Giaume, C. (2008). Gap junction-mediated astrocytic networks in the mouse barrel cortex. The Journal of Neuroscience : The Official Journal of the Society for Neuroscience, 28(20), 5207–17. http://doi.org/10.1523/JNEUROSCI.5100-07.2008

Ihrie, R. A., Shah, J. K., Harwell, C. C., Levine, J. H., Guinto, C. D., Lezameta, M., … Alvarez-Buylla, A. (2011). Persistent Sonic Hedgehog Signaling in Adult Brain Determines Neural Stem Cell Positional Identity. Neuron, 71(2), 250–262. http://doi.org/10.1016/j.neuron.2011.05.018

Imayoshi, I., Sakamoto, M., Ohtsuka, T., Takao, K., Miyakawa, T., Yamaguchi, M., … Kageyama, R. (2008). Roles of continuous neurogenesis in the structural and functional integrity of the adult forebrain. Nature Neuroscience, 11(10), 1153–1161. http://doi.org/10.1038/nn.2185

Imura, T., Kornblum, H. I., & Sofroniew, M. V. (2003). The predominant neural stem cell isolated from postnatal and adult forebrain but not early embryonic forebrain expresses GFAP. The Journal of Neuroscience : The Official Journal of the Society for Neuroscience, 23(7), 2824–32. Retrieved from http://www.ncbi.nlm.nih.gov/pubmed/12684469

Isaacson, J. S., & Strowbridge, B. W. (1998). Olfactory reciprocal synapses: dendritic signaling in the CNS.

Neuron, 20(4), 749–61. Retrieved from http://www.ncbi.nlm.nih.gov/pubmed/9581766

Itasaki, N., Bel-Vialar, S., & Krumlauf, R. (1999). "Shocking" developments in chick embryology: electroporation and in ovo gene expression. Nat Cell Biol, 1(8), E203-7. http://doi.org/10.1038/70231

Kanca, O., Caussinus, E., Denes, A. S., Percival-Smith, A., & Affolter, M. (2014). Raeppli: a whole-tissue labeling tool for live imaging of Drosophila development. Development, 141(2), 472–480. http://doi.org/10.1242/dev.102913

Kempermann, G., Kuhn, H. G., & Gage, F. H. (1997). More hippocampal neurons in adult mice living in an enricged environment. Nature, 386(3), 493–495.

Kim, W. R., Kim, Y., Eun, B., Park, O. -h., Kim, H., Kim, K., … Sun, W. (2007). Impaired Migration in the Rostral Migratory Stream But Spared Olfactory Function after the Elimination of Programmed Cell Death in Bax Knock-Out Mice. Journal of Neuroscience, 27(52), 14392–14403. http://doi.org/10.1523/JNEUROSCI.3903-07.2007

Kita, Y., Kawakami, K., Takahashi, Y., & Murakami, F. (2013). Development of cerebellar neurons and glias revealed by in utero electroporation: Golgi-like labeling of cerebellar neurons and glias. PloS One, 8(7), e70091. http://doi.org/10.1371/journal.pone.0070091

Kohwi, M., Osumi, N., Rubenstein, J. L. R., & Alvarez-Buylla, A. (2005). Pax6 is required for making specific subpopulations of granule and periglomerular neurons in the olfactory bulb. The Journal of Neuroscience : The Official Journal of the Society for Neuroscience, 25(30), 6997–7003. http://doi.org/10.1523/JNEUROSCI.1435-05.2005

Kohwi, M., Petryniak, M. A., Long, J. E., Ekker, M., Obata, K., Yanagawa, Y., … Alvarez-Buylla, A. (2007). A subpopulation of olfactory bulb GABAergic interneurons is derived from Emx1- and Dlx5/6-expressing progenitors. J Neurosci, 27(26), 6878–6891. http://doi.org/10.1523/JNEUROSCI.0254-07.2007

Kosaka, K., & Kosaka, T. (2005). synaptic organization of the glomerulus in the main olfactory bulb: compartments of the glomerulus and heterogeneity of the periglomerular cells. Anatomical Science International, 80(2), 80–90. http://doi.org/10.1111/j.1447-073x.2005.00092.x

Kosodo, Y., Röper, K., Haubensak, W., Marzesco, A.-M., Corbeil, D., & Huttner, W. B. (2004). Asymmetric distribution of the apical plasma membrane during neurogenic divisions of mammalian neuroepithelial cells. The EMBO Journal, 23(11), 2314–24. http://doi.org/10.1038/sj.emboj.7600223

Kretzschmar, K., & Watt, F. M. (2012). Lineage tracing. Cell, 148(1–2), 33–45. http://doi.org/10.1016/j.cell.2012.01.002

Kriegstein, A., & Alvarez-Buylla, A. (2009). The glial nature of embryonic and adult neural stem cells. Annual Review of Neuroscience, 32, 149–84. http://doi.org/10.1146/annurev.neuro.051508.135600

Kriegstein, A. R., & Götz, M. (2003). Radial glia diversity: a matter of cell fate. Glia, 43(1), 37–43. http://doi.org/10.1002/glia.10250

Kriegstein, A. R., & Noctor, S. C. (2004). Patterns of neuronal migration in the embryonic cortex. Trends in Neurosciences, 27(7), 392–9. http://doi.org/10.1016/j.

tins.2004.05.001

Kuan, C. Y., Elliott, E. A., Flavell, R. A., & Rakic, P. (1997). Restrictive clonal allocation in the chimeric mouse brain. Proceedings of the National Academy of Sciences of the United States of America, 94(7), 3374–9. http://doi.org/10.1073/pnas.94.7.3374

Lacar, B., Young, S. Z., Platel, J.-C., & Bordey, A. (2010). Imaging and recording subventricular zone progenitor cells in live tissue of postnatal mice. Frontiers in Neuroscience, 4(July), 1–16. http://doi.org/10.3389/fnins.2010.00043

Lacar, B., Young, S. Z., Platel, J. C., & Bordey, A. (2011). Gap junction-mediated calcium waves define communication networks among murine postnatal neural progenitor cells. European Journal of Neuroscience, 34(12), 1895–1905. http://doi.org/10.1111/j.1460-9568.2011.07901.x

Laywell, E. D., Rakic, P., Kukekov, V. G., Holland, E. C., & Steindler, D. a. (2000). Identification of a multipotent astrocytic stem cell in the immature and adult mouse brain. Proceedings of the National Academy of Sciences of the United States of America, 97(25), 13883–8. http://doi.org/10.1073/pnas.250471697

Le Douarin, N. (2005). The Nogent Institute--50 years of embryology. The International Journal of Developmental Biology, 49(2–3), 85–103. http://doi.org/10.1387/ijdb.041952nl

Levison, S. W., Chuang, C., Abramson, B. J., & Goldman, J. E. (1993). The migrational patterns and developmental fates of glial precursors in the rat subventricular zone are temporally regulated. Development (Cambridge, England), 119(3), 611–22. Retrieved from http://www.ncbi.nlm.nih.gov/pubmed/8187632

Liu, X., Wang, Q., Haydar, T. F., & Bordey, A. (2005). Nonsynaptic GABA signaling in postnatal subventricular zone controls proliferation of GFAP-expressing progenitors. Nature Neuroscience, 8(9), 1179–1187. http://doi.org/10.1038/nn1522

Livet, J., Weissman, T. a, Kang, H., Draft, R. W., Lu, J., Bennis, R. a, … Lichtman, J. W. (2007). Transgenic strategies for combinatorial expression of fluorescent proteins in the nervous system. Nature, 450(7166), 56–62. http://doi.org/10.1038/nature06293

Lledo, P.-M., Alonso, M., & Grubb, M. S. (2006). Adult neurogenesis and functional plasticity in neuronal circuits. Nature Reviews. Neuroscience, 7(3), 179–93. http://doi.org/10.1038/nrn1867

Lledo, P. M., & Saghatelyan, A. (2005). Integrating new neurons into the adult olfactory bulb: Joining the network, life-death decisions, and the effects of sensory experience. Trends in Neurosciences, 28(5), 248–254. http://doi.org/10.1016/j.tins.2005.03.005

Llorens-Bobadilla, E., Zhao, S., Baser, A., Saiz-Castro, G., Zwadlo, K., & Martin-Villalba, A. (2015). Single-Cell Transcriptomics Reveals a Population of Dormant Neural Stem Cells that Become Activated upon Brain Injury. Cell Stem Cell, 17(3), 329–340. http://doi.org/10.1016/j.stem.2015.07.002

Lois, C., & Alvarez-Buylla, A. (1994). Long-distance neuronal migration in the adult mammalian brain. Science (New York, N.Y.), 264(5162), 1145–8.

Lois, C., Hong, E. J., Pease, S., Brown, E. J., & Baltimore, D. (2002). Germline transmission and tissue-specific expression of transgenes delivered by

lentiviral vectors. Science (New York, N.Y.), 295(5556), 868–72. http://doi.org/10.1126/science.1067081

Long, J. E., Garel, S., Alvarez-Dolado, M., Yoshikawa, K., Osumi, N., Alvarez-Buylla, A., & Rubenstein, J. L. R. (2007). Dlx-Dependent and -Independent Regulation of Olfactory Bulb Interneuron Differentiation. Journal of Neuroscience, 27(12), 3230–3243. http://doi.org/10.1523/JNEUROSCI.5265-06.2007

López-Júarez, A., Howard, J., Ullom, K., Howard, L., Grande, A., Pardo, A., … Nakafuku, M. (2013). Gsx2 controls region-specific activation of neural stem cells and injury-induced neurogenesis in the adult subventricular zone. Genes and Development, 27(11), 1272–1287. http://doi.org/10.1101/gad.217539.113

López-Mascaraque, L., De Carlos, J. A., & Valverde, F. (1986). Structure of the olfactory bulb of the hedgehog (Erinaceus europaeus): description of cell types in the granular layer. The Journal of Comparative Neurology, 253(2), 135–52. http://doi.org/10.1002/cne.902530202

López-Mascaraque, L., & de Castro, F. (2002). The olfactory bulb as an independent developmental domain. Cell Death and Differentiation, 9(12), 1279–86. http://doi.org/10.1038/sj.cdd.4401076

Loulier, K., Barry, R., Mahou, P., Le Franc, Y., Supatto, W., Matho, K. S., … Livet, J. (2014). Multiplex cell and lineage tracking with combinatorial labels. Neuron, 81(3), 505–20. http://doi.org/10.1016/j.neuron.2013.12.016

Luo, J., Daniels, S. B., Lennington, J. B., Notti, R. Q., & Conover, J. C. (2006). The aging neurogenic subventricular zone. Aging Cell, 5(2), 139–52. http://doi.org/10.1111/j.1474-9726.2006.00197.x

Luskin, M. B. (1993). Restricted proliferation and migration of postnatally generated neurons derived from the forebrain subventricular zone. Neuron, 11(1), 173–89.

Luskin, M. B. (1998). Neuroblasts of the postnatal mammalian forebrain: their phenotype and fate. Journal of Neurobiology, 36(2), 221–33. Retrieved from http://www.ncbi.nlm.nih.gov/pubmed/9712306

Luskin, M. B., Pearlman, A. L., & Sanes, J. R. (1988). Cell lineage in the cerebral cortex of the mouse studied in vivo and in vitro with a Recombinant Retrovirus. Neuron, 1(8), 635–647. http://doi.org/10.1016/0896-6273(88)90163-8

Luzzati, F., Nato, G., Oboti, L., Vigna, E., Rolando, C., Armentano, M., … Peretto, P. (2014). Quiescent neuronal progenitors are activated in the juvenile guinea pig lateral striatum and give rise to transient neurons. Development, 141(21), 4065–4075. http://doi.org/10.1242/dev.107987

Ma, D. K., Kim, W. R., Ming, G. L., & Song, H. (2009). Activity-dependent extrinsic regulation of adult olfactory bulb and hippocampal neurogenesis. Annals of the New York Academy of Sciences, 1170, 664–673. http://doi.org/10.1111/j.1749-6632.2009.04373.x

Mackay-Sim, A., & Kittel, P. (1991). Cell dynamics in the adult mouse olfactory epithelium: a quantitative autoradiographic study. The Journal of Neuroscience : The Official Journal of the Society for Neuroscience, 11(4), 979–84.

Magavi, S., Friedmann, D., Banks, G., Stolfi, A., & Lois, C. (2012). Coincident generation of pyramidal neurons and protoplasmic astrocytes in neocortical columns. The Journal of Neuroscience : The Official Journal of

the Society for Neuroscience, 32(14), 4762–72. http://doi.org/10.1523/JNEUROSCI.3560-11.2012

Magnusson, J. P., & Frisén, J. (2016). Stars from the darkest night: unlocking the neurogenic potential of astrocytes in different brain regions. Development (Cambridge, England), 143(7), 1075–86. http://doi.org/10.1242/dev.133975

Malatesta, P., Hack, M. a, Hartfuss, E., Kettenmann, H., Klinkert, W., Kirchhoff, F., & Götz, M. (2003). Neuronal or glial progeny: regional differences in radial glia fate. Neuron, 37(5), 751–64. Retrieved from http://www.ncbi.nlm.nih.gov/pubmed/12628166

Martynoga, B., Drechsel, D., Guillemot, F., Ochoa-espinosa, A., Affolter, M., Fedoriw, A., & Mugford, J. (2012). Molecular Control of Neurogenesis : A View from the Mammalian Cerebral Cortex Molecular Control of Neurogenesis : AView from the Mammalian Cerebral Cortex. Cold Spring Harbor Perspectives in Biology, 4, 1–14. http://doi.org/10.1101/cshperspect.a008359

McQuiston, A. R., & Katz, L. C. (2001). Electrophysiology of Interneurons in the Glomerular Layer of the Rat Olfactory Bulb. J Neurophysiol, 86(4), 1899–1907.

Menn, B., Garcia-Verdugo, J. M., Yaschine, C., Gonzalez-Perez, O., Rowitch, D., & Alvarez-Buylla, A. (2006). Origin of oligodendrocytes in the subventricular zone of the adult brain. The Journal of Neuroscience : The Official Journal of the Society for Neuroscience, 26(30), 7907–7918. http://doi.org/10.1523/JNEUROSCI.1299-06.2006

Merkle, F. T., Fuentealba, L. C., Sanders, T. a, Magno, L., Kessaris, N., & Alvarez-Buylla, A. (2014). Adult neural stem cells in distinct microdomains generate previously unknown interneuron types. Nature Neuroscience, 17(2), 207–14. http://doi.org/10.1038/nn.3610

Merkle, F. T., Mirzadeh, Z., & Alvarez-Buylla, A. (2007). Mosaic organization of neural stem cells in the adult brain. Science (New York, N.Y.), 317(5836), 381–4. http://doi.org/10.1126/science.1144914

Merkle, F. T., Tramontin, A. D., García-Verdugo, J. M., & Alvarez-Buylla, A. (2004). Radial glia give rise to adult neural stem cells in the subventricular zone. PNAS, 101(50), 17528–32. http://doi.org/10.1073/pnas.0407893101

Miller, F. D., & Gauthier, A. S. (2007). Timing is everything: making neurons versus glia in the developing cortex. Neuron, 54(3), 357–69. http://doi.org/10.1016/j.neuron.2007.04.019

Miron, V. E., Kuhlmann, T., & Antel Jack P., J. P. (2011). Cells of the oligodendroglial lineage, myelination, and remyelination. Biochimica et Biophysica Acta - Molecular Basis of Disease, 1812(2), 184–193. http://doi.org/10.1016/j.bbadis.2010.09.010

Mirzadeh, Z., Merkle, F. T., Soriano-Navarro, M., Garcia-Verdugo, J. M., & Alvarez-Buylla, A. (2008a). Neural stem cells confer unique pinwheel architecture to the ventricular surface in neurogenic regions of the adult brain. Cell Stem Cell, 3(3), 265–78. http://doi.org/10.1016/j.stem.2008.07.004

Mobley, A. S., Bryant, A. K., Richard, M. B., Brann, J. H., Firestein, S. J., & Greer, C. A. (2013). Age-dependent regional changes in the rostral migratory stream. Neurobiology of Aging, 34(7), 1873–1881. http://doi.org/10.1016/j.neurobiolaging.2013.01.015

Mombaerts, P., Wang, F., Dulac, C., Chao, S. K., Nemes, A., Mendelsohn, M., … Axel, R. (1996). Visualizing an olfactory sensory map. Cell, 87(4), 675–86.

Murdoch, B., & Roskams, A. J. (2008). A novel embryonic nestin-expressing radial glia-like progenitor gives rise to zonally restricted olfactory and vomeronasal neurons. The Journal of Neuroscience : The Official Journal of the Society for Neuroscience, 28(16), 4271–82. http://doi.org/10.1523/JNEUROSCI.5566-07.2008

Nato, G., Caramello, a., Trova, S., Avataneo, V., Rolando, C., Taylor, V., … Luzzati, F. (2015). Striatal astrocytes produce neuroblasts in an excitotoxic model of Huntington's disease. Development, 142(5), 840–845. http://doi.org/10.1242/dev.116657

Nishiyama, A., Komitova, M., Suzuki, R., & Zhu, X. (2009). Polydendrocytes (NG2 cells): multifunctional cells with lineage plasticity. Nature Reviews. Neuroscience, 10(1), 9–22. http://doi.org/10.1038/nrn2495

Niu, W., Zang, T., Zou, Y., Fang, S., Smith, D. K., Bachoo, R., & Zhang, C.-L. (2013). In vivo reprogramming of astrocytes to neuroblasts in the adult brain. Nature Cell Biology, 15(10), 1164–75. http://doi.org/10.1038/ncb2843

Noctor, S. C., Flint, a C., Weissman, T. a, Dammerman, R. S., & Kriegstein, a R. (2001). Neurons derived from radial glial cells establish radial units in neocortex. Nature, 409(6821), 714–20. http://doi.org/10.1038/35055553

Nolte, C., Matyash, M., Pivneva, T., Schipke, C. G., Ohlemeyer, C., Hanisch, U. K., … Kettenmann, H. (2001). GFAP promoter-controlled EGFP-expressing transgenic mice: A tool to visualize astrocytes and astrogliosis in living brain tissue. GLIA, 33(1), 72–86. http://doi.org/10.1002/1098-1136(20010101)33:1<72::AID-GLIA1007>3.0.CO;2-A

Ortega, F., & Costa, M. R. (2016). Live Imaging of Adult Neural Stem Cells in Rodents. Frontiers in Neuroscience, 10(March), 1–14. http://doi.org/10.3389/fnins.2016.00078

Ortega, F., Costa, M. R., Simon-Ebert, T., Schroeder, T., Götz, M., & Berninger, B. (2011). Using an adherent cell culture of the mouse subependymal zone to study the behavior of adult neural stem cells on a single-cell level. Nature Protocols, 6(12), 1847–59. http://doi.org/10.1038/nprot.2011.404

Ortega, F., Gascón, S., Masserdotti, G., Deshpande, A., Simon, C., Fischer, J., … Berninger, B. (2013). Oligodendrogliogenic and neurogenic adult subependymal zone neural stem cells constitute distinct lineages and exhibit differential responsiveness to Wnt signalling. Nature Cell Biology, 15(6), 602–613. http://doi.org/10.1038/ncb2736

Pan, Y. A., Freundlich, T., Weissman, T. a, Schoppik, D., Wang, X. C., Zimmerman, S., … Schier, A. F. (2013). Zebrabow: multispectral cell labeling for cell tracing and lineage analysis in zebrafish. Development (Cambridge, England), 140(13), 2835–46. http://doi.org/10.1242/dev.094631

Pan, Y. A., Livet, J., Sanes, J. R., Lichtman, J. W., & Schier, A. F. (2011). Multicolor brainbow imaging in Zebrafish. Cold Spring Harbor Protocols, 6(1), 1–8. http://doi.org/10.1101/pdb.prot5546

Petit, A., Legué, E., & Nicolas, J. (2005). Methods in clonal analysis and applications. Reprod. Nutr. Dev.,

45, 321–339. http://doi.org/10.1051/rnd

Petreanu, L., & Alvarez-Buylla, A. (2002). Maturation and death of adult-born olfactory bulb granule neurons: role of olfaction. The Journal of Neuroscience : The Official Journal of the Society for Neuroscience, 22(14), 6106–6113. http://doi.org/20026588

Pfenninger, C. V., Steinhoff, C., Hertwig, F., & Nuber, U. A. (2011). Prospectively isolated CD133/CD24-positive ependymal cells from the adult spinal cord and lateral ventricle wall differ in their long-term in vitro self-renewal and in vivo gene expression. Glia, 59(1), 68–81. http://doi.org/10.1002/glia.21077

Ponti, G., Obernier, K., Guinto, C., Jose, L., Bonfanti, L., & Alvarez-Buylla, A. (2013). Cell cycle and lineage progression of neural progenitors in the ventricular-subventricular zones of adult mice. Proceedings of the National Academy of Sciences of the United States of America, 110(11), E1045-54. http://doi.org/10.1073/pnas.1219563110

Poon, A., Li, Z., Wolfe, G. W., Lu, L., Williams, R. W., Hayes, N. L., … Goldowitz, D. (2010). Identification of a Chr 11 quantitative trait locus that modulates proliferation in the rostral migratory stream of the adult mouse brain. European Journal of Neuroscience, 32(4), 523–537. http://doi.org/10.1111/j.1460-9568.2010.07316.x

Porlan, E., Perez-Villalba, A., Delgado, A. C., & Ferrón, S. R. (2013). Paracrine regulation of neural stem cells in the subependymal zone. Archives of Biochemistry and Biophysics, 534(1–2), 11–19. http://doi.org/10.1016/j.abb.2012.10.001

Price, J. L., & Powell, T. P. (1970). The synaptology of the granule cells of the olfactory bulb. Journal of Cell Science, 7(1), 125–55.

Ramón y Cajal, S. (1894). Croonian Lecture: la fine structure des centres nerveux. Proc. R. Soc.508 Lond., 55, 444–468.

Ramón y Cajal, S. (1904). Textura del Sistema Nervioso del Hombre y los Vertebrados. Madrid: Moya.

Ramón y Cajal, S. (1913). Estudios sobre la Degeneración y Regeneración del Sistema Nervioso. Madrid: Moya.

Ramón y Cajal, S. (1931). Pensamientos de tendencia educativa. Archivo de La Palabra.

Reynolds, B. A., & Weiss, S. (1996). Clonal and population analyses demonstrate that an EGF-responsive mammalian embryonic CNS precursor is a stem cell. Developmental Biology, 175(1), 1–13. http://doi.org/10.1006/dbio.1996.0090

Rhodes, K. E., Raivich, G., & Fawcett, J. W. (2006). The injury response of oligodendrocyte precursor cells is induced by platelets, macrophages and inflammation-associated cytokines. Neuroscience, 140(1), 87–100. http://doi.org/10.1016/j.neuroscience.2006.01.055

Ribeiro Xavier, A. L., Kress, B. T., Goldman, S. A., Lacerda de Menezes, J. R., & Nedergaard, M. (2015). A Distinct Population of Microglia Supports Adult Neurogenesis in the Subventricular Zone. Journal of Neuroscience, 35(34), 11848–11861. http://doi.org/10.1523/JNEUROSCI.1217-15.2015

Richardson, W. D., Young, K. M., Tripathi, R. B., & McKenzie, I. (2011). NG2-glia as Multipotent Neural Stem Cells: Fact or Fantasy? Neuron, 70(4), 661–673. http://doi.org/10.1016/j.neuron.2011.05.013

Rochefort, C., Gheusi, G., Vincent, J.-D., & Lledo, P.-M. (2002). Enriched odor exposure increases the number of newborn neurons in the adult olfactory bulb and improves odor memory. The Journal of Neuroscience : The Official Journal of the Society for Neuroscience, 22(7), 2679–2689. http://doi.org/20026260

Rojczyk-Gołębiewska, E., Pałasz, A., & Wiaderkiewicz, R. (2014). Hypothalamic subependymal niche: A novel site of the adult neurogenesis. Cellular and Molecular Neurobiology, 34(5), 631–642. http://doi.org/10.1007/s10571-014-0058-5

Rouach, N. (2009). Hippocampal Synaptic Transmission. Science, 1551(2008), 1551–1555. http://doi.org/10.1126/science.1164022

Roux, L., Benchenane, K., Rothstein, J. D., Bonvento, G., & Giaume, C. (2011). Plasticity of astroglial networks in olfactory glomeruli. Proceedings of the National Academy of Sciences of the United States of America, 108(45), 18442–6. http://doi.org/10.1073/pnas.1107386108

Rowitch, D. H., & Kriegstein, A. R. (2010). Developmental genetics of vertebrate glial–cell specification. Nature, 468(7321), 214–222. http://doi.org/10.1038/nature09611

Ryu, J. R., Hong, C. J., Kim, J. Y., Kim, E.-K., Sun, W., & Yu, S.-W. (2016). Control of adult neurogenesis by programmed cell death in the mammalian brain. Molecular Brain, 9, 43. http://doi.org/10.1186/s13041-016-0224-4

Salipante, S. J., & Horwitz, M. S. (2006). Phylogenetic fate mapping. Proceedings of the National Academy of Sciences of the United States of America, 103(14), 5448–5453. http://doi.org/10.1073/pnas.0601265103

Sato, Y., Kasai, T., Nakagawa, S., Tanabe, K., Watanabe, T., Kawakami, K., & Takahashi, Y. (2007). Stable integration and conditional expression of electroporated transgenes in chicken embryos. Developmental Biology, 305(2), 616–24. http://doi.org/10.1016/j.ydbio.2007.01.043

Sauvageot, C., & Stiles, D. (2002). Molecular mechanisms controlling cortical gliogenesis. Current Opinion in Neurobiology, 12(3), 244–249. http://doi.org/10.1016/S0959-4388(02)00322-7

Schneider, S. P., & Macrides, F. (1978). Laminar distributions of internuerons in the main olfactory bulb of the adult hamster. Brain Research Bulletin, 3(1), 73–82.

Schoppa, N. E., Kinzie, J. M., Sahara, Y., Segerson, T. P., & Westbrook, G. L. (1998). Dendrodendritic inhibition in the olfactory bulb is driven by NMDA receptors. The Journal of Neuroscience : The Official Journal of the Society for Neuroscience, 18(17), 6790–802. Retrieved from http://www.ncbi.nlm.nih.gov/pubmed/9712650

Schwarting, G. A., Gridley, T., & Henion, T. R. (2007). Notch1 expression and ligand interactions in progenitor cells of the mouse olfactory epithelium. Journal of Molecular Histology, 38(6), 543–53. http://doi.org/10.1007/s10735-007-9110-9

Shaner, N. C., Steinbach, P. A., & Tsien, R. Y. (2005). A guide to choosing fluorescent proteins. Nature Methods, 2(12), 905–909. http://doi.org/10.1038/NMETH819

Shapiro, L. A., Ng, K., Zhou, Q. Y., & Ribak, C. E. (2009). Subventricular zone-derived, newly generated neurons populate several olfactory and limbic forebrain

regions. Epilepsy and Behavior, 14(1 SUPPL. 1), 74–80. http://doi.org/10.1016/j.yebeh.2008.09.011

Shepherd, G. M., Chen, W., & Greer, C. (2004). Olfactory bulb. In The Synaptic Organization of the Brain (pp. 165–216). New York: Oxford Univ. Press.

Siddiqi, F., Chen, F., Aron, A. W., Fiondella, C. G., Patel, K., & LoTurco, J. (2014). Fate Mapping by PiggyBac Transposase Reveals That Neocortical GLAST+ Progenitors Generate More Astrocytes Than Nestin+ Progenitors in Rat Neocortex. Cerebral Cortex, 24(2), 508–520. http://doi.org/10.1093/cercor/bhs332

Smith, C. M., & Luskin, M. B. (1998). Cell cycle length of olfactory bulb neuronal progenitors in the rostral migratory stream. Developmental Dynamics, 213(2), 220–227. http://doi.org/10.1002/(SICI)1097-0177(199810)213:2<220::AID-AJA7>3.0.CO;2-I

Smith D.K., Wang L.L. & Zhang.L. (2016). Physiological, pathological, and engineered cell identity reprogramming in the central nervous system. Wiley Interdiscip Rev Dev Biol. 2016 Jul;5(4):499-517. doi: 10.1002/wdev.234.

Snippert, H. J., van der Flier, L. G., Sato, T., van Es, J. H., van den Born, M., Kroon-Veenboer, C., … Clevers, H. (2010). Intestinal crypt homeostasis results from neutral competition between symmetrically dividing Lgr5 stem cells. Cell, 143(1), 134–144. http://doi.org/10.1016/j.cell.2010.09.016

Sohn, J., Orosco, L., Guo, F., Chung, S. H., Bannerman, P., Mills Ko, E., … Pleasure, D. (2015). The subventricular zone continues to generate corpus callosum and rostral migratory stream astroglia in normal adult mice. J Neurosci, 35(9), 3756–3763. http://doi.org/10.1523/JNEUROSCI.3454-14.2015

Son, J. H., Min, N., & Joh, T. H. (1996). Early ontogeny of catecholaminergic cell lineage in brain and peripheral neurons monitored by tyrosine hydroxylase-lacZ transgene. Molecular Brain Research, 36(2), 300–308. http://doi.org/10.1016/0169-328X(95)00255-Q

Song, J., Zhong, C., Bonaguidi, M. a, Sun, G. J., Hsu, D., Gu, Y., … Song, H. (2012). Neuronal circuitry mechanism regulating adult quiescent neural stem-cell fate decision. Nature, 489(7414), 150–4. http://doi.org/10.1038/nature11306

Spalding, K. L., Bergmann, O., Alkass, K., Bernard, S., Salehpour, M., Huttner, H. B., … Frisén, J. (2013). Dynamics of hippocampal neurogenesis in adult humans. Cell, 153(6), 1219–27. http://doi.org/10.1016/j.cell.2013.05.002

Spassky, N., Heydon, K., Mangatal, a, Jankovski, a, Olivier, C., Queraud-Lesaux, F., … Zalc, B. (2001). Sonic hedgehog-dependent emergence of oligodendrocytes in the telencephalon: evidence for a source of oligodendrocytes in the olfactory bulb that is independent of PDGFRalpha signaling. Development (Cambridge, England), 128(24), 4993–5004.

Sternberg, N., & Hamilton, D. (1981). Bacteriophage Pl Site-specific Recombination. Journal of Molecular Biology, 4, 467–486.

Sulston, J. E., Schierenberg, E., White, J. G., & Thomson, J. N. (1983). The embryonic cell lineage of the nematode Caenorhabditis elegans. Developmental Biology, 100(1), 64–119. http://doi.org/10.1016/0012-1606(83)90201-4

Temple, S. (1989). Division and differentiation of isolated CNS blast cells in microculture. Nature, 340(6233), 471–3. http://doi.org/10.1038/340471a0

Temple, S. (2001). The development of neural stem cells. Nature, 414(6859), 112–117. http://doi.org/10.1038/35102174

Toresson, H., & Campbell, K. (2001). A role for Gsh1 in the developing striatum and olfactory bulb of Gsh2 mutant mice. Development (Cambridge, England), 128(23), 4769–80.

Valverde, F., & Lopez-Mascaraque, L. (1991). Neuroglial arrangements in the olfactory glomeruli of the hedgehog. The Journal of Comparative Neurology, 307(4), 658–674. http://doi.org/10.1002/cne.903070411

Valverde, F., Santacana, M., & Heredia, M. (1992). Formation of an olfactory glomerulus: morphological aspects of development and organization. Neuroscience, 49(2), 255–75.

Ventura, R. E., & Goldman, J. E. (2007). Dorsal radial glia generate olfactory bulb interneurons in the postnatal murine brain. The Journal of Neuroscience : The Official Journal of the Society for Neuroscience, 27(16), 4297–302. http://doi.org/10.1523/JNEUROSCI.0399-07.2007

Waclaw, R. R., Wang, B., Pei, Z., Ehrman, L. A., & Campbell, K. (2009). Distinct Temporal Requirements for the Homeobox Gene Gsx2 in Specifying Striatal and Olfactory Bulb Neuronal Fates. Neuron, 63(4), 451–465. http://doi.org/10.1016/j.neuron.2009.07.015

Watt, F. M., & Jensen, K. B. (2009). Epidermal stem cell diversity and quiescence. EMBO Molecular Medicine, 1(5), 260–267. http://doi.org/10.1002/emmm.200900033

Weber, K., Bartsch, U., Stocking, C., & Fehse, B. (2008). A multicolor panel of novel lentiviral "gene ontology" (LeGO) vectors for functional gene analysis. Molecular Therapy : The Journal of the American Society of Gene Therapy, 16(4), 698–706. http://doi.org/10.1038/mt.2008.6

Weber, K., Thomaschewski, M., Warlich, M., Volz, T., Cornils, K., Niebuhr, B., … Fehse, B. (2011). RGB marking facilitates multicolor clonal cell tracking. Nature Medicine, (May 2010). http://doi.org/10.1038/nm.2338

Whitman, C. (1887). A contribution to the history of germ layers in clepsine. Journal of Morphology, 1, 105–182. Retrieved from http://scholar.google.com/scholar?hl=en&btnG=Search&q=intitle:A+contribution+to+the+history+of+germ+layers+in+clepsine#0

Wichterle, H., Turnbull, D. H., Nery, S., Fishell, G., & Alvarez-Buylla, A. (2001). In utero fate mapping reveals distinct migratory pathways and fates of neurons born in the mammalian basal forebrain. Development (Cambridge, England), 128(19), 3759–3771.

Willaime-Morawek, S., Seaberg, R. M., Batista, C., Labbé, E., Attisano, L., Gorski, J. a, … van der Kooy, D. (2006). Embryonic cortical neural stem cells migrate ventrally and persist as postnatal striatal stem cells. The Journal of Cell Biology, 175(1), 159–68. http://doi.org/10.1083/jcb.200604123

Winner, B., Cooper-Kuhn, C. M., Aigner, R., Winkler, J., & Kuhn, H. G. (2002). Long-term survival and cell death of newly generated neurons in the adult rat olfactory bulb. European Journal of Neuroscience, 16(9), 1681–1689. http://doi.org/10.1046/j.1460-9568.2002.02238.x

Woltjen, K., Michael, I. P., Mohseni, P., Desai, R.,

Mileikovsky, M., Hämäläinen, R., … Nagy, A. (2009). piggyBac transposition reprograms fibroblasts to induced pluripotent stem cells. Nature, 458(7239), 766–70. http://doi.org/10.1038/nature07863

Yamaguchi, M., & Mori, K. (2005). Critical period for sensory experience-dependent survival of newly generated granule cells in the adult mouse olfactory bulb. Proceedings of the National Academy of Sciences of the United States of America, 102(27), 9697–9702. http://doi.org/10.1073/pnas.0406082102

Yoshida, A., Yamaguchi, Y., Nonomura, K., Kawakami, K., Takahashi, Y., & Miura, M. (2010). Simultaneous expression of different transgenes in neurons and glia by combining in utero electroporation with the Tol2 transposon-mediated gene transfer system. Genes to Cells : Devoted to Molecular & Cellular Mechanisms, 15(5), 501–12. http://doi.org/10.1111/j.1365-2443.2010.01397.x

Young, K. M., Fogarty, M., Kessaris, N., & Richardson, W. D. (2007). Subventricular zone stem cells are heterogeneous with respect to their embryonic origins and neurogenic fates in the adult olfactory bulb. The Journal of Neuroscience : The Official Journal of the Society for Neuroscience, 27(31), 8286–96. http://doi.org/10.1523/JNEUROSCI.0476-07.2007

Yu, Y.-C., Bultje, R. S., Wang, X., & Shi, S.-H. (2009). Specific synapses develop preferentially among sister excitatory neurons in the neocortex. Nature, 458(7237), 501–4. http://doi.org/10.1038/nature07722

Yu, Y.-C., He, S., Chen, S., Fu, Y., Brown, K. N., Yao, X.-H., … Shi, S.-H. (2012). Preferential electrical coupling regulates neocortical lineage-dependent microcircuit assembly. Nature, 486(7401), 113–7. http://doi.org/10.1038/nature10958

Yusa, K., Zhou, L., Li, M. A., Bradley, A., & Craig, N. L. (2011). A hyperactive piggyBac transposase for mammalian applications. Proceedings of the National Academy of Sciences of the United States of America, 108(4), 1531–6. http://doi.org/10.1073/pnas.1008322108

Zerlin, M., Milosevic, A., & Goldman, J. E. (2004). Glial progenitors of the neonatal subventricular zone differentiate asynchronously, leading to spatial dispersion of glial clones and to the persistence of immature glia in the adult mammalian CNS. Developmental Biology, 270(1), 200–13. http://doi.org/10.1016/j.ydbio.2004.02.024

Zhang, X., & Firestein, S. (2002). The olfactory receptor gene superfamily of the mouse. Nature Neuroscience, 5(2), 124–133. http://doi.org/10.1038/nn800

Zong, H., Espinosa, J. S., Su, H. H., Muzumdar, M. D., & Luo, L. (2005). Mosaic analysis with double markers in mice. Cell, 121(3), 479–92. http://doi.org/10.1016/j.cell.2005.02.012

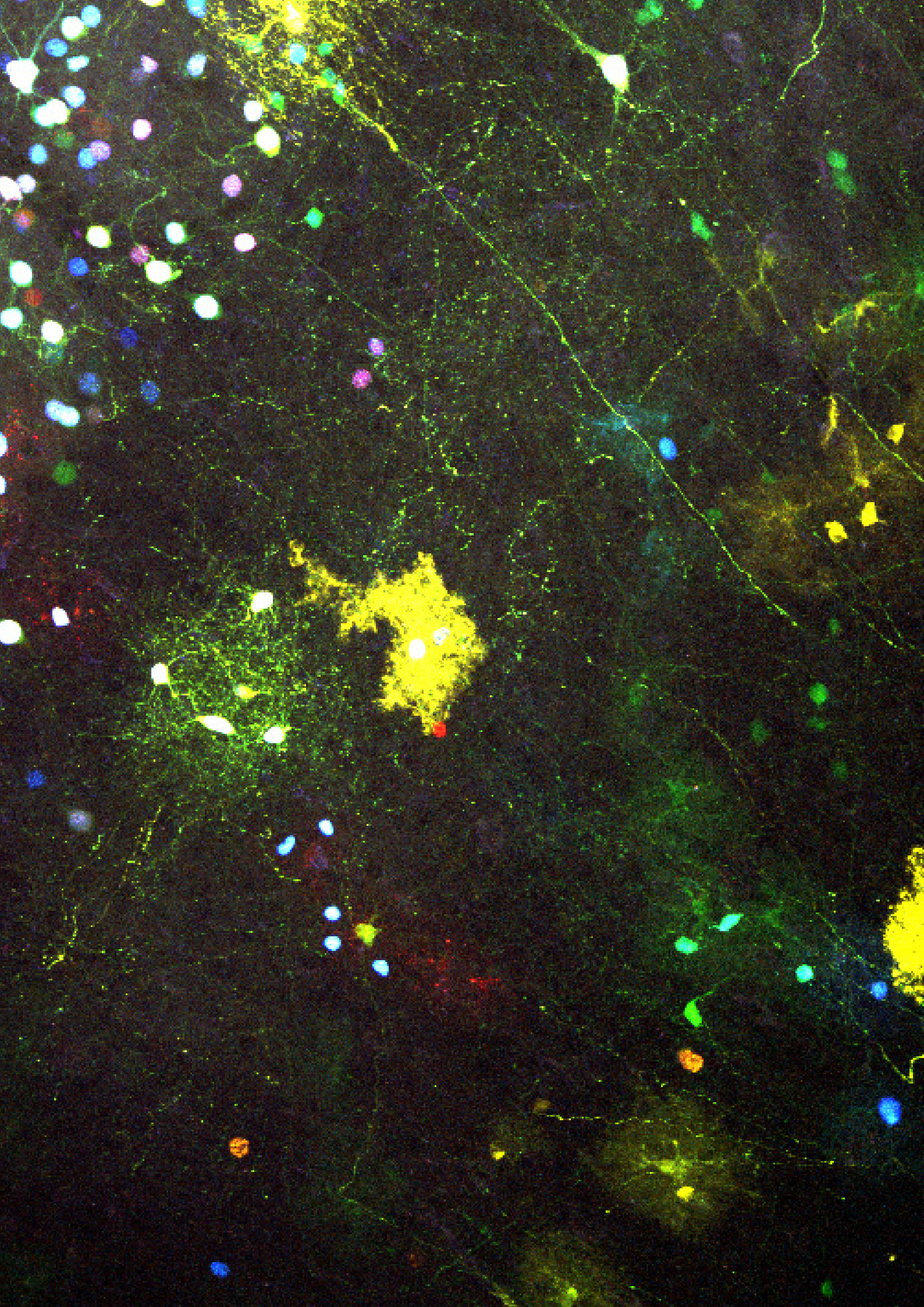

RELATED PUBLICATIONS

frontiers in
NEUROANATOMY

REVIEW ARTICLE
published: 02 July 2014
doi: 10.3389/fnana.2014.00055

Unraveling Cajal's view of the olfactory system

María Figueres-Oñate†, Yolanda Gutiérrez† and Laura López-Mascaraque*

Department of Molecular, Cellular, and Developmental Neurobiology, Instituto Cajal (CSIC), Madrid, Spain

Edited by:
Fernando De Castro, Hospital Nacional de Parapléjicos-SESCAM, Spain

Reviewed by:
Alino Martinez-Marcos, Universidad de Castilla, Spain
Richard S. Nowakowski, Florida State University, USA

***Correspondence:**
Laura López-Mascaraque, Instituto Cajal (CSIC), Avenida del Doctor Arce, 37, Madrid 28002, Spain
e-mail: mascaraque@cajal.csic.es

† These authors have contributed equally to this work.

The olfactory system has a highly regular organization of interconnected synaptic circuits from the periphery. It is therefore an excellent model for understanding general principles about how the brain processes information. Cajal revealed the basic cell types and their interconnections at the end of the XIX century. Since his original descriptions, the observation and analysis of the olfactory system and its components represents a major topic in neuroscience studies, providing important insights into the neural mechanisms. In this review, we will highlight the importance of Cajal contributions and his legacy to the actual knowledge of the olfactory system.

Keywords: olfactory bulb, olfactory cortex, olfactory epithelium, glia, neuron

INTRODUCTION

Santiago Ramón y Cajal is called the father of modern neuroscience for our current understanding of the nervous system really began through his work. Cajal postulated the main principle of neuroscience, the Neuron Doctrine, which recognizes the neuron as the basic anatomical and functional unit of the nervous system (Ramón y Cajal, 1891). His view was opposed to the reticular theory developed by Golgi (1873). The principal advantage that Cajal had over his contemporaries was the better understanding of the Golgi method allowing thus its correct interpretation. With this edge Cajal was able to give a successful explanation to the static view of the sections impregnated by the Golgi method. He was even able to make predictions on physiological brain properties that are being demonstrated nowadays thanks to more sophisticated techniques. Based on observations done using the Golgi method Cajal concluded: "It happens sometimes that the reaction of Golgi runs from one fiber to another when two of them intersect, resembling branches or anastomotic examples. This error can only be avoided by using high magnifying lenses and not giving credit to other branches other than those that appear in the focal plane and on the level of those triangular thickenings that are never absent in cases of a legitimate branch" (Ramón y Cajal, 1890b). In birds' cerebellum, Cajal correctly described that the surface of Purkinje cells "appears bristling with thorns or short spines" (Ramón y Cajal, 1888); Golgi instead, rejected the existence of these spines, considering them artifacts of the silver staining technique. He also established the connections between neurons and drew the maps of the trajectory of nerve currents and impulses that led him to formulate the Law of Dynamic Polarization: "The protoplasmic expansions, dendrites, and the cellular body have axipetal conduction (i.e., toward the axon); whereas the axon has dendrifugal and somatofugal conduction (i.e., it comes from the dendrites or the cellular body)" (Ramón y Cajal, 1899). Furthermore, Cajal described the growth cone as a "concentration of protoplasm of conical form, endowed with amoeboid movements" (Ramón y Cajal, 1890a). Another of Cajal's contributions was the formulation of the Neurotropic Theory (Ramón y Cajal, 1892a); which shows how nerve cells find their way to their targets during development. In the formulation of these Laws explaining the morphological and functional organization of the nervous system, the analyses of the olfactory system was critical; this due to its accessibility, its orderly organization in layers and the easy identification of the main direction of the nervous message flow. Thus, the aim of this article is to give a brief outline of Cajal's main contributions to the knowledge of the olfactory system along with some key developments in our current understanding of this system.

OLFACTORY CIRCUIT

> "The flow of the nervous movement in the bulb would be the following: the olfactory imprint is collected in the mucosa by the peripheral expansion of the bipolar cells and is then transferred to the glomeruli where both the mitral corpuscles as well as the pyramidal or fusiform cells from the molecular layer collect said imprint to raise it to the brain. [...] In summary, there are two main junctions: one in the glomeruli and another one in the cortex of the olfactory lobe. In each one of these junctions the movement acquires more diffusion, partaking in its conduction an increasingly larger number of nervous corpuscles" (Ramón y Cajal, 1892b).

The olfactory system represents an excellent model of the cellular interaction between the periphery and the central nervous system. In the nasal cavity is located the olfactory epithelium (OE) where the olfactory sensory neurons (OSNs), in direct contact with the environment, are contained. OSNs project their axons, through the cribriform plate, to contact target cells in the olfactory bulb (OB). OB projection cells send the olfactory signal to the olfactory cortex (OC), which includes the olfactory

tubercle, piriform cortex, amygdala, and entorhinal cortex. The olfactory information is then further transmitted to the thalamus, hypothalamus, or hippocampus (**Figure 1A**). One of Cajal's most important contributions, the *Law of dynamic polarization*, was possible by the observation of the direction of the signal flow from one neuron to the next in this system. In particular, he used arrows to represent in his histological drawings the flow of information from the periphery (OE) to the OB in the brain and then onto the OC (**Figure 1B**): "Excitation is conducted at the glomeruli, where numerous olfactory fibers end. Here, the motion is transmitted along several currents directed along the path of the projection cells (mitral or superior, medial, and inferior tufted cells), from the intraglomerular tufts, to the axis-cylinders and their cerebral endpoints in the olfactory centers" (Ramón y Cajal, 1890b). Thus, even without a functional frame, Cajal proposed the direction of the information flow that was later corroborated by physiological studies (reviewed in Shepherd and Erulkar, 1997), although the presence of axonless granule cells in this system challenged the *Law of dynamic polarization* (Shepherd et al., 2007; Sassoè-Pognetto, 2011).

Cajal's detailed study of the olfactory system and its components (**Figure 2A**) (Ramón y Cajal, 1890b) laid the foundations for later contemporary studies (**Figures 2B,C**). In his book "*Recuerdos de mi vida*" (Ramón y Cajal, 1917), he defines the OB as an accessible and regular structure, comparable to the cerebellum and retina. In this system, once again, he evidenced the nerve propagation by contact and the important role of dendrites: "The history of the physiological interpretation of the structure of the olfactory bulb provides a typical case of the crippling influence of theoretical prejudices. Golgi had already discovered before us the most important facts of that structure, the singularly invaluable concurrency within the glomeruli of the olfactory fibers, on the one hand, and the dendritic tuft of mitral cells on the other; but his rigid conception of the diffuse nervous network did not allow him to recognize the great physiological scope of such provision" (Ramón y Cajal, 1917).

These characteristics are reinforced by the incorporation of new cellular elements not only during development, but also during adulthood (Altman, 1969; Lois and Alvarez-Buylla, 1994). The plastic process in the OB is the result of the combination of cellular contributions from either the telencephalic subventricular zone as a part of the central nervous system, and the olfactory placode/epithelium, which "represents a peripheral nervous center" (Ramón y Cajal, 1892b).

OLFACTORY EPITHELIUM

> "The olfactory mucosa contains the nervous cells from where the olfactory fibers that reach the brain through the ethmoid's lamina cribrose; it thus represents a peripheral nervous center. [...] The bipolar or olfactory cell represents the real reception organ of the odorant impulse or stimulus" (Ramón y Cajal, 1892b).

The olfactory epithelium is the place where volatile odorant molecules are initially detected and it is composed by three cell types: OSNs, supporting cells and basal cells. OSNs (**Figure 3**) are bipolar cells located in the intermediate OE region, distributed between the supporting cells. Their apical processes end at the lumen in non-motile cilia, while the thinner descending axon "gives neuronal character to the bipolar cell" (Ramón y Cajal, 1892b) and transmits the impulse to the OB. The supporting

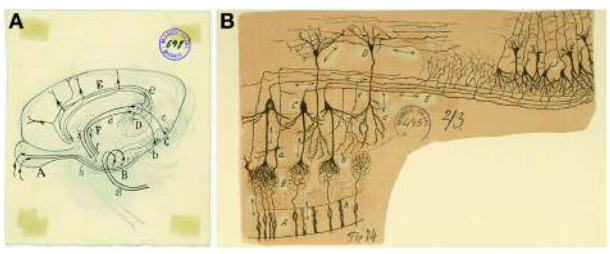

FIGURE 1 | Overall view of the olfactory circuit. (A) Unpublished original Cajal cartoon of the olfactory system. **(B)** Cajal's diagram outlining the circuitry and the trajectory of the nerve impulse (arrows). *(A)* Bipolar cells of the olfactory mucosa. *(B)* Olfactory glomeruli. *(C)* Mitral cells. *(D)* Grains. *(E)* External root (lateral olfactory tract). *(F)* Olfactory cortex. *(a)* Small tufted cell; *(b)* main dendrite of a mitral cell; *(c)* terminal branch of a grain; *(e)* recurrent collaterals of a mitral cell; *(g)* surface triangular cells of the olfactory cortex; *(h)* epithelial cells of the nasal mucosa (Ramón y Cajal, 1894). Cajal Legacy (Instituto Cajal, CSIC, Madrid, Spain).

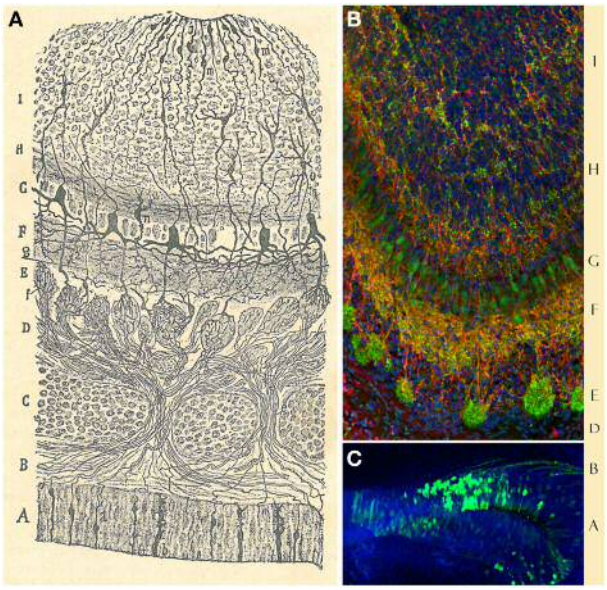

FIGURE 2 | Olfactory bulb and epithelium. (A) Original Cajal drawing showing the "antero-posterior view of the olfactory bulb and nasal mucosa of the newly-born mouse." *(A)* olfactory epithelium; *(a)* olfactory sensory neuron; *(b)* sustentacular cell. *(B)* Dermis. *(C)* Ethmoid bone. *(D)* Fibrillar layer. *(E)* Glomerular layer. *(F)* Inferior molecular layer. *(G)* Mitral cells layer. *(H)* Superior molecular region. *(I)* Granular zone. *(c)* Cartilage. *(e)* Olfactory nerve. *(f)* Arborization of the olfactory fibers within the glomeruli. *(g)* Central cyllinder-axis of an inferior tufted cell. *(h)* Mitral cell. *(i)* Grains. *(j)* Epithelial cells. *(n)* Lower grain. *(o)* Large stellated cell (Ramón y Cajal, 1890b). **(B)** Immunohistochemical staining for Dab1 protein (reelin signaling mediator, green) and Map2a,b protein (microtubule associated protein, red) on mouse olfactory bulb sections at P3. Nuclei counterstained with Hoechst (blue) (Martín-López et al., 2011). **(C)** Olfactory sensory neurons (green) at E17, labeled after *in utero* electroporation of an EGP-expressing plasmid into the olfactory placode at E11. Nuclei counterstained with Hoechst (blue). Sagittal mouse brain section.

or sustentacular cells exhibit an irregular morphology, but their nuclei are mostly located apically, thereby being narrower on their basal side (**Figures 3A,B**). The characteristic morphology of these cells offers "numerous facets or hollow molds in order to adapt to the bipolar corpuscles [...] and their mission appears to be no other than preventing any contact between them, avoiding any horizontal current communication" (Ramón y Cajal, 1892b). Basal cells, not described by Cajal, form a single cell layer in the basal lamina, near the underlying bone of the OE (Retzius, 1892). They have a constant turnover (Graziadei, 1973) being the precursors of OSNs (Suzuki et al., 2013).

One of the main advances in the study of this system was the cloning of the olfactory signal transduction molecules, in particular the odorant receptors (Buck and Axel, 1991) located on the OSNs cilia. In mice there are over five million OSNs, each expressing just one among the thousand odorant receptor genes (Zhang and Firestein, 2002). These chemosensory receptors are odorant-binding proteins with seven transmembrane domains coupled to G-proteins. Each receptor is codified by the allele of a single gene (Buck and Axel, 1991) and binds only odor molecules of a certain family. They are responsible of transforming the chemical information into electric signals in the olfactory circuit. Genetic tools reported that OSNs, expressing a given odorant receptor, are intermingled and randomly distributed within four large OE zones. These zones are symmetric in both sides of the nasal cavities and are divided based on the expression pattern of some odorant receptors (Ressler et al., 1993; Vassar et al., 1993). Furthermore, OSNs expressing the same receptor converge upon a stereotypical pair of glomeruli (Mombaerts et al., 1996). Nonetheless, the mechanisms by which a set of OSNs, expressing certain odorant receptor, innervates a discrete amount of glomeruli are not well-known; although it seems to be dependent on environmental cues, as well as on intrinsic OSN/odorant receptor factors (reviewed in Mombaerts, 2006; Blanchart and López-Mascaraque, 2011).

Cajal showed that OSNs axons ended into the glomeruli (**Figure 4A**): "This fibril goes through a part of the dermis indivisible and without anastomosing, then gathering with others in tight bundles, goes upwards later, always preserving its individuality, through the ethmoid's lamina cribrosa and assaults, finally, the olfactory bulb, ending arborizing in the thickness of one glomeruli of this central nervous system organ" (Ramón y Cajal, 1892b). Even when the past decades have seen enormous achievements by the implementation of new technologies, Cajal's morphological descriptions provided the basis for subsequent studies. *In situ* hybridization and immunohistochemistry revealed the molecular features of OSNs (**Figures 3C–E**). Later, the use of HRP, retrograde fluorescent markers (Fast Blue, Diamidino Yellow), biotinylated dextrans and lipophilic fluorescent tracers (e.g., DiI, DiO, DiA) confirmed the pathway of OSN axons from the periphery to the OB. At this respect, **Figure 4D** shows the path of retrogradely OSN labeled cells after a DiI injection into the OB. Furthermore, techniques such as *in utero* electroporation of an EGP-expressing plasmid used to study the olfactory pit cell migrations allowed also a further visualization of these nerve bundles (**Figure 4C**). These axons do not ramify until they reach the glomeruli (**Figure 4B**), where they will make contacts with the dendrites of the projection neurons. It is within these specialized structures where the information from the periphery is integrated and then conducted to the rest of the brain. Additionally, the development of the OB is not dependent on the presence of the OE or the synaptic input from the OSNs (López-Mascaraque et al., 1996; López-Mascaraque and De Castro, 2002), although OSN axons are critical during OB

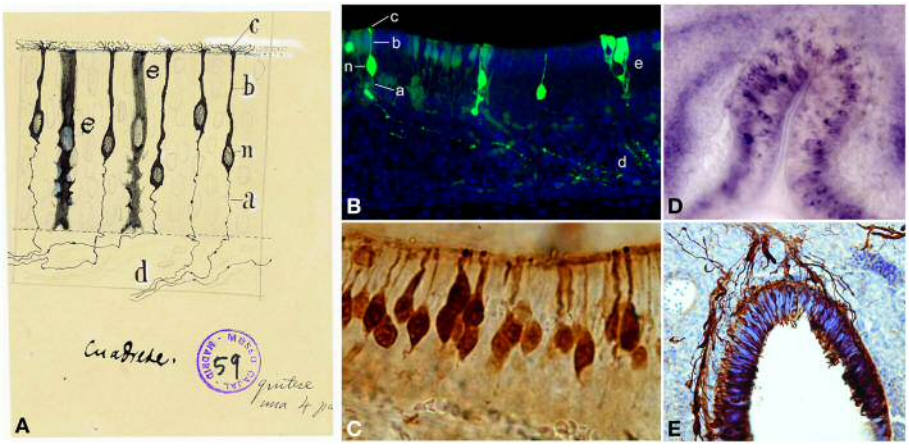

FIGURE 3 | Olfactory sensory neurons (OSNs). (A) Cajal drawing illustrating the cell types and their morphologies in the olfactory epithelium. OSN components: *(n)* nucleus; *(b)* dendrite; *(c)* apical cilia; *(a)* axon. *(d)* OSNs axons bundle. *(e)* supporting or sustentacular cell. The drawing shows the handwriting of Cajal with specific instructions for the required reduction publication factor in the margins (Ramón y Cajal, 1917). Cajal Legacy (Instituto Cajal, CSIC, Madrid, Spain). **(B)** Olfactory epithelium labeled E18 cells after *in utero* electroporation of an EGP-expressing plasmid injected into the olfactory placode at E14 (green). Hoechst (blue). Sagittal mouse section. *a–e, n* correspond to the counterpart structures labeled by Cajal in **(A)**. **(C)** Immunohistochemistry for the Tuj1 marker in mouse olfactory epithelium shows both mature and immature OSNs. **(D)**. *In situ* hybridization for *Nrp-II mRNA* in coronal sections of mouse olfactory epithelium at E14. **(E)** Immunohistochemistry for Tuj1 marker in a mouse olfactory placode coronal section at E11. Panels **(C–E)** were taken by Albert Blanchart.

layering in the final orientation of mitral cells (López-Mascaraque et al., 2005).

SPATIAL CELL ARRANGEMENTS IN THE OLFACTORY BULB

Next station in the olfactory pathway is the olfactory bulb: "the olfactory nerves, which bore into the cranium base through several holes in considerable numbers, and assault the olfactory bulb where they end" (Ramón y Cajal, 1890b). One of the most important of Cajal findings was the demonstration of the entire course of the olfactory fibers. Cajal made the real assumption that these fibers come from the mucosa (OE) and end into the glomerulus at the OB not as a network, as Golgi thought, but by free varicose arborizations.

The OB has a well-defined laminar structure and is formed by different cell populations divided into projection neurons (mitral cells and some tufted cells), interneurons (periglomerular cells, external tufted cells, short axon cells, granule cells, Van Gehuchten cells, and Blanes cells) and glial cells (astrocytes, oligodendrocytes, olfactory ensheathing cells, NG2, and microglia). The innermost part of the OB, the ependymal zone, contains progenitor cells.

Golgi considered the OB formed by three layers (Golgi, 1875) while Schwalbe (1881) proposed six layers. The definitive description of cell types and disposition in six layers was given by Cajal and his disciples (Ramón y Cajal, 1890b; Blanes, 1898). From the outside in, the OB is organized in the following layers: the olfactory nerve layer (ONL), glomerular layer (GL), the external plexiform layer (EPL), the mitral cell layer (MCL), the internal plexiform layer (IPL) and the granule cell layer (GcL) (**Figures 5A,B**). Cajal stated that the ONL was formed by unbranched "*nerve fibrils*" which preserve the same thickness along their trajectory from the OE. Besides, this layer contains an extremely interesting population restricted exclusively to the olfactory system regions, the olfactory ensheathing cells (Valverde and López-Mascaraque, 1991). During development, olfactory ensheathing cells coexist with astrocytes as part of the migratory mass (Doucette, 1990; De Carlos et al., 1996; Blanchart and López-Mascaraque, 2011; Blanchart et al., 2011). Olfactory ensheathing cells maintain certain progenitor characteristics (Schwarting et al., 2007) and are responsible, among other things, for the permissibility within the OB to OSNs axons growth during development and adulthood, thus being a key component of the ability of the OE to continually regenerate.

Next stratum, the GL, is defined by Cajal as the target of the fibrils coming from the OSNs: "Under the peripheral fibrillar

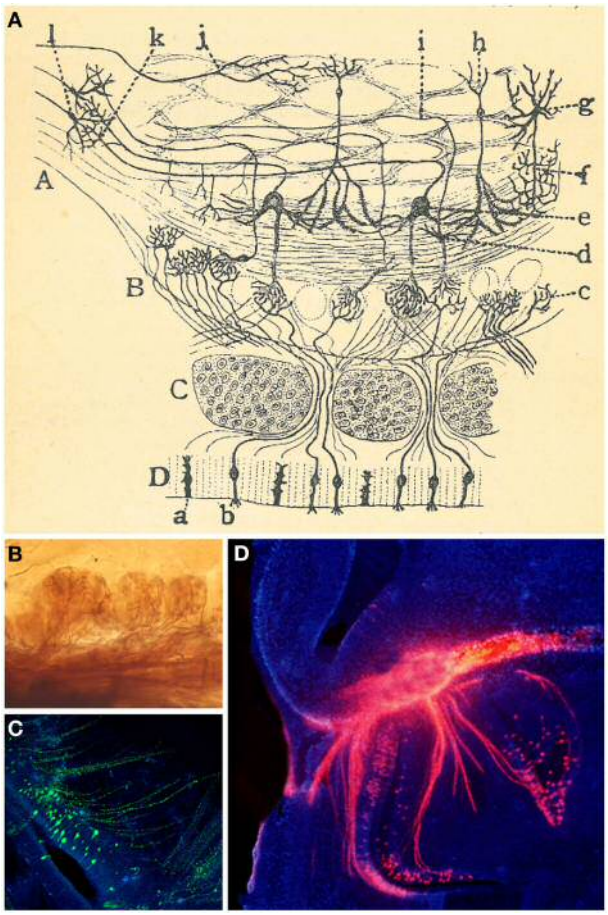

FIGURE 4 | Connection between the olfactory epithelium and the olfactory bulb. (A) Cajal schematic drawing of the mammal's olfactory system. *(A)* Olfactory lobe. *(B)* Olfactory bulb's glomerular layer. *(C)* Cribriform plate. *(D)* Olfactory epithelium or nasal mucosa; *(a)* supporting cells; *(b)* OSNs (Ramón y Cajal, 1892b). **(B)** Axonal arborizations of OSNs axons in several glomeruli stained with the Golgi method. **(C)** Olfactory sensory neurons (green) at E17, labeled after *in utero* electroporation of an EGP-expressing plasmid into the olfactory placode at E11. Nuclei counterstained with Hoechst (blue). Sagittal mouse section. **(D)** Retrogradely labeled OSN cells after a DiI crystal application into the OB (red). Hoechst (blue).

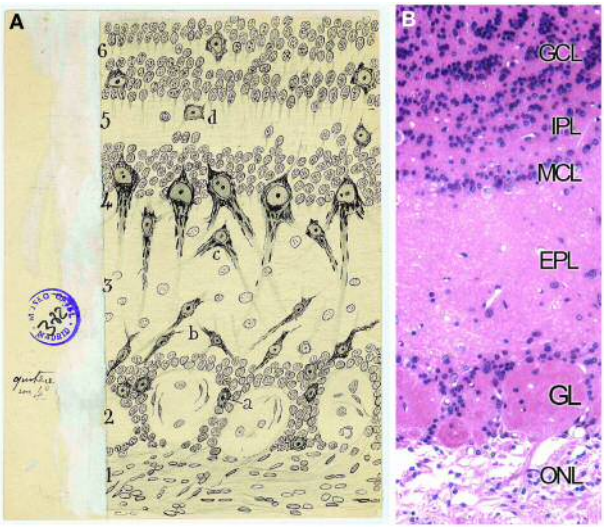

FIGURE 5 | Layers distribution of the Olfactory bulb. (A) Original Cajal drawing of the frontal section of the rabbit olfactory bulb (Ramón y Cajal, 1901). *(1)* Nerve layer (ONL). *(2)* Glomerular layer (GL). *(3)* External plexiform layer (EPL). *(4)* Mitral cells layer (MCL). *(5)* Inner plexiform layer (IPL). *(6)* Grains and white matter layer (GcL). *(a)* Peripheral tufted cells; *(b)* middle; *(c)* internal *(d)* short axon cells. Cajal Legacy (Instituto Cajal, CSIC, Madrid, Spain). **(B)** Olfactory bulb mouse coronal section of hematoxylin and eosin nuclei staining showing the different layers described by Cajal in **(A)**.

layer lays an irregular area of two or more rows of disordered ovoid masses called olfactory glomeruli. [...] They are composed of the terminal branches of olfactory fibers, the thick plume of dendrites arriving from deeper zones, certain tiny nerve corpuscles and, finally, some neuroglial elements" (Ramón y Cajal, 1890b). More than a century ago Cajal stated the exact input of the OSNs into the glomeruli, although Golgi reported the intraglomerular branching of the olfactory fibers (Golgi, 1875). In 1890 Cajal described the composition of each glomerulus (**Figure 6A**): the terminal arborization of the olfactory fibers, the thick apical dendrites from deeper regions, considerable tiny nervous corpuscles and several neuroglial elements (Ramón y Cajal, 1890b). Those tiny nervous corpuscles correspond to tufted or fusiform nerve cells, that collaborate in the formation of what he called intraglomerular plexus (**Figures 6B,C**), and external grains or short axon nerve cells, which branch within glomeruli, cells classified by Golgi as glial cells. Nowadays, a further characterization can be achieved either by the specific expression of different markers for each cell type presents or by the cell's physiological properties. Moreover, while Cajal studied the development of this system both in younger and/or phylogenetically less complex animals, nowadays we describe the cellular contributions, e.g., to the OB, after *in utero* viral infections (Blanchart et al., 2011) or by electroporation of different plasmids. In fact, a clonal analysis of glial cell populations can be performed with the Star Track approach (García-Marqués and López-Mascaraque, 2013). Moreover, a modification of this technique that uses an ubiquitous promoter (*UbC-Star Track*, (Figueres-Oñate and López-Mascaraque, 2013) allows a more comprehensive lineage study of all the cell populations (**Figure 6D**).

Since the apical dendrite of mitral cells and 2–3 dendrites of tufted cells penetrate into the territory of each glomerulus, Cajal noted that "the propagation of the nerve impulse is not individual, from a single neuron to another, but collective, from a group of nerve fibers to a group of ganglion corpuscles" (Ramón y Cajal, 1901). Nowadays, the characterization of the functional glomerular map has led to a more thorough understanding of how the positional domain information translates to different odor responses such as innate or learned responses (reviewed in Mori and Sakano, 2011).

Below the glomeruli is located the EPL, similar to the molecular area of the cerebellum or the retina. This layer includes lateral dendrites of the mitral and tufted cells and apical dendritic processes of granular cells (**Figure 7A**). Cajal named tufted cells as that because of their robust peripheral dendrite branching into the olfactory glomeruli. They are divided into external, middle and deep, dependent on the location of their soma. Cajal also described the presence of axonal collaterals from mitral cells in this molecular layer.

The next stratum is the MCL, composed by mitral cells. Mitral cell bodies, as described by Cajal, form a regular single row and owe their name to their appearance (**Figure 7A**). They are the principal output cells of the OB and, in most mammals, are characterized by a single apical dendrite through the EPL that branches into an apical tuft within the glomerulus (**Figure 7B**). Mitral cells are one type of the projection neurons (**Figure 7C**), whose entire development terminates at postnatal stages (Blanchart et al., 2006). Within the glomeruli, mitral cells interact and receive inputs through synaptic contacts with periglomerular and granule cells. Mitral cells are the bridge connecting directly the periphery with higher integrative structures (Ramón y Cajal, 1904; reviewed in Gire et al., 2013). Their inputs come from OSNs and external tufted cells and send their outputs to various cortical structures (Hayar et al., 2004; Gire et al., 2012).

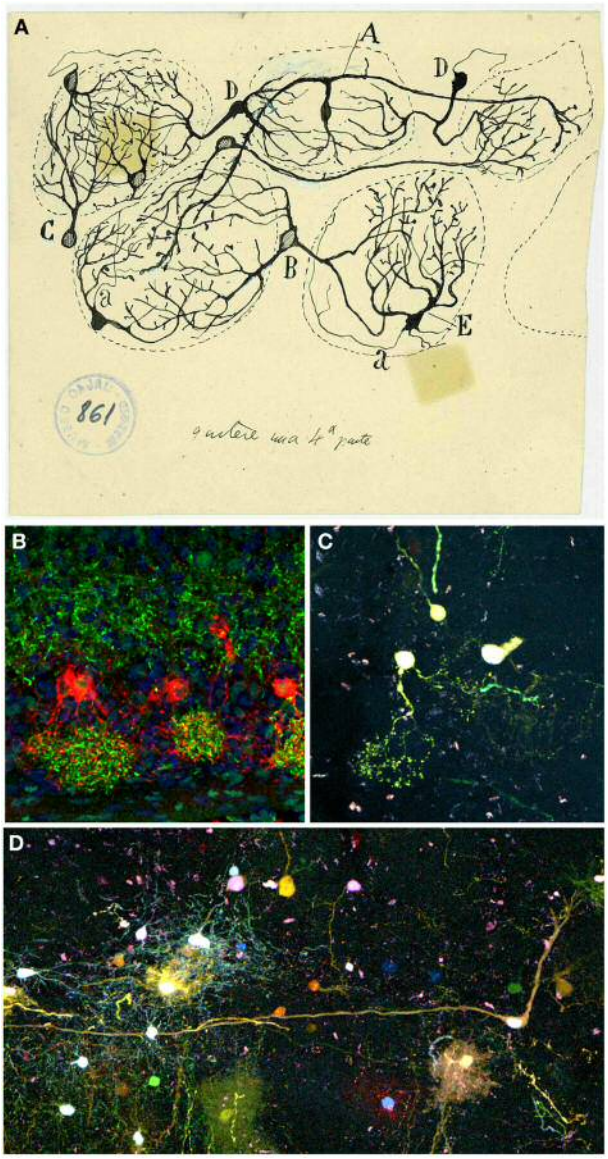

FIGURE 6 | Periglomerular cells. (A) Original drawing by Cajal's disciple Blanes, showing periglomerular cells of a cat glomerular layer (Blanes, 1898). Cell branching into three glomeruli *(A)*. Biglomerular cells *(B–D)*. Monoglomerular cells *(C–E)*. *(a)* Axon. Cajal Legacy (Instituto Cajal, CSIC, Madrid, Spain). **(B)** Periglomerular cells immunolabeled for tyrosine hydroxylase (TH, red) protein and Dab1 protein (green) on mouse olfactory bulb sections at P3. Panel was taken by Eduardo Martin-López. **(C,D)** Adult periglomerular cells contributing to one **(C)** or more glomeruli **(D)** labeled after E13 *in utero* electroporation of different plasmids with the *UbC-Star Track method* (Figueres-Oñate and López-Mascaraque, 2013).

Cajal also described the centrifugal feedback that mitral cells receive from cortical structures (Ramón y Cajal, 1901), and recent studies provided a functional explanation to these projections (for review see Gire et al., 2013).

Below the MCL layer, the IPL is populated by most axon collaterals of tufted cells (**Figure 8A**), while the GcL contains many interneurons like the granule cells and the short-axon cells. The granule cells are small spiny ovoid cells with an apical process extending radially into the EPL and short secondary dendrites confined to the GcL (**Figures 8B–E**). Golgi reported that these cells showed no evidence of axons Golgi (1875) and Blanes (1898) stated that they were not glia as Kölliker claimed (Kölliker, 1891). Additionally, Cajal described different types of short-axon cells within the GcL: Golgi cells, Cajal cells, and Blanes cells. Blanes cells are interneurons with a significant electrophysiological role, as they provide inhibitory inputs onto granule cells and appear to be excited by mitral cells, which could be a novel mechanism for encoding short-term olfactory information (Pressler and Strowbridge, 2006). The different subpopulations of these interneurons were classified by Cajal on morphological and

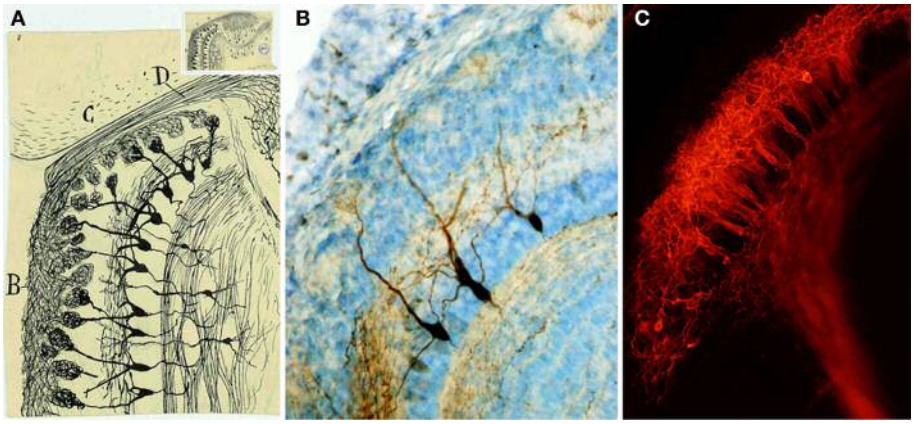

FIGURE 7 | Mitral cells. (A) Magnified detail of the original Cajal figure (upper inset). Horizontal mouse olfactory bulb section at 20-days-old (Ramón y Cajal, 1901). Olfactory bulb *(B)*, frontal cortex *(C)*, Olfactory nerve *(D)*. Cajal Legacy (Instituto Cajal, CSIC, Madrid, Spain). **(B)** Mitral cells labeled after BDA injection into the lateral olfactory tract at P5 (Blanchart et al., 2006). **(C)** Retrograde labeling of mitral cells after DiI injection into the lateral olfactory tract at E17 (Blanchart et al., 2006).

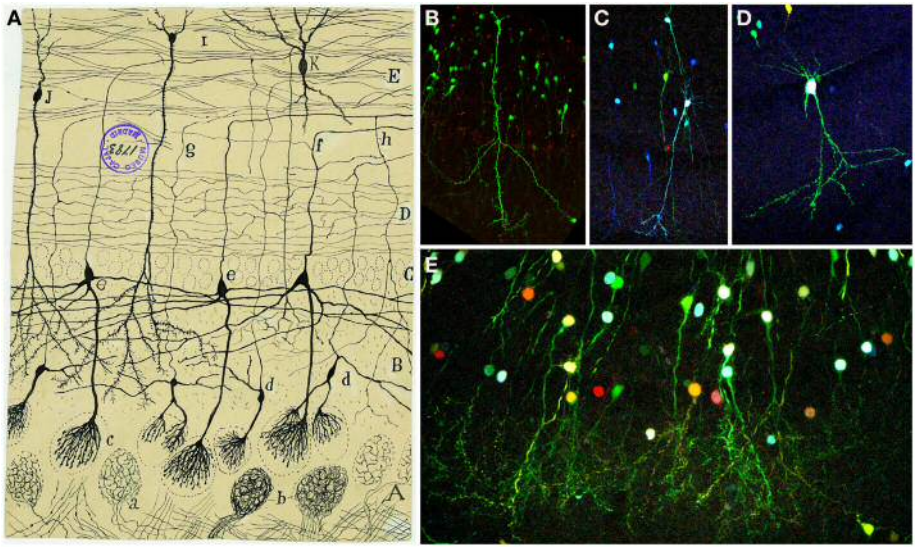

FIGURE 8 | Granular cells. (A) Original Cajal drawing of an olfactory bulb section from a few days cat brain (Ramón y Cajal, 1901). *G*lomerular layer *(A)*, outer plexiform layer *(B)*, mitral cell layer *(C)*, inner plexiform layer *(D)*, grains layer and white matter *(E)*. *(a)* Terminal arborization of an olfactory fiber; *(b)* glomerulus with several endings; *(c)* mitral plume; *(d)* tufted cells. Cajal Legacy (Instituto Cajal, CSIC, Madrid, Spain). **(B–E)** Granule cells in the olfactory bulb of young adult mice (P20) labeled after E12-14 *in utero* electroporation of different plasmids with the *UbC-Star Track* method. (Figueres-Oñate and López-Mascaraque, 2013). **(B,C)** Granule cells with similar to (i,j) in Cajal's drawing. **(D)** Tufted cell. **(E)** Granular cells branching their processes in the glomeruli.

spatial basis. Since his work, the diversity of GcL cells has also been based on molecular and physiological features (Price and Powell, 1970; Schneider and Macrides, 1978; López-Mascaraque et al., 1986; Crespo et al., 2001; Kosaka and Kosaka, 2005).

In summary, Cajal plotted the dynamic scheme of the OB, pointing out the need to give a special significance to the protoplasmic processes of mitral and tufted cells, which penetrate into the glomerulus and are in intimate contact with the olfactory fibrils. The olfactory fibers never depart from the glomerular territory and neither axons of central origin enter in the glomeruli, which is against Golgi's assertion. Cajal was also a pioneer in the description of different axonal projections of tufted and mitral cells to the OC (Ramón y Cajal, 1904).Indeed anatomical and physiological differences suggests that mitral and tufted cells may serve different functions and possibly contribute to different aspects of the olfactory code including perception of odorants (Nagayama et al., 2004; Shepherd et al., 2004). Although mitral and tufted cells innervate different cortical targets, the circuitry and projection sites of the tufted cells are not yet well-understood and are still one of the main focus of research in the field (for review see Mori and Sakano, 2011). Besides, the two main inhibitory interneuron types described by Cajal in the OB have a significant role in the olfactory processing: periglomerular cells mediate lateral inhibition at the level of the glomeruli (Aungst et al., 2003), while granule cells mediate dendrodendritic inhibition onto the lateral collaterals of mitral cells (Schoppa et al., 1998). These synapses formed between lateral dendrites of mitral cells and granule cells was suggested to be inconsistent with Cajal's Law of Dynamic Polarization (for extensive reviews see Shepherd et al., 2007; Sassoè-Pognetto, 2011).

NEUROGLIA IN THE OLFACTORY BULB

Cajal and his colleagues played an important role in describing glial cells. They initiated an active discussion regarding where to encompass those, at that time, unknown cells into the functional map of the brain. In different species, Cajal identified these cells, closely related to the cell bodies of neurons, as neuroglia. Then, he could not draw any definitive conclusion about the physiological role of neuroglial cells, but he presupposed an insulating role: protection to prevent contact between nerve fibers (Ramón y Cajal, 1896). This insulating theory of the neuroglia was originally developed by Cajal's brother, Pedro, and it was always supported by Cajal: "By rational conjecture, we have defended in several manuscripts the thesis, initially suggested by my brother, that both the epithelial and neuroglial cells have a role insulating the fibers and nervous cells, preventing contacts between close but dynamically independent elements" (Ramón y Cajal, 1897).

Focusing on the OB, Golgi briefly described the glia in this structure, but one the most important descriptions was done by Cajal's disciple, De Castro (1920). De Castro made a careful comparison between the neuroglia of human OB to other higher mammals by using the Cajal-improved sublimated-gold technique and the reduced silver impregnation method (**Figures 9A,D**). With these staining methods, Fernando de Castro showed the neuroglial distribution in the OB as well as the abundance and importance of the vascular glial end-feet in different brain areas. He also suggested that neuroglial cells may release neuroactive substances and directly participate in neural transmission (De Castro, 1951). In addition, he noticed how astrocytes were closely related to blood vessels through their end-feet, raising questions about their specific function: "What role does the neuroglia play in the vascular foot? Would it be entrusted with any function or would it be just a mere support organ? Difficult in every respect is the solution to the problem" (De Castro, 1920). Recently, the processes of protoplasmic astrocytes arranged around blood vessels (**Figures 9B,C**) were labeled after *in utero* electroporation of the Star Track plasmid mix (García-Marqués and López-Mascaraque, 2013) into the lateral ventricles. After embryonic electroporation of the OB progenitors with *UbC-Star Track* method (Figueres-Oñate and López-Mascaraque, 2013), clones of glial cells surrounding several glomeruli are located in adult olfactory bulbs (**Figure 9E**).

While the glomerular structure and neuronal connectivity has been extensively described, both the role and connectivity of neuroglia in the OB have yet to be characterized. Within the OB, astrocytes do not just play an insulating or supporting role, but they are also an active part of the sensory integration in the olfactory glomeruli, interacting with their neuronal counterparts, in a glomerulus-specific manner (Roux et al., 2011). Although the olfactory astroglia was defined as a syncytium, the advent of molecular and genetic techniques changed the experimental approaches to determine the progeny of single cells, shedding light to a further network specialization (Houades et al., 2008). A promising approach is the *in vivo* clonal analysis, Star Track, based on the combinatorial expression of different gene reporters (García-Marqués and López-Mascaraque, 2013; García-Marqués et al., 2014) that makes possible to trace the progeny of targeted GFAP progenitors (**Figures 9D,E**). Besides the classification based on morphology and location of glial cells, we show the presence homogeneous glial clones which indicates the existence of separate progenitors for each glial population (García-Marqués and López-Mascaraque, 2013).

Regardless from the glial elements mentioned above, Cajal also described the presence of myelin fibers within the OB using the Weigert-Pal staining technique (**Figure 10A**). "The medullated fibers are relatively abundant around the glomeruli and even within them. The periglomerular fibers are generally very thin and correspond with cylinder-axis of the inferior tufted cells [...]. The intraglomerular fibers have a more difficult interpretation. [...] In general, it can be assumed that said fibers [...] end within the same glomerular area. [...] As is well known, the olfactory fibers and the grains expansions lack myelin" (Ramón y Cajal, 1890b). Cajal and his disciples also observed what they called "*third element*" or "*adendritic cells*" (De Castro, 1920), known today as microglia. The use of molecular markers, selectively expressed by these cells in the OB, revealed the distinct glia subtypes (**Figure 10B**).

OLFACTORY CORTEX

The olfactory cortex is a phylogenetically old cortical structure. It is formed by all brain regions receiving direct axonal input from mitral and some tufted cells (Allison, 1954; Price, 1973), making the olfactory system the only sensory modality without thalamic relays. Among several areas, the OC includes the

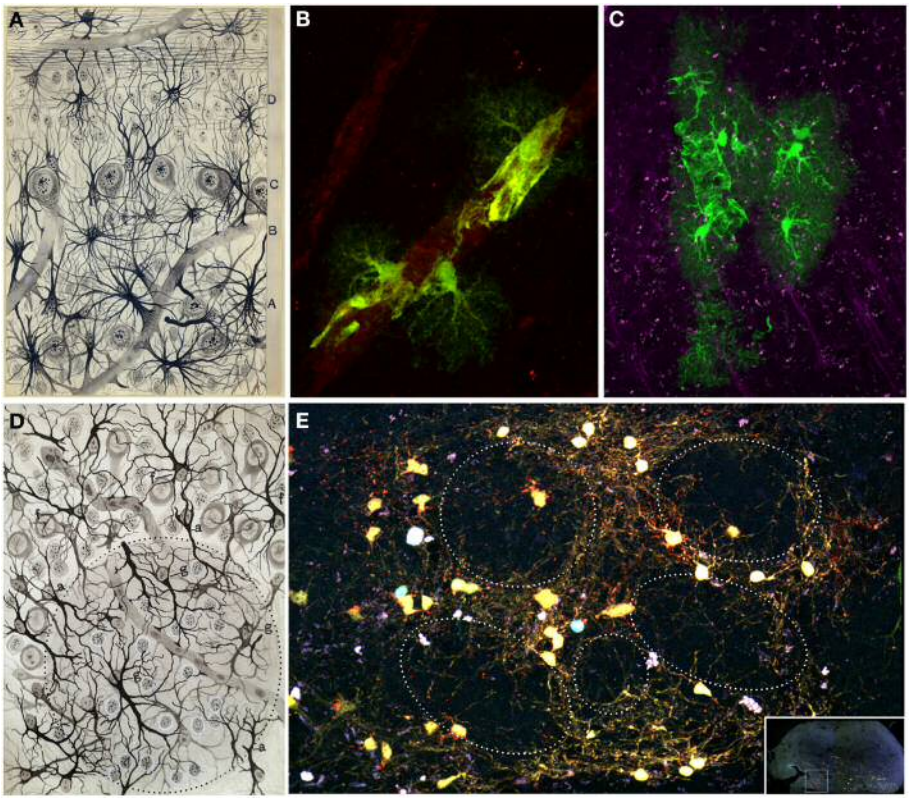

FIGURE 9 | Glial cells. (A) Original Fernando de Castro drawing of human olfactory bulb stained with Cajal's gold chloride sublimate method. Superficial substratum of the molecular layer with numerous cephalopodic cells *(A)*, deep substratum *(B)*, mitral cell layer *(C)*, grains layer *(D)* (De Castro, 1920). **(B,C)** Processes of protoplasmic astrocytes arranged around a blood vessel labeled after *in utero* electroporation of the *Star Track* plasmid mix (García-Marqués and López-Mascaraque, 2013) into the lateral ventricles. These perivascular end feet are represented in the olfactory bulb **(A)** by Fernando de Castro. Panel **(B)** modified from Martín-López et al. (2013) and panel **(C)** were taken by Eduardo Martin-López. **(D)** Fernando de Castro drawing illustrating the glomerular layer of the adult dog stained by the Cajal's gold chloride sublimate method. *(g)* Intraglomerular fibrous elements; *(a)* radioglomerular corpuscles; *(f)* fibrous cells located superficial to the molecular zone, displaying most of their extensions oriented toward deepest layers. Note numerous nuclei located in this region, corresponding to Cajal's adendritic glia (De Castro, 1920). **(E)** Clone of glial cells surrounding several glomeruli in an adult (7 months) olfactory bulb labeled after E13 *in utero* electroporation of different plasmids with the *UbC-Star Track* method (Figueres-Oñate and López-Mascaraque, 2013).

anterior olfactory nucleus, the entorhinal cortex, the piriform cortex (primary OC), *tenia tecta*, cortical amygdaloid nucleus and the olfactory tubercle. Axons from the OB projecting to the OC constitute the lateral olfactory tract (LOT), located on the outer and lower side of the olfactory pedicle named by Calleja and Cajal as the "*external root*" (Calleja, 1893; Ramón y Cajal, 1901).

Despite its heterogeneity throughout the rostro-caudal axis, the OC displays a three-layer organization: layer 1 is subdivided in layers 1a and 1b; layer 2 contains semilunar cells and a large number of pyramidal-like cells and layer 3 is formed by different pyramidal cells (Valverde, 1965). Cajal and his disciple Calleja (1893) distinguished five layers in the OC: fibrillar layer or outer root layer, molecular or plexiform layer, layer of small and large pyramids, layer of polymorphs corpuscles and white matter (**Figure 11A**).

The fibrillar layer (layer 1a) is formed by LOT fibers while the molecular or plexiform layer (layer 1b) receives associational fibers from deeper cells and includes collaterals of the olfactory fibers, tufts of pyramidal cells and dendrites of deeper horizontal cells. The layer of small and large pyramids (layer 2) appears like a "flexible and undulating belt quite well demarcated from the bordering areas" (Ramón y Cajal, 1901). It contains cells with different morphologies, including semilunar cells (superficial part) and a large number of pyramidal-like cells (in deeper regions). While the semilunar cells usually lack descendent axonal projections, deeper cells display axonal processes penetrating into the white matter. As Cajal postulated, "the configuration of the neurons from said layer is highly variable, being able to discover, even in the deepest planes, multiple elements whose shape is triangular, stellated or fusiform, though they never lack a radial dendrite directed to the second layer" (Ramón y Cajal, 1901). At the deepest level, the polymorph cells layer (layer 3) includes the most voluminous cells with descending axonal collaterals that penetrate into the white matter. Recently, the development of novel tools for the clonal analysis of the brain neural lineages, the *UbC-Star Track* method (Figueres-Oñate and López-Mascaraque, 2013), evidenced the large variety of morphologies within the OC (**Figures 11B–F**). Finally, the white matter is formed by the

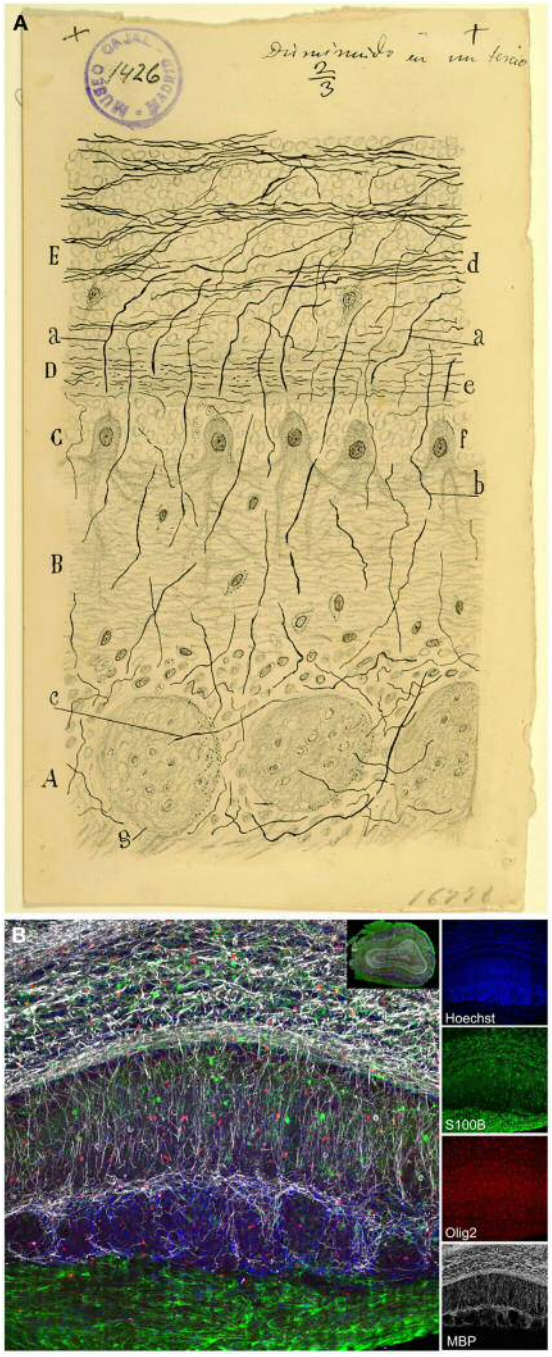

FIGURE 10 | Myelin. (A) Original drawing from Cajal of an olfactory bulb section of a month-old rat. Weigert-Pal method (Ramón y Cajal, 1890b). Layer of the glomeruli *(A)*, lower molecular layer *(B)*, mitral layer *(C)*, higher molecular layer *(D)*, coating the grains *(E)*. *(a)* myelin fiber corresponding to the cylinder-axis of mitral cells; *(b)* cylinder-axis of mitral cells; *(c)* core fiber from within the glomeruli; *(d)* bundles of fibers in the layer of grains; *(e)* thin horizontal strands from the higher molecular area; *(f) mitral* cells; *(g)* glomerulus; Cajal Legacy (Instituto Cajal, CSIC, Madrid, Spain). **(B)** Immunohistochemistry with different glial markers: Olig2 (oligodendrocyte progenitors, red), S100β (astrocytes, green), and myelin binding protein (MBP, gray). Nuclei labeled with Hoechst (blue). Inset shows overall view of the olfactory bulb (coronal section) labeled with the markers explained above.

concurrence of axonal projections from overlying layers, forming a labyrinthic and irregular plexus, that complicates the definition of their routes: "In summary, the fibers or second order conductors coming from the bulbar and frontal cortex, underlying the external root, follow two routes: ones, the majority, go backwards deeply to reach the corpus striatum incorporating to the corona radiata; others travel toward the inside and backwards and enter the anterior commissure. Being unable to sufficiently follow those conductors, we ignore if any of them reach Ammon's horn" (Ramón y Cajal, 1901).

This anatomical organization may underlie the fact that mitral and tufted cells project to the OC through different pathways and toward different targets suggesting the possibility that they carry different odor information (reviewed in Mori and Sakano, 2011). The diverse cortical projections of a single mitral cell, the broad distribution of mitral cells axons and the overlapping of their information at their target neurons provide the basis for a diversification and combinatorial integration of the olfactory information processing (Ghosh et al., 2011). Recent work using anatomical and physiological techniques demonstrated that individual neurons in the piriform cortex receive convergent input from mitral/tufted cells connected to multiple glomeruli located all over the OB (Apicella et al., 2010; Davison and Ehlers, 2011; Miyamichi et al., 2011). The precise scheme of the olfactory pathway displayed by Cajal (**Figure 1A**) opened the door to the anatomical basis of olfactory processing (Gire et al., 2013). OSNs expressing the same odorant receptor converge in one glomeruli of each hemisphere (Mombaerts et al., 1996; Mombaerts, 2006). This spatial pattern, termed *odotopic map* is just applied for the first olfactory station (OSN to OB). However, although much is known about how odors are represented at the level of OB, the nature of odor representations in this cortex and the integration of the odor activity of output OB neurons into higher brain regions, essential for the cortical odor representations, are still debated (for review see Bekkers and Suzuki, 2013).

OLFACTORY SYSTEM PERSPECTIVES

> "The functional specialization of the brain imposes to the neurons two main gaps: inability to proliferate and irreversibility of the intra-protoplasmatic differentiation. It is because this reason that, once development is over, the growth and regeneration of axons and dendrites are irrevocably dried up. In the adult brains the nervous pathways are fixed, finished, immutable. Everything may die nothing is regenerated itself. It belongs to the science of the future to change, if possible, this cruel decree" (Ramón y Cajal, 1913).

Unlike other brain structures, the OB is not a simple relay nucleus, but a center for information processing and storage. Cajal missed one of the most important characteristics of the OB, the cell turnover: "Nature has given us a limited amount of brain cells. Here is a capital, large or small, that nobody can increase as the neuron is unable to multiply" (Ramón y Cajal, 1931). However, adult neurogenesis is among the most important brain discoveries opening new debate about the function and integration of these cells into the system. The adult mice brain retains a proliferative area, the subventricular zone (SVZ), which maintains proliferative functions through live. Astrocyte-like cells (B cells)

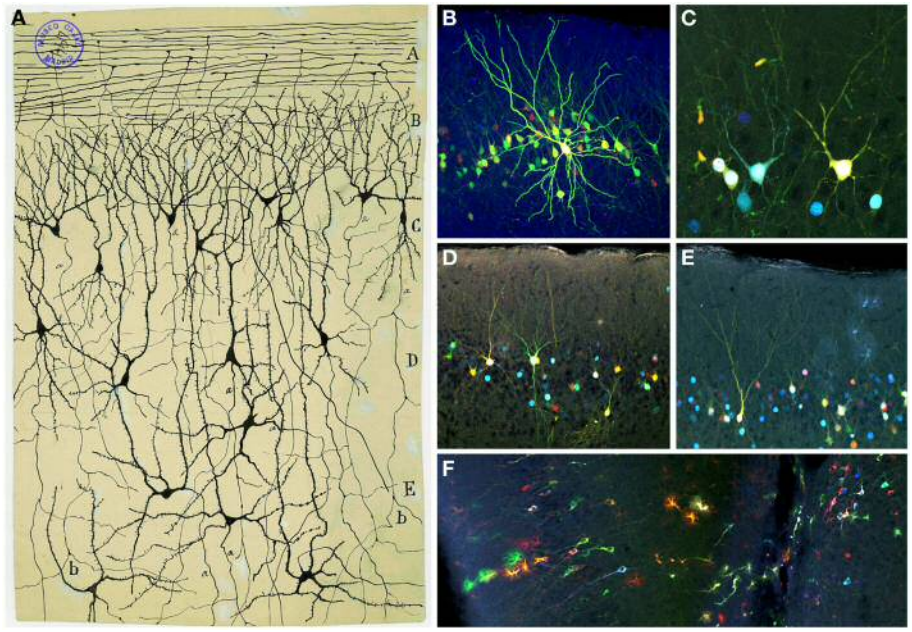

FIGURE 11 | Olfactory cortex. (A) Original Cajal drawing showing the olfactory cortex layers (Ramón y Cajal, 1901). *O*lfactory fibers layer *(A)*; plexiform layer *(B)*; layer of polymorphic superficial cells *(C)*; layer of the pyramids *(D);* deep polymorphous cells *(D). (b)* Bifurcation of axons. Cajal Legacy (Instituto Cajal, CSIC, Madrid, Spain). **(B–F)** Different cell morphologies in the adult mouse olfactory cortex labeled after E12 *in utero* electroporation of different plasmids with the *UbC-Star Track method* (Figueres-Oñate and López-Mascaraque, 2013). Note the presence of cells with either arachnoid morphologies, similar to those in **(B)**, and crescent-shaped cells similar to **(C)**. **(D,E)**. View of different morphological neuronal types. **(F)** Several neurons along with different glial clones.

divide to produce neuroblasts via intermediate progenitors. These neuroblasts migrate along the rostral migratory stream to the OB, where they differentiate and migrate to their final positions in the granular or periglomerular layers (Kriegstein and Alvarez-Buylla, 2009). Strikingly, a spatial patterning within the SVZ indicates that interneuron subtypes depend on their generation area (Merkle et al., 2007). Moreover, the temporal differences in the production of interneurons are related to their subtype specification and functional integration in the system (Batista-Brito et al., 2008).

To conclude, Cajal opened up an essential work to our current understanding of this system. These classical studies provided the basis for anatomical, physiological, and molecular studies. Now, more than a century later, the use of state-of-the-art approaches such as cell type specific optogenetic manipulations, *in utero* electroporation, *in vivo* genetic fate mapping and cell ablation, electrophysiological and live-cell imaging techniques, patch-clamp recordings and two-photon microscopy *in vivo* and in brain slice preparations can help understanding how odor information is represented and processed by the olfactory system.

ACKNOWLEDGMENTS

We would like to thank Drs. Albert Blanchart and Eduardo Martin-Lopez for their contribution with the images. We especially thank Dr. Agenor Limon for his careful review and editing of the manuscript. Cajal drawings and micrographs were provided by the Legado Cajal (Instituto Cajal, CSIC, Madrid, Spain) thanks to Dr. Juan A. de Carlos. Fernando de Castro drawings belong to the Fernando de Castro Archives and were provided by his grandson Fernando de Castro. This work was supported by research Grant BFU2010-15564 from the Spanish Ministry of Economy and Competitiveness.

REFERENCES

Allison, A. C. (1954). The secondary olfactory areas in the human brain. *J. Anat.* 88, 481–488.

Altman, J. (1969). Autoradiographic and histological studies of postnatal neurogenesis. IV. Cell proliferation and migration in the anterior forebrain, with special reference to persisting neurogenesis in the olfactory bulb. *J. Comp. Neurol.* 137, 433–457. doi: 10.1002/cne.901370404

Apicella, A., Yuan, Q., Scanziani, M., and Isaacson, J. S. (2010). Pyramidal cells in piriform cortex receive convergent input from distinct olfactory bulb glomeruli. *J. Neurosci.* 30, 14255–14260. doi: 10.1523/JNEUROSCI.2747-10.2010

Aungst, J. L., Heyward, P. M., Puche, A. C., Karnup, S. V, Hayar, A., Szabo, G., et al. (2003). Centre-surround inhibition among olfactory bulb glomeruli. *Nature* 426, 623–629. doi: 10.1038/nature02185

Batista-Brito, R., Close, J., Machold, R., and Fishell, G. (2008). The distinct temporal origins of olfactory bulb interneuron subtypes. *J. Neurosci.* 28, 3966–3975. doi: 10.1523/JNEUROSCI.5625-07.2008

Bekkers, J. M., and Suzuki, N. (2013). Neurons and circuits for odor processing in the piriform cortex. *Trends Neurosci.* 36, 429–438. doi: 10.1016/j.tins.2013.04.005

Blanchart, A., Carlos, J. A. D. E., and Lo, L. (2006). Time frame of mitral cell development. *J. Comp. Neurol.* 543, 529–543. doi: 10.1002/cne

Blanchart, A., and López-Mascaraque, L. (2011). From the periphery to the brain: wiring the olfactory system. *Transl. Neurosci.* 2, 293–309. doi: 10.2478/s13380-011-0038-x

Blanchart, A., Martín-López, E., De Carlos, J. A., and López-Mascaraque, L. (2011). Peripheral contributions to olfactory bulb cell populations (migrations towards the olfactory bulb). *Glia* 59, 278–292. doi: 10.1002/glia.21100

Blanes, T. (1898). Sobre algunos puntos dudosos de la estructura del bulbo olfatorio. *Rev. Trimest. Microgr.* 3, 99–127.

Buck, L. B., and Axel, R. (1991). A novel multigene family may encode odorant receptors: a molecular basis for odor recognition. *Cell* 65, 175–187. doi: 10.1016/0092-8674(91)90418-X

Calleja, C. (1893). *La Región Olfatoria del Cerebro*. Madrid: Moya.

Crespo, C., Blasco-Ibáñez, J. M., Marqués-Marí, A. I., and Martínez-Guijarro, F. J. (2001). Parvalbumin-containing interneurons do not innervate granule cells in the olfactory bulb. *Neuroreport* 12, 2553–2556. doi: 10.1097/00001756-200108080-00052

Davison, I. G., and Ehlers, M. D. (2011). Neural circuit mechanisms for pattern detection and feature combination in olfactory cortex. *Neuron* 70, 82–94. doi: 10.1016/j.neuron.2011.02.047

De Carlos, J. A., López-Mascaraque, L., and Valverde, F. (1996). Early olfactory fiber projections and cell migration into the rat telencephalon. *Int. J. Dev. Neurosci.* 14, 853–866. doi: 10.1016/S0736-5748(96)00055-X

De Castro, F. (1920). Estudios sobre la neuroglia de la corteza cerebral del hombre y de los animales. *Trab. Lab. Invest. Biol.* 18, 1–35.

De Castro, F. (1951). Anatomical aspects of the ganglionic synaptic transmission in mammalians. *Arch. Int. Physiol.* 59, 479–525.

Doucette, R. (1990). Glial influences on axonal growth in the primary olfactory system. *Glia* 3, 433–449. doi: 10.1002/glia.440030602

Figueres-Oñate, M., and López-Mascaraque, L. (2013). "Clonal cell analysis in the olfactory bulb," in *Poster Session Presented at: 43th Annual Meeting of the Society for Neuroscience*. Available online at: http://www.abstractsonline.com/Plan/ViewAbstract.aspx?sKey=ca564d3b-67c2-414d-8b86-f5cd0137c118&cKey=fe484196-5b7d-46b3-b110-d8f00ffaabfe&mKey={8D2A5BEC-4825-4CD6-9439-B42BB151D1CF}

García-Marqués, J., and López-Mascaraque, L. (2013). Clonal identity determines astrocyte cortical heterogeneity. *Cereb. Cortex* 23, 1463–1472. doi: 10.1093/cercor/bhs134

García-Marqués, J., Nunez-Llaves, R., and Lopez-Mascaraque, L. (2014). NG2-glia from pallial progenitors produce the largest clonal clusters of the brain: time frame of clonal generation in cortex and olfactory bulb. *J. Neurosci.* 34, 2305–2313. doi: 10.1523/JNEUROSCI.3060-13.2014

Ghosh, S., Larson, S. D., Hefzi, H., Marnoy, Z., Cutforth, T., Dokka, K., et al. (2011). Sensory maps in the olfactory cortex defined by long-range viral tracing of single neurons. *Nature* 472, 217–220. doi: 10.1038/nature09945

Gire, D. H., Franks, K. M., Zak, J. D., Tanaka, K. F., Whitesell, J. D., Mulligan, A. A., et al. (2012). Mitral cells in the olfactory bulb are mainly excited through a multistep signaling path. *J. Neurosci.* 32, 2964–2975. doi: 10.1523/JNEUROSCI.5580-11.2012

Gire, D. H., Restrepo, D., Sejnowski, T. J., Greer, C., De Carlos, J. A., and López-Mascaraque, L. (2013). Temporal processing in the olfactory system: can we see a smell? *Neuron* 78, 416–432. doi: 10.1016/j.neuron.2013.04.033

Golgi, C. (1873). Sulla struttura della sostanza grigia del cervelo. *Gazz. Med. Ital. Lomb.* 33, 244–246.

Golgi, C. (1875). Sulla fina struttura dei bulbi olfactorii. *Riv. Sper. Freniatr. Med. Leg.* 1, 66–78.

Graziadei, P. P. C. (1973). Cell dynamics in the olfactory mucosa. *Tissue Cell* 5, 113–131. doi: 10.1016/S0040-8166(73)80010-2

Hayar, A., Karnup, S., Ennis, M., and Shipley, M. T. (2004). External tufted cells: a major excitatory element that coordinates glomerular activity. *J. Neurosci.* 24, 6676–6685. doi: 10.1523/JNEUROSCI.1367-04.2004

Houades, V., Koulakoff, A., Ezan, P., Seif, I., and Giaume, C. (2008). Gap junction-mediated astrocytic networks in the mouse barrel cortex. *J. Neurosci.* 28, 5207–5217. doi: 10.1523/JNEUROSCI.5100-07.2008

Kölliker, A. (1891). Ueber den feineren Bau des Bulbus olfactorius. Aus den Sitzungsber der Würzb. *Phys. Med.* 1, 1–5.

Kosaka, K., and Kosaka, T. (2005). Synaptic organization of the glomerulus in the main olfactory bulb: compartments of the glomerulus and heterogeneity of the periglomerular cells. *Anat. Sci. Int.* 80, 80–90. doi: 10.1111/j.1447-073x.2005.00092.x

Kriegstein, A., and Alvarez-Buylla, A. (2009). The glial nature of embryonic and adult neural stem cells. *Annu. Rev. Neurosci.* 32, 149–184. doi: 10.1146/annurev.neuro.051508.135600

Lois, C., and Alvarez-Buylla, A. (1994). Long-distance neuronal migration in the adult mammalian brain. *Science* 264, 1145–1148. doi: 10.1126/science.8178174

López-Mascaraque, L., De Carlos, J. A., and Valverde, F. (1986). Structure of the olfactory bulb of the hedgehog (*Erinaceus europaeus*): description of cell types in the granular layer. *J. Comp. Neurol.* 253, 135–152. doi: 10.1002/cne.902530202

López-Mascaraque, L., De Carlos, J. A., and Valverde, F. (1996). Early onset of the rat olfactory bulb projections. *Neuroscience* 70, 255–266. doi: 10.1016/0306-4522(95)00360-U

López-Mascaraque, L., and De Castro, F. (2002). The olfactory bulb as an independent developmental domain. *Cell Death Differ.* 9, 1279–1286. doi: 10.1038/sj.cdd.4401076

López-Mascaraque, L., García, C., Blanchart, A., and De Carlos, J. A. (2005). Olfactory epithelium influences the orientation of mitral cell dendrites during development. *Dev. Dyn.* 232, 325–335. doi: 10.1002/dvdy.20239

Martín-López, E., Blanchart, A., De Carlos, J. A., and López-Mascaraque, L. (2011). Dab1 (Disable homolog-1) reelin adaptor protein is overexpressed in the olfactory bulb at early postnatal stages. *PLoS ONE* 6:e26673. doi: 10.1371/journal.pone.0026673

Martín-López, E., García-Marques, J., Núñez-Llaves, R., and López-Mascaraque, L. (2013). Clonal astrocytic response to cortical injury. *PLoS ONE* 8:e74039. doi: 10.1371/journal.pone.0074039

Merkle, F. T., Mirzadeh, Z., and Alvarez-Buylla, A. (2007). Mosaic organization of neural stem cells in the adult brain. *Science* 317, 381–384. doi: 10.1126/science.1144914

Miyamichi, K., Amat, F., Moussavi, F., Wang, C., Wickersham, I., Wall, N. R., et al. (2011). Cortical representations of olfactory input by trans-synaptic tracing. *Nature* 472, 191–196. doi: 10.1038/nature09714

Mombaerts, P. (2006). Axonal wiring in the mouse olfactory system. *Annu. Rev. Cell Dev. Biol.* 22, 713–737. doi: 10.1146/annurev.cellbio.21.012804.093915

Mombaerts, P., Wang, F., Dulac, C., Chao, S. K., Nemes, A., Mendelsohn, M., et al. (1996). Visualizing an olfactory sensory map. *Cell* 87, 675–686. doi: 10.1016/S0092-8674(00)81387-2

Mori, K., and Sakano, H. (2011). How is the olfactory map formed and interpreted in the mammalian brain? *Annu. Rev. Neurosci.* 34, 467–499. doi: 10.1146/annurev-neuro-112210-112917

Nagayama, S., Takahashi, Y. K., Yoshihara, Y., and Mori, K. (2004). Mitral and tufted cells differ in the decoding manner of odor maps in the rat olfactory bulb. *J. Neurophysiol.* 91, 2532–2540. doi: 10.1152/jn.01266.2003

Pressler, R. T., and Strowbridge, B. W. (2006). Blanes cells mediate persistent feed-forward inhibition onto granule cells in the olfactory bulb. *Neuron* 49, 889–904. doi: 10.1016/j.neuron.2006.02.019

Price, J. L. (1973). An autoradiographic study of complementary laminar patterns of termination of afferent fibers to the olfactory cortex. *J. Comp. Neurol.* 150, 87–108. doi: 10.1002/cne.901500105

Price, J. L., and Powell, T. P. (1970). The synaptology of the granule cells of the olfactory bulb. *J. Cell Sci.* 7, 125–155.

Ramón y Cajal, S. (1888). Estructura de los centros nerviosos de las aves. *Rev. Trim. Histol. Norm. Pat.* 1, 1–10.

Ramón y Cajal, S. (1890a). A quelle epoque apparaissent les expansions des cellules nerveuses de la moëlle épinière du poulet? *Anat. Anz.* 5, 609–613, 631–639.

Ramón y Cajal, S. (1890b). *Origen y Terminación de las Fibras Nerviosas Olfatorias*. Bacelona: GacSan, 1–21.

Ramón y Cajal, S. (1891). Significación fisiológica de las expansiones protoplásmicas y nerviosas de las células de la sustancia gris. *Rev. Cienc. Méd. Barc.* 22:23.

Ramón y Cajal, S. (1892a). La rétine des vertébrés. *Cellule* 9, 121–133.

Ramón y Cajal, S. (1892b). Nuevo concepto de la Histología de los centros nerviosos. Conferencia III. *Rev. Cienc. Méd. Barc.* 18, 457–476.

Ramón y Cajal, S. (1894). Croonian Lecture: la fine structure des centres nerveux. *Proc. R. Soc. Lond.* 55, 444–468. doi: 10.1098/rspl.1894.0063

Ramón y Cajal, S. (1896). Sobre las relaciones de las células nerviosas con las neuróglicas. *Rev. Trimest. Microgr.* 1, 123–126.

Ramón y Cajal, S. (1897). Algo sobre la significación fisiológica de la neuroglia. *Rev. Trimest. Microgr.* 1, 33–47.

Ramón y Cajal, S. (1899). *Textura del Sistema Nervioso del Hombre y de los Vertebrados*. Madrid: Moya.

Ramón y Cajal, S. (1901). Estudios sobre la corteza cerebral humana. IV. Estructura de la corteza cerebral olfativa del hombre y mamíferos. *Trab. Lab. Invest. Biol.* 1, 1–140.

Ramón y Cajal, S. (1904). *Textura del Sistema Nervioso del Hombre y los Vertebrados*. Madrid: Moya.

Ramón y Cajal, S. (1913). *Estudios sobre la Degeneración y Regeneración del Sistema Nervioso*. Madrid: Moya.

Ramón y Cajal, S. (1917). *Recuerdos de mi Vida.* Vol. 2*: Historia de mi Labor Científica*. Madrid: Alianza Editorial.

Ramón y Cajal, S. (1931). *Pensamientos de Tendencia Educativa. Audiobook*. Madrid: Archivo de la Palabra.

Ressler, K. J., Sullivan, S. L., and Buck, L. B. (1993). A zonal organization of odorant receptor gene expression in the olfactory epithelium. *Cell* 73, 597–609. doi: 10.1016/0092-8674(93)90145-G

Retzius, G. (1892). "Die endigungsweise des riechnerven," in *Biologisches Untersuchungen. Neue Folge*, ed G. Retzius (Stockholm: Samson and Wallin), 25–28.

Roux, L., Benchenane, K., Rothstein, J. D., Bonvento, G., and Giaume, C. (2011). Plasticity of astroglial networks in olfactory glomeruli. *Proc. Natl. Acad. Sci. U.S.A.* 108, 18442–18446. doi: 10.1073/pnas.1107386108

Sassoè-Pognetto, M. (2011). Molecular and functional heterogeneity of neural circuits: an example from the olfactory bulb. *Brain Res. Rev.* 66, 35–42. doi: 10.1016/j.brainresrev.2010.06.003

Schneider, S. P., and Macrides, F. (1978). Laminar distributions of internuerons in the main olfactory bulb of the adult hamster. *Brain Res. Bull.* 3, 73–82. doi: 10.1016/0361-9230(78)90063-1

Schoppa, N. E., Kinzie, J. M., Sahara, Y., Segerson, T. P., and Westbrook, G. L. (1998). Dendrodendritic inhibition in the olfactory bulb is driven by NMDA receptors. *J. Neurosci.* 18, 6790–6802.

Schwalbe, G. A. (1881). *Lehrbuch der Neurologie*. Erlanger: E. Besold.

Schwarting, G. A., Gridley, T., and Henion, T. R. (2007). Notch1 expression and ligand interactions in progenitor cells of the mouse olfactory epithelium. *J. Mol. Histol.* 38, 543–553. doi: 10.1007/s10735-007-9110-9

Shepherd, G. M., Chen, W., and Greer, C. (2004). "Olfactory bulb," in *The Synaptic Organization of the Brain* (New York, NY: Oxford University Press), 165–216

Shepherd, G. M., Chen, W. R., Willhite, D., Migliore, M., and Greer, C. (2007). The olfactory granule cell: from classical enigma to central role in olfactory processing. *Brain Res. Rev.* 55, 373–382. doi: 10.1016/j.brainresrev.2007.03.005

Shepherd, G. M., and Erulkar, S. D. (1997). Centenary of the synapse: from Sherrington to the molecular biology of the synapse and beyond. *Trends Neurosci.* 20, 385–392. doi: 10.1016/S0166-2236(97)01059-X

Suzuki, J., Yoshizaki, K., Kobayashi, T., and Osumi, N. (2013). Neural crest-derived horizontal basal cells as tissue stem cells in the adult olfactory epithelium. *Neurosci. Res.* 75, 112–120. doi: 10.1016/j.neures.2012.11.005

Valverde, F. (1965). *Studies of the Pyriform Lobe*. Cambridge, MA: Harvard University Press.

Valverde, F., and López-Mascaraque, L. (1991). Neuroglial arrangements in the olfactory glomeruli of the hedgehog. *J. Comp. Neurol.* 307, 658–674. doi: 10.1002/cne.903070411

Vassar, R., Ngai, J., and Axel, R. (1993). Spatial segregation of odorant receptor expression in the mammalian olfactory epithelium. *Cell* 74, 309–318. doi: 10.1016/0092-8674(93)90422-M

Zhang, X., and Firestein, S. (2002). The olfactory receptor gene superfamily of the mouse. *Nat. Neurosci.* 5, 124–133. doi: 10.1038/nn800

Conflict of Interest Statement: The authors declare that the research was conducted in the absence of any commercial or financial relationships that could be construed as a potential conflict of interest.

Received: 14 March 2014; paper pending published: 07 April 2014; accepted: 10 June 2014; published online: 02 July 2014.

Citation: Figueres-Oñate M, Gutiérrez Y and López-Mascaraque L (2014) Unraveling Cajal's view of the olfactory system. Front. Neuroanat. ***8****:55. doi: 10.3389/fnana. 2014.00055*

This article was submitted to the journal Frontiers in Neuroanatomy.

Please cite this article in press as: Bribián A et al. Decoding astrocyte heterogeneity: New tools for clonal analysis. Neuroscience (2015), http://dx.doi.org/10.1016/j.neuroscience.2015.04.036

Neuroscience xxx (2015) xxx–xxx

REVIEW

DECODING ASTROCYTE HETEROGENEITY: NEW TOOLS FOR CLONAL ANALYSIS

A. BRIBIÁN,[‡] M. FIGUERES-OÑATE,[‡] E. MARTÍN-LÓPEZ[†] AND L. LÓPEZ-MASCARAQUE[*]

Instituto Cajal-CSIC, Madrid, Spain

Abstract—The importance of astrocyte heterogeneity came out as a hot topic in neurosciences especially over the last decades, when the development of new methodologies allowed demonstrating the existence of big differences in morphological, neurochemical and physiological features between astrocytes. However, although the knowledge about the biology of astrocytes is increasing rapidly, an important characteristic that remained unexplored, until the last years, has been the relationship between astrocyte lineages and cell heterogeneity. To fill this gap, a new method called *StarTrack* was recently developed, a powerful genetic tool that allows tracking astrocyte lineages forming cell clones. Using *StarTrack*, a single astrocyte progenitor and its progeny can be specifically labeled from its generation, during embryonic development, to its final fate in the adult brain. Because of this specific labeling, astrocyte clones, exhibiting heterogeneous morphologies and features, can be easily analyzed in relation to their ontogenetic origin. This review summarizes how astrocyte heterogeneity can be decoded studying the embryonic development of astrocyte lineages and their clonal relationship. Finally, we discuss about some of the challenges and opportunities emerging in this exciting area of investigation.

This article is part of a Special Issue entitled: Astrocyte-Neuron Interact.

Key words: glial cells, clonal, progenitor, lineage, NG2-glia, cortical lesion.

Contents

INTRODUCTION

In recent years, the development of new and innovative genetic techniques opened up the possibility of studying the heterogeneity of brain cell populations in relation to their ontogenetic origin. In particular, *in vivo* single-cell analysis offers a direct correlation between the embryonic origin of brain cells and their adult fate and heterogeneity (García-Marqués and López-Mascaraque, 2013; García-Moreno et al., 2014; Loulier et al., 2014; Siddiqi et al., 2014; Figueres-Oñate et al., 2015).

Among all cells forming the Central Nervous System (CNS), astrocytes are one of the most abundant and heterogeneous cell types in the brain and spinal cord, representing nearly 20% of the total number of cells in humans (Pelvig et al., 2008). Classically astrocytes were classified into two general categories: protoplasmic and fibrous; protoplasmic astrocytes occupy the gray matter whereas fibrous astrocytes reside in the white matter (Fig. 1A, B; Kölliker, 1889; Andriezen, 1893; Lenhossek, 1893; Cajal, 1913; Rio-Hortega, 1928). Cajal already used this general distinction of astrocytes at the beginning of the last century (1913), describing the presence of morphologically distinct types of astrocytes in the human hippocampus (Fig. 1C). Nowadays, these differences are easily highlighted using genetic tools that allow visualizing the totality of cell bodies such as dye-filling (Bushong et al., 2002; Ogata and Kosaka, 2002; Wilhelmsson et al., 2004; Pekny and Nilsson, 2005), fluorescent protein labeling either by specific transgenic mice and viral injections (Buffo et al., 2008), or by the most recently developed, DNA fluorescent reporter vectors like the *StarTrack* method (García-Marqués and López-Mascaraque, 2013). Unlike the dye-filling or the viral or transgenic mediated fluorescent labeling of astrocytes, the *StarTrack* technique specifically labels astrocyte progeny distinguishing unequivocally each individual cell clone at the end of the

*Corresponding author. Address: Instituto Cajal-CSIC, Avda. Dr. Arce, 37, 28002 Madrid, Spain
E-mail address: mascaraque@cajal.csic.es (L. López-Mascaraque).
† Present address: Yale School of Medicine, New Haven, CT 06520-8082, USA.
‡ These authors contributed equally to this work.

Abbreviations: hGFAP, human glial fibrillary acidic protein promoter; NPC, neural progenitor cell; NSCs, neural stem cells; OPCs, oligodendrocyte precursor cells; RGCs, radial glial cells; SGZ, subgranular zone.

http://dx.doi.org/10.1016/j.neuroscience.2015.04.036

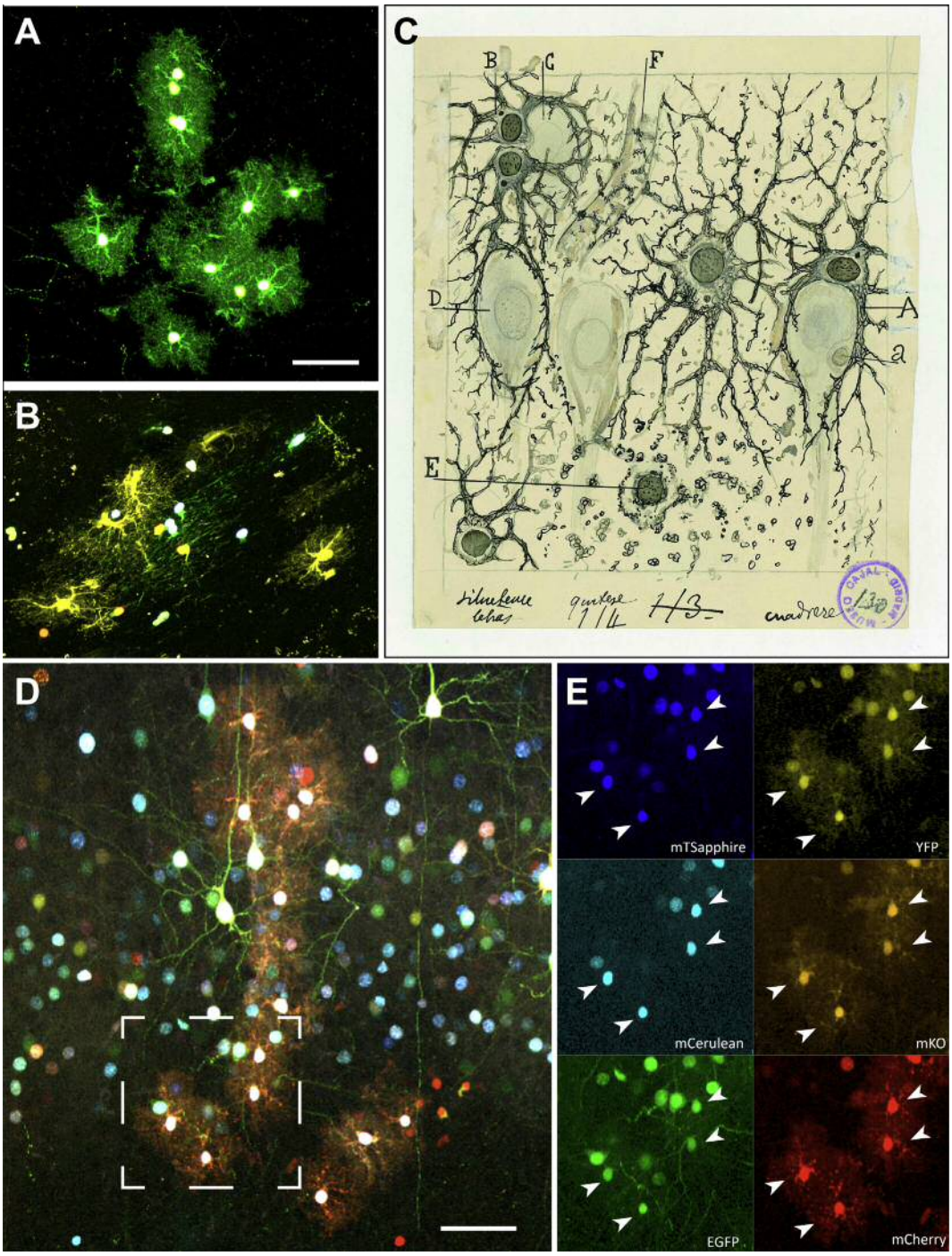

Fig. 1. Astrocyte classification. (A) Characteristic morphology of protoplasmic astrocytes after embryonic electroporation using the *StarTrack* method. (B) Typical morphologies of fibrous astrocytes within the white matter after embryonic electroporation using the *StarTrack* method. (C) Original Cajal drawing illustrating the human neuroglia in the pyramidal and radiated layers of Ammon's horn with the gold chloride method: *A* represents thick astrocyte wrapping a pyramidal cell; *B*, sibling astrocytes forming a nest around a cell (*C*), one of them extend two processes to another nest (*D*); *E*: cell ''with autolysis signs''. *F*: Astrocyte close to blood vessels. Cajal Legacy, Instituto Cajal, CSIC. (D) General view of the ubiquitous modification of the *StarTrack* method. The *UbC-StarTrack* allows the tracking of the whole neural progeny from single cells. This modification is based on the combinatorial expression of six fluorescent reporter proteins expressed both, in the cell nucleus and the cytoplasm under a ubiquitous promoter (Ubiquitin C). Decomposition of each fluorescent protein expression in the cells included in the box is represented in E. (E) Details of each confocal channel of labeled cells in D dotted box. Each clone is defined by analyzing the fluorescent expressing vectors incorporated in each cell. Separate confocal channels isolated each single emission of the six different reporter proteins. Fluorescent proteins are, organized by the spectral emission–excitation: mTsapphire, mCerulean, EGFP, Yellow fluorescent protein (YFP), monomeric Kusabira Orange (mKO) and mCherry. The *UbC-StarTrack* is driven by a ubiquitous promoter, which allows the tracing of the whole-cell progeny. Arrowheads point to the different fluorescent combination in astrocytes, although some neurons were also labeled, Fluorescent proteins mTsapphire, mCerulean, EGFP are expressed in those astrocytes just in the nuclear form while YFP, mKO and mCherry are expressed both in the nucleus and the cell cytoplasm. Scale bars: A, B 50 μm; D, E 50 μm.

Please cite this article in press as: Bribián A et al. Decoding astrocyte heterogeneity: New tools for clonal analysis. Neuroscience (2015), http://dx.doi.org/10.1016/j.neuroscience.2015.04.036

embryonic development (Fig. 1A, B). Over the years, the use of all these genetic tools of cell labeling has revealed that, at least morphologically, astrocytes are much more heterogeneous than the classical and simple distinction between fibrous and protoplasmic astrocytes. Additionally, complementary studies of cell function have revealed that astrocytes exhibit a wide range of molecular phenotypes, plasticity and functional properties. Indeed, astrocytes within different brain regions can express different types and levels of ion channels, thus may have subtle differences in electrophysiological properties, including their resting membrane potentials (Kettenmann and Ransom, 2005; Freeman, 2010; Oberheim et al., 2012).

Although these classifications described in depth the morphological and physiological heterogeneity of astrocytes, the unresolved questions about whether or not this heterogeneity is specified during the embryonic development or affects equally all sibling cells, have recently been able to be comprehended. The development of genetic tools such as *StarTrack* (García-Marqués and López-Mascaraque, 2013), which specifically label sibling cells derived from the same progenitor, allows addressing questions such as: *is astrocyte heterogeneity genetically specified during the CNS development and hence dependent on the cell lineage? Is this heterogeneity exclusively influenced by environmental factors?* Or, *is this heterogeneity the result of both, genetic and environmental factors?* Recently our group has found that different classes of astrocytes have clonal identity, suggesting that astrocyte heterogeneity is specified early during CNS development (García-Marqués and López-Mascaraque, 2013). Detailed information about the current knowledge explaining the relationships of astrocyte heterogeneity with the ontogeny is summarized in this review.

CURRENT APPROACHES TO STUDY CELL LINEAGES

During the last decades different works explain the complexity and heterogeneity of astrocytes in the CNS suggesting that they are grouping on cell clusters with clonal identity (Price and Thurlow, 1988; Gray and Sanes, 1991; Muroyama et al., 2005). However, the absence of a technique for specifically labeling all cells derived from the same progenitor, has impeded establishing the influence of genetic specification of astrocyte lineages with their final destination and heterogeneity. Thus, the question about whether adult cells, that belong to a particular clone, are inheriting a similar phenotype affecting the establishment of astrocytic domains in the CNS parenchyma, is being addressed through the improvement of new genetic tools for cell tracking of progeny, like the *StarTrack* method (García-Marqués and López-Mascaraque, 2013).

The idea of tracking cell fate from neural progenitors to their final fate destination was developed together with the onset of some genetic tools making the permanent cell labeling feasible. In particular, Cre-loxP recombination system (Sauer, 1987) was a key technique to address questions about progeny. This technology was later introduced in transgenic mice (Feil et al., 1996), and greatly expanded the possibilities of cellular studies involving genetic modifications. Since then, the use of Cre-loxP technology has been widely extended in the scientific community by combining it with fluorescent reporter genes, increasing dramatically the possibilities to study cell lineages and/or mapping neural circuits, as reported by *Brainbow* technology (Livet et al., 2007; Cai et al., 2013). Another approach is using modified retrovirus to label cell lineages by infecting progenitors (Cepko et al., 1995; Reid et al., 1995; Li et al., 2012), a widely used technology for tracking cells (Heins et al., 2002; Weber et al., 2011). The use of virus with the purpose of tracking cells or modifying their phenotypes is a widely used technology (Heins et al., 2002; Weber et al., 2011). Other approaches included DNA site-specific recombination (Raymond and Soriano, 2007), mosaic analysis with double-marker system (MADM; Zong et al., 2005; Gao et al., 2014) and Flybow (Hadjieconomou et al., 2011; Hampel et al., 2011).

However, while all these technologies open up a wide range of possibilities for studying genetically modified cell populations, the question about whether final phenotypes in adult organisms are already specified in progenitor cells is a question that is beginning to be solved from the recent development of new techniques.

STARTRACK AS A TOOL TO STUDY CELL PROGENY

The *StarTrack* method was designed by our group as an approach to answer the question of whether a neural progenitor cell (NPC) is already specified to give rise to a specific population of heterogeneous astrocytes, since the beginning of its generation in the CNS (García-Marqués and López-Mascaraque, 2013). This technique is based on the combinatorial expression of six fluorescent reporter proteins under the regulation of human glial fibrillary acidic protein promoter (hGFAP) expressed either in the cytoplasm or in the nucleus. The different fluorescent reporters are incorporated in a plasmid containing the hGFAP promoter and PiggyBac transposase recognition sites to guarantee the permanent expression of these proteins in randomly electroporated cells. *StarTrack* produces a specific labeling of progenitor cells, based on the combination of reporter genes that are inherited by their progenies. This permanent labeling allows to specifically study cell clones at adult stages or when they reach their final destinations. Using this technology it is possible to track astrocyte progenies originating from a single NPC and hence analyze their migrations, final destinations and some features such as morphological heterogeneity. A characteristic regularly observed is the similarity between all astrocytes belonging to the same clone. These features together with the high diversity of clones, strongly suggest the existence of subtypes of clones or functional categories, although further functional analyses must be performed. All together provide us with a more comprehensive understanding of astrocyte heterogeneity that can be applied further to study functional differences between clones or their response to

Please cite this article in press as: Bribián A et al. Decoding astrocyte heterogeneity: New tools for clonal analysis. Neuroscience (2015), http://dx.doi.org/10.1016/j.neuroscience.2015.04.036

events such as brain injuries. Complementarily we have recently developed a modification of the *StarTrack* method, *UbC-StarTrack*, which uses a ubiquitous promoter to extend the study of clones to the other CNS cell types (Fig. 1D, E; Figueres-Oñate et al., 2014; Parmigiani et al., 2015).

ASTROCYTE DEVELOPMENT: FROM SINGLE CELL TO ADULT HETEROGENEITY

During embryonic development, the differentiation of all CNS cells follows a sequential paradigm of cell generation. The first groups of cells that are generated are neurons, followed by astrocytes and finally oligodendrocytes, all happening in partially overlapping waves (Sauvageot and Stiles, 2002; Rowitch and Kriegstein, 2010). Focusing on the cortical development of glial cells, they are classified into astrocytes, oligodendrocytes, microglia, ependymal cells, tanycytes and NG2 cells or polydendrocytes (Nishiyama et al., 2002; Nishiyama, 2007; Richardson et al., 2011). During CNS development, the differentiation of neural cells from their NPCs involves many genetic and environmental factors, including patterning of spatial cues along the rostrocaudal or dorsoventral axes of the CNS (Jessell, 2000; Kohwi and Doe, 2013). NPCs, also named neural stem cells (NSCs), are clustered in domains in the ventricular zone whose cells share neurogenic and gliogenic potencies (McCarthy et al., 2001; Rowitch and Kriegstein, 2010). The switch that determines if a NPC is going to be a neuron or a glial cell is influenced by both genetic and environmental factors affecting their differentiation programs (Götz and Sommer, 2005; Rowitch and Kriegstein, 2010). Radial glial cells (RGCs) are an important subtype of NSCs in the neuroepithelium (Doetsch et al., 1999). RGCs are pluripotent progenitor cells that divide mostly asymmetrically in the ventricular zone (reviewed in Parnavelas and Nadarajah, 2001; Campbell and Götz, 2002; Malatesta et al., 2008). These particular progenitor cells generate both neurons and later glial cells including ependymal cells, astrocytes and oligodendrocytes (Doetsch et al., 1999; Malatesta et al., 2000; Noctor et al., 2001; Kriegstein and Götz, 2003; Pinto and Götz, 2007; Kriegstein and Alvarez-Buylla, 2009; Dimou and Götz, 2014). At embryonic and perinatal stages, RGCs are mainly located in the subventricular zone (SVZ) extending their processes to the pial surface (Fig. 2A). At perinatal stages some RGCs transform themselves into multipolar astrocytes, suggesting that astrogenesis is linked to the terminal phases of RGC differentiation (Fig. 2B). However, there is still much controversy about the origin of macroglial cells derived from bipotential precursors; so far, how the transformation of NSCs varies as they progress through distinct developmental stages is a pending question.

On the other hand, multipotent cells remain in the adult brain located in neurogenic niches acting as NSCs. There are two neurogenic niches in the adult brain: the SVZ and the hippocampal subgranular zone (SGZ). GFAP-positive progenitors located in the SVZ and SGZ (type B cells) generate large numbers of new cells (Doetsch et al., 1999). In the adult SGZ the majorities of B cells differentiate into granule cells that project their dendrites into the molecular layer and axons to the CA3 pyramidal cell layer via the mossy fiber pathway (Stanfield and Trice, 1988; Markakis and Gage, 1999; Seri et al., 2001) and establish synaptic connection with local neurons (McDonald and Wojtowicz, 2005).

In the case of the SVZ B cells give rise to neuroblasts that migrate in chains to the olfactory bulb through the rostral migratory stream where they differentiate into granule and periglomerular neurons (Corotto et al., 1993; Lois and Alvarez-Buylla, 1994; Lois et al., 1996). In addition, B cells could also give rise to oligodendrocytes (Menn et al., 2006; Gonzalez-Perez and Alvarez-Buylla, 2011) and mature astrocytes (Merkle et al., 2007).

ASTROCYTE CLONES

The existence of mixed clones, containing either astrocytes/oligodendrocytes (Levison and Goldman, 1993; McCarthy et al., 2001) or astrocytes/interneurons (Grimaldi et al., 2009; Sudarov et al., 2011) during embryonic development suggests that both cell lineages might be related. This fact is clearly observed at early developmental stages, but changes over development show that cell clones seem to be restricted to neurons, astrocytes or oligodendrocytes clones (Grove et al., 1993; Luskin et al., 1993; Luskin and McDermott, 1994). These data are consistent with the model characterized by a progressive restriction on cell generation of NSCs, so that they changed their potency from mixed neuronal–glial, through glial, to purely astrogenic or oligogenic fate (Mallamaci, 2013). Although this is the common rule, some precursors may retain their tripotency until relatively later developmental stages or even during the adulthood (Reynolds and Weiss, 1992; Morshead and van der Kooy, 2004; Neumeister et al., 2009). An example of the retained tripotency is what occurs to progenitors (B cells) that form the SVZ. Thus, it is demonstrated that B cells give rise to interneurons, astrocytes (Merkle et al., 2007) and oligodendrocytes (Menn et al., 2006; Gonzalez-Perez and Alvarez-Buylla, 2011) in the adult CNS. It is remarkable that, NG2 cells could also act as precursor cells since they could generate oligodendrocyte, astrocytes and neurons (Dimou et al., 2008; Rivers et al., 2008; Zhu et al., 2008). In fact, *in vivo* cell fate analyses revealed that NG2 cells are oligodendrocyte precursor cells in the white matter (OPCs), while the in gray matter only rarely give rise to oligodendrocytes or astrocytes but keep their phenotype throughout postnatal life (Dimou et al., 2008; Zhu et al., 2008; Trotter et al., 2010).

Independently, whether astrocytes come from bi- or tri-potent precursors, what is clearly established is that lineages of astrocytes display different morphologies and functional domains (García-Marques et al., 2010; García-Marqués and López-Mascaraque, 2013).

One question that still remains unclear is the precise timing for astrogenesis. The lack of stage-specific markers for astrocyte precursors (Molofsky et al., 2012) makes difficult monitoring astrocyte generation and proliferation at early developmental stages. Thus, once the progenitor is astrocyte committed, it continues

Please cite this article in press as: Bribián A et al. Decoding astrocyte heterogeneity: New tools for clonal analysis. Neuroscience (2015), http://dx.doi.org/10.1016/j.neuroscience.2015.04.036

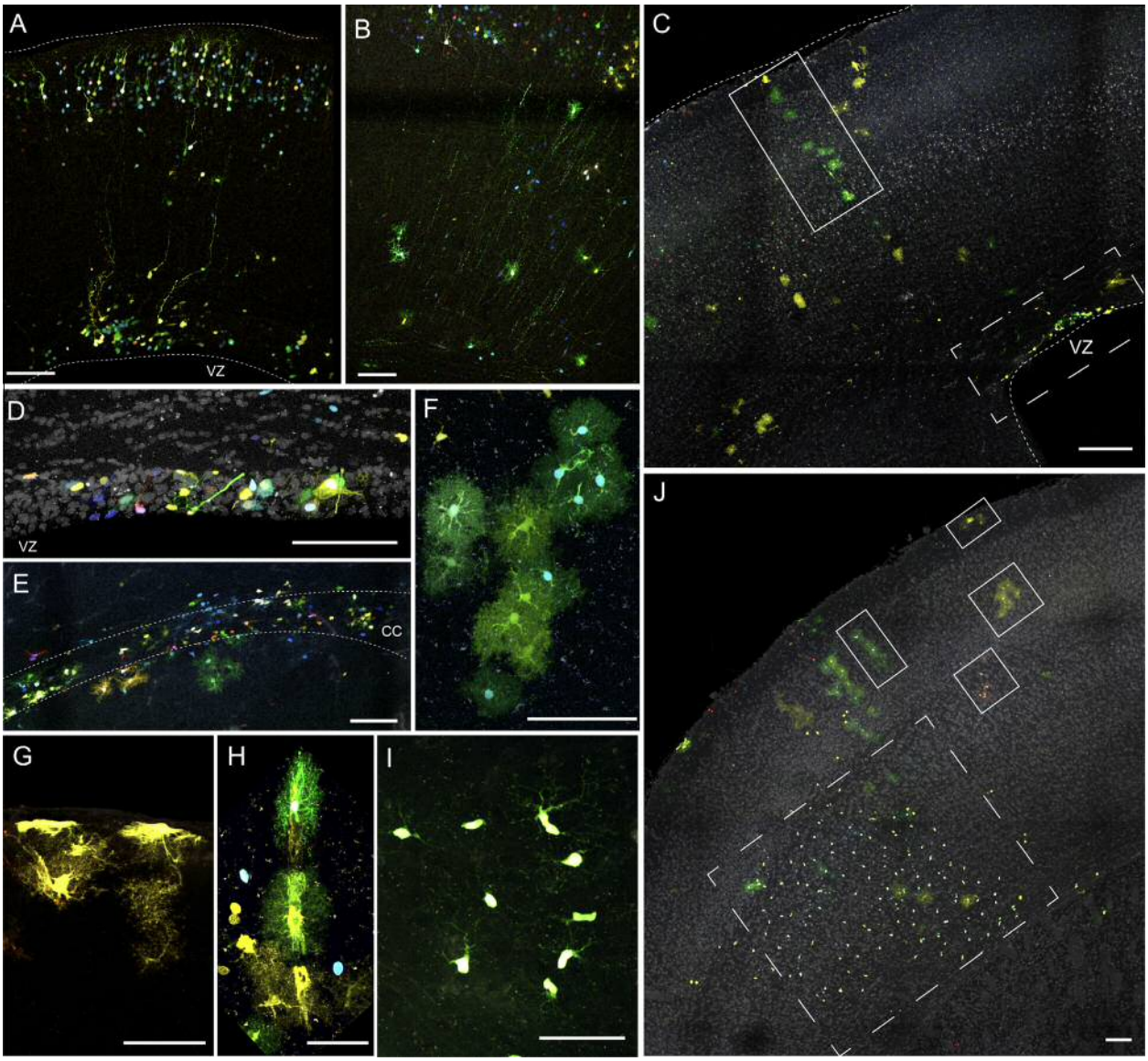

Fig. 2. Clonal astrocyte heterogeneity after E14 electroporation. (A) Electroporation of the ubiquitous *UbC-StarTrack*. At P0 radial glia cells connect both pial and ventricular surface. (B) After *UbC-StarTrack* electroporation, at P5, radial glia cells transform into clonally related immature astrocytes. (C) General view of the dispersion of adult cortical astrocytes after *StarTrack* electroporation. Some astrocyte clones colonize several cortical areas showing a columnar dispersion (vertical box), whereas labeled cells positioned in the SVZ reveal targeted area (dashed box). (D) Clonal hGFAP labeled cells within the proliferative adult SVZ. Nuclei labeled with Draq5™. (E) Adult white matter magnification after *StarTrack* electroporation. Typical fibrous astrocyte morphologies in corpus callosum. (F) Two different clones of protoplasmic astrocytes labeled by *StarTrack*. (G) Clone of restricted pial astrocytes. (H) Two different clones of astrocytes surrounding the same blood vessel. (I) Typical morphology of clonally related NG2-labeled cells with *StarTrack*. (J) Clonal distribution of cells after *StarTrack* electroporation. Some clones are positioned in defined cortical layers (boxes), although others occupied several cortical layers (NG2 cells, dashed box). CC: Corpus callosum; VZ: ventricular zone. Scale bar = 100 μm.

proliferating in the neonatal brain parenchyma, remaining within delimited domains from where they radially migrate (Hochstim et al., 2008; Ge et al., 2012; Tsai et al., 2012; García-Marqués and López-Mascaraque, 2013). As soon as they achieve their final destiny, they proliferate by symmetric divisions (Ge et al., 2012; García-Marqués and López-Mascaraque, 2013).

All these changes in the timing of generation, proliferation, migration and final destination make astrocytes a widely distributed type of cells in the CNS being involved in a large number of functions (Sofroniew and Vinters, 2010; Dimou and Götz, 2014). The consequence of that is astrocytes are a large heterogeneous population, although the cellular nature of this heterogeneity is just starting to emerge and it is of crucial relevance to explain their function (Chaboub and Deneen, 2012). For example, is established the existence of anatomical and functional astrocytic domains, forming astroglial networks in different brain areas (Giaume and McCarthy, 1996; Giaume et al., 2010) that can be coupled by GAP junctions suggesting they form specific functional domains, as described for astrocytes located within barrels in the somatosensory cortex (Houades et al., 2006). Similarly, within the olfactory bulb exists a preferential

Please cite this article in press as: Bribián A et al. Decoding astrocyte heterogeneity: New tools for clonal analysis. Neuroscience (2015), http://dx.doi.org/10.1016/j.neuroscience.2015.04.036

communication between astrocytes within a glomerulus but not between astrocytes in adjacent glomeruli (Roux et al., 2011). Furthermore, as sibling neurons have higher probability to be electrically coupled with each other via GAP junctions than non-sister cells (Yu et al., 2013), sibling astrocytes may be preferentially connected by GAP junctions. Additionally, Tsai and collaborators (Tsai et al., 2012) highlighted the importance of region-restricted astrocyte allocation, since the depletion of an astrocytic specific spinal cord domain results in abnormal formation of specific synapses onto motoneurons. In this respect, we are wondering whether clonally related astrocytes may overlap with functional neural domains or networks, although further functional assays must be performed to clarify this question. Thus, performing clonal analysis is essential to understand all these questions from single progenitor cells at a precise time point during development.

DECODING ASTROCYTE HETEROGENEITY: ANALYSES OF CLONAL DISPERSION

Astrocytes differ in their morphology, developmental origin, gene expression profile, electrophysiological properties, function and response to injury and disease (García-Marques et al., 2010; Zhang and Barres, 2010). The distribution and final location of astrocytes vary depending on the region in which they are generated (early in the ventral spinal cord and later in the brain cortex; Guérout et al., 2014) and migration routes, all influenced by intrinsic and extrinsic factors forming the different type of astrocyte clones. In cortical areas, the precursors of astrocyte clones migrate from the ventricular zone in a pattern similar to radial glia (Fig. 2A). In the perinatal cerebral cortex, RGCs forming the ventricular zone transform into clones of mature and immature astrocytes, characterized by thick and poorly branched processes, resembling protoplasmic astrocytes (Fig. 2B). Interestingly, in adult brains some clone-related progenitors are still present within the wall of the ventricular zones in the electroporated areas (SVZ; Fig. 2C, D) indicating that proliferative niches are still present during the adult stage. Taken together, astrocyte clones visualized by *StarTrack* were classified into the following subtypes: (1) Cells attached to the ventricular zone with long processes (Fig. 2D) resembling B cells (proposed as the NSC of the adult brain); (2) Fibrous astrocytes flanking or within the corpus callosum (Fig 2E); (3) Protoplasmic astrocytes occupying several or restricted layers of the cerebral cortex (Boxes in Fig. 2C, F, J); (4) Pial astrocytes (Fig. 2G) with morphology similar to the lamellar astrocytes (Holen, 2011). These pial astrocytes, lying underneath the pial surface, are also clonally related cells and they are classified as a new astrocyte subtype coming from different progenitors (García-Marqués and López-Mascaraque, 2013).

The dispersion of astrocytes suggests that the arrangement of these cells is related to their final location and probably influenced by their function (García-Marqués and López-Mascaraque, 2013). For example, pial astrocytes (Fig. 2G) are probably functionally related to the glia limitans (Liu et al., 2013). On the other hand, clonally related cells with protoplasmic morphologies are also found arranged in columns with their end foot processes surrounded by a single blood vessel suggesting a role in blood vessel uptake (Fig. 2H).

Another important observation, is that clones of protoplasmic astrocytes form domains of spatially restricted cells showing diverse arrangements throughout the cortical layers: Some clones are located throughout several cortical layers (Fig. 2C) while others occupy restricted layers (Fig. 2J). Even using a cell labeling regulated under the GFAP promoter, we find very large NG2-glia clones distributed by the cortex (Fig. 2J, dotted lines box and Fig. 2I). Expression of the hGFAP promoter in other cell types as NG2 and neurons was previously reported (Matthias et al., 2003; Su et al., 2004). This topic was extensively addressed in our recent work (García-Marqués et al., 2014).

In summary, we state that the *StarTrack* method is a powerful approach to describe clonally related cells forming homogeneous cell clusters. The high degree of homogeneity within astrocyte clones clearly demonstrates that fibrous and protoplasmic astrocytes come from separate cell lineages. Similarly, pial clones and those surrounded blood vessels are derived from separate lineage branches.

GLIAL CLONAL RESPONSE TO BRAIN DAMAGE

Astroglia actively respond to CNS damages (neurodegenerative diseases, traumatic injuries, stroke…), classically known as reactive gliosis. Reactive gliosis is characterized by the generation of a glial scar, a barrier constituted by reactive astrocytes, microglia, fibroblasts, pericytes, endothelial and meningeal cells (Sofroniew and Vinters, 2010). Reactive astrocytes are characterized by hypertrophied cell bodies due to different cellular events such as hyperplasia, cytoplasmic enlargement, elongated cell processes and overexpression of intermediate filament proteins such as GFAP, vimentin, nestin and S100β (Mathewson and Berry, 1985; Pekny, 2001; Sofroniew, 2005, 2009; Dimou and Götz, 2014; Gallo and Dennen, 2014). In addition, besides reactive gliosis, astrocytes are also affected in some CNS pathologies that undergo functional loss and degeneration (Maragakis and Rothstein, 2006; Olabarria et al., 2010).

Between these events, GFAP upregulation in astrocyte cytoplasm can be highlighted using the *StarTrack* technique (Fig. 3A, B). Upon brain injury (Fig. 3C), astroglia are thought to be involved in the repair and wound healing process, since reactive astrocytes migrate to the lesion site border also proliferating to form the glial scar (Miyake et al., 1988; Buffo et al., 2005; Sofroniew, 2005). However, to date there is still some controversy about what is the origin of reactive astrocytes. Some works describe that reactive astrocytes proliferate within or close to the area injured (Buffo et al., 2005; Sofroniew, 2005; Martín-López et al., 2013); others suggest these cells arise from endogenous progenitors located in the adult brain parenchyma such as NG2 cells (Alonso, 2005; Buffo et al.,

Please cite this article in press as: Bribián A et al. Decoding astrocyte heterogeneity: New tools for clonal analysis. Neuroscience (2015), http://dx.doi.org/10.1016/j.neuroscience.2015.04.036

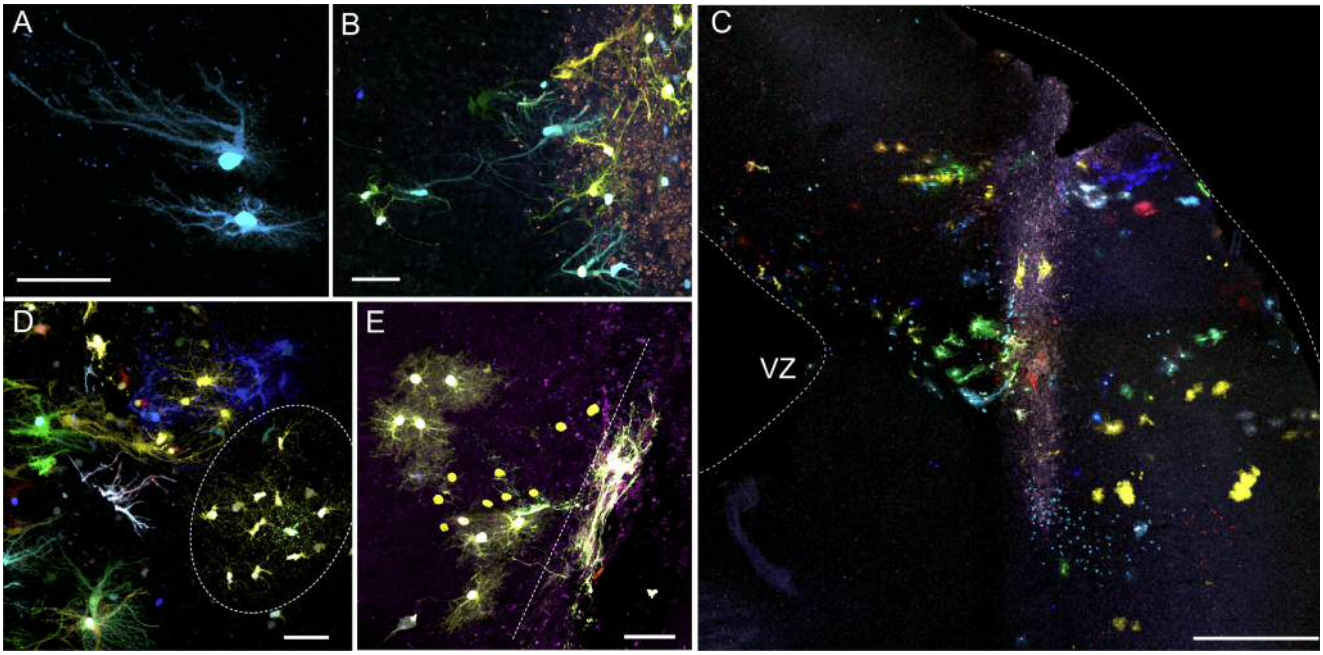

Fig. 3. Clonal astrocyte response to cortical injury. *StarTrack* labeling, 7 days after injury to the adult cortex in E14-electroporated mice embryos. (A) Representative image of two reactive astrocytes, showing the typical hypertrophied morphology. (B) Clones of reactive astrocytes located around and into the injury site (bright tissue made of cellular debris). (C) Low-magnification image of a cortical area 7 days post injury using the fine needle method. Needle track is highlighted as a ''clear'' tissue surrounded by several clones of astrocytes, exhibiting reactive morphologies. (D) Different shapes of reactive astrocytes around and into the injured area with reactive morphology. Clonally related NG2-like cells with a non-altered morphology close to the injured area (dotted area). (E) Different astrocyte reactivity related to their distance to the lesion. Dotted line limits the lesion site. VZ: ventricular zone. Scale bar = 100 μm.

2008; Komitova et al., 2011; García-Marqués et al., 2014; Nishiyama et al., 2014); and a third hypothesis could be that reactive astrocytes dedifferentiate toward an immature state as occurs in the SVZ and hippocampus (Doetsch et al., 1999; Seri et al., 2001). However, although the source of reactive astrocyte is still unclear, their migration to the lesion border directing their hypertrophied cellular processes to the injury to form the glial scar is widely demonstrated (Sofroniew and Vinters, 2010; Martín-López et al., 2013). A particularity of reactive astrocytes is that, unlike OPCs, astrocytes do not cover long distances and they remain stationary with less migration toward the injury site (Tsai et al., 2012; Bardehle et al., 2013; Martín-López et al., 2013). It is remarkable that the difference in cell migration between astrocytes and OPCs is also found during embryonic development, where OPCs migrate longer distances than astrocyte progenitors at early post-natal stages. Moreover, astrocytes are not alone in responding to brain injuries; NG2 cells (Fig. 3D, dashed line) have also been involved in repairing processes and contribute to the proliferative activity close to the injury (Buffo et al., 2008; Simon et al., 2011; Dimou and Götz, 2014).

Considering that all astrocytes in the CNS form clones, an open question is whether there is a clonal response to the injury. Astrocytes whose cell bodies are labeled in their totality are shown around the lesion area forming clones close to the injury. From these clones, all sibling cells show the characteristic hypertrophied processes typical of reactive astrocytes, sending thick cellular processes to the injury border (Fig. 3E, right hypertrophied clone). However, other clones, located at comparable distances, did not display altered cell morphologies (Fig. 3E, left non-hypertrophied clone). This study, completed with cell proliferation analysis, opens up a new perspective on the putative relationship between the diversity of astrocyte clones and their response in damaged brain (Martín-López et al., 2013).

In summary, clonal analysis from a single-cell progenitor opens up new perspectives on glial diversity, highlighting the relevance of astrocytes during CNS development and homeostasis maintenance in healthy and damaged brain.

Acknowledgments—This work was supported by research Grant BFU2013-48807-R from the Spanish Ministry of Economy and Competitiveness. Cajal original drawing was provided by Cajal Legacy (Instituto Cajal, CSIC, Madrid, Spain) thanks to Dr. Juan A. de Carlos.

REFERENCES

Andriezen WL (1893) The neuroglia elements in the human brain. Br Med J 2:227–230.

Alonso G (2005) NG2 proteoglycan-expressing cells of the adult rat brain: possible involvement in the formation of glial scar astrocytes following stab wound. Glia 49:318–338.

Bardehle S, Krüger M, Buggenthin F, Schwausch J, Ninkovic J, Clevers H, Snippert HJ, Theis FJ, Meyer-Luehmann M, Bechmann I, Dimou L, Götz M (2013) Live imaging of astrocyte responses to acute injury reveals selective juxtavascular proliferation. Nat Neurosci 16:580–586.

Buffo A, Vosko MR, Ertürk D, Hamann GF, Jucker M, Rowitch D, Götz M (2005) Expression pattern of the transcription factor Olig2 in response to brain injuries: implications for neuronal repair. Proc Natl Acad Sci USA 102:18183–18188.

Buffo A, Rite I, Tripathi P, Lepier A, Colak D, Horn AP, Mori T, Götz M (2008) Origin and progeny of reactive gliosis: a source of multipotent cells in the injured brain. Proc Natl Acad Sci USA 105:3581–3586.

Bushong EA, Martone ME, Jones YZ, Ellisman MH (2002) Protoplasmic astrocytes in CA1 stratum radiatum occupy separate anatomical domains. J Neurosci 22:183–192.

Cajal SR (1913) Contribución al conocimiento de la neuroglia del cerebro humano. Trab Lab Invest Biol 11:255–315.

Cai D, Cohen KB, Luo T, Lichtman JW, Sanes JR (2013) Improved tools for the Brainbow toolbox. Nat Methods 10:540–547.

Campbell K, Götz M (2002) Radial glia: multi-purpose cells for vertebrate brain development. Trends Neurosci 25:235–238.

Cepko C, Ryder EF, Austin CP, Walsh C, Fekete DM (1995) Lineage analysis using retrovirus vectors. Methods Enzymol 254:387–419.

Chaboub LS, Deneen B (2012) Developmental origins of astrocyte heterogeneity: the final frontier of CNS development. Dev Neurosci 34:379–388.

Corotto FS, Henegar JA, Maruniak JA (1993) Neurogenesis persists in the subependymal layer of the adult mouse brain. Neurosci Lett 149:111–114.

Dimou L, Simon C, Kirchhoff F, Takebayashi H, Götz M (2008) Progeny of Olig2-expressing progenitors in the gray and white matter of the adult mouse cerebral cortex. J Neurosci 28:10434–10442.

Dimou L, Götz M (2014) Glial cells as progenitors and stem cells: new roles in the healthy and diseased brain. Physiol Rev 94:709–737.

Doetsch F, Caillé I, Lim DA, García-Verdugo JM, Alvarez-Buylla A (1999) Subventricular zone astrocytes are neural stem cells in the adult mammalian brain. Cell 97:703–716.

Feil R, Brocard J, Mascrez B, LeMeur M, Metzger D, Chambon P (1996) Ligand-activated site-specific recombination in mice. Proc Natl Acad Sci USA 93:10887–10890.

Figueres-Oñate M, Gutiérrez Y, López-Mascaraque L (2014) Unraveling Cajal's view of the olfactory system. Front Neuroanat 8:1–12.

Figueres-Oñate M, García-Marqués J, Pedraza M, De Carlos JA, López-Mascaraque L (2015) Spatiotemporal analyses of neural lineages after embryonic and postnatal progenitor targeting combining different reporters. Front Neurosci 9:1–11.

Freeman MR (2010) Specification and morphogenesis of astrocytes. Science 330:774–778.

Gallo V, Deneen B (2014) Glial development: the crossroads of regeneration and repair in the CNS. Neuron 83:283–308.

Gao P, Postiglione MP, Krieger TG, Hernandez L, Wang C, Han Z, Streicher C, Papusheva E, Insolera R, Chugh K, Kodish O, Huang K, Simons BD, Luo L, Hippenmeyer S, Shi SH (2014) Deterministic progenitor behavior and unitary production of neurons in the neocortex. Cell 159:775–788.

García-Marqués J, De Carlos JA, Greer CA, López-Mascaraque L. García-Marqués, López-Mascaraque (2010). Different astroglia permissivity controls the migration of olfactory bulb interneuron precursors. Glia 58:218–230.

García-Marqués J, López-Mascaraque L (2013) Clonal identity determines astrocyte cortical heterogeneity. Cereb Cortex 23:1463–1472.

García-Marqués J, Núñez-Llaves R, López-Mascaraque L (2014) NG2-glia from pallial progenitors produce the largest clonal clusters of the brain: time frame of clonal generation in cortex and olfactory bulb. J Neurosci 34:2305–2313.

García-Moreno F, Vasistha NA, Begbie J, Molnár Z (2014) CLoNe is a new method to target single progenitors and study their progeny in mouse and chick. Development 141:1589–1598.

Ge WP, Miyawaki A, Gage FH, Jan YN, Jan LY (2012) Local generation of glia is a major astrocyte source in postnatal cortex. Nature 484:376–380.

Giaume C, McCarthy KD (1996) Control of gap-junctional communication in astrocytic networks. Trends Neurosci 19:319–325.

Giaume C, Koulakoff A, Roux L, Holcman D, Rouach N (2010) Astroglial networks: a step further in neuroglial and gliovascular interactions. Nat Rev Neurosci 11:87–99.

Gonzalez-Perez O, Alvarez-Buylla A (2011) Oligodendrogenesis in the subventricular zone and the role of epidermal growth factor. Brain Res Rev 67:147–156.

Götz M, Sommer L (2005) Cortical development: the art of generating cell diversity. Development 132:3327–3332.

Gray GE, Sanes JR (1991) Migratory paths and phenotypic choices of clonally related cells in the avian optic tectum. Neuron 6:211–225.

Grimaldi P, Parras C, Guillemot F, Rossi F, Wassef M (2009) Origins and control of the differentiation of inhibitory interneurons and glia in the cerebellum. Dev Biol 328:422–433.

Grove EA, Williams BP, Li DQ, Hajihosseini M, Friedrich A, Price J (1993) Multiple restricted lineages in the embryonic rat cerebral cortex. Development 117:553–561.

Guérout N, Li X, Barnabé-Heider F (2014) Cell fate control in the developing central nervous system. Exp Cell Res 321:77–83.

Hadjieconomou D, Rotkopf S, Alexandre C, Bell DM, Dickson BJ, Salecker I (2011) Flybow: genetic multicolor cell labeling for neural circuit analysis in *Drosophila melanogaster*. Nat Methods 8:260–266.

Hampel S, Chung P, McKellar CE, Hall D, Looger LL, Simpson JH (2011) Drosophila Brainbow: a recombinase-based fluorescence labeling techniqueto subdivide neural expression patterns. Nat Methods 8:253–259.

Heins N, Malatesta P, Cecconi F, Nakafuku M, Tucker KL, Hack MA, Chapouton P, Barde YA, Götz M (2002) Glial cells generate neurons: the role of the transcription factor Pax6. Nat Neurosci 5:308–315.

Hochstim C, Deneen B, Lukaszewicz A, Zhou Q, Anderson DJ (2008) Identification of positionally distinct astrocyte subtypes whose identities are specified by a homeodomain code. Cell 133:510–522.

Holen T (2011) The ultrastructure of lamellar stack astrocytes. Glia 59:1075–1083.

Houades V, Rouach N, Ezan P, Kirchhoff F, Koulakoff A, Giaume C (2006) Shapes of astrocyte networks in the juvenile brain. Neuron Glia Biol 2:3–14.

Jessell TM (2000) Neuronal specification in the spinal cord: inductive signals and transcriptional codes. Nat Rev Genet 1:20–29.

Kettenmann H, Ransom BR (2005) The concept of neuroglia: a historical perspective. In: Kettenmann H, Ransom BR, editors. Neuroglia, 2nd ed.. Oxford: Oxford University Press. p. 1–8.

Kohwi M, Doe CQ (2013) Temporal fate specification and neural progenitor competence during development. Nat Rev Neurosci 14:823–838.

Kölliker A, von (1889) Handbuch der Gewebelehre des Mensachen 6th ed vol 1. Die allgemeineGewebelehre und die systeme der Haut, knochen und Muskeln. Engelmann, Leipzig.

Komitova M, Serwanski DR, Lu QR, Nishiyama A (2011) NG2 cells are not a major source of reactive astrocytes after neocortical stab wound injury. Glia 59:800–809.

Kriegstein AR, Alvarez-Buylla A (2009) The glial nature of embryonic and adult neural stem cells. Annu Rev Neurosci 32:149–184.

Kriegstein AR, Götz M (2003) Radial glia diversity: a matter of cell fate. Glia 43:37–43.

Lenhossek (1893). Der feinere Bau des Nervensystems. Ed. Fischer's Medicinische Buchhandlung.

Levison SW, Goldman JE (1993) Both oligodendrocytes and astrocytes develop from progenitors in the subventricular zone of postnatal rat forebrain. Neuron 10:201–212.

Li Y, Lu H, Cheng P-L, Ge S, Xu H, Shi S-H, Dan Y (2012) Clonally related visual cortical neurons show similar stimulus feature selectivity. Nature 486:118–121.

Please cite this article in press as: Bribián A et al. Decoding astrocyte heterogeneity: New tools for clonal analysis. Neuroscience (2015), http://dx.doi.org/10.1016/j.neuroscience.2015.04.036

Liu X, Zhang Z, Guo W, Burnstock G, He C, Xiang Z (2013) The superficial glia limitans of mouse and monkey brain and spinal cord. Anat Rec (Hoboken) 296:995–1007.
Livet J, Weissman TA, Kang H, Draft RW, Lu J, Bennis RA, Sanes JR, Lichtman JW (2007) Transgenic strategies for combinatorial expression of fluorescent proteins in the nervous system. Nature 450:56–62.
Lois C, Alvarez-Buylla A (1994) Long-distance neuronal migration in the adult mammalian brain. Science 264(5162):1145–1148.
Lois C, García-Verdugo JM, Alvarez-Buylla A (1996) Chain migration of neuronal precursors. Science 271(5251):978–981.
Loulier K, Barry R, Mahou P, Le Franc Y, Supatto W, Matho KS, Ieng S, Fouquet S, Dupin E, Benosman R, Chédotal A, Beaurepaire E, Morin X, Livet J (2014) Multiplex cell and lineage tracking with combinatorial labels. Neuron 81:505–520.
Luskin MB, Parnavelas JG, Barfield JA (1993) Neurons, astrocytes, and oligodendrocytes of the rat cerebral cortex originate from separate progenitor cells: an ultrastructural analysis of clonally related cells. J Neurosci 13:1730–1750.
Luskin MB, McDermott K (1994) Divergent lineages for oligodendrocytes and astrocytes originating in the neonatal forebrain subventricular zone. Glia 11:211–226.
Malatesta P, Hartfuss E, Götz M (2000) Isolation of radial glial cells by fluorescent-activated cell sorting reveals a neuronal lineage. Development 127:5253–5263.
Malatesta P, Appolloni I, Calzolari F (2008) Radial glia and neural stem cells. Cell Tissue Res 331:165–178.
Mallamaci A (2013) Developmental control of cortico-cerebral astrogenesis. Int J Dev Biol 57:689–706.
Maragakis NJ, Rothstein JD (2006) Mechanisms of disease: astrocytes in neurodegenerative disease. Nat Clin Pract Neurol 2:679–689.
Markakis EA, Gage FH (1999) Adult-generated neurons in the dentate gyrus send axonal projections to field CA3 and are surrounded by synaptic vesicles. J Comp Neurol 406:449–460.
Martín-López E, García-Marques J, Núñez-Llaves R, López-Mascaraque L (2013) Clonal astrocytic response to cortical injury. PLoS One 8(9):e74039.
Mathewson AJ, Berry M (1985) Observations on the astrocyte response to a cerebral stab wound in adult rats. Brain Res 327:61–69.
Matthias K, Kirchhoff F, Seifert G, Hüttmann K, Matyash M, Kettenmann H, Steinhäuser C (2003) Segregated expression of AMPA-type glutamate receptors and glutamate transporters defines distinct astrocyte populations in the mouse hippocampus. J Neurosci 23:1750–1758.
McCarthy M, Turnbull DH, Walsh CA, Fishell G (2001) Telencephalic neural progenitors appear to be restricted to regional and glial fates before the onset of neurogenesis. J Neurosci 21:6772–6781.
McDonald HY, Wojtowicz JM (2005) Dynamics of neurogenesis in the dentate gyrus of adult rats. Neurosci Lett 385:70–75.
Menn B, Garcia-Verdugo JM, Yaschine C, Gonzalez-Perez O, Rowitch D, Alvarez-Buylla A (2006) Origin of oligodendrocytes in the subventricular zone of the adult brain. J Neurosci 26:7907–7918.
Merkle FT, Mirzadeh Z, Alvarez-Buylla A (2007) Mosaic organization of neural stem cells in the adult brain. Science 317:381–384.
Miyake T, Hattori T, Fukuda M, Kitamura T, Fujita S (1988) Quantitative studies on proliferative changes of reactive astrocytes in mouse cerebral cortex. Brain Res 451:133–138.
Molofsky AV, Krencik R, Ullian EM, Tsai HH, Deneen B, Richardson WD, Barres BA, Rowitch DH (2012) Astrocytes and disease: a neurodevelopmental perspective. Genes Dev 26:891–907.
Morshead CM, van der Kooy D (2004) Disguising adult neural stem cells. Curr Opin Neurobiol 14:125–131.
Muroyama Y, Fujiwara Y, Orkin SH, Rowitch DH (2005) Specification of astrocytes by bHLH protein SCL in a restricted region of the neural tube. Nature 438:360–363.
Neumeister B, Grabosch A, Basak O, Kemler R, Taylor V (2009) Neural progenitors of the postnatal and adult mouse forebrain retain the ability to self-replicate, form neurospheres, and undergo multipotent differentiation in vivo. Stem Cells 27:714–723.
Nishiyama A, Watanabe M, Yang Z, Bu J (2002) Identity, distribution, and development of polydendrocytes: NG2-expressing glial cells. J Neurocytol 31:437–455.
Nishiyama A (2007) Polydendrocytes: NG2 cells with many roles in development and repair of the CNS. Neuroscientist 13:62–76.
Nishiyama A, Suzuki R, Zhu X (2014) NG2 cells (polydendrocytes) in brain physiology and repair. Front Neurosci 8:133.
Noctor SC, Flint AC, Weissman TA, Dammerman RS, Kriegstein AR (2001) Neurons derived from radial glial cells establish radial units in neocortex. Nature 409:714–720.
Oberheim NA, Goldman SA, Nedergaard M (2012) Heterogeneity of astrocytic form and function. Methods Mol Biol 814:23–45.
Ogata K, Kosaka T (2002) Structural and quantitative analysis of astrocytes in the mouse hippocampus. Neuroscience 113:221–233.
Olabarria M, Noristani HN, Verkhratsky A, Rodríguez JJ (2010) Concomitant astroglial atrophy and astrogliosis in a triple transgenic animal model of Alzheimer's disease. Glia 58:831–838.
Parmigiani E, Leto K, Rolando C, Figueres-Oñate M, López-Mascaraque L, Buffo A, Rossi F (2015) Heterogeneity and bipotency of astroglial-like cerebellar progenitors along the interneuron and glial lineages. J Neuroscience (in press).
Parnavelas JG, Nadarajah B (2001) Radial glial cells are they really glia? Neuron 31:881–884.
Pekny M (2001) Astrocytic intermediate filaments: lessons from GFAP and vimentin knock-out mice. Prog Brain Res 132:23–30.
Pekny M, Nilsson M (2005) Astrocyte activation and reactive gliosis. Glia 50:427–434.
Pelvig DP, Pakkenberg H, Stark AK, Pakkenberg B (2008) Neocortical glial cell numbers in human brains. Neurobiol Aging 29:1754–1762.
Pinto L, Götz M (2007) Radial glial cell heterogeneity–the source of diverse progeny in the CNS. Prog Neurobiol 83:2–23.
Price J, Thurlow L (1988) Cell lineage in the rat cerebral cortex: a study using retroviral-mediated gene transfer. Development 104:473–482.
Raymond CS, Soriano P (2007) High-efficiency FLP and PhiC31 site-specific recombination in mammalian cells. PLoS One 2(1):e162.
Reid CB, Liang I, Walsh C (1995) Systematic widespread clonal organization in cerebral cortex. Neuron 15:299–310.
Reynolds BA, Weiss S (1992) Generation of neurons and astrocytes from isolated cells of the adult mammalian central nervous system. Science 255:1707–1710.
Richardson WD, Young KM, Tripathi RB, McKenzie I (2011) NG2-glia as multipotent neural stem cells: fact or fantasy? Neuron 70:661–673.
Rio-Hortega P (1928) Tercera aportacion al conocimiento morfologico e interpretación funcional de la oligodendroglia. Mem Real Soc Esp Hist Nat 14:5–122.
Rivers LE, Young KM, Rizzi M, Jamen F, Psachoulia K, Wade A, Kessaris N, Richardson WD (2008) PDGFRA/NG2 glia generate myelinating oligodendrocytes and piriform projection neurons in adult mice. Nat Neurosci 11:1392–1401.
Roux L, Benchenane K, Rothstein JD, Bonvento G, Giaume C (2011) Plasticity of astroglial networks in olfactory glomeruli. Proc Natl Acad Sci USA 108:18442–18446.
Rowitch DH, Kriegstein AR (2010) Developmental genetics of vertebrate glial-cell specification. Nature 468:214–222.
Sauer B (1987) Functional expression of the Cre-lox site-specific recombination system in the yeast *Saccharomyces cerevisiae*. Mol Cell Biol 7:2087–2096.
Sauvageot CM, Stiles CD (2002) Molecular mechanisms controlling cortical gliogenesis. Curr Opin Neurobiol 12:244–249.
Seri B, García-Verdugo JM, McEwen BS, Alvarez-Buylla A (2001) Astrocytes give rise to new neurons in the adult mammalian hippocampus. J Neurosci 21:7153–7160.
Siddiqi F, Chen F, Aron AW, Fiondella CG, Patel K, LoTurco JJ (2014) Fate mapping by piggyback transposase reveals that

Please cite this article in press as: Bribián A et al. Decoding astrocyte heterogeneity: New tools for clonal analysis. Neuroscience (2015), http://dx.doi.org/10.1016/j.neuroscience.2015.04.036

neocortical GLAST+ progenitors generate more astrocytes than nestin+ progenitors in rat neocortex. Cereb Cortex 24:508–520.
Simon C, Götz M, Dimou L (2011) Progenitors in the adult cerebral cortex: cell cycle properties and regulation by physiological stimuli and injury. Glia 59:869–881.
Sofroniew MV (2005) Reactive astrocytes in neural repair and protection. Neuroscientist 11:400–407.
Sofroniew MV (2009) Molecular dissection of reactive astrogliosis and glial scar formation. Trends Neurosci 32:638–647.
Sofroniew MV, Vinters HV (2010) Astrocytes: biology and pathology. Acta Neuropathol 119:7–35.
Stanfield BB, Trice JE (1988) Evidence that granule cells generated in the dentate gyrus of adult rats extend axonal projections. Exp Brain Res 72:399–406.
Su M, Hu H, Lee Y, d'Azzo A, Messing A, Brenner M (2004) Expression specificity of GFAP transgenes. Neurochem Res 29:2075–2093.
Sudarov A, Turnbull RK, Kim EJ, Lebel-Potter M, Guillemot F, Joyner AL (2011) Ascl1 genetics reveals insights into cerebellum local circuit assembly. J Neurosci 31:11055–11069.
Trotter J, Karram K, Nishiyama A (2010) NG2 cells: properties, progeny and origin. Brain Res Rev 63:72–82.
Tsai HH, Li H, Fuentealba LC, Molofsky AV, Taveira-Marques R, Zhuang H, Tenney A, Murnen AT, Fancy SP, Merkle F, Kessaris N, Alvarez-Buylla A, Richardson WD, Rowitch DH (2012) Regional astrocyte allocation regulates CNS synaptogenesis and repair. Science 337:358–362.
Weber K, Thomaschewski M, Warlich M, Volz T, Cornils K, Niebuhr B, Täger M, Lütgehetmann M, Pollok JM, Stocking C, Dandri M, Benten D, Fehse B (2011) RGB marking facilitates multicolor clonal cell tracking. Nat Med 17:504–508.
Wilhelmsson U, Li L, Pekna M, Berthold CH, Blom S, Eliasson C, Renner O, BushongE Ellisman M, Morgan TE, Pekny M (2004) Absence of glial fibrillary acidic protein and vimentin prevents hypertrophy of astrocytic processes and improves post-traumatic regeneration. J Neurosci 24:5016–5021.
Zhang Y, Barres BA (2010) Astrocyte heterogeneity: an underappreciated topic in neurobiology. Curr Opin Neurobiol 20:588–594.
Zhu X, Bergles DE, Nishiyama A (2008) NG2 cells generate both oligodendrocytes and gray matter astrocytes. Development 135:145–157.
Zong H, Espinosa JS, Su HH, Muzumdar MD, Luo L (2005) Mosaic analysis with double markers in mice. Cell 121:479–492.
Yu HH, Awasaki T, Schroeder MD, Long F, Yang JS, He Y, Ding P, Kao JC, Wu GY, Peng H, Myers G, Lee T (2013) Clonal development and organization of the adult Drosophila central brain. Curr Biol 23:633–643.

(Accepted 15 April 2015)
(Available online xxxx)

Please cite this article in press as: Bribián A et al. Decoding astrocyte heterogeneity: New tools for clonal analysis. Neuroscience (2015), http://dx.doi.org/10.1016/j.neuroscience.2015.04.036

Development/Plasticity/Repair

Heterogeneity and Bipotency of Astroglial-Like Cerebellar Progenitors along the Interneuron and Glial Lineages

Elena Parmigiani,[1,2] Ketty Leto,[1,2] Chiara Rolando,[1,2] María Figueres-Oñate,[3] Laura López-Mascaraque,[3] Annalisa Buffo,[1,2] and Ferdinando Rossi[1,2]†

[1]Department of Neuroscience Rita Levi-Montalcini and Neuroscience Institute Cavalieri Ottolenghi, University of Turin, I-10126 Turin, Italy, [2]Neuroscience Institute Cavalieri Ottolenghi, I-10043 Orbassano, Turin, Italy, and [3]Department of Molecular, Cellular, and Developmental Neurobiology, Cajal Institute, Spanish National Research Council, E-28002 Madrid, Spain

Cerebellar GABAergic interneurons in mouse comprise multiple subsets of morphologically and neurochemically distinct phenotypes located at strategic nodes of cerebellar local circuits. These cells are produced by common progenitors deriving from the ventricular epithelium during embryogenesis and from the prospective white matter (PWM) during postnatal development. However, it is not clear whether these progenitors are also shared by other cerebellar lineages and whether germinative sites different from the PWM originate inhibitory interneurons. Indeed, the postnatal cerebellum hosts another germinal site along the Purkinje cell layer (PCL), in which Bergmann glia are generated up to first the postnatal weeks, which was proposed to be neurogenic. Both PCL and PWM comprise precursors displaying traits of juvenile astroglia and neural stem cell markers. First, we examine the proliferative and fate potential of these niches, showing that different proliferative dynamics regulate progenitor amplification at these sites. In addition, PCL and PWM differ in the generated progeny. GABAergic interneurons are produced exclusively by PWM astroglial-like progenitors, whereas PCL precursors produce only astrocytes. Finally, through *in vitro*, *ex vivo*, and *in vivo* clonal analyses we provide evidence that the postnatal PWM hosts a bipotent progenitor that gives rise to both interneurons and white matter astrocytes.

Key words: **Bergmann glia; cerebellum; mouse brain; multipotent progenitors; neurogenesis; prospective white matter**

Introduction

The anatomic complexity of the cerebellum originates embryonically from the epithelium of the fourth ventricle [ventricular zone (VZ)] and the anterior rhombic lip (RL). In these germinal niches, progenitors with astroglial features [bona fide radial glia (RG); Mori et al., 2006] give rise to all the glutamatergic and GABAergic cerebellar neurons, respectively (Carletti and Rossi, 2008). Interestingly, cerebellar development continues after birth, when secondary proliferative sites replace the embryonic niches. Postnatally, proliferative progenitors reside in the external granular layer (EGL), in the prospective white matter (PWM), and along the Purkinje cell layer (PCL; Altman and Bayer, 1997). Although the EGL exclusively produces granule neurons (Hallonet et al., 1990; Alvarez-Otero et al., 1993), the PWM comprises cells belonging to the interneuronal, astroglial, and oligodendroglial lineages (Leto et al., 2012). The PCL instead hosts a subset of postmitotic Bergmann glia (BG) and precursors for this astroglial type (Yamada and Watanabe, 2002; Sudarov et al., 2011; Buffo and Rossi, 2013). However, a neurogenic potential has also been hypothesized for PCL-residing progenitors (Alcock et al., 2007; Alcock and Sottile 2009).

Notably, progenitors in both PCL and PWM display similar traits of immature astroglia and prospective neural stem cell (NSC) markers (Yamada and Watanabe, 2002; Anthony et al., 2004; Lee et al., 2005; Alcock et al., 2007; Alcock and Sottile, 2009; Silbereis et al., 2009; Fleming et al., 2013). Beside these similarities, the specific features and progenies of PCL and PWM progenitors are not well known. For instance, despite evidence that the PWM is the main source of cerebellar interneurons (Leto et al., 2009; Silbereis et al., 2009; Fleming et al., 2013), a direct proof excluding other sources including the PCL is still missing.

Moreover, it is still unclear whether a lineage relationship exists between interneurons and astrocytes, as suggested by previous studies (Leto et al., 2012). Mice lacking the transcription factor Achaete-scute homolog-1 show increased astrocyte production at the expense of interneurons, suggesting that these lineages might originate from the same progenitor (Grimaldi et al.,

Received Dec. 23, 2014; revised March 22, 2015; accepted March 28, 2015.

Author contributions: E.P., K.L., A.B., and F.R. designed research; E.P., K.L., and C.R. performed research; C.R., M.F.-O., and L.L.-M. contributed unpublished reagents/analytic tools; E.P., K.L., C.R., and A.B. analyzed data; E.P., K.L., and A.B. wrote the paper.

This work was supported by the Ministry of Universities and Research [Research Programs of Relevant National Interest 2009 Program TBCZJB (F.R.) and Research Fund for the Promotion of Basic Research Grant RBFR10A01S (K.L.)] and the University of Turin. This study was also partly funded by the research grant BFU2013-48807-R from the Spanish Ministry of Economy and Competitivenes to Laura López-Mascaraque. We thank Mikio Hoshino, Silvia De Marchis, and Annarita DeLuca for critical reading of this manuscript and helpful suggestions. We are also indebted to Alexandra Lepiez and Magdalena Götz for kindly providing the LCMV plasmids, Verdon Taylor for the gift of the Confetti mutant line, Annarita DeLuca for technical help, and Daniele Imperiale for cyclin stainings. We dedicate this work in memory of Prof. F. Rossi for his continuous support and encouragement.

†Deceased on January 24, 2014.

The authors declare no competing financial interests.

Correspondence should be addressed to Annalisa Buffo, Department of Neuroscience Rita Levi-Montalcini, University of Turin, Neuroscience Institute Cavalieri Ottolenghi, Regione Gonzole 10, I-10043 Orbassano, Turin, Italy. E-mail: annalisa.buffo@unito.it.

C. Rolando's present address: Department of Biomedicine, University of Basel, CH-4058 Basel, Switzerland.

DOI:10.1523/JNEUROSCI.5255-14.2015

 0270-6474/15/357388-15$15.00/0